



The
University
Of
Sheffield.

**Towards the development of a tractable model
to study innate immune responses of the
respiratory tract to
Staphylococcus aureus infection**

ZEYAD ALHARBI

A thesis submitted for the degree of
Doctor of Philosophy (Ph.D.)

December 2022

The University of Sheffield
Faculty of Medicine, Dentistry and Health
Department of Infection, Immunity and Cardiovascular Disease

Supervisors: Professor Colin Bingle
Dr Lynne Bingle

Dedicated to my family

*To the people who believe, support, and encourage me to strive for
excellence and follow my dreams*

Abstract

The epithelium of the human airway provides critical protection to the respiratory tract because the cells are always exposed to inhaled microbes. The epithelial lining therefore acts as a physical shield against pathogens. This layer contains several cell types that are specialized to perform the functions of the innate defence system. Studies of interactions between the host and pathogens require the establishment of differentiated epithelial cell cultures that recapitulate the airway epithelium. *Staphylococcus aureus* is a bacterium found in 30% of the population in the upper tract of the respiratory system. The aim of this study was to develop *in vitro* models of the human airway epithelium that can be used to study the initial stages of infection of the respiratory tract. HBEC3-KT and BMI-1 cells (human immortalised bronchial epithelial cell lines) were differentiated at the air liquid interface (ALI) for three weeks. A direct comparison of these cells was performed with primary human bronchial epithelial cells (HBECs) cultured in the same manner. RT-PCR and qPCR was performed with several markers specific for different cell types (e.g., *BPIFA1*, *BPIFB1*, *SCGB1A1*, *TEKT1*) and this confirmed the differentiation of cells at the ALI. Expression of these markers were lower in the cell lines compared to the HBECs. Protein corresponding to some of these genes was examined under IF microscopy. An unbiased proteomic analysis was performed to directly compare the apical secretions of differentiated HBEC3-KT cells and differentiated primary HBECs. The proteomics data indicated that HBECs and differentiated HBEC3-KT cells appear phenotypically similar. Many proteins were shared between the two ALI cultures, but the production of primary mucus protein components and some host defence proteins was less in the HBEC3-KTs, which may limit the use of this cell line as a surrogate for the human airway epithelium. Effects of *S. aureus* infection were studied by using differentiated and undifferentiated cells with GFP-labelled *S. aureus* (SH1000) at different MOIs. Primary differentiated HBECs were also infected following treatment of the cells with IL-13. Bacterial infections were more marked in differentiated cells. qPCR and RT PCR was performed with several pro-inflammatory markers (e.g., *CXCL10*, *CXCL1* and *IL6*). Inflammatory responses were also examined using IF microscopy and protein-based assays (cytokine arrays). It appeared that differentiated cells expressed higher levels of inflammatory mediators and induction was greater than in undifferentiated cells. This study established a number of *in vitro* models that can be used for the identification of pathogen and host factors that are necessary for the initial stages of *S. aureus* infection of the respiratory tract.

Acknowledgment

First, I would like to express my gratitude to Prof Colin Bingle, my mentor, and project supervisor. His assistance has been of utmost importance during my Ph.D. journey. It was my pleasure to work with you since your wisdom and guidance allowed me to learn a great deal and gain new skills that will be useful in my future research. I cannot thank you enough for believing in my potential to take on this project. I also want to convey my appreciation to Dr. Lynne Bingle. Her constant reassurance, advice, and teachings helped me design my experiments and get the best possible results during the four years of my study. I am grateful for the opportunity to do this study at their facilities. The skills and knowledge I gained there were indispensable.

Thank you very much to everyone in the Bingle group and my friends for making my Ph.D. studies entertaining and worthwhile. Fawaz, Aziz, Miraj, and Cameron! Thank you for being such great partners and companions. Priyanka, I will always be in debt to you for being there while things were not easy at work, particularly in my first year. I would like to acknowledge the assistance of technical personnel at the University of Sheffield as well as group of Dr. Lynne Prince.

During this time, particularly helpful to me were the Saudi Arabia government, which sponsored my Ph.D. studies and living expenses. I also appreciate the University of Tabuk for providing me with this great opportunity. Above all, I want to express my gratitude to my family. I can never pay my father and mother back for their unwavering support in all of my decisions. Their prayers for me have helped me push through every obstacle in life. Words cannot explain how grateful I am for all they have done for me.

Without the support, encouragement, and nurturing of my loving wife Bashayr Alqattan, children Mohammad, Sultana and Sattam, and siblings, my dream would never have become a reality. My family's patience and genuine care have been my backbone throughout this journey. Lastly, I would not have completed my Ph.D. without my friends Ali, Asim, Faisal, Abdullah, Hussam, Hatim, Yahea and Saad. Their presence cannot be underestimated.

Abstract publication

- Alharbi, Z., Chowdhury, M.M.K., Bingle, L. and Bingle, C., 2020. Air liquid interface (ALI)-grown immortalized human cell lines: a promising tractable model for human airway. *European Respiratory Journal* 2020 56: 4327; **DOI:** 10.1183/13993003.congress-2020.4327

Conference presentations

- **Poster presentation:** Development of a tractable model of the human airway using immortalised cell lines grown at the ALI. Medical School Research Day, Sheffield, UK, June 2019.
- **Poster presentation:** Development of a tractable model of the human airway using immortalised cell lines grown at the ALI. British Association of Lung Research (BALR), Cambridge, UK, September 2019.
- **Podium presentation:** Air liquid interface (ALI)-grown immortalized human cell lines: a promising tractable model for human airway. European Respiratory Society International Congress 2020, Vienna, Austria.
- **Poster presentation:** Using differentiated and undifferentiated airway epithelium to understand the intracellular fate of *Staphylococcus aureus*. British Association of Lung Research (BALR), Exeter, UK, June 2021.

Abbreviations

Agr	Accessory gene regulator
ALI	Air-liquid interface
AM	Alveolar Macrophage
AMPs	Antimicrobial Peptides
AMR	Antimicrobial resistance
ANOVA	Analysis of variance
APCs	Antigen-presenting cells
ASL	Airway Surface Liquid
AT1	Alveolar Type 1 cell
AT2	Alveolar Type 2 cell
BEGM	Bronchial Epithelial Growth Medium
BHI	Brain Heart Infusion
BPIFA1	Bactericidal / Permeability-increasing fold containing member A1
BPIFB1	Bactericidal / Permeability-increasing fold containing member B1
CBE1	Ciliated bronchial epithelium 1
CCSP	Clara cell secretory protein.
CdK4	Cyclin-dependent kinase 4
cDNA	Complementary Deoxyribonucleic Acid
CF	Cystic fibrosis
CFTR	CF transmembrane conductance regulator
CFU	Colony forming unit
CHIPS	Chemotaxis inhibitory protein of Staphylococcus
CIFA	Clumping factor, A
CLRs	C-type lectin receptors
COPD	Chronic obstructive pulmonary disease
CRCs	Conditionally reprogrammed cells
CRs	Compliment Receptors
CT	Cycle threshold
CXCL	Chemokine (C-X-C motif) ligand
CysLT	Cysteinyl leukotriene
DAMPs	Damage-Associated Molecular Patterns
DAPI	4',6-diamidino-2-phenylindole
DAPT	Dual Antiplatelet Therapy
DCs	Dendritic cells
dNTP	Deoxyribonucleotide Triphosphate
EAP	Extracellular adherence protein
Eap	Extra-cellular adherence protein
EGFR	Epidermal growth factor receptor
EGFR	Epidermal growth factor receptor
EU	European union
Fc	Fragment crystallisable.
FcγRs	Fcγ receptors
FOXJ1	Forkhead box protein J1
GPCR	G-protein-coupled receptor (C5aR, C5a receptor)
HBEC	Culture of Human Bronchial Epithelial Cells.
HBSS	Hank's Balanced Salt Solution
HBSS	Hank's balanced salt solution
HDPs	Host defence peptides
HE4	Human Epididymis Protein 4

Hlg	Hemolysin-gamma
hTERT	Human Telomerase Reverse Transcriptase
ICAM-1	Intracellular adhesion molecule 1
IFNs	Interferons
IgE	Immunoglobulin E
IgG	Immunoglobulin G
IL-1	Interleukin-1
IL-13	Interleukin-13
IL-6	Interleukin-6
iNKT	invariant NKT
KT	The cytotoxic T
LPS	Lipopolysaccharide
LTA	Lipoteichoic Acids
LUK	leucocidin
MCC	Mucociliary clearance
MOI	Multiplicities of Infection
MRSA	Methicillin-resistant <i>Staphylococcus aureus</i>
MUC5B	Mucin protein 5B
MUC5AC	Mucin 5 AC
NADPH	Nicotinamide Adenine Dinucleotide Phosphate
NHLBI	The National Heart, Lung, and Blood Institute
NK	Natural kill cells
NLRs	Nod-like receptors
OAZ1	Ornithine decarboxylase antizyme 1
PAMPs	Pathogen-Associated Molecular Patterns
PBS	Phosphate-buffered saline.
PCA	Principle component analysis
PCD	Primary ciliary dyskinesia
PCR	Polymerase chain reaction
PGN	Peptidoglycan layer
PMN	Polymorphonuclear
PNECs	Pulmonary neuroendocrine cells
PRRs	Pattern Recognise Receptors
PSGL-1	P-selectin glycoprotein ligand-1
PVL	Panton-Valentine leucocidin
qPCR	Quantitative polymerase chain reaction
RNA	Ribonucleic acid
ROCK	Rho-associated protein kinase
ROS	Reactive Oxygen Species
RT	Room Temperature
RT-PCR	Reverse Transcription - Polymerase chain reaction
<i>S. aureus</i>	<i>Staphylococcus aureus</i>
SCGB1A1	Secretoglobin family 1A member 1
SCGB3A1	Secretoglobin family 3A member 1
SEA/SEB	Staphylococcal Enterotoxin A/B
SEB	Staphylococcal enterotoxin B
SEM	Standard error of the mean
SLPI	Secretory Leukoprotease Inhibitor
SPA	Staphylococcal Protein A
SPDEF	SAM pointed domain containing Ets transcription factor

SSL	Staphylococcal super antigen-like protein
SV40	Simian Virus 40
TE	Trypsin EDTA
Th	T helper
TLRs	Toll Like Receptors.
TNF-1	Tumour necrosis factor receptor 1
TSST	Toxic shock syndrome toxin
TSST	Toxic shock syndrome toxin
VRSA	<i>S. aureus</i> that is resistant to vancomycin
WFDC2	WAP four-disulfide core domain protein 2
μ	Micro
3D	Three-dimensional

Contents

Abstract	IV
Acknowledgment	V
Abstract publication	VI
Conference presentations	VI
Abbreviations	VII
Contents	X
List of figures	XV
List of tables	XVIII
CHAPTER 1: Introduction	1
1.1 Respiratory System	2
1.2 Airway Epithelium.....	3
1.2.1 Basal cells	5
1.2.2 Club cells	6
1.2.3 Goblet cells	7
1.2.4 Ciliated cells.....	7
1.2.4 Rare cells.....	9
1.2.4.1 Pulmonary neuroendocrine cells	9
1.2.4.2 Tuft (brush) cells	9
1.2.4.3 Pulmonary ionocytes	10
1.2.5 Alveolar epithelial cells	10
1.3 Respiratory Immunity	12
1.3.1 Crucial defensive functions of the immune system	12
1.3.2 Barrier function of the airway epithelium.....	14
1.3.2.1 Physical barrier function	14
1.3.2.2 Chemical barrier function	15
1.3.3 Immune Cells	17
1.3.3.1 Neutrophils.....	17
1.3.3.2 Macrophages	18
1.3.3.3 Natural killer cells.....	19
1.3.3.4 Dendritic cells	20
1.4 Respiratory Infection	20

1.5 <i>S. aureus</i>	21
1.5.1 The life cycle of <i>S. aureus</i>	23
1.5.2 <i>S. aureus</i> as a cause of pulmonary infection.....	23
1.5.3 Virulence factors of <i>S. aureus</i>	24
1.6 Evasion of the Innate Immune System by <i>S. aureus</i>	29
1.6.1 Evading extravasation.....	29
1.6.2 Inhibition of complement activation and chemotaxis	30
1.7 Induction of Host Defence Responses by <i>S. aureus</i> Infection	31
1.8 Host Responses to <i>S. aureus</i> Infection.....	33
1.9 Respiratory Cell Cultures for Studying Pulmonary-Specific Responses	34
1.10 ALI Models of the Airway.....	36
1.11 Improvements in Primary Cell Culturing.....	39
1.12 Signaling pathway of interleukin 13 (IL-13) in the airway.....	40
1.13 Host-Pathogen Interaction Models for Studying <i>S. aureus</i>	42
1.14 Hypothesis.....	45
1.15 Objectives	45
1.15 This project consisted of three major aims:	45
CHAPTER 2: Material and Methods.....	46
2.1 Culture of immortalized and primary human bronchial epithelial cells.....	47
2.1.1 Cell culture, splitting and maintenance of growth	47
2.1.2 Seeding cells onto transwells and differentiation at the ALI	48
2.1.3 Seeding undifferentiated cells.....	49
2.2 Ribonucleic acid (RNA) extraction.....	51
2.3 Complementary DNA (cDNA) synthesis	51
2.4 Reverse transcription polymerase chain reaction (RT-PCR).....	51
2.4.1 Primers for PCR.....	52
2.5 Agarose gel electrophoresis	53
2.6 Quantitative polymerase chain reaction (qPCR).....	54
2.7 Immunostaining and immunofluorescence microscopy of ALI cultures	55
2.7.1 ALI Culture Sample fixation.....	55
2.7.2 Fluorescence immunocytochemistry.....	55
2.8 Protein analysis	56
2.8.1 Proteomic data analysis.....	56
2.8.2 Human Cytokine Array.....	57
2.9 Culture of <i>Staphylococcus aureus</i> (<i>S. aureus</i>)-GFP	57

2.10 Miles Misra protocol for colony forming unit (CFU) count	59
2.11 Infection of cell cultures with <i>S. aureus</i>	59
2.11.1 Undifferentiated cell infection	59
2.11.2 Differentiated cell infection	59
2.11.3 Visualization of HBEC3-KT and HBE cells exposed to <i>S. aureus</i>	60
2.12 Statistics	60
CHAPTER 3: Rationalizing a tractable model for human airway using cells grown at the air liquid interface (ALI).....	61
3.1 Introduction.....	62
3.1.1 Aims:.....	64
3.2 Results.....	66
3.2.1 Characterization of HBEC3-KT cells	66
3.2.2 Differentiation of HBEC3-KT cells when grown at the ALI.....	68
3.2.2.1 Gene expression by RT-PCR	68
3.2.2.2 Validation of gene expression in differentiating HBEC3-KT cells by RT- qPCR	70
3.2.3 Immunofluorescence microscopy of airway epithelial markers during ALI culture of HBEC3-KT cells.....	72
3.2.4 Modulation of HBEC3-KT cells differentiation with DAPT and IL13	75
3.2.5 Differentiation of BMI-1 cells when grown at the ALI	79
3.2.5.1 Gene expression by RT-PCR	79
3.2.5.2 Validation of gene expression in BMI-1 cell RNA samples by RT- qPCR	81
3.2.6 Immunofluorescence microscopy of airway epithelial markers during ALI culture of BMI-1 cells	83
3.2.7 Differentiation of HBECs when grown at the ALI	86
3.2.7.1 Gene expression by RT-PCR	86
3.2.7.2 Validation of gene expression in HBECs RNA samples by RT- qPCR	88
3.2.8 Immunofluorescence microscopy of airway epithelial markers during ALI culture of HBECs	90
3.2.9 Comparison of expression of cell-specific marker genes in ALI differentiated HBEC3-KT, BMI-1 and HBEC cells.....	92
3.2.10 Quantitative proteomics analysis of the secretome in HBEC3-KT cells and HBECs	94
3.2.11 Comparison of the quantitative proteomics analysis of the HBEC3-KT cells and Calu-3 cell secretome	108
3.2.12 Comparison of the quantitative proteomics analysis of HBECs secretomes from different studies	110
3.13 Discussion.....	112

3.13.1 The differentiation of HBEC3-KT cells.....	113
3.13.2 Modulation of HBEC3-KT cells differentiation	115
3.13.3 The differentiation of BMI-1 and HBECs	116
3.13.4 Comparison of ALI-differentiated of HBEC3-KT cell and HBEC secretomes.....	119
3.13.5 Variation in this study.....	120
CHAPTER 4: <i>Staphylococcus aureus</i> infection in undifferentiated airway cells.....	123
4.1 Introduction.....	124
4.1.1 Aims:.....	125
4.2 Results.....	127
4.2.1 Growth of <i>S. aureus</i> in tissue culture media	127
4.2.2 Determination of MOI in undifferentiated HBEC3-KT cells	129
4.2.3 Establishing infections in uHBEC3-KT cells	131
4.2.4 Responses of uHBEC3-KT cells infected with <i>S. aureus</i>	137
4.2.4.1 Induction of host cell gene expression	137
4.2.5 Cytokine and chemokine production by <i>S. aureus</i> exposed uHBEC3-KT cells.....	141
4.2.5 Determination of MOI in undifferentiated HBECs.....	144
4.2.6 Establishing infections in uHBECs.....	146
4.2.7 Determination infection of uHBECs with <i>S. aureus</i>	154
4.2.7.1 Validation of host cell gene expression	154
4.2.8 Cytokine and chemokine production by <i>S. aureus</i> exposed uHBEC.....	158
4.2.9 Comparison of the cytokine and chemokine production by <i>S. aureus</i> exposed uHBEC3-KT cells and uHBECs	161
4.10 Discussion.....	163
CHAPTER 5: <i>Staphylococcus aureus</i> infection in differentiated primary human bronchial epithelial cells.	169
5.1 Introduction.....	170
5.1.1 Aims:.....	171
5.2 Results.....	173
5.2.1 Determining the number of <i>S. aureus</i> in differentiated HBECs	173
5.2.2 Infection of differentiated HBECs with <i>S. aureus</i>	175
5.2.3 Response of differentiated HBECs infected with <i>S. aureus</i>	178
5.2.3.1 induction of host cell gene expression	178
5.2.4 Cytokine and chemokine production by <i>S. aureus</i> exposed differentiated HBECs.....	181
5.2.5 Determining <i>S. aureus</i> numbers in differentiated HBECs in the presence of IL-13.....	186
5.2.6 Infection of differentiated HBECs with <i>S. aureus</i> in the presence of IL-13.....	188

5.2.7 Determination infection of HBECs with <i>S. aureus</i> in the presence of.....	191
IL-13	191
5.2.7.1 Validation of host cell gene expression	191
Figure 5.10: Comparison of gene expression in early time points in the presence of IL-13 using <i>CXCL10</i> and <i>IL6</i>	191
5.2.8 Cytokine and chemokine production by IL-13 treated differentiated HBECs infected with <i>S. aureus</i>	194
5.2.9 Comparison of the infection of differentiated HBECs with <i>S. aureus</i> in absence and presence of IL-13	197
5.10 Discussion.....	201
CHAPTER 6: General discussion.....	206
6.1 Strengths and Weaknesses	211
6.2 Future Directions	212
Appendix 1 – List of cytokines and chemokines.....	213
Appendix 2 – List of the top 100 extracellular proteins.	214
References.....	217

List of figures

Figure 1.1 Schematic diagram of the respiratory tract.	3
Figure 1.2 Cellular components of airway epithelium.	4
Figure 1.3 Relationships between cells that generate the pseudostratified airway epithelium of the lung.	6
Figure 1.4 The structure of a motile cilia.	8
Figure 1.5 Overview of the alveolar unit.	11
Figure 1.6 Extravasation of a neutrophil to an infection site and the antimicrobial mechanisms.	18
Figure 1.7 Schematic representation of the structure of <i>S. aureus</i>	22
Figure 1.8 <i>S. aureus</i> approach to destabilize neutrophils extravasation.	30
Figure 1.9 Neutrophil attack and evasion of activation.	31
Figure 1.10 Schematic of ALI culture.	37
Figure 1.11 Gene expression during ALI differentiation of human bronchial epithelial cells.	38
Figure 1.12 Potential mechanisms of IL-13-induced airway hyperresponsiveness.	42
Figure 2.1. Schematic of the timeline and method of ALI culture experiments.	50
Figure 2.2 Schematic to show the method of culture of <i>S. aureus</i>	58
Figure 3.1 Morphological characteristics of HBEC3-KT cells during ALI differentiation on different days.	67
Figure 3.2 RT-PCR of gene expression during ALI differentiation of HBEC3-KT cells.	69
Figure 3.3 RT-qPCR analysis of gene expression during ALI differentiation of HBEC3-KT cells.	71
Figure 3.4 Immunofluorescence microscopy of differentiation of secretory and ciliated for HBEC3-KT cells.	74
Figure 3.5 Gene expression during ALI differentiation of HBEC3-KT cells treated with DAPT and IL-13.	76
Figure 3.6 RT-qPCR analysis of gene expression during ALI differentiation of HBEC3-KT cells with DAPT and IL-13 treatments on day 21.	78
Figure 3.7 RT-PCR of gene expression during ALI differentiation of BMI-1 cells.	80
Figure 3.8 RT-qPCR analysis of gene expression during ALI differentiation of BMI-1 cells.	82
Figure 3.9 Immunofluorescence microscopy reflecting the differentiation of ciliated and secretory BMI-1.	85
Figure 3.10 RT-PCR of gene expression during ALI differentiation of HBECs.	87
Figure 3.11 RT-qPCR analysis of gene expression during ALI differentiation of HBECs.	89
Figure 3.12 Immunofluorescence microscopy reflecting the differentiation of ciliated and secretory HBECs.	91
Figure 3.13 RT-qPCR analysis of gene expression during ALI differentiation of HBEC, BMI-1 and HBEC3-KT cells on day 21	93
Figure 3.14 PCA of differentiated of HBECs and HBEC3-KT cells.	95

Figure 3.15 Proteomic characterisation of the apical secretome of the human bronchial epithelium in HBEC3-KT and HBEC models.	97
Figure 3.16 Differential analysis of the secretome in HBEC3-KT cells and HBECs.	98
Figure 3.17 Relative abundance of the secretome in HBECs and HBEC3-KT cells.	100
Figure 3.18 Comparison of the HBEC3-KT and HBEC secretomes.	101
Figure 3.19 Proteomic characterisation of the apical secretome of the human bronchial epithelium in HBEC3-KT cells and HBECs models.	104
Figure 3.20 Relative abundance of proteins during the ALI differentiation of HBECs and HBEC3-KT cells.	106
Figure 3.21 Relative abundance of certain innate defence proteins during the ALI differentiation of HBECs and HBEC3-KT cells.	107
Figure 3.22 Venn diagram showing the percentage of individual proteins from HBEC3-KT cells and Calu-3 cells as well as common proteins.	108
Figure 3.23 Venn diagram showing the distribution of proteins unique to HBEC (A) and HBEC (B) and the common/combined candidates (HBEC (A) and HBEC (B)).	110
Figure 3.24 Phase contrast images of HBEC3-KT cells grown in KFSM and PALI media exhibit different phenotypes that also differ with DAPT and IL-13 treatment	118
Figure 4.1. Viable Counts of 4 hours <i>S. aureus</i> infections in different growth medium....	128
Figure 4.2. Viable Counts of <i>S. aureus</i> infections in uHBEC3-KT cells.	130
Figure 4.3. Infection uHBEC3-KT cells with <i>S. aureus</i> at MOI (1).	132
Figure 4.4. Infection uHBEC3-KT cells with <i>S. aureus</i> at MOI (0.1).	133
Figure 4.5. Infection uHBEC3-KT cells with <i>S. aureus</i> at MOI (0.01).	134
Figure 4.6. Comparison of mean fluorescence intensity of GFP in uHBEC3-KT cells infected with <i>S. aureus</i> at different MOIs.	136
Figure 4.7. RT-PCR of gene expression during the infection of uHBEC3-KT with <i>S. aureus</i>	138
Figure 4.8. Comparison of <i>CXCL10</i> and <i>IL6</i> in uHBEC3-KT cells infected with three different MOIs of <i>S. aureus</i>	140
Figure 4.9. Cytokine Array from uHBEC3-KT cells with <i>S. aureus</i> for 4 hours.	142
Figure 4.10. Comparison of immune mediators released by <i>S. aureus</i> -exposed for 4 hours uHBEC3-KT cells (MOI-1).	143
Figure 4.11. Viable Counts of <i>S. aureus</i> infections in uHBECs.	144
Figure 4.12. Infection uHBEC with <i>S. aureus</i> at MOI (1).	147
Figure 4.13. Infection uHBEC with <i>S. aureus</i> at MOI (0.1).	148
Figure 4.14. Infection uHBEC with <i>S. aureus</i> at MOI (0.01).	149
Figure 4.15. Comparison of mean fluorescence intensity in uHBEC exposed to <i>S. aureus</i> at three different MOIs.	151

Figure 4.16. Comparison of mean fluorescence intensity in uHBEC exposed to <i>S. aureus</i> at different MOIs.	153
Figure 4.17. Comparison of <i>CXCL10</i> and <i>IL6</i> in uHBEC infected with three doses for 4 hours of <i>S. aureus</i>	155
Figure 4.18. Comparison of <i>CXCL10</i> and <i>IL6</i> in uHBEC infected with three doses for 4 hours of <i>S. aureus</i>	157
Figure 4.19. Cytokine Array from uHBECs with <i>S. aureus</i> for 4 hours.	159
Figure 4.20. Comparison of immune mediators released by <i>S. aureus</i> -exposed for 4 hours uHBECs (MOI-1)	160
Figure 4.21. Comparison of immune mediators released by <i>S. aureus</i> -exposed for 4 hours uHBECs and uHBEC3-KT cells (MOI-1).	162
Figure 5.1. Viable counts of <i>S. aureus</i> infections in differentiated HBECs.	174
Figure 5.2. Immunofluorescence quantitation in differentiated HBEC infected with <i>S. aureus</i>	177
Figure 5.3. Comparison of expression of <i>CXCL10</i> and <i>IL6</i> after infection.	178
Figure 5.4. Comparison of <i>IL6</i> , <i>CXCL10</i> and <i>CXCL1</i> in differentiated HBECs infected with <i>S. aureus</i>	180
Figure 5.5. Cytokine secretion from HBECs infected with <i>S. aureus</i>	182
Figure 5.6. Densitometry analysis of cytokine array from HBECs infected with <i>S. aureus</i>	183
Figure 5.7. Cytokine secretion from uHBECs and HBECs infected with <i>S. aureus</i> as compared to mock cells.....	185
Figure 5.8. Viable counts of <i>S. aureus</i> infections in differentiated HBECs in the presence of IL-13.	187
Figure 5.9. Immunofluorescence microscopy of HBECs differentiated in the presence of IL-13 infected with <i>S. aureus</i>	190
Figure 5.10. Comparison of gene expression in early time points using <i>CXCL10</i> and <i>IL6</i>	191
Figure 5.11. Comparison of <i>CXCL10</i> , <i>CXCL1</i> and <i>IL6</i> in IL-13 treated differentiated HBECs infected with <i>S. aureus</i>	193
Figure 5.12. Cytokine array from IL-13 treated HBECs infected with <i>S. aureus</i>	195
Figure 5.13. Densitometry analysis performed on cytokine array from IL-13 treated HBECs infected with <i>S. aureus</i>	196
Figure 5.14. Comparison of viable counts of <i>S. aureus</i> during infections on differentiated HBECs in absence and presence of IL-13.....	198
Figure 5.15. Comparison of immune mediators released by HBECs in the absence and presence of IL-13 (MOI-1).....	199
Figure 5.16 Comparison of immune mediators released by <i>S. aureus</i> -exposed for 16 hours HBECs in the absence and presence of IL-13 (MOI-1)	200

List of tables

Table 1-1 Virulence factors implicated in adhesion to host cells and toxicity and various other enzymes..	26
Table 1-2 Virulence factors implicated in immune evasion at different levels.....	28
Table 2-1 List of Primary Cell Donors (Lot Nos.)	48
Table 2-2 PCR program for RT-PCR	52
Table 2-3. List of primers.	53
Table 2-4 TaqMan® gene expression assays used for qPCR experiments.	54
Table 2-5 Primary antibodies in immunostaining.	55
Table 2-6 Secondary antibodies in immunostaining.	56
Table 3-1 Proteins identified in the HBEC3-KT cells and HBECs secretomes at day 21 of ALI. Only the 50 most abundant proteins were considered.	102
Table 3-2 List of proteins identified in the HBEC3-KT cell and Calu-3 cell secretomes following ALI. Only the 50 most abundant proteins were considered.	109
Table 3-3 List of proteins identified in the HBEC (A) and HBEC (B) secretomes following ALI. Only the 50 most abundant proteins were considered.	111

CHAPTER 1: Introduction

1.1 Respiratory System

The fundamental process of breathing, which is also known as pulmonary ventilation, is performed by the lungs. More specifically, the exchange of gases occurs in the lungs through air sacs known as alveoli. These alveoli have a substantial capillary blood flow that allows for gaseous exchange to occur through the thin alveolar layer, which brings air into contact with the blood. All of the alveolar tissues are connected to the external surface via a number of airways (Hsia et al., 2016) that are collectively known as the respiratory tract. This tract starts in the nose, which comes into direct contact with external air. The nasal cavity is connected to the pharynx, a common route for both breathing and food ingestion. The larynx represents the next part of the respiratory tract, consisting of a cartilaginous tube-shaped air passageway (Ghorani-Azam et al., 2016). The larynx is also known as the voice box, as it allows for the production of sound due to the air passing through it producing different patterns of vibrations. The larynx opens into the trachea, which connects the voice box to the bronchi and consists of a long tube made up of C-shaped rings (Santacroce et al., 2020). The functions of the trachea are facilitated by mucus-producing cells that help to keep debris, dust particles and allergens out of the lungs. The bronchi are two large tubes that take air from the windpipe (i.e. the trachea) and forward it into the lungs. These main bronchi are further divided into smaller tubes known as bronchioles, which open into the alveoli, that is, the basic functional units of the lungs, where gaseous exchange occurs (Shukla et al., 2020).

As a whole, the respiratory system is a network of organs maintained by the lungs. It is divided into two main parts, namely the upper and lower tracts (Figure 1.1). The upper respiratory tract comprises the nasal cavities, which filter inhaled air to prevent any external particles or microorganisms from entering the lungs, as well as the pharynx and the larynx, which serve to conduct air into the lungs. The lower tract of the respiratory system consists of the trachea and the bronchi, which are lined with a mucociliated epithelium all the way to the bronchioles, in addition to the peripheral lung tissue that contains clusters of alveoli (Kumpitsch et al., 2019).

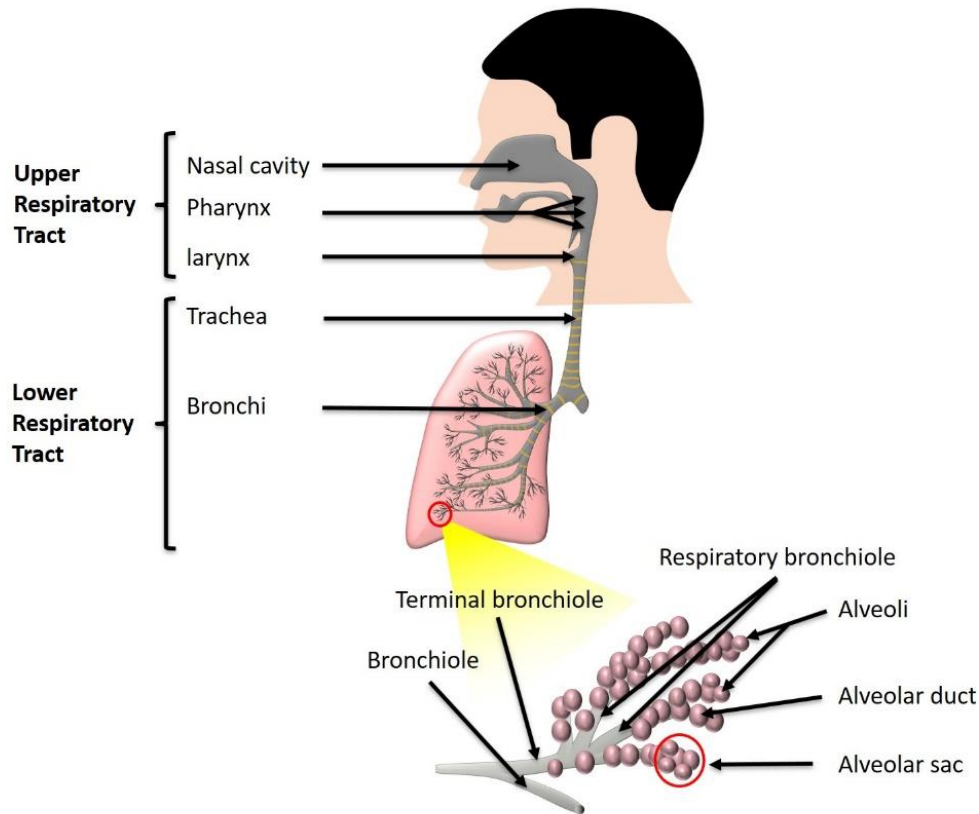


Figure 1.1: Schematic diagram of the respiratory tract.

An illustration of the upper respiratory tract, which comprises the pharynx, nasal cavity, laryngopharynx and oropharynx, and the lower respiratory tract, which comprises the trachea, bronchia and peripheral lung.

1.2 Airway Epithelium

The epithelium is tissue that covers both the internal and external surfaces of the body. More specifically, it covers the body in the form of skin and also lines internal surfaces of the body such as the digestive, reproductive and respiratory tracts (Alysandratos et al., 2021). The epithelium serves a wide variety of functions depending on its location, including sensory reception, diffusion, filtration, excretion, absorption, secretion and protection (Arnellos and Keijzer, 2019). As the lungs are constantly exposed to inhaled pathogens, including viruses and bacteria, the airway epithelium plays a critical role in maintaining the normal function of the alveoli and trachea (Whitsett and Alenghat, 2015). Indeed, it not only functions as a physical barrier, but also triggers various innate and adaptive immune responses through its mucociliary apparatus (Ganjian et al., 2020). The majority of the human respiratory tract, including the nasal cavity, trachea and bronchi, is lined by a complex pseudostratified

epithelium composed of multiple cell types. The other types of epithelia found in the respiratory tract include cuboidal epithelia that line the surfaces of the bronchioles and the simple squamous epithelium that lines the alveoli in order to facilitate the exchange of gases (Basil et al., 2020).

The airway epithelium is a dynamic type of tissue that undergoes gradual but constant renewal (Maurizi et al., 2021). The nasal, bronchial and tracheal epithelia are composed of multiple cell types, including secretory cells (goblet and club), basal cells, ciliated cells and rare cells such as neuroendocrine cells, ionocytes and tuft/brush cells (Zaragosi et al., 2020) (Figure 1.2). Moreover, Type I and Type II cells are found in the alveolar epithelium (Whitsett and Alenghat, 2015, Whitsett, 2018). The airway epithelium is pseudostratified, with single cells of differing heights all resting alongside each other on the basement membrane.

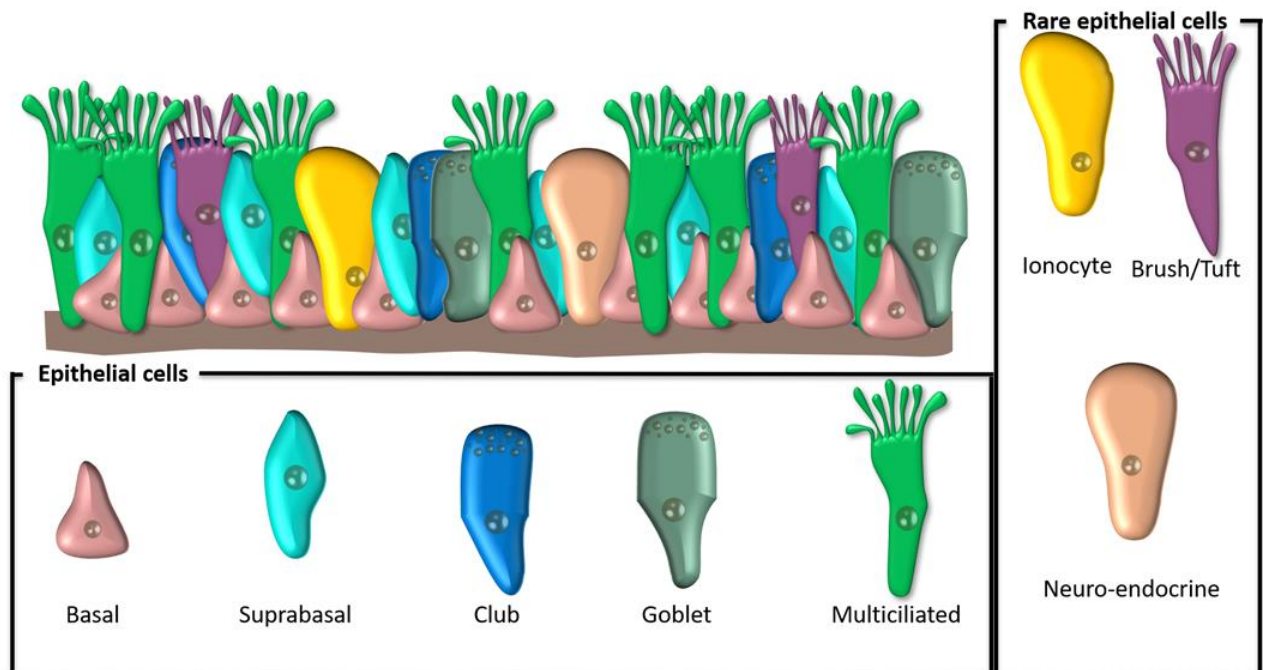


Figure 1.2: Cellular components of airway epithelium.

The airway epithelium comprises pseudostratified epithelial cells, including ciliated cells and a smaller number of club cells, goblet cells, tuft cells (brush cells) and neuroendocrine cells that are layered on top of basal cells. The image has been modified from Zaragosi et al. (2020).

1.2.1 Basal cells

Conducting airways rely on basal cells to serve as essential progenitor cells (Rock et al., 2009, Rock et al., 2010, Cole et al., 2010). Basal cells represent the primary airway stem cells, and they exhibit both self-renewal ability and the capacity to develop into club cells, goblet cells, tuft cells, neuroendocrine cells, pulmonary ionocytes and multiciliated cells (as shown in Figure 1.3) (Davis and Wypych, 2021). In mice, the smaller airways are known to lack basal cells, although such cells are abundant in the trachea and major bronchi (Hogan et al., 2014). By contrast, in human airways, basal cells are present throughout the entire airway, although smaller airways below 0.5 mm in diameter have a two-fold lower basal cell density (Zaragosi et al., 2020). Basal cells represent a heterogeneous population of cells that includes true epithelial stem cells. However, such cells differ in terms of the expression levels of the cytokeratins 8 and 14 (Rock et al., 2010). The role of the basal cells is not limited to tissue repair, as they also play a role in the immunological memory of exposure to certain pathogens. A number of studies have used the TP63 transcription factor, keratins 5 and 14 (KRT5 and KRT14), podoplanin (PDPN), nerve growth factor receptor (NGFR) and galectin 1 (LGALS1) as basal cell markers (Rock et al., 2009, Kotton and Morrisey, 2014).

In a recent comprehensive study of basal cells, the coupling of cell lineage algorithms with single-cell RNA sequencing (RNAseq) revealed the heterogeneous natures of the populations of basal cells found in humans and mice (Zaragosi et al., 2020). The results also showed the presence of ‘hybrid’ mucous-multiciliated cells and progenitors of rare cells in the human model cells. In terms of the mouse trachea experiment, three populations were identified following the genetic differentiation of the basal cells: club cells, goblet cells and multiciliated cells (Zaragosi et al., 2020).

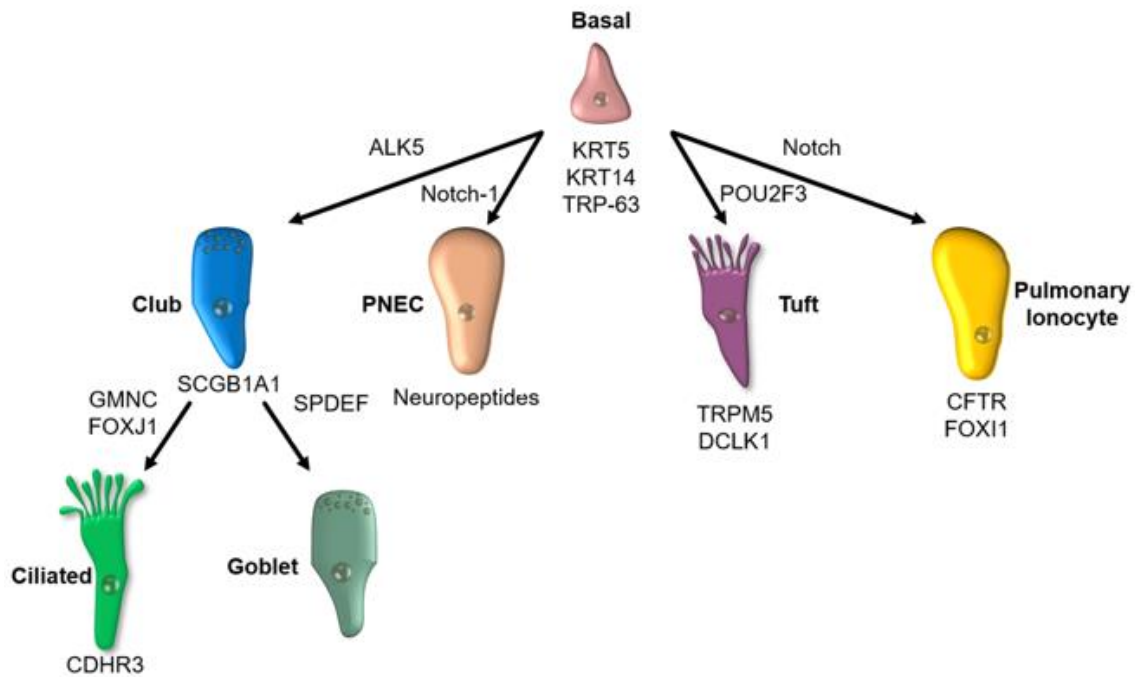


Figure 1.3: Relationships between cells that generate the pseudostratified airway epithelium of the lung.

The main airway stem cells, that is, the basal cells, differentiate into most other epithelial cell types. The expression of specific genes can be used to distinguish these different cell types. The image has been modified from Davis and Wypych (2021).

1.2.2 Club cells

The bronchiolar and tracheal epithelia both contain club cells. These cells were once known as Clara cells, although that term has now become obsolete (Boers et al., 1998). Club cells act as progenitors for the ciliated and goblet cells found in the smaller airways (Dean and Snelgrove, 2018). Single-cell RNAseq has been used to identify new significant hallmarks in the field of cell lineage analysis. Cell differentiation experiments have shown that in the trachea, club cells first mature into goblet cells and then differentiate into multiciliated cells (Zaragosi et al., 2020). When used in combination with a cell lineage analysis, single-cell RNAseq has been applied to reveal the differentiation among pathological and normal cells. Club cells are found in the luminal epithelium and exhibit a columnar shape. They play a role in xenobiotic metabolism and contain secretory granules that include anti-microbial and anti-inflammatory peptides (Malvin et al., 2019). The anti-inflammatory secretoglobin, SCGB1A1 is the most commonly investigated marker of club cells. Indeed, the fate of club cells has previously been traced using SCGB1A1, which revealed that they differentiate into multiciliated cells that can

be identified by the expression of the transcription factor Forkhead box protein J1 (FOXJ1)(Rawlins et al., 2009, Schilders et al., 2016, Ruiz García et al., 2019) and goblet cells that can be identified by the expression of mucin MUC5AC (Kotton and Morrisey, 2014, Liu et al., 2019).

1.2.3 Goblet cells

The differentiation of basal cells and club cells gives rise to goblet cells (Davis and Wypych, 2021). These goblet cells can be identified by their globular shape, and they are considered to be the primary mucus-producing cells within the airways. Goblet cells and submucosal glands secrete mucins such as MUC5B and MUC5AC (Kotton and Morrisey, 2014) onto the surfaces of the airways (Yang and Yu, 2021). Along with ciliated cells, they enhance the process of mucociliary clearance. Different metabolites, electrolytes, fluids, mucins and anti-microbial products contribute to the formation of mucus (Whitsett, 2018). In addition, goblet cells respond to environmental stimuli by expressing both cytokines and chemokines, which recruit and educate innate immune cells such as innate lymphoid cells (ILC2), dendritic cells and eosinophils, all of which play a role in the Th2 immune responses seen in individuals with asthma (Chen et al., 2009, Lambrecht et al., 2019). Increasing the level of ligand binding with the receptors of Notch signalling induces the basal cells and other secretory cells to differentiate into goblet cells (Shaykhiev, 2019). As shown in Figure 1.3, the transcriptional pathway involved in the formation of goblet cells from club cells is regulated by the sterile alpha motif (SAM) pointed domain-containing ETF transcription factor (SPDEF) (Davis and Wypych, 2021). High levels of SPDEF lead to goblet cell hyperplasia, while its absence inhibits the formation of goblet cells in the laryngeal submucosal glands and trachea (Yang and Yu, 2021).

1.2.4 Ciliated cells

Similar to other respiratory tract cells, ciliated cells are located above the basal cells (Yaghi and Dolovich, 2016). The percentage of ciliated cells normally increases with airway branching, rising from approximately 50% in the trachea to around 70% in the small airways (Yaghi and Dolovich, 2016). There are two transcriptionally distinct subsets of columnar ciliated cells located across the proximal-distal axis (Travaglini et al., 2020), and they are also present throughout the airways. These columnar ciliated cells trap and expel microorganisms and debris using the rhythmic beating of the hair-like cilia in a process known as mucociliary clearance (Tilley et al., 2015, Håheim, 2020). Both goblet cells and club cells can serve as the progenitors of ciliated cells (Ruiz Garcia et al., 2019). More specifically, a complex

transcriptional network involving Notch signalling, geminin coiled-coil domain-containing protein 1 and the activation of MYB protooncogene control regulates the differentiation of club cells and goblet cells into ciliated cells (Whitsett, 2018).

In addition, the transcription factor FOXJ1 plays an important role in the formation of cilia (Yu et al., 2008, Koay et al., 2021). Cilia are microtubule-based cell organelles that extend from a basal body to a centriole located at the apical surface of the cells. They contain either 9 + 0 or 9 + 2 axonemes surrounded by a specialised ciliary membrane (Figure 1.4). The 9 + 0 pattern is found in non-motile primary cilia. The 0 represents the missing central pair of single microtubules, while the 9 + 2 pattern has 9 doublet microtubules that surround a central pair of microtubules (Satir, 2005, Loreng and Smith, 2017). The 9 + 0 cilia also lack axonemal dyneins, that are the molecular motors critical for ciliary movement, whereas the 9 + 2 cilia are motile. 200–300 motile cilia found on the surface of ciliated cells in the airways (Kuek and Lee, 2020).

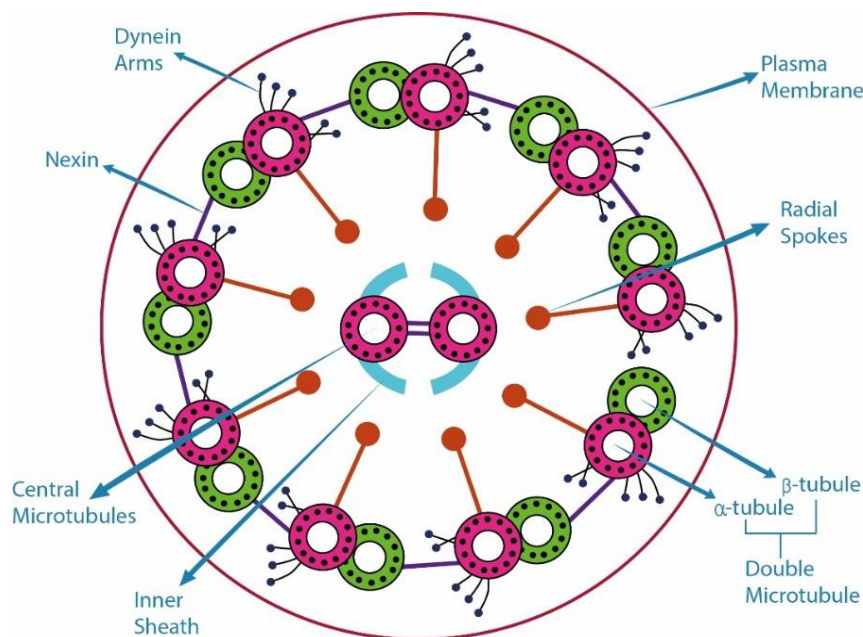


Figure 1.4: Structure of a motile cilium.

The axoneme of the cilia is composed of two tubules that are positioned centrally. They are surrounded by nine doublet microtubules comprising alpha (α)- and beta (β)-tubules. Motile cilia beat with a wave like motion, which is driven by the radial spoke, inner and outer dynein arms and nexin links. The image has been modified from Sleight (2016).

1.2.4 Rare cells

As well as the more abundant cells, there are three types of rare cells present in the airway epithelium: neuroendocrine cells, tuft cells and ionocytes.

1.2.4.1 Pulmonary neuroendocrine cells

First identified in the 1950s (Feyrter, 1954), pulmonary neuroendocrine cells (PNECs) play an important role in the interaction between the immune and neurological systems. There remain many unanswered questions regarding the ontogeny of PNECs and their relationships with other types of lung cells during homeostasis and lung injury. PNECs are present in the airway from the windpipe to the bronchioles as either isolated single cells or small bunches of cells referred to as neuroepithelial bodies (NEBs) (Noguchi et al., 2020). Moreover, they are present in the intrapulmonary airways, most commonly at airway bifurcations or bronchioalveolar duct junctions (Mou et al., 2021). The progressive cell-type specification in the lungs starts with progenitors of a neuroendocrine nature (Noguchi et al., 2020). Airway development and hypoxia-sensitive chemoreceptor development are highly dependent on PNECs (Van Lommel, 2001, Zaragosi et al., 2020). They perform vital functions in this regard through the formation of corpuscle-neuroepithelial bodies and their membrane receptors. These receptors sense changes in oxygen concentration, immune cells response and regulate the blood flow during pulmonary disease progression (Hewitt and Lloyd, 2021). Furthermore, they have the ability to act as neuroendocrine and secrete bioactive substances such as serotonin (Van Lommel, 2001, Zaragosi et al., 2020). In addition, studies involving naphthalene-induced lung injury have shown that PNECs are linked to tuft cells in a similar way to which they are linked to both club cells and basal cells (Song et al., 2012, Ouadah et al., 2019). Epithelial injury can cause some PNECs to adopt differing cell fates, thereby behaving as stem cells (Alysandratos et al., 2021).

1.2.4.2 Tuft (brush) cells

Tuft cells, which are also known as brush cells or solitary chemosensory cells, are present in many epithelia (Schneider et al., 2019). Their name is derived from their microvillar appendages, which extend into the lumen (Sell et al., 2021). Tuft cells play an important role in immune function, as they are involved in the initiation of the Th2 response against parasites (Davis and Wypych, 2021). Moreover, tuft cells replace the missing tracheal ciliated cells in the airway epithelium in patients with immotile cilia (Ting and von Moltke, 2019). A recent study comprehensively investigated the transcriptional factors that play a role in the innate type

2 immunity related to airway tuft cells (Ualiyeva et al., 2020). The findings of this study suggested that tuft cells can sense local damage and provide an immune function. Tuft cells generate a high level of cysteinyl leukotriene (CysLT) and P2Y2, a purinergic receptor. Thus, the automatic train protection (ATP) signalling that occurs during epithelial stress generates CysLT mediated by P2Y2 activation (Ualiyeva et al., 2020). The respiratory reflexes that provide protection in the case of bacterial infection originate in tuft cells. A murine tuft cell analysis performed by means of single-cell RNAseq revealed the high expression of *Trpm5*, *Gnat3* and *Tas2r18* genes, which are involved in bitter taste signalling and other sensory functions. In addition, the gene-encoding; the cholinergic receptor is also highly expressed by tuft cells (Hollenhorst et al., 2020).

1.2.4.3 Pulmonary ionocytes

Pulmonary ionocytes are generated from basal cell progenitors and were recently identified in the airways (Montoro et al., 2018, Davis and Wypych, 2021). A genetic profiling analysis has recently suggested their involvement in the development of cystic fibrosis (CF) as pulmonary ionocytes represent the main source of the transcripts of the cystic fibrosis transmembrane conductance regulator (CFTR) ion channel in both mice (*Cftr*) and humans (Scudieri et al., 2020). When compared with other airway epithelial cells, pulmonary ionocytes express CFTR to a greater extent (Shah et al., 2022). According to scRNA-seq data, only 0.42% of mouse airway cells are ionocytes (Montoro et al., 2018), whereas the corresponding proportion in humans is 0.5%–1.5%. These cells also express a number of other markers including *FOXII* and *ASCL3* (Okuda et al., 2021). Moreover, the level of ionocyte-specific gene expression in human airway epithelial cultures is enhanced by FOXI1 transcriptional activation (Plasschaert et al., 2018).

1.2.5 Alveolar epithelial cells

In addition to protecting the lungs against damage by hazards such as pathogens, the alveolar epithelium is important in relation to gaseous exchange. If the lungs are injured, the alveolar epithelium is able to regenerate and repair itself quickly so as to restore the epithelial barrier (Wang et al., 2018c). There are two main types of alveolar epithelial cells, namely Type I cells and Type II cells, as shown in Figure 1.5. Type I cells (AT1) cover approximately 90% of the total surface of the alveoli (Guillot et al., 2013, Whitsett and Alenghat, 2015). The most important role of AT1 cells involves facilitating gas exchange between the blood and alveolar lumen. The very thin structure of AT1 cells means that they well adapted for the transfer of gas

from the blood capillaries to the lumen of the alveoli. Type II cells (AT2) secrete surfactant proteins and lipids that serve to lower the surface tension in the alveolar sacs and, therefore, prevent alveolar collapse during the ventilatory cycle (Barkauskas et al., 2013). Furthermore, AT2 cells can act as alveolar stem cells, which can differentiate into AT1 cells following injury so that the gaseous exchange capacity of the epithelium is quickly restored (Barkauskas et al., 2013, Wu and Tang, 2021). Both types of cells are differentiated from alveolar progenitor cells during the late embryonic stage to form distal epithelial saccules (Nikolić et al., 2017). The alveoli, which form the basic unit of the gaseous exchange surface, are formed from epithelial saccules after birth through a process known as alveologensis. During this process, AT1 cells become flattened to increase their surface area (Yang et al., 2016). These cells have traditionally been considered to be terminally differentiated as they lose the capacity to divide. However, it has previously been shown that they do demonstrate some degree of cellular plasticity and can proliferate and differentiate into AT2 cells (Jain et al., 2015).

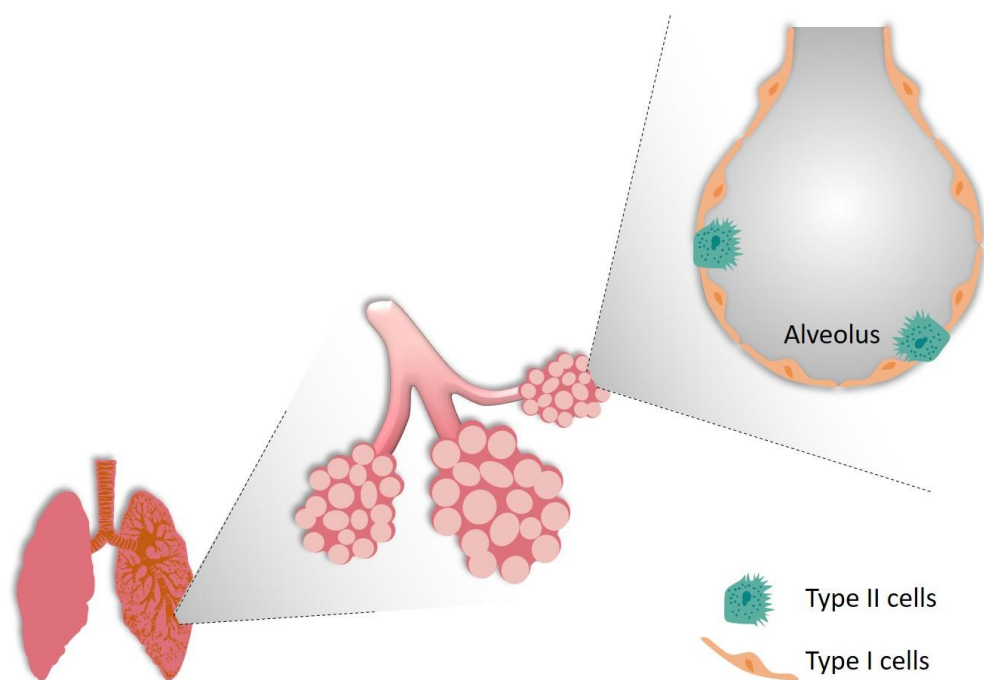


Figure 1.5: Overview of the alveolar unit.

Type I cells make up most of the alveolar surface due to their long and thin cytoplasmic processes, whereas the cuboidal type II cells, which are more numerous, lower the surface tension and contribute to the alveolar host defence mechanism by interacting with immune cells.

1.3 Respiratory Immunity

1.3.1 Crucial defensive functions of the immune system

The human immune system can be divided into four layers, namely the physical and chemical barrier, intrinsic immunity, innate immunity and adaptive immunity layers. To establish an infection, an invading pathogen must overcome all of these barriers (Abdulmannan et al., 2018). The first line of defence against any invading pathogen is the combination of the physical and chemical barriers that exist in the airways in the form of the hairs present in the nasal cavity and the cilia and mucus of the respiratory tract (Günther and Seyfert, 2018). Innate and adaptive immunity are the most studied aspects of immunity (Marshall et al., 2018). Innate immunity is based on responses which are activated immediately after infection (Kubelkova and Macela, 2019). The cells involved in innate immunity include the epithelial cells, neutrophils, basophils, eosinophils, macrophages, natural killer (NK) cells, mast cells and dendritic cells (Domínguez-Andrés et al., 2019). The main limitation of the innate immune response is its lack of pathogen specificity (Simon et al., 2015). Furthermore, it cannot produce a memory response, which means that future exposure requires the response to be activated again from the initial stages (Iwasaki and Medzhitov, 2015, Italiani and Boraschi, 2017). By contrast, adaptive immunity is based on memory cells, that is, B and T cells (Riera Romo et al., 2016). These cells are activated by the production of certain cytokines and chemokines by the innate immune system; therefore, the main limitation of adaptive immunity is the slow response. However, this type of immune response is more specific because B and T cells produce antibodies that are active against specific pathogens (Annunziato et al., 2015). Additionally, adaptive immunity has a memory function, which means that following subsequent exposure to the pathogen, the memory cells against the specific pathogen are activated more quickly (Carsetti et al., 2020). Intrinsic immunity is a more recently identified immune response, which specifically protects against viral infections (Yan and Chen, 2012). Intrinsic immunity consists of cell cycle restriction factors that directly block the replication and assembly of viral particles. These proteins are constantly synthesised, meaning that they can act against viruses more effectively than the innate and adaptive immune responses (Schilling et al., 2021).

Among the most important components of innate immunity are phagocytes (macrophages and neutrophils). They fulfil their role by phagocytosing any pathogens that are able to breach the physical and chemical barriers of the immune system (Kaur and Secord, 2019). This leads to the activation of mechanisms for the destruction of invading particles, such as phagocytosis,

endocytosis and inflammation (Yates et al., 2018). However, these cells may not recognise some invading pathogens. Other components of the innate immune system play different roles, including the activation of inflammation, opsonisation, clearance of immune complexes and lysis of pathogens (Kumar et al., 2021). A series of innate immune receptors work to achieve the identification of microorganisms by recognising the specific expression patterns of those organisms (Brubaker et al., 2015, Nie et al., 2018). The recognition of pathogen-associated molecular patterns (PAMPs) initiates the interaction between the host and the pathogen. Host-pathogen interactions have also been reported following the recognition of endogenous danger signals, for example, interleukin-1 (IL-1) (Janeway Jr and Medzhitov, 2002, Murphy and Weaver, 2016). Moreover, the pattern recognition receptors (PRRs) work towards the detection of molecules that result from tissue damage in the body, known as damage-associated molecular patterns (DAMPs) (Dib et al., 2020). This recognition results in the promotion of the inflammatory response (Iwasaki and Medzhitov, 2015).

The innate immune response is triggered in immune cells through the recognition of PAMPs by PRRs (Bauer et al., 2018). This recognition is followed by the swift induction of a complex series of signalling pathways, thereby resulting in the induction of the inflammatory responses regulated by chemokines and cytokines, which facilitates the elimination of pathogens (Yates et al., 2018). The best-studied examples of PRRs are the Toll-like receptors (TLRs), such as TLR1/2 and TLR4, located on the cell surface (Lumb, 2016).

The cells associated with adaptive immunity, which are also known as lymphocytes, destroy any pathogens that escape from the innate defence response through different mechanisms (Levinson, 2014, Rao et al., 2020). Moreover, the memory provided by the adaptive immune response leads to enhanced protection against certain pathogens in the future. T cells or T lymphocytes are activated by antigen-presenting cells such as dendritic cells and macrophages (Hilligan and Ronchese, 2020). Furthermore, B cells are activated in response to the cytokines and chemokines released by T cells and then start to produce antibodies that are specific against the relevant pathogen (Lam et al., 2020), specificity is achieved through genetic rearrangements of the gene-encoding antibodies following activation by T cells (Waldman et al., 2020). The memory provided by the adaptive immune system ensures that this type of specific immune response is activated quickly if the host encounters the same infection again in the future (Jones et al., 2021).

1.3.2 Barrier function of the airway epithelium

1.3.2.1 Physical barrier function

Physical barriers play a vital role in preventing microbes from reaching tissues that are vulnerable to infection. A major function of the airway epithelial tissue involves serving as a physical barrier against foreign substances. Motile cilia, which represent the key component of the mucociliary clearance (MCC) process, move mucus in order to entrap particles and pathogens and, therefore, keep them out of the lungs (Nawroth et al., 2020). Thus, the MCC process controls the movement of the mucus present on the inside of the respiratory tract and also regulates the osmolarity, viscoelasticity and resultant quality of that mucus (Button et al., 2013). Typically, the mucus and cilia layers are considered to form separate components of the MCC process (the 'sol' and 'gel' layers) (Bustamante-Marin and Ostrowski, 2017). Mucus is composed of globular proteins, mucins, salts, water, lipids, DNA, cells and cellular debris (Button et al., 2012). The elastic mucus layer covers the cilia (Lafforgue et al., 2017), which are bathed in the pericellular lining fluid (or sol). Consequently, the airway surface controls the cilia and mucus homeostasis in a manner known as the 'gel-on-brush' model, which promotes both cilia motility and MCC (Button et al., 2012). Mucins can exist in the form of either membrane-bound (tethered mucins) or soluble (secreted) mucins. The membrane-bound mucins consist of large glycoproteins that remain bound to the surface of cells. Prominent examples of such mucins include MUC1, MUC4 and MUC16 (Govindarajan and Gipson, 2010, Bonser and Erle, 2017). By contrast, soluble secreted gel-forming mucins such as MUC5AC and MUC5B are synthesised intracellularly and then secreted by means of vesicular transport. They consist of protein components along with complex oligosaccharides that can influence the hydration of cellular surfaces due to their structures and the charge present on the surface of molecules. The function of these mucins is to prevent pathogens from reaching cellular surfaces, and they achieve this by performing MCC (Delaveris et al., 2020).

In cases of CF, primary ciliary dyskinesia (PCD), chronic obstructive pulmonary disease (COPD) and asthma, the abnormal thickening of the mucus reduces ciliary motility and dysregulates the production of MUC5AC and MUC5B (Johnson, 2011, Bonser and Erle, 2017). The mucociliary function of the airway epithelial tissue is directly dependent on the wave-like motion of the cilia (Seibold et al., 2020). In addition, the system protects the smaller (lower) airways against infection by foreign particles such as viruses and microorganisms through the action of MUC5AC and MUC5B (Ostedgaard et al., 2017, Seibold, 2018). Both proteins form

an integral part of mucus layer, which protects the epithelial surface of the air passageways. More specifically, Amini et al. (2019) reported the secretion of these two types of mucins in nasal respiratory epithelium. They found that both the MUC5AC and MUC5B to be expressed at the cell surface of goblet cell present in the respiratory epithelium. However, the cells in olfactory epithelium do not secrete MUC5AC, rather the Bowman's gland present under the olfactory epithelium secrete only MUC5B. MUC5B deficiency results in the depletion of this gland (Amini et al., 2019).

The physical barrier of the epithelial layer is maintained by the functioning of tight and adherens junctions. Tight junctions are intercellular adhesion complexes that control the movement of ions and solutes across the epithelium, while adherens junctions both mediate cell-to-cell adhesion and promote the formation of tight junctions (Zihni et al., 2016, Claesson-Welsh et al., 2021). The tight junctions have an important role in preventing the free passage of ions between epithelial cells so loss of function of tight junctions has a critical role in human diseases such as inflammatory bowel disease (Lee et al., 2018b). Tight junctions maintain the permeability of the airway epithelium at an optimum level. Increase in the permeability due to degradation of the junctions, causes hyperreactivity and exacerbation of asthma. Besides this erosion of epithelial barrier is also associated with respiratory distress syndrome (Zhou et al., 2021).

1.3.2.2 Chemical barrier function

The cells of the airway epithelium secrete a range of proteins that constitute a chemical barrier on the airway surface. These host defence peptides (HDPs) are important in relation to host cell immune responses. They consist of a wide range of short cationic and amphipathic peptides that are synthesised and released by a broad spectrum of cells. These peptides are generally shorter than 50 amino acids in length and have a positive charge ranging from +2 to +9 at the physiological pH (Mookherjee et al., 2020). These peptides can be divided into four groups based on their structures: extended flexible loop peptides, cyclic peptides, peptides based on β -sheets with disulphide bonds, and peptides based on α -helices (Hancock et al., 2016). As previously mentioned, chemical barriers destroy pathogens on the airway surface. Mucus and airway secretions contain multiple proteins derived from epithelial and non-epithelial cells that are capable of killing pathogens (Krismer et al., 2014, Sharma et al., 2020). Prominent examples include, Cathelicidin (LL37), Motif chemokine ligand 20 (CCL20), lysozyme, defensins and lactoferrin (Tavares et al., 2020, Wang et al., 2022).

HDPs play important roles in both infectious diseases (e.g. infected diabetic ulcers, burn wounds, dermatitis, fungal nail infections, renal infections, hematopoietic stem cell transplantation-related infections) and chronic inflammatory diseases (e.g. arthritis, asthma, colitis) (Van der Does et al., 2018). In fact, dysregulation of HDPs is associated with infectious and inflammatory pathology (Prasad et al., 2019). For example, a decrease in the defensins level in a burn injury will facilitate both infection and sepsis (Berkestedt et al., 2010, Chen et al., 2022). Furthermore, HDPs are currently being investigated in relation to the development of novel anti-microbial and immunoregulatory drugs (Steinstraesser et al., 2011, Mookherjee et al., 2020).

Broadly speaking, there are three main groups of HDPs. The first group comprises proteins that can destroy microbes, such as the lysozyme enzyme found in the secretions of the airway epithelium. This exerts an anti-microbial effect against Gram-positive bacteria such as *Staphylococcus aureus* (*S. aureus*) by degrading their peptidoglycan (PGN) layer (Cheung et al., 2021). The second group comprises peptides that use a metallic element as a cofactor, including lactoferrin, which is an iron-restricting protein found in the serum and mucosal secretions. Lactoferrin and lysozyme together demonstrate synergistic activity against Gram-negative and Gram-positive bacteria (Tavares et al., 2020). The third group comprises peptides that can infiltrate biofilms, such as defensins and cathelicidins (Ohlsen et al., 2008).

HDPs can be either constitutively expressed or induced by specific stressors (Moretta et al., 2021). For example, α -defensins are generally expressed constitutively, whereas most β -defensins are inducible (Van Cleemput et al., 2020). α -defensins are primarily localised within phagosomes in inflammatory cells, whereas β -defensins are primarily secreted by tissue cells (Yeasmin et al., 2021). Lipopolysaccharide (LPS) and the pro-inflammatory cytokines IL-1 β and TNF- α increase the level of HDP expression (Xu and Lu, 2020). The anti-microbial and cytotoxic characteristics of defensins and HDPs are associated with their ability to induce pore formation within the pathogen's membrane (Solanki et al., 2021). Biologically, HDPs influence the adaptive and innate immunity against infection of inflammatory responses and the effective determination of infections (Hemshkhar et al., 2016). In addition to the direct anti-microbial action of HDPs and their function in relation to the immune modulatory response, they also play a role in wound healing and angiogenesis and also possess anti-cancer activities (Yeasmin et al., 2021).

1.3.3 Immune Cells

Aside from the epithelial cells found within the lungs that I have described above, there are a number of immune cells that play key roles in the host defence function of the respiratory tract.

1.3.3.1 Neutrophils

Neutrophils are leukocytes that are involved in the immune response (Stray-Pedersen et al., 2017, Kalafati et al., 2022), with neutrophil activation and recruitment being amongst the first responses to infection. Neutrophils represent the most abundant granulocytes, and they contain secretory granules containing various HDPs (Levinson, 2014, Mohamed and Alawna, 2020).

Neutrophils are short-lived and fast-moving, and they account for approximately 70% of all the leukocytes in circulation (Rosales, 2018). The principal role of neutrophils involves engulfing and degrading bacteria in order to either control commensal populations or prevent infection. This is achieved through the generation of reactive oxygen species (ROS) in a process known as a metabolic burst (Spaan et al., 2015). In the case of a respiratory metabolic burst, nicotinamide adenine dinucleotide phosphate (NADPH) oxidase produces ROS, including superoxide (Brubaker et al., 2015). The superoxide then decays to form hypochlorous acid that kills bacteria. The granules of neutrophils and the materials inside them can be discharged extracellularly. Lactoferrin, cathelicidins, defensins, LL-37 and lysozymes are among the HDPs discharged by neutrophils (Kanashiro et al., 2020). These cells can release and form neutrophil extracellular traps (NETs)—molecular traps made up of anti-microbial proteins, decondensed chromatin, some proteases and histone proteins (Sollberger et al., 2018).

The recruitment of neutrophils from the circulation begins with endothelial activation and neutrophil rolling. During the activation process, the neutrophils stop rolling and adhere firmly to the endothelium (Brubaker et al., 2015). They then transmigrate through the endothelium to the underlying tissue. This process is known as extravasation. Within the underlying tissue, the neutrophils are directed by a chemotactic gradient that steers them towards the invading bacterium (Spaan et al., 2015). This is followed by phagocytosis, which depends on the deposition of immunoglobulins within the tissues and complements their recognition by complement receptors (CRs) and Fc γ receptors (Fc γ Rs) (Brubaker et al., 2015). Within the neutrophil phagosome, antimicrobial peptides (AMPs) are released following the fusion of granules with the phagosome, while the NADPH oxidase-derived ROS then kill bacteria (Ulfig and Leichert, 2021) (Figure 1.6).

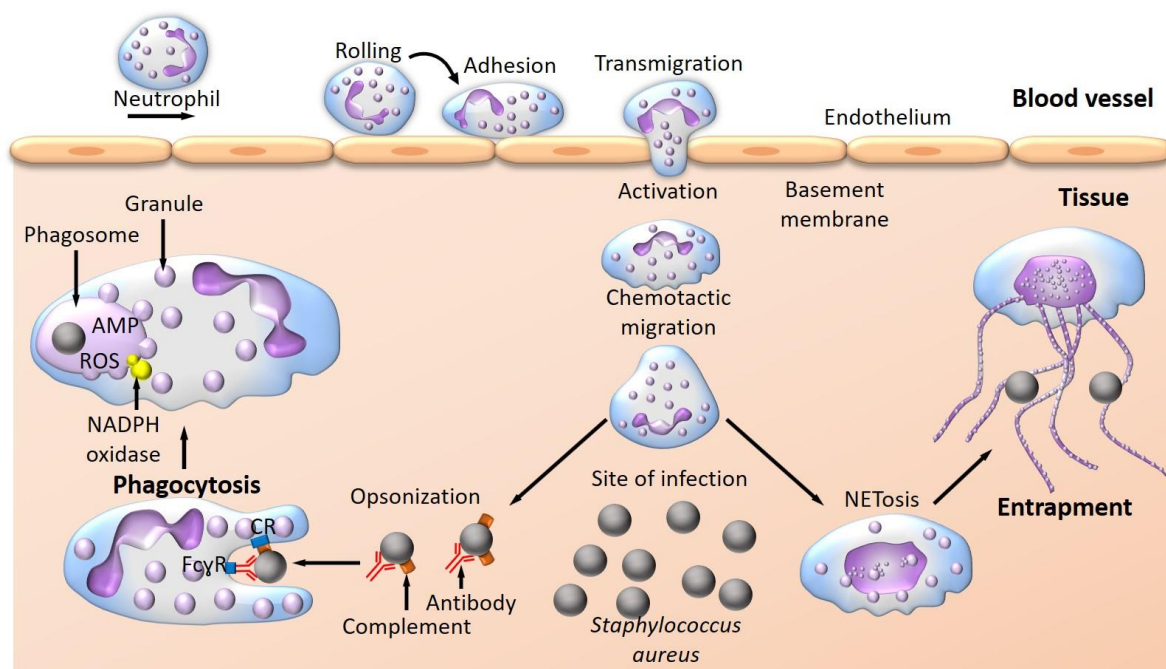


Figure 1.6: Extravasation of a neutrophil to an infection site and the associated anti-microbial mechanisms.

The activated endothelium recruits neutrophils that roll on it. Upon stimulus, the neutrophils firmly adhere to the endothelium. Following host tissue invasion by a pathogen, neutrophils undergo extravasation, chemotactic migration, opsonization, phagocytosis and ultimately cause pathogen lysis. Image has been modified from Spaan et al. (2013).

1.3.3.2 Macrophages

Macrophages are ‘professional’ phagocytic cells derived from monocytes. They have a longer lifespan than neutrophils (Murphy and Weaver, 2016) and are relatively resistant to apoptotic stimuli (Gordon and Plüddemann, 2018). Macrophages are found in low numbers within a variety of host tissues, although a range of signals have the ability to increase the number of macrophages (Randolph, 2011, Arora et al., 2018). Macrophages are fundamental facilitators of the innate immune responses to various infections, and they are considered to represent the frontline of defence against infection because they are the resident tissue phagocytes (Brubaker et al., 2015).

Macrophages perform a variety of roles, such as killing pathogens, coordinating inflammatory responses through the release of mediators and clearing apoptotic cells (Levinson, 2014, Pidwill et al., 2021). After ingestion, pathogens are trapped in a phagosome, which then fuses with a lysosome to form a phagolysosome. Phagolysosomes contain multiple toxic agents and

enzymes capable of killing ingested bacteria. Phagolysosomes also interface with the adaptive immune system through presenting peptides to T-helper cells (Zhai et al., 2019). Moreover, they participate in the detection of and response to infection, and they generate signals that lead to the recruitment of inflammatory cells, including neutrophils (Nguyen et al., 2012).

The tissue-resident macrophages of the lungs are the alveolar macrophages (AMs), which are restricted to the airspaces inside the alveoli and situated to react to pathogens in the lower airways (Neupane et al., 2020). The AMs represent the frontline defence mechanism by which the lung defends itself against bacteria (Spaan et al., 2015, Heukels et al., 2019). The interaction between bacteria and AMs results in a complex response involving the opsonisation of bacteria, the migration of macrophages and monocytes towards the infection site, the attachment of bacteria to the macrophage phagocytic receptors, bacterial internalisation and, finally, the killing of intracellular bacteria (Flannagan et al., 2016).

1.3.3.3 Natural killer cells

The lungs are routinely challenged by various potentially injurious factors, such as pathogens (e.g. bacteria, viruses, fungi), tumours and other environmental insults. For this reason, a huge number of immune cells occupy the respiratory system. Recent studies have identified natural killer (NK) cells as a diverse population comprising various subpopulations with distinct qualities (Cong and Wei, 2019). NKT cells are considered the primary member of the CD1d-restricted T cell family. CD1d-restricted T cells can be further divided into three classes, which are usually known as type I NKT (or invariant), type II NKT (or variant) and a third class that function according to their antigen specificity and T cell receptor (TCR) use. The identification of the specific markers of NK cells on a T cell subset led to the initial discovery of NKT cells (Trottein and Paget, 2018). During infection, NKT cells are quickly stimulated to activate their regulatory and effector functions. Indeed, NKT cells have the potential to respond to a diverse set of pathogens and stressors, including bacteria, viruses, fungi, inflammation, dust, pollens and helminthic parasites (Paget and Trottein, 2013). During lung infection by *S. aureus*, the invariant NKT (iNKT) cells detect staphylococcal enterotoxin B (SEB), a potent toxin, through the major histocompatibility complex class 1 (MHC-I). As a result, the iNKT cells secrete a plethora of cytokines, including interleukin-12 (IL-12), type I interferons (IFNs) and IL-8 (Rieder et al., 2011). These cytokines further activate the NKT cells through the indirect activation pathway. Once all of the required T cells have been activated, they release more

cytokines and, consequently, control the lung infection and associated tissue damage (Rieder et al., 2011).

1.3.3.4 Dendritic cells

The innate immune system defends against various microbial infections by detecting foreign antigens and killing the associated microorganisms. Dendritic cells (DCs) are the main innate immune cells that perform this function through the expression of specific receptors. These receptors detect foreign antigens based on the pathogen-related molecular patterns. The triggering of DCs leads to the stimulation of antigen-specific adaptive immune responses, thereby activating both the innate and adaptive immune systems (Bieber and Autenrieth, 2020). DCs are present beneath the epithelial layer of the lung tissues. Due to their high environmental sensitivity and expression of diverse PRRs, such as TLRs, NOD-like receptors (NLRs) and C-type lectin receptors (CLRs), DCs have the potential to detect a broad range of microbes and pathogens (Cook and MacDonald, 2016). During the infection of the lung with *S. aureus*, DCs become activated and their TLRs (TLR2 and TLR4) detect the staphylococcal PGN. The DCs then act as antigen-presenting cells (APCs), presenting the recognised antigen to the T-helper (Th1) cells and triggering the Th1-mediated immune responses (Wu and Xu, 2014). Meanwhile, the DCs also begin to release cytokines such as IL-12 and IL-23 in order to stimulate the Th1/Th17 immune cells, thereby further helping to eliminate *S. aureus* and prevent tissue damage (Wu and Xu, 2014). The activation of T cells by APCs such as DCs results in the activation of adaptive immunity (Armentrout et al., 2020). During this process, more specific immune responses are activated, whereby specific T cells and, subsequently, specific B cells are recruited to act against specific pathogens such as *S. aureus* (Uebele et al., 2020). The mechanisms of action of these two cell types differ, as T cells are involved in the direct destruction of the pathogen, while B cells produce antibodies that tag the pathogen for destruction (Pelzek et al., 2018).

1.4 Respiratory Infection

A wide variety of bacterial, viral and fungal pathogens can infect the human lungs. The most common bacterial infections are *S. aureus*, *Moraxella catarrhalis*, *Haemophilus influenzae*, *Chlamydia pneumoniae*, *Bordetella pertussis*, *Mycoplasma pneumoniae* and *Streptococcus pneumoniae* (*pneumococcus*) (MacIntyre et al., 2017). The most common viral infections of the respiratory system are rhinovirus A, B and C, respiratory syncytial virus, influenza virus A and B, parainfluenza virus 1, 2 and 3, coronaviruses OC43/HKU1 and 229E/NL63, human

metapneumovirus and adenovirus (MacIntyre et al., 2017, Tchatchouang et al., 2018). Viral infection of the human respiratory system is a hugely topical issue at the moment, as the SARS-CoV-2 pandemic has ravaged the globe and resulted in a huge number of fatalities (Smith et al., 2022). Indeed, the estimated number of deaths caused by SARS-CoV-2 worldwide currently stands at around 5 million (Worldometer, n.d.), whereas the 1918 flu pandemic killed an estimated 45–50 million (Agrawal et al., 2021). Fungal infections of the respiratory system affect hundreds of thousands of people every year, and they include *Pneumocystis jirovecii*, *Cryptococcus neoformans*, *Aspergillus fumigatus*, *Candida albicans*, mucormycetes and endemic dimorphic fungi (Barac et al., 2018, Firacative, 2020).

Respiratory disease is amongst the foremost causes of death in both adults and children, with an estimate of over 540 million deaths being caused by respiratory disease worldwide in 2017 alone (Soriano et al., 2020). Moreover, respiratory disease causes approximately 1.4–1.8 million deaths of children under the age of five each year, rendering it a more significant cause of death among this population than AIDS or malaria (Black et al., 2010, Reiner et al., 2019).

Staphylococcus bacteria are commonly involved in the infection of the human respiratory tract (Kumpitsch et al., 2019). This observation is relevant because these bacteria reside on the human skin without causing disease or damage and, therefore, can be considered part of the normal microbiota of human skin (McNeil et al., 2021). Yet, these bacteria are opportunistic and will cause infection whenever they get the opportunity to infect the human respiratory tract. Their presence on the human body provides them with a greater opportunity to infect the human respiratory system than many other bacterial species. Thus, they are commonly associated with bacterial respiratory infections (Limoli and Hoffman, 2019).

1.5 *S. aureus*

Initially discovered by Sir Alexander Ogston in 1880, *S. aureus* is a Gram-positive bacterium that, when cultured on a blood agar plate, forms golden or yellow colonies, thereby leading to the name *aureus*, which means ‘golden’ in Latin (Lowy, 1998). *S. aureus* is commonly found in the respiratory tract, including the nasal passage and throat, as well as on the skin and in the intestines. It has been estimated that methicillin-resistant *S. aureus* (MRSA) is present on or in 2–53 million people, and it may cause infections in those people (Xiao et al., 2019). Structurally, *S. aureus* has cell walls that are composed of a thick peptidoglycan (PGN) layer, lipoteichoic acids (LTA) that are associated with the membrane and proteins (Figure 1.7). PGN is composed of N-acetylglucosamine, which can be linked through peptide bonds and polymers

of the acid N-acetylglucosamine (Kim et al., 2015). *S. aureus* is an extremely successful colonising pathogen of the upper respiratory tract (Graham et al., 2021). Indeed, approximately 30% of people worldwide are colonised with *S. aureus* (Etter et al., 2020).

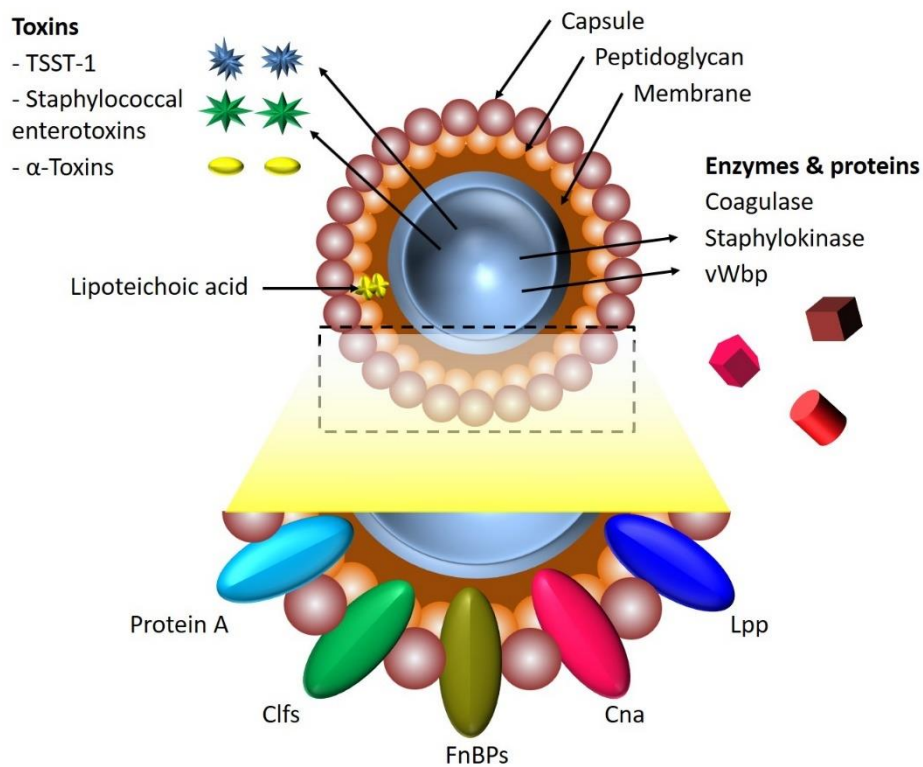


Figure 1.7: Schematic representation of the structure of *S. aureus*.

The cell wall structure of *S. aureus* consists of two layers, one composed of PNG and the other of polysaccharide capsules. As well as the production of toxins, adhesion to and invasion of host tissue, and immune evasion, *S. aureus* possess an extensive arsenal of virulence factors. Clfs = clumping factors, Cna = Collagen adhesin, FnBPs = fibronectin binding proteins, Lpp = lipoproteins, TSST-1 = Toxic shock syndrome toxin-1, vWbp = von Willebrand factor-binding protein. Image has been modified from Jin et al. (2021).

1.5.1 The life cycle of *S. aureus*

S. aureus pathogenesis involves five stages (Gnanamani et al., 2017); colonisation; spreading local infection; development of sepsis; metastatic infection and toxinosis (Gnanamani et al., 2017). *S. aureus* is predominantly localised in the anterior nasal cavity, which serves as a reservoir for potential infection. Under certain circumstances, colonisation becomes infection when the organism penetrates through the skin/mucosal surface and enters the blood, thereby causing invasive disease (Huitema et al., 2021). The disease can spread to cause serious presentations such as abscesses, particularly at sites close to the initial infection site. This systematic and gradual infection can later lead to septic shock (Lee et al., 2018). Furthermore, a cytokine-driven host response can lead to poor blood flow to the organs and, therefore, low blood pressure, which is associated with a substantial degree of mortality (Pietrocola et al., 2017).

1.5.2 *S. aureus* as a cause of pulmonary infection

S. aureus is known to cause infections in both community and healthcare settings (Taylor and Unakal, 2021). The treatment of these infections remains challenging due to the emergence of multidrug-resistant strains. For instance, the first case of resistance by *S. aureus* against methicillin, a semi-synthetic antibiotic, was reported in 1961, leading to the identification of MRSA (Wang et al., 2022). MRSA stimulates immune reactions and mortality (DeLeo et al., 2010), and it is now recognised as one of the major etiological agents of nosocomial and community-acquired infections worldwide (Haque et al., 2018) and there are approximately 150,000 healthcare-acquired MRSA infections per year in the European Union (Mkrtchyan et al., 2017). MRSA can result in mild to severe respiratory failure with septic shock (Pickens and Wunderink, 2022).

While early studies of *S. aureus* infection revealed that it has a variety of virulence factors, it has become increasingly clear that the host immune reaction is a major determinant of disease progression (Klevens et al., 2007, Mrochen et al., 2020). The pathogenic characteristics of *S. aureus* depend on their virulence factors, and it has been determined that the most functional virulence factor is α -hemolysin exotoxin, which causes tissue destruction (Divyakolu et al., 2019). Aside from methicillin, *S. aureus* can acquire resistance to a variety of antibiotics, either through mutations of chromosomal genes or horizontal acquisition of resistance genes (Vestergaard et al., 2019).

Up to 60% of humans host *S. aureus* at any one time, with a further 30% being considered to be persistent carriers. The remaining 10% never host the organism and so are referred to as non-carriers (Hurley, 2018). Approximately 30% of healthy children transmit *S. aureus* from the outer nostrils, and this rate is even higher in children with CF (52.4%) (Stone et al., 2009). In fact, the prevalence of *S. aureus* infection is increased in CF patients in general. For example, in the United States, the prevalence of MRSA in CF patients is 27% (Akil and Muhlebach, 2018). Thus, MRSA is more common in patients with CF than in other populations, leading to the worsening of their symptoms. This has raised concerns regarding the involvement of MRSA in bronchiectasis (Metersky et al., 2018). The mucus in the respiratory tract of a CF patient is much thicker than the mucus present in patients with infectious diseases such as bronchitis (Kreda et al., 2012, Kiedrowski and Bomberger, 2018). Thick mucus clogs the airways to a greater extent when compared with hydrated mucus. MRSA infection is usually chronic, and the respiratory tract slowly and irreversibly deteriorates over time. Genome plasticity has allowed *S. aureus* to adapt, which facilitates its persistence (Schwartbeck et al., 2016). The adaptive strategies here include biofilm formation, the acquisition of anti-microbial resistance (AMR), the appearance of persistent phenotypes and the regulation of virulence genes (Hsu et al., 2021). The whole-genome sequencing process provides information about the timeline of the adaptations that occur in an organism during its interaction with its host (Harkins et al., 2018). Various factors are transcribed from the genome of *S. aureus* to govern its virulence within the host. For instance, Accessory gene regulator (*agr*), which is an accessory gene regulator, is one factor responsible for the regulation of many surface proteins and secreted proteins necessary for virulence (Balasubramanian et al., 2016). Quorum sensing or signalling (QS) is important in terms of how these bacteria control their virulence factors. During QS, bacteria regulate the expression of genes according to the variations in the density of the cell population (Pena et al., 2019).

1.5.3 Virulence factors of *S. aureus*

As mentioned above, there are a number of secreted and cell wall-anchored virulence factors present in *S. aureus* that increase its potential to cause infection (Table 1.1). For the bacterium to cause an infection, it must first adhere to and enter a host cell. The cell wall-anchored virulence factors, such as clumping factors A and B (Hair et al., 2010, Elkhatab et al., 2015, Farnsworth et al., 2017), collagen adhesion, fibronectin-binding proteins FnBPA and FnBPB (Foster, 2016) and staphylococcal protein A (SpA) (Falugi et al., 2013, Pauli et al., 2014, Zhu et al., 2019, Fox et al., 2021), facilitate both adherence and internalisation. These factors bind

to the extracellular matrix proteins of the host cell, such as fibronectin, fibrinogen and elastin (Roche et al., 2004). The FnBPs are necessary for invasion (Shinji et al., 2011), while mutations in FnBPA and FnBPB are known to reduce the renal burden and mortality rate in mice (Lee et al., 2018a). One of the key virulence factors of *S. aureus*, SpA, binds to the cell wall and can be secreted (O'Halloran et al., 2015). It binds to the Fab and Fcγ portions of immunoglobulin and so aids in immune evasion. SpA also contributes to inflammation and pneumonia in a murine model by interacting with the epidermal growth factor receptor (EGFR) (Soong et al., 2011). SpA then leads to the activation of the RhoA/Rho-associated protein kinase/myosin light chain, which is followed by MAPK signalling and calpain activity in the epithelial cells of the respiratory tract (Soong et al., 2011). It cleaves the transmembrane portion of the junctional protein and supports the transmigration of polymorphonuclear leukocytes (PMNs) to the airway (Soong et al., 2011).

Table 1.1. Virulence factors implicated in adhesion to host cells and toxicity and various another enzyme. Table has been modified from Zecconi and Scali (2013).

Adhesion to host cells; <i>S. aureus</i> virulence factors		
Name	Abbreviation	Function
Von Willebrand factor binding protein	vWbp	Binding to vW factor, fibrinogen, and prothrombin, and activation of last one
Immunoglobulin-binding protein	Sbi	Binding to C3 protein of complement system and involved in C3-C3b conversion, part of Fc domain of immunoglobulin
Plasmin-sensitive protein	Pls	Binding to nasal epithelial cells and lipids of host cells
Extracellular adherence protein	Eap/Map	Impairs wound healing and angiogenesis; stimulation of secretion of IL-6 / MHC-II analog protein and TNF α ; biofilm formation through adhesion to host cells and <i>S. aureus</i> cells
Extracellular matrix protein-binding protein	Emp	Biofilm formation through binding with extracellular matrix
Serine-rich surface protein	SraP	Binding to platelets
<i>S. aureus</i> surface protein G	SasG	Biofilm formation through binding with the extracellular matrix
Fibronectin binding proteins A, B	FnBPA, B	Adhesins for elastin, fibronectin, and fibrinogen (FnBPA only)
Iron-regulated surface determinant A, B, C and H	IsdA, B, C, H	Bind haptoglobin, fetuin, hemin, hemoglobin, transferrin, fibrinogen, fibronectin, and haptoglobin-hemoglobin complex
Polysaccharide intercellular adhesin	PIA	Biofilm formation through aggregation by adhesin
Elastin-binding protein	EbpS	Adhesin through transmembrane for tropoelastin and elastin
Bone sialoprotein-binding protein	Bbp	Binding to fibrinogen, adhesin for bone sialoprotein (SdrE)
Serin-aspartate repeat proteins C, D and E	Sdrs	Adhesins
Collagen-binding adhesin	Cna	Adhesin for collagen (both types IV and I)
Toxins ; <i>S. aureus</i> virulence factors		
Toxic shock syndrome toxin 1	TSST1	Superantigen activity, Endothelial toxicity
Enterotoxin-like proteins	SEls	Superantigen activity to immunomodulate, No or unknown gastroenteric toxicity
Enterotoxins	SEs	Superantigen activity for immunomodulation, Gastroenteric toxicity
Exfoliative toxins A, B and D	ETA/B/D	Digestion of desmoglein 1 through serine proteases which act specifically through glutamate, superantigen activity through exotoxins
β toxin	Hlb	Cytolytic effects through sphingomyelinase
Phenol soluble modulins	PSMs	Detergent activity along with pore-forming toxins
Leukocidins D, E and M	LukD/E/M	Leukocytes are killed while also part leukotoxins which causes pore formation
α toxin	Hla	Toxin causing cytolytic effect through pore formation
Enzymes and other proteins; <i>S. aureus</i> virulence factors		
Formyl-peptide receptor-like 1 inhibitory protein	FLIPr	Binding to formyl peptide receptor
Enolase	Eno	Binding to laminin and help in formation of phosphoenol-pyruvate from phosphor-glycerate
Phospholipase C	Plc	Lipase activity through phosphatidylinositol
O-acetyltransferase	OatA	Peptidoglycan O-acetylation
Coagulase	Coa	Helps to convert fibrinogen to fibrin while activation of prothrombin after activation
Fatty acid-modifying enzyme	FAME	Modification of fatty acids
Glycerol ester hydrolases	lip, geh, beh	Degradation of triacylglycerols
V8 protease	SspA	Serine protease

SpA blocks the IgG-mediated activation of the complement system and promotes cell death by interfering with the IgG hexamer formation. It can also block IgG-mediated phagocytosis (Cruz et al., 2022). SpA relies on the EGFR, TNFR1 and Fas ligands to stimulate IL-16 secretion from the CD4 cells, which is controlled by the calcium ion flux and calpain activity (Ahn et al., 2014). IL-16 is involved in tissue inflammation. The multiple virulence factors associated with *S. aureus* render it a pathogen, as explained by the detailed description of all the factors given in Table 1.2 (Pietrocola et al., 2017).

Table 1.2. Virulence factors implicated in immune evasion at different levels. Table has been modified from Zecconi and Scali (2013).

Prevention of neutrophil migration; Virulence factors of <i>S. aureus</i>		
Name	Abbreviation	Function
Staphylococcal superantigen-like 7	SSL7	Blocking the recognition by neutrophils, also bind to with IgA through Fc region
Chemotaxis inhibitory protein	CHIPS	Blocks formyl peptide receptors and C5a receptor
Staphylococcal superantigen-like 5	SSL5	Blocks PMN rolling through binding with P-selectin glycoprotein ligand-1
Staphylococcal superantigen-like 1	SSL10	Binding with chemokine receptors
Lysis of leukocytes; Virulence factors of <i>S. aureus</i>		
Leukocidins A /B or H/G	LukAB/HG	PMNs killing through pore-formation
Panton-Valentine leukocidin	PVL	Leukocytes killing through pore formation
γ toxin	Hlg	Causes hemolysis through becoming part of leukocidin
δ toxin	Hld	Binding to monocytes and neutrophils to cause cytolytic effects
Resisting to oxidative burst; Virulence factors of <i>S. aureus</i>		
Thioredoxin and thioredoxin reductase	-	Inactivation of ROS
Staphyloxanthin	-	Carotenoid
Catalase and alkylhydroxide reductase	CatA, AhpC	Helps in colonization of nasal cavity, also role in inactivation of hydrogen peroxide
Evasion of complement activation; Virulence factors of <i>S. aureus</i>		
<i>S. aureus</i> surface protein E	SdrE	Binding to factor H of complement regulation
Clumping factor A	ClfA	Binding to complement regulator factor I and helps in platelets adhesion
Extracellular complement-binding protein	Ecb	Inhibition of convertase
Extracellular fibrinogen-binding protein	Efb	Binding to complement C3 and fibrinogen; also inhibition of C5 and C3
Staphylococcal complement inhibitor	SCIN	Inhibition of convertase
Staphylokinase	Sak	Activates plasminogen
Capsular polysaccharides	CPSs	Modifies C3b and C3 and C3b role
Degradation of immunoglobulins; Virulence factors of <i>S. aureus</i>		
Staphylokinase	Sak	Activation of plasminogen
Protein A	SpA	Role in conversion of C3–C3b through binding with C3, also binds Fc domain of TNFR-1, von Willebrand factor and immunoglobulin
Cloaking of opsonin; Virulence factors of <i>S. aureus</i>		
Clumping factor B	ClfB	Adhesion to cytokeratin 10 and platelets
Clumping factor A	ClfA	Binding to factor 1 of complement regulation, adhesion to platelets
Evasion of innate immune defences related to antimicrobial peptides; Virulence factors of <i>S. aureus</i>		
Dlt operon	Dlt	Modification of teichoic acids through insertion of D-alanine
Multiple peptide resistance factor F	MprF	Modification of lipids through insertion of lysine
Antimicrobial peptide sensor	Aps	Impairing the antimicrobial peptides through binding
Gra regulatory system	GraR/S	Impairing the function of LL-37 and phagocytosis
Resisting to lysozyme activity; Virulence factors of <i>S. aureus</i>		
OatA gene	OatA	Modifications in N-acetylmuramic acid
Resisting to the action of cathelicidin; Virulence factors of <i>S. aureus</i>		
Aureolysin	Aul	Cleavage of LL-37
Staphylokinase	Sak	Binding to Alpha-defensin

1.6 Evasion of the Innate Immune System by *S. aureus*

S. aureus has developed multiple mechanisms through which it can evade the innate immune system. These mechanisms include the prevention of phagocytosis, inhibition of anti-microbial responses in host cells and blockage of the migration of leukocytes (Flannagan et al., 2015).

1.6.1 Evading extravasation

Neutrophils are the first responder to a pathogenic breach as they are the first to reach the infection site. Their response takes place in three stages: Firstly, neutrophils adhere to the endothelial cells and roll on them. It is followed by their attachment to the endothelial cells that causes neutrophil arrest. Finally, neutrophils cross the endothelial barrier and migrate to the infection site (Teng et al., 2017). The initial stage of extravasation, that is, the rolling of a neutrophil along the cells of the endothelium, can be modulated by SSL5, which acts on the PSGL-1 (Zhang et al., 2016) by inhibiting its interaction with P-selectin and preventing the further rolling of the neutrophil on the endothelium (Kappelmayer and Nagy, 2017).

The second stage of neutrophil extravasation, namely firm adhesion to the endothelium, is also targeted by *S. aureus*. More specifically, ICAM-1, which is the essential molecule involved in the interaction process, is bound and inhibited by Eap, which blocks the final stage of molecular adherence and transmigration near the site of infection (Sökeland and Schumacher, 2019). Figure 1.8 illustrates the functions of these modulators. SSL3 modulates the monocyte and neutrophil responses by inhibiting the interactions of TLR2 with its ligands (Bardoel et al., 2012). Moreover, when SSL3 binds the extracellular TLR2 domain, it blocks the stimulation of macrophages (Yokoyama et al., 2012, Askarian et al., 2018).

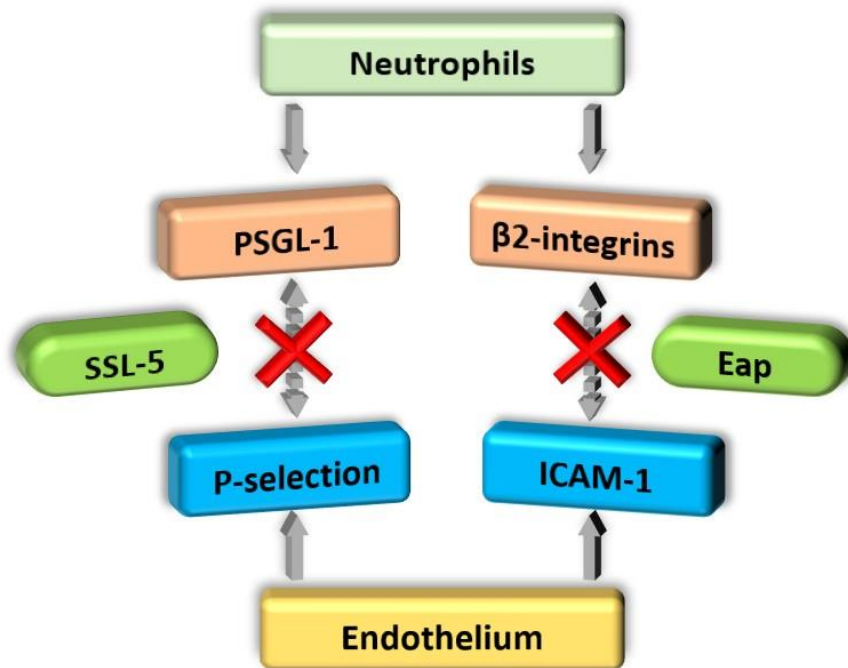


Figure 1.8: *S. aureus* approach to destabilize neutrophils extravasation.

The first stage is regulated by the interaction between the glycoprotein (PSGL-1) of the neutrophils and the P-selectin/E-selectin of the endothelial cells, while the second stage involves the interaction of the $\beta 2$ integrins of the neutrophils with the ICAM-1 present on the endothelial cells. Finally, the host-derived chemokines act as potent proinflammatory mediators and recruit an increasing number of neutrophils. The SSL-5 from *S. aureus* blocks the interaction of P-selectin with PSGL-1, while the Eap (*S. aureus*) interferes with the binding of ICAM-1 to the $\beta 2$ -integrins, which blocks the neutrophil-endothelium adhesion and starts the pathogenesis by surpassing the adhesion mechanism. Image has been modified from Teng et al. (2017).

1.6.2 Inhibition of complement activation and chemotaxis

S. aureus also secretes numerous proteins that affect chemokine signalling, as illustrated in Figure 1.9. In addition to inhibiting PSGL-1, SSL5 is also responsible for inhibiting the chemokine-induced activation of leukocytes through inhibiting the leukocyte response to the CC, CX3C and CXC chemokines as well as to the complement fragments C5a and C3a (Bestebroer et al., 2010). Neutrophils that have been exposed to Staphopain A (a secreted cysteine protease) do not respond to the activation of chemokine CXCR2 due to the cleavage of the N-terminal domain (Laarman et al., 2012). Furthermore, Staphopain A inhibits the CXCR2-mediated migration of neutrophils towards chemokines.

Based on the results of experiments involving mutant isogenic Staphopain A and wild-type MRSA, it appears that Staphopain A is the only secreted protease that exhibits activity against CXCR2 (Laarman et al., 2012). The CHIPS binds to the neutrophil chemoattractant receptors,

thereby blocking ligand binding (Thammavongsa et al., 2015). In addition, CHIPS is essential during the initial stages of infection because it allows *S. aureus* to colonise particular niches (McGuinness et al., 2016). However, as the bacteria multiply and reach a high density, the host chemokines are capable of overcoming the inhibition by CHIPS (de Vor et al., 2020).

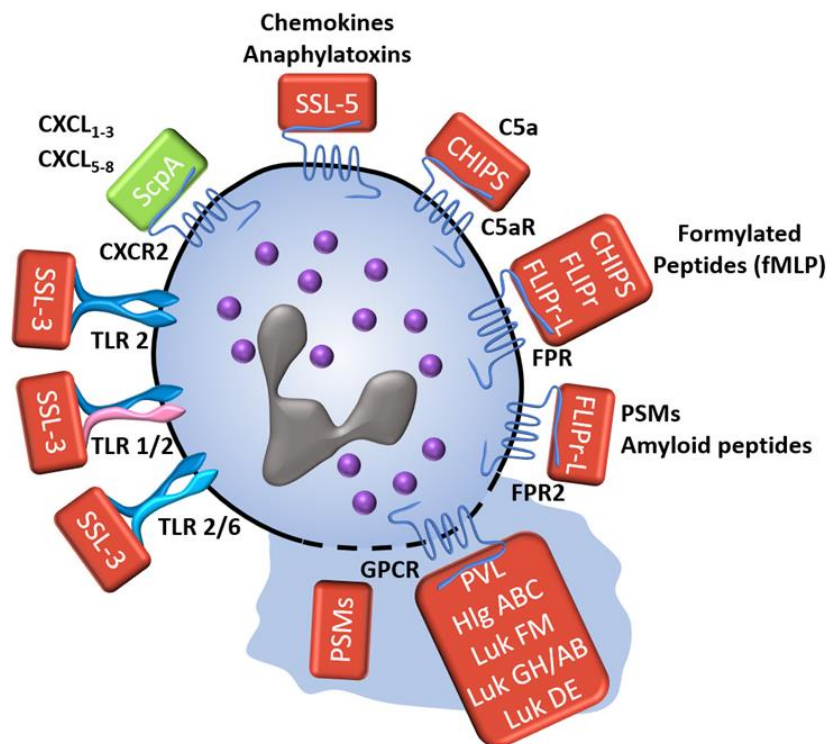


Figure 1.9: Neutrophil attack and evasion of activation.

The red boxes represent the antagonising proteins of *S. aureus*, while the green box represents a protease. Image has been modified from Span et al. (2013).

1.7 Induction of Host Defence Responses by *S. aureus* Infection

S. aureus expresses toxic molecules, such as exfoliative toxins, pore-forming peptides, proteolytic enzymes and superantigens, which work against immune system activation and cause diarrhoea, vomiting and food poisoning (Tam and Torres, 2019). *S. aureus* can also prompt the development of toxin-specific IgE (Kim et al., 2019), which can cause allergic reactions, asthma and atopic dermatitis (Stentzel et al., 2017). Mast cells can respond directly to the compounds produced by microorganisms via the G protein-coupled receptors and TLR (Redegeld et al., 2018, Arifuzzaman et al., 2019, Pundir et al., 2019), which contributes to the activation of the innate host defence (Piliponsky and Romani, 2018, Arifuzzaman et al., 2019).

The *S. aureus* genome features a number of regulatory systems that coordinate the expression of its virulence factors. For instance, *Agr* represents an important regulatory mechanism that controls the expression levels of secreted toxins and surface proteins. *AgrD* (a peptide bacteria used for QS), *AgrB* (the export protein of *AgrD*), a response regulator (*AgrA*) and a sensor histidine kinase (*AgrC*) are all encoded by the *Agr* regulon. The expression of *AgrA* is regulated by its binding to its promoter sequence in coordination with RNAIII (Jenul and Horswill, 2019). Additionally, *Agr* mutations have been reported in several clinical isolates (Traber et al., 2008). Both *Agr* and the *Agr* regulon are redundant in relation to the lungs' inflammatory signals, although they play an essential role in invasive pulmonary infection. Moreover, *Agr* plays an important role in animal models of pneumonia, as reported in several prior studies (Montgomery et al., 2010).

Aside from the immunological effects of the haemolytic toxins, the proteins of *S. aureus* can trigger the activation of B and T cells. Initially, these *S. aureus* proteins result in the activation of T cells by means of the TSST and staphylococcal enterotoxin A/B (SEA/SEB) (Karauzum and Datta, 2017). Furthermore, these proteins can lead to the activation of both platelets and polyclonal B cells with the help of protein A (Bekeredjian-Ding et al., 2007, Tam and Torres, 2019), while the *S. aureus* IgG-binding protein (*Sbi*) works along with protein A to sequester immunoglobulins (Smith et al., 2011) and α -haemolysin is responsible for inflammasome activation (Craven et al., 2009). TSST-1 is the causative toxin behind toxic shock syndrome (TSS), which results in symptoms of fever, multisystem involvement, hypertension and rash. TSS was previously considered to be a result of highly absorbent tampon use during menstruation (Farage and Maibach, 2006, Reame, 2020), although this notion was later proven wrong when TSS was reported in different patient populations (Low, 2013).

While the direct role of TSST-1 in pathogenesis remains unclear, *S. aureus* has been reported to be the causative agent of a number of respiratory diseases, including post-flu infection, laryngotracheitis, pneumonia and pharyngitis (Parker and Prince, 2012). (Bachert et al., 2003, Bachert et al., 2020) observed correlation between IgE antibodies (immunoglobulins E) and both asthma and enterotoxin. Moreover, the correlation between the eosinophil cationic protein, which is the marker of rhinitis and asthma, and enterotoxin IgE antibodies was investigated by Pietrocola et al. (2017).

1.8 Host Responses to *S. aureus* Infection

The immune system helps the host to remove any harmful substances (e.g. pathogens, toxins, allergens) from the body. The genes responsible for the immune response are known as immune response (IR) genes, and they are present in MHC. The IR genes encode MHC II molecules, which recognise different protein antigens through receptors and then display the peptides for the initiation of an antigen-specific immune response (van den Elsen, 2011). MHC complexes can be recognised by T-helper cells. These T cells then help B cells to produce antibodies (Rao, 2018). The host generates a response to ensure the elimination of infectious agents from the body through the innate and adaptive immune systems. The involved cells are initially very low in number, but once triggered they proliferate and reach the maximum number required for an effective response (Evavold and Kagan, 2018). In the case of an infection inside the body, the epithelium is affected first due to being the first layer of all the internal organs (Walters et al., 2013).

The infected epithelial cells exhibit the least ability to respond to the infection. The normal regulation of epithelial cells against infection is induced by genes such as B94 and Zfp36 (interleukin) (Makita et al., 2021). IL-6 is an interleukin that is well known for its pro-inflammatory (enhances the inflammation) and anti-inflammatory (reduces the inflammation) properties (Borsini et al., 2020). Soluble IL-6R fulfils a pro-inflammatory role through the activation of the immune system (O'Callaghan, 2018). As the recruitment of monomers occurs, both T-cell apoptosis and Treg differentiation are inhibited, whereas the anti-inflammatory role performed by the membrane-bound IL-6R leads to the activation of signal transducer and activator of transcription 3 (STAT3) (O'Callaghan, 2018). Moreover, the proliferation of epithelial cells can be observed alongside the inhibition of epithelial cell apoptosis. This interleukin is encoded by the IL-6 gene and helps to protect epithelial cells against infection (O'Callaghan, 2018). In addition, the IP-10 (also known as CXCL10) protein is also highly important with regard to *S. aureus* because it plays a critical role in the recruitment of NK cells (Li et al., 2017).

Epithelial cells significantly contribute to the initiation of the adaptive response in the airways. Specifically, epithelial cells recognise the specific and unique patterns of receptors and then release anti-microbial agents into the airways in order to eliminate infectious agents. The epithelial cells keep interacting with the interepithelial and subepithelial DCs so that the DCs are no longer able to skew the T cells (Zhang et al., 2018). When an inflammatory or immune response is required, chemokines are released from the epithelial cells, which help in recruiting

those subsets of granulocytes and T cells required for the necessary immune response (Evavold and Kagan, 2018).

1.9 Respiratory Cell Cultures for Studying Pulmonary-Specific Responses

Pulmonary function can be investigated at different levels, both *in vitro* and *in vivo*. As direct studies are difficult to conduct on humans, model organisms such as mice or primates are used for *in vivo* studies, while respiratory cell lines are used for *in vitro* studies (Bosch et al., 2021). Both *in vitro* and *in vivo* studies are associated with specific advantages and limitations. Animal studies can be used as an alternative to human studies when investigating pathogens or treatment options within the context of whole-body exposure. Cell lines, such as A549, can be used as an *in vitro* model because they are derived from humans (Gharebaghi et al., 2020). For this reason, they may prove more relevant for any human-related investigation. In contrast to primary cells that have been freshly isolated from tissues, immortalised cell lines are modified by means of the genetic insertion of transforming genes that allow the cells to proliferate indefinitely. Therefore, such cells have the ability to evade normal cellular senescence. The defined genetic changes that transform human immortalised cell lines are similar to the changes that transform normal human cells into cancer cells (Hynds et al., 2018a). As immortalised cell lines can grow for extended periods of time and multiple passages, they can be used to make stable cell lines and genetically modified via the process of gene editing (Jin et al., 2018).

Primary cultures of human lung epithelial cells are increasingly recognised as the ‘best’ model of lung epithelial cells. However, despite recent advances in the methods available for their extended culture (Hiemstra et al., 2018), these cells typically experience a restriction in terms of their growth capacity that constrains their utility, particularly the capacity to disseminate the cells and their clones to the wider research community. To combat this limitation, the immortalisation of normal human lung epithelial cells to generate cell lines is considered a significant goal. Such cell lines, the best example of which is arguably the BEASE2B cell line, have been generated by means of transfection with oncogenic viral proteins such as the SV40 large T antigen (Ke et al., 1988, Park et al., 2015). However, such cells are not able to differentiate in the same way as air-liquid interface (ALI) cultured primary cells (Calvert and Ryan, 2020).

Ramirez et al. (2004) reported that the transduction of both hTERT and Cdk4 (but neither alone) could reproducibly immortalise human bronchial epithelial cells (referred to as HEBC-KTs) isolated from biopsy specimens retrieved from donors with and without lung cancer.

HBEC-KTs exhibit several properties typical of human bronchial epithelial cells, including (albeit not limited to) their morphology and the ability to form monolayers. In the organotypic culture conditions in which cells are placed at the ALI, HBEC-KT cells form ciliated cells, goblet cells and basal cells, thereby forming a structure similar to the human bronchial epithelium, which indicates that the cells retain the properties of typical pluripotent immature basal cells (Ramirez et al., 2004). The HBEC-KT collection has subsequently been utilised extensively in research (Vaz et al., 2017). The collection currently includes more than 40 HBEC lines generated from different donors. Several of these lines, such as the HBEC3-KT and HBEC4-KT lines, are maintained by the American Type Culture Collection, while others are widely disseminated by the Minna and Shay Labs (Ramirez et al., 2004).

In other immortalised cell lines, the polycomb complex protein BMI-1, has been shown to extend the proliferative capacity of human bronchial epithelial cells while maintaining their mucociliary differentiation capacity. To increase their proliferation, primary HBECs were transduced with either viral oncogenes or mouse Bmi-1 and hTERT, and the resultant cell lines underwent mucociliary differentiation (Munye et al., 2017). Fulcher et al. (2009) established a number of human bronchial epithelial cell lines for research into CF. They introduced the catalytic subunit of telomerase and BMI-1 into the primary cells and demonstrated that, after this treatment, the lifespan of the cells increased, while following frequent passaging (after the 15th passage), the cells showed the presence of the diploid karyotype (Fulcher et al., 2009).

It was postulated that human BMI-1 alone would serve to increase the proliferative capacity of bronchial epithelial cells while maintaining their differentiation potential. Both CF and non-CF bronchial epithelial cells were transduced with a lentivirus expressing BMI-1, after which their morphology, replication and karyotype were evaluated. The knockdown of DNAH5 in the BMI-1 cells using shRNA led to a PCD-like phenotype (Munye et al., 2017). The BMI-1-transduced basal cells exhibited normal cell morphology, karyotype and division times throughout the extensive passaging. Moreover, the BMI-1 cell lines underwent mucociliary differentiation when cultured at the ALI, as indicated by the formation of cilia and the expression of the gel-forming mucins *MUC5AC* and *MUC5B* (Munye et al., 2017).

Other immortalised airway epithelial cell lines have been generated. Walters et al. (2013) reported the preparation of an epithelial basal cell line of the human airway that has multipotent differentiation potential. In this study, they brushed the primary cells obtained from healthy non-smokers and infected them with telomerase. The differentiation and non-differentiation

analyses were performed using the ALI. The single-cell clone analysis of the newly prepared cell line demonstrated that it continued exhibiting the characteristics of the original cells upon 40 passages and then differentiated into ciliated (*FOXJ1*, *DNAI1*), club (*SCGB1A1/CC10*), goblet (*TFF3*) and secretory (*MUC5B* and *MUC5AC*) cells (Walters et al., 2013). Similarly, Wang et al. (2019) demonstrated the preparation and immortalisation of a small airway epithelium. For this, they infected healthy cells obtained from non-smokers with retroviral-based telomerase reverse transcriptase and a model drug. Their results indicated that the single-cell clone kept proliferating up to 200 doubling times and more than 70 passages, whilst maintaining basal cell properties (KRT5+ and TP63+) (Wang et al., 2019).

1.10 ALI Models of the Airway

ALI cultures are increasingly used as the culture system of choice for differentiating primary respiratory epithelial cells and studying them *in vitro* (Wang et al., 2018a). The ALI approach generates a pseudostratified mucociliary epithelium that replicates the epithelium of the native airway (Tata et al., 2013). The first ALI culture of tracheobronchial cells was described in 1990 (Wu et al., 1990), and since then the approach has become an established tool for respiratory research. There are now multiple published methods for culturing airway cells at the ALI on diverse platforms, using different media and with different differentiation times (Luengen et al., 2020). The most commonly utilised methods involve the use of polycarbonate transwell filters. When cultured at the ALI, pulmonary cells (from the nose to the small airways) develop a phenotype that is considered to mimic normal physiological conditions (Baldassi et al., 2021). In an ALI culture, the cells are exposed to air from the top (the apical surface), while nutrition is provided from below (the basal surface) through the transwell filter. In a native respiratory epithelia, the epithelial cells obtain nutrients from the lamina propria, which lies beneath them, while the apical surface is covered with mucus that cleans and protects the airways. Thus, the ALI approach provides conditions that are very similar to those experienced by native airway epithelial cells. The advantages of using the ALI include the ability to reconstruct a pseudostratified epithelium in an *in vitro* system that is comparable to an *in vivo* epithelium (Wang et al., 2018). For this reason, the ALI culture approach is now considered the best way to model a physiological epithelium that undergoes both ciliogenesis and mucus secretion. The cells are permitted to differentiate for a given period of time, generally 14–28 days (Yang et al., 2015). This process is depicted in Figure 1.10. The growth media required for successful ALI differentiation require multiple growth factors, including retinoic acid, insulin, bovine pituitary extract, hydrocortisone, human epidermal growth factor, epinephrine and transferrin

(O'Boyle et al., 2018). One of the most significant growth factors required for differentiation is retinoic acid, as it is required for lung development and maturation through the stimulation of retinoid X receptors in order to activate diverse genes (Yang et al., 2015).

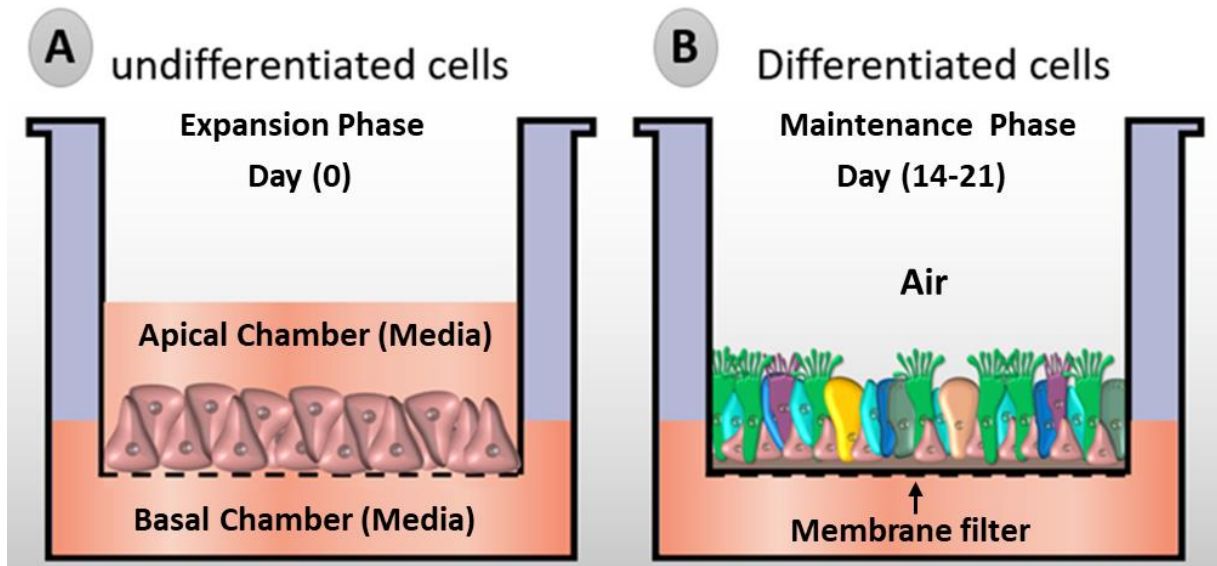


Figure 1.10: Schematic illustration of the ALI culture process.

(A) Undifferentiated cells are grown in submerged culture and fed from above and below. (B) Differentiated cells are exposed to air from the top (apical surface) and fed from below (basal surface) through the transwell filter. When the cells are submerged in the culture from above, they are unable to differentiate. However, when the cells are fed from below and air is provided from the top, the cells engage in the differentiation process.

The physiologically relevant phenotype of the ALI *in vitro* cell culture model means that it can be used for the investigation of respiratory biology, to model diseases and to support drug development (Langhans, 2018). Moreover, cell differentiation in this model results in the development of cell specialisation, which can be observed via the analysis of tissue-specific genes during the process of differentiation of human bronchial cells (Figure 1.11). According to the data obtained by Ross et al. (2007), the expression of multiple cell-specific marker gene was induced during differentiation. In addition, in this data set, *BPIFA1* and *BPIFB1* were the most highly expressed genes within the differentiated cells.

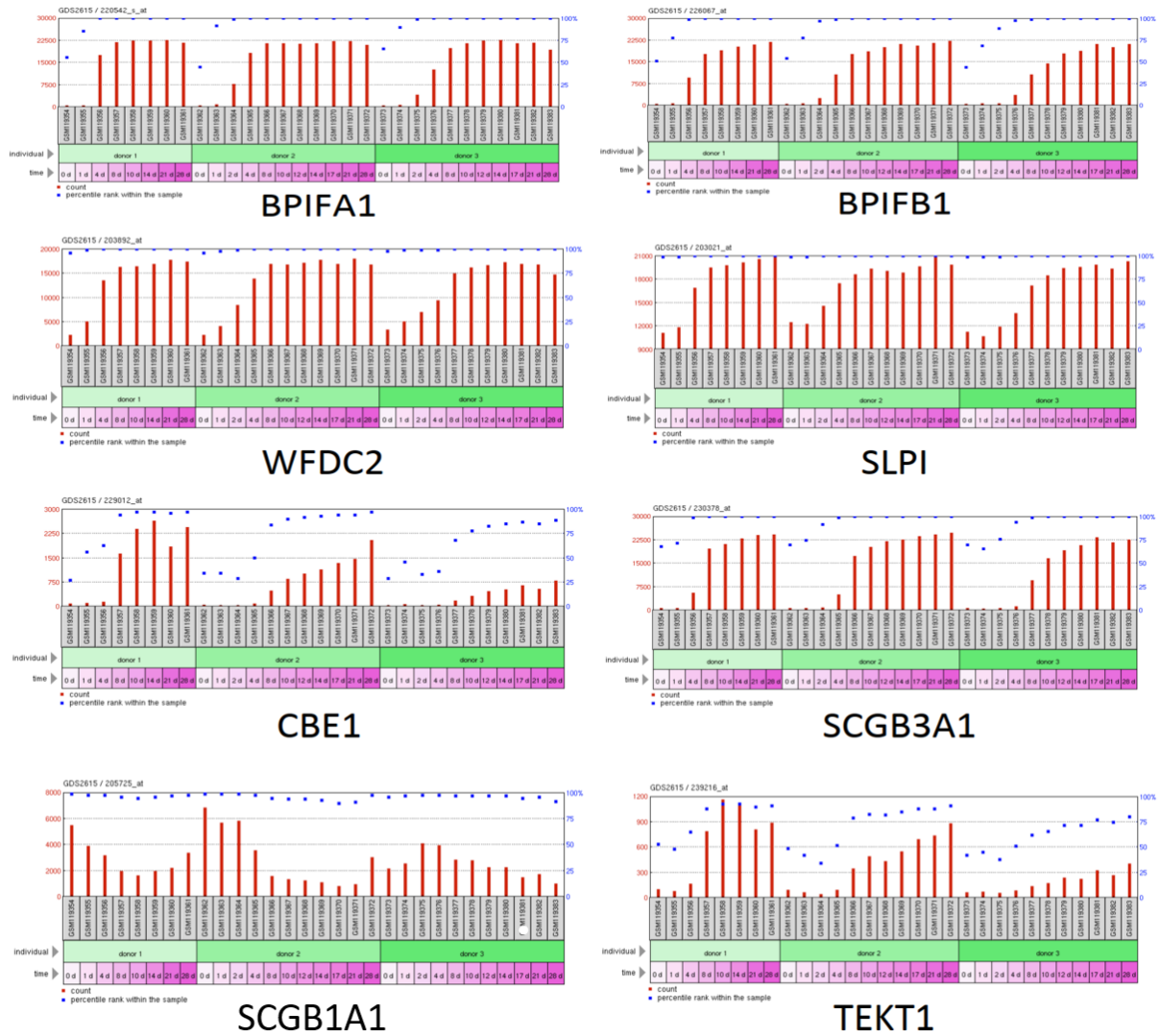


Figure 1.11: Gene expression during ALI differentiation of human bronchial epithelial cells.

The gene expression profiles of a number of cell-specific marker genes were extracted from NCBI GEO (<https://www.ncbi.nlm.nih.gov/geo/>). The data were obtained from the microarray study conducted by Ross et al. (2007). The data show the induction of the expression of multiple markers (red bars) during the differentiation process. *BPIFA1*, *BPIFB1*, *WFDC2*, *SLPI*, *SCGB3A1* and *SCGB1A1* are markers of secretory cells, whereas *TEKT1* and *CBE1* are markers of ciliated cells.

1.11 Improvements in Primary Cell Culturing

Although primary cells are very useful tools when it comes to research, they are associated with a number of limitations. For instance, as primary airway cells cannot grow for extended periods and multiple passages, they cannot be used to make stable cell lines. They also cannot be isolated in very large numbers, and it is well known that they suffer from donor-to-donor variability. Primary cell cultures also require a rich mix of micronutrients, amino acids and other nutrients (Hynds et al., 2018b). Thus, in addition to retinoic acid, other growth factors have been used to modify and improve primary airway cell cultures. For example, SMAD pathway inhibition has been shown to promote the expansion of basal cells, thereby increasing the number of primary cells in the culture (Mou et al., 2016). Rho-associated protein kinase (ROCK) inhibition also improves epithelial cultures (Park et al., 2004, Saadeldin et al., 2020). Y-27632 is commonly used to inhibit ROCK, resulting in improved cloning and increased survival of both human pluripotent stem cells and embryonic stem cells (Horani et al., 2013, Martinovich et al., 2017).

The conditionally reprogrammed cell (CRC) technique is gaining interest in relation to its use in cell culturing in human epithelial models (Wolf et al., 2017) and has been successfully used in a number of studies (Liu et al., 2012, Reynolds et al., 2016, Wolf et al., 2017, Rayner et al., 2019), which revealed that different media generate model cell cultures that are slightly different. Wolf et al. (2017) described a robust life-extended model of paediatric airway epithelial cells with the help of the CRC technique. The medium used for the culturing included the ROCK (Y-27632) inhibitor and the method used mitotically inactivated fibroblasts. The results confirmed that the CRC technique aids in the development of a model for airway epithelial cells that preserves the phenotype of the cells after multiple passages, extends the lifespan of the cells, augments the proliferation potential of the cells and produces an immune response through the expression anti-viral genes (Wolf et al., 2017).

The findings of Reynolds et al. (2016) supported the efficacy of CRC technology with regard to the production of nasal airway epithelial cells, highlighting noticeable advantages when compared with standard cultures. The standard medium is based on bronchial epithelial growth media (BEGM). It has been reported that feeder cells, along with ROCK (Y-27632), can be used for the induction of tumour epithelial and normal cells in order to multiply their number *in vitro*. The continuous cell propagation or augmentation was based on both Y-27632 and feeder cells, whereas the CRC technique produces a normal karyotype and retains the non-tumorigenic nature of the cells. Rayner et al. (2019) showed the development of a differentiated

culture medium (PneumaCult-ALI) for the production of primary normal human bronchial epithelial (NHBE) cells. Multiple culture conditions were tested against NHBE cells, and it was found that the cells maintained the airway epithelial properties after four passages.

Ruiz García et al. (2019) reported the use of the single-cell RNAseq technique for the differentiation of nasal epithelial cells grown in different media: PneumaCult and BEGM. Differentiation by means of single-cell RNAseq showed that the cells assembled in six populations with the PneumaCult medium and seven populations with the BEGM medium. Cyclic basal cell, non-cyclic basal cell, suprabasal cell, club cell, goblet cell and multiciliated cell populations were observed with the PneumaCult medium, whereas goblet cell and club cell populations were mainly observed with the BEGM medium. The study resulted in an intriguing finding: the PneumaCult-ALI model was associated with higher expression of *MUC5AC* (Ruiz García et al., 2019). Thus, it was concluded that different culture media give rise to different characteristic populations and gene expression levels.

1.12 Signaling pathway of interleukin 13 (IL-13) in the airway

One of the best studied pathways modulating airway epithelium is IL-13. IL-13 is the signature cytokine of the type II inflammatory response, and it plays important roles in regulating the responses of lymphocytes, myeloid cells, and non-hematopoietic cells (Junttila, 2018). Th2 cells, natural killer T cells, innate immune cells, and innate lymphoid cells can produce IL-13, which helps to trigger and sustain a chronic idiopathic intestinal inflammatory response (Giuffrida et al., 2019). Asthma and related traits are strongly associated with tissue IL-13 levels and genetic variants in the IL-13 gene, supporting the significance of IL-13 in allergic disorders in humans (Townley et al., 2011). The IL-13 signaling pathway shown in figure 1.12 demonstrate the effects of IL-13 on the cell, as well as the roles of IL-13 in the airway. One potential mechanism of IL-13-induced airway hyperresponsiveness is through the production of goblet cells (Boonpiyathad et al., 2019). Mucus production can lead to airway obstruction and hyperresponsiveness. Additionally, IL-13 has been shown to increase the production of pro-inflammatory cytokines, such as IL-4, IL-5, and IL-13, these cytokines can contribute to airway inflammation and hyperresponsiveness (Gandhi et al., 2017). IL-13 binds to the IL-13 receptor (IL-13R), which is expressed on a variety of cell types, including airway smooth muscle cells, epithelial cells, and macrophages. IL-13R is a heterodimeric receptor that consists of IL-13R alpha 1 and IL-13R alpha 2 subunits (Onyiah and Colgan, 2016).

IL-13 signaling leads to the activation of a number of different signaling pathways, including Mitogen-activated protein kinase (MAPK), Phosphoinositide 3-kinase (PI3K), and Janus kinase (JAK)-signal transducer and activator of transcription (STAT) pathways (Favoino et al., 2021). These pathways lead to the activation of a number of different transcription factors, including STAT6, which is responsible for the transcription of a number of genes involved in the inflammatory response as shown in the Figure 1.12 (Favoino et al., 2021). IL-13 is also involved in the regulation of airway smooth muscle contraction. IL-13 signaling leads to the production of cyclooxygenase-2, which is responsible for the synthesis of prostaglandins. Prostaglandins are involved in the regulation of airway smooth muscle contraction. IL-13 also upregulates the expression of a number of other genes that are involved in the contraction of airway smooth muscle, including endothelin-1 and thromboxane A2 (Lam et al., 2019).

In addition to its role in the contraction of airway smooth muscle, IL-13 also plays a role in the production of mucus. IL-13 signaling leads to the upregulation of a number of genes that are involved in the production of mucus, including MUC5AC and MUC5B (Ma et al., 2018).

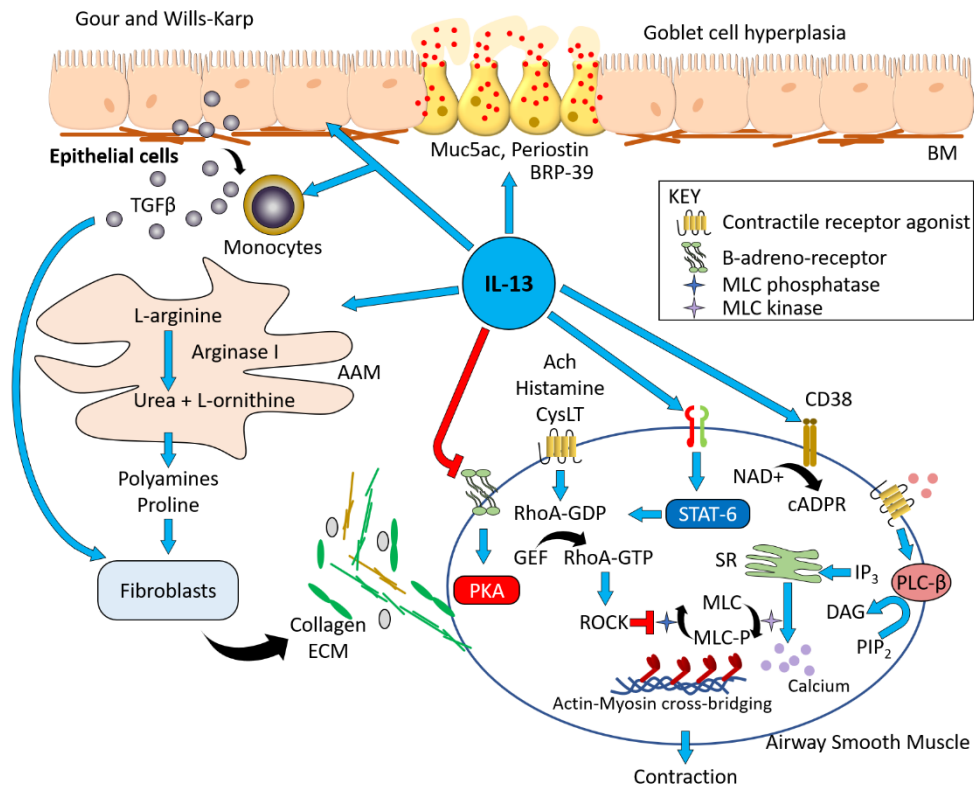


Figure 1.12: Potential mechanisms of IL-13-induced airway hyperresponsiveness.

IL-13 causes several cellular alterations in the airway wall that may help explain airway hyperresponsiveness, the primary physiological symptom of asthma. These include generation of mucus and mucus cell metaplasia; contraction of the smooth muscles of the airways; and deposition and fibrosis of collagen. Image has been modified from Gour and Wills-Karp (2015).

1.13 Host-Pathogen Interaction Models for Studying *S. aureus*

Different models have been used to investigate *S. aureus* colonisation and infection of the human respiratory tract, which has led to the development of colonisation models that make it possible to study the interaction of *S. aureus* with the respiratory tract. The development of an effective model of *S. aureus* infection is crucial for the development of an effective vaccine against the disease (Kiedrowski et al., 2016), and it will also aid in understanding of the process of infection.

Medina et al. (2019) investigated the interaction between the host and the pathogen using bronchial epithelium cells and *S. aureus* bacterial strains. An *in vitro* infection model was developed using an 16HB14o epithelial cell line with differentiation, polarisation and a tight junction barrier, characteristics that render the cell line feasible for use in regenerating phenotypes (Callaghan et al., 2020). Furthermore, the protein profiling indicated that the

bacteria activate relatively similar responses to ensure adaptation to the intracellular environment irrespective of the polarisation of the epithelial cells (Medina et al., 2019).

A study that analysed the interaction between the skin and *S. aureus* showed that the corneal layer present in the skin epidermal cells differs from that present in other types of epithelial cells. The corneal cell layer provides an important barrier against *S. aureus*, although *S. aureus* can invade the host cell using different mechanisms and promote both colonisation and skin infection by disrupting the host defence (Krishna and Miller, 2012).

Cultured human airway Epithelial cells (calu-3) cells have also been successfully used to model *S. aureus* infections, specifically, the USA300 clinical isolate of community-associated MRSA (CA-MRSA). Calu-3 cells are a human cell line from an adenocarcinoma that grow as adherent culture and exhibit epithelial morphology (Zhu et al., 2010). The viability of the Calu-3 airway epithelial cells was reduced when they were infected with *S. aureus*, likely because *S. aureus* secretes a damaging agent that destroys the epithelial cell layer (Kiedrowski et al., 2016).

Furthermore, ALI co-culture models have been used to study the interaction between *S. aureus* and the airway (Kiedrowski et al., 2016). This study investigated how infection with *S. aureus* triggers the immune responses of epithelial cells in conjunction with the inflammatory cells and using either primary cells or cell lines. The colonisation of the bacteria take place on the apical surface of the epithelial cells, as observed via microscopy, with clumps and single-cell interactions being seen between the host and pathogen. The qPCR technique was used for the expression analysis of *S. aureus* grown in the co-culture media. Here, alpha-toxin (Hla) was reported to be the main damaging agent with regard to the epithelial cells. A similar three-dimensional (3D) culture model has also been developed to study the interaction between *S. aureus* and skin tissue (Shambat et al., 2015). This model allows for the investigation of how the pathogen attaches itself to the skin, grows and manipulates layers of the epidermis.

As previously described, *S. aureus* is an important bacterium that causes generally colonises the upper respiratory tract and the colonial complex group CC30 strains are known to be associated with colonisation, although the mechanism behind their colonisation process remains unclear (Sharma-Kuinkel et al., 2015). A co-culture model was developed whereby *S. aureus* colonised the apical surface of the polarised human airway epithelial cells (Deplanche et al., 2019). The results were clear, as the wild-type *S. aureus* killed the airway epithelial cells in less than 24 hours, whereas the mutated variant that lacked alpha-toxin (HLA) persisted for more than 24 hours (Deplanche et al., 2019). These strains showed a lack of severe toxicity

towards the airway epithelial cells. The results were validated by means of qPCR, whereby the PCR of known virulence factors showed the expression profile of *S. aureus* grown in the co-culture to correlate with that reported in previous human colonisation studies (Wood et al., 2021). Moreover, noteworthy changes in the physiology of *S. aureus* were observed during a microarray analysis in the co-culture model involving lipid and amino acid metabolism. This subject needs to be studied further in order to determine the specific *S. aureus* interactions that occur with the host epithelia *in vitro* (Morgene et al., 2018).

1.14 Hypothesis

The hypothesis of this work is that human bronchial epithelial cell lines or primary cells can be used *in vitro* to study the mode of initial *S. aureus* infection of respiratory tract.

1.15 Objectives

The objectives of the study were to validate the use of immortalized bronchial epithelial cell lines (HBEC3-KT and BMI-1) in direct comparison with the use of primary airway cells as models to investigate the pathogenesis of *S. aureus* infection, and to investigate the host factors associated with *S. aureus* infection in cultured and differentiated bronchial epithelial cells.

1.15 This project consisted of three major aims:

1. To undertake differentiation studies with immortalized airway cell lines in comparison with primary human bronchial epithelial cells to see if they could be used as tractable models of the differentiated mucociliary epithelium.
2. To establish *S. aureus* infections in undifferentiated HBEC3-KT cells and primary HBECs
3. To establish and characterize *S. aureus* infections in differentiated human airway epithelial cell models.

CHAPTER 2: Material and Methods.

2.1 Culture of immortalized and primary human bronchial epithelial cells

2.1.1 Cell culture, splitting and maintenance of growth

For my thesis work, I used two types of human airway cells, immortalized cell lines and primary airway cells. I used two immortalized cell lines, human bronchial epithelial cell line (HBEC3-KT) and BMI-1 cells. HBEC3-KT cells were originally generated from primary human bronchial epithelial cells (HBEC) via overexpression of hTERT and CDK4 (Ramirez et al., 2004). The cells were provided by Dr. Frank McCaughan (Department of Biochemistry, University of Cambridge). The cells were routinely cultured in T25cm² tissue culture flasks using Keratinocyte-SFM (Gibco) containing 25 mg/ml bovine pituitary extract and 2.5 µg/ml human recombinant EGF (Davis et al., 2015). BMI-1 cells were derived from primary HBECs immortalized via transduction with the polycomb complex protein BMI-1. They have been reported to differentiate in ALI culture (Munye et al., 2017, Torr et al., 2016). Cells were provided by Professor Steve Hart (UCL GOS Institute of Child Health), who cultured the cells in a growth factor-supplemented bronchial epithelial cell growth medium (BEGM) (Munye et al., 2017). In my study, BMI-1 cells were cultured in T25cm² tissue culture flasks using Pneumacault™ Expansion Plus medium containing 10 ml Pneumacult Ex⁺ 50X Supplement and 96 µg/ml hydrocortisone (STEMCELL Technologies Inc.).

I also undertook studies with human primary cells (PromoCell) isolated from the surface epithelium of bronchi. Information about the batches is given in Table 2.1. Primary cells were cultured in T25cm² tissue culture flasks using Pneumacault™ Expansion Plus medium containing 10 ml Pneumacault™ Ex⁺ 50X Supplement and 96 µg/ml hydrocortisone.

All cells were incubated in an incubator set at 37 °C with a 5% carbon dioxide level and 95% humidity. Cells were cultured for 3 to 5 days until they reached a confluence of 70–90%. At this stage, the cells were split and introduced into new tissue culture flasks using the Detach Kit from PromoCell as follows. The culture medium was removed and the cells were washed twice with Hank's Balanced Salt Solution (HBSS; Gibco by Life Technologies). In the next step, the cells were trypsinized using trypsin-EDTA (TE) (Detach Kit, Promo Cell) to remove them from the tissue culture flask. Next, a trypsin inhibitor was added at an equal volume. The suspension was transferred to a 15 ml centrifuge tube and centrifuged at 1000 rpm for 5 min in order to pellet the cells. The cell pellet was resuspended in freshly prepared Keratinocyte-SFM for HBEC3-KT cells and Pneumacault™ Ex⁺ for BMI-1 and HBE cells and then centrifuged again.

The cells were split in different ratios to ensure that they would not become too confluent. The splitting ratio used generally was 1:5, where 1 ml of cells was diluted with 5 ml of the Keratinocyte-SFM and Pneumacault™ Expand⁺ media.

Table 2.1. List of Primary Cell Donors (Lot Nos.).

Donor	Age	Sex	Lot Nos.
Donor 1	50	Male	446Z036.9
Donor 2	52	Female	455Z016.1
Donor 3	62	Male	458Z015
Donor 4	74	Male	458Z006.1
Donor 5	65	Female	404Z008.2
Donor 6	59	Female	424Z015.3
Donor 7	69	Male	451Z006
Donor 8	56	Female	432Z016.5
Donor 9	79	Male	458Z009
Donor 10	60	Male	459Z013

2.1.2 Seeding cells onto transwells and differentiation at the ALI

For this step, cells were seeded either with and without the use of rat-tail collagen type I (Corning). Collagen coating helps cells to stick to the wells (Vaughan et al., 2006). Transwells were coated with 50µg/ml of rat-tail collagen type I for 3 hours at (37 °C), later washed with HBSS and air-dried. 0.4 µm pore Falcon A Corning Brand Polyethylene terephthalate (PET) membrane filters were used in all cases.

25,000 HBEC3-KT cells and 30,000 HBEC and BMI-1 cells were plated in each transwell. The cells were allowed to grow in the medium for 5 to 7 days until the submerged cultures became confluent. The composition of the medium for each cell line at this stage was as described above.

PneumaCult-ALI Basal Medium (STEMCELL Technologies Inc.) was used for the differentiation culture when the apical media was removed and the transwells were exposed to

the ALI. Fresh PneumaCult-ALI Basal Medium (supplemented with ALI maintenance supplement, heparin solution and hydrocortisone stock solution) was used to feed the cells in the basal compartment of the plates and their apical surfaces were washed with 200 μ l of warm HBSS every two days. Apical washes were stored frozen at -20°C for further use. The ALI culturing process was performed for 14–28 days. This step allows the cells to differentiate into a complex mucociliary epithelium that displays many characteristics of the native airway. During ALI culture, samples of cells were taken at days 0, 7, 14, 21, and 28 for RNA analysis. Some wells were also fixed for microscopy (see Section 2.7.1). The culture process is outlined in Figure 2.1.

In additional experiments, HBEC3-KT cells were subjected to one of two treatments. Some cells were treated with the γ -secretase inhibitor, N-[N-(3,5-Difluorophenacetyl)-L-alanyl]-S-phenylglycine t-butyl ester (DAPT; TOCRIS Bioscience). DAPT is a compound that inhibits the Notch signaling pathway. 10 mM DAPT in DMSO was diluted in PneumaCult-ALI Medium and added to the basolateral side of the cell cultures every 2 days (Wolfe, 2006, Gerovac et al., 2014). The resulting inhibition of the Notch signaling pathway was expected to enhance the production of FOXJ1⁺ ciliated cells (Gomi et al., 2015).

The second set of experiments involved stimulation of the basolateral compartment of the cell culture transwell using human recombinant interleukin 13 (IL-13; Sino Biological) at a concentration of 10ng/ml. This treatment was expected to induce the proliferation of goblet cells (Turner et al., 2011b). IL-13 diluted in PneumaCult-ALI Medium was added freshly to the basolateral side of the cell culture every 2 days.

2.1.3 Seeding undifferentiated cells

Undifferentiated (u) HBEC3-KT and HBE cells were seeded and grown to confluence in 24-well tissue culture plates. 25,000 HBEC3-KT cells and 30,000 HBECs were plated per well. The cells were allowed to grow in the medium for 5 to 7 days until the cultures became confluent.

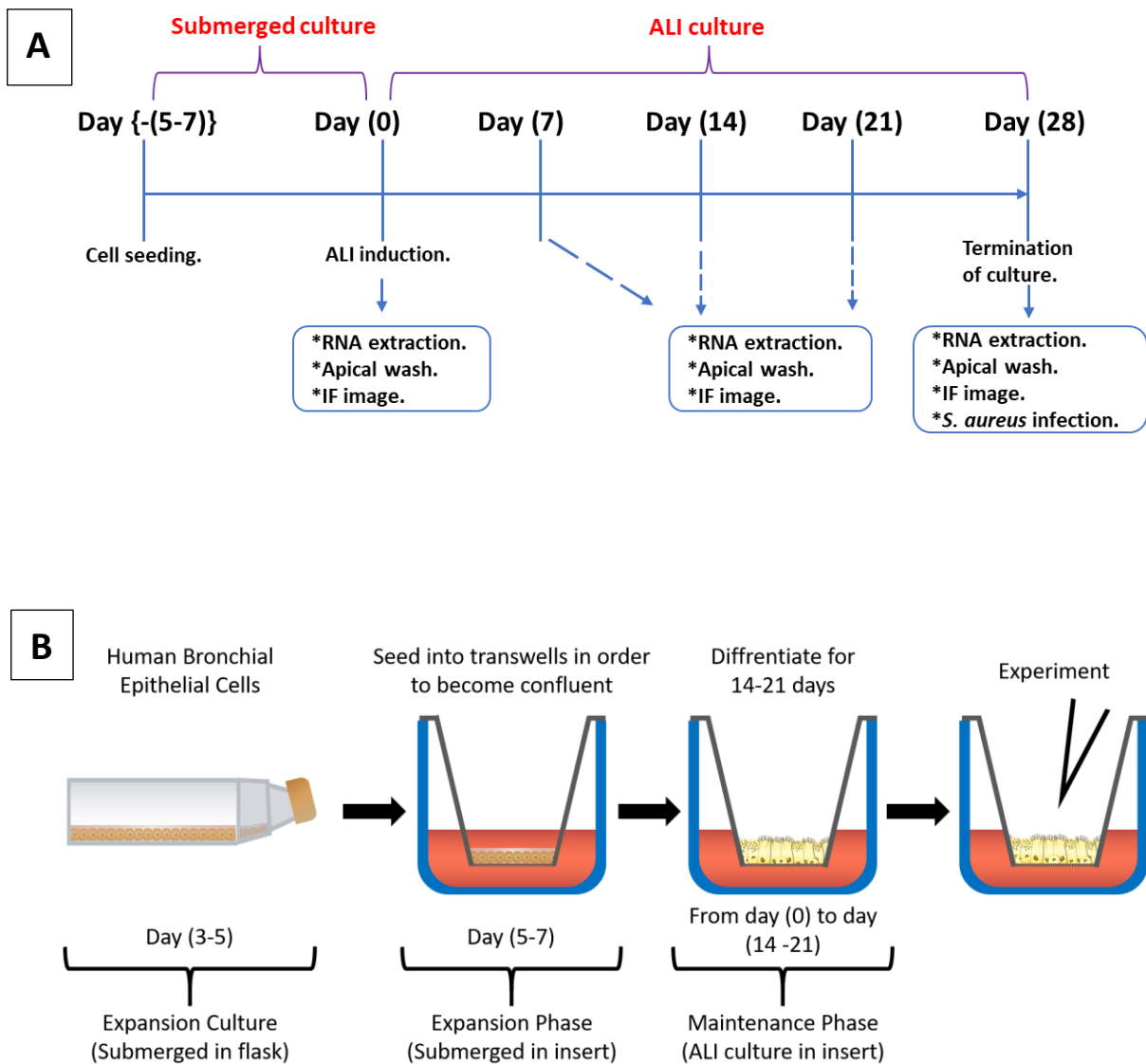


Figure 2.1. Schematic of the timeline and method of ALI culture experiments.

The timeline for culture of cells lines and HBECs is outlined. ALI conditions were induced upon the cells reaching confluence. At regular intervals, samples for transcriptional and protein analyses were taken (A). Cells were cultured in flasks to increase their number cells; they were then cultured in a submerged phase on transwells until they reached a confluent state. Then the apical medium was removed, and the cells were cultured at the ALI for 14-28 days prior to being used in experiments (B).

2.2 Ribonucleic acid (RNA) extraction

Washed cells were directly lysed in wells or on Transwells using 250 μ l TRIreagent (Sigma-Aldrich) as described previously (Rio et al., 2010) and RNA was extracted using the Direct-zol RNA MicroPrep (Zymopure) method as follows. An equal volume of ethanol was added to the lysed cell suspension, which was then processed through a mini-column (Stead and Kushner, 2016). Subsequently, the columns were treated with deoxyribonuclease (DNase) in DNA Digestion Buffer to digest the genomic DNA and the solution was allowed to stand at room temperature (RT) for 15 minutes. Following this, washing steps were performed according to the supplier's protocol (Supplementary Protocol VI). Finally, to elute the RNA, 15 μ l of DNase/RNase-free water was added directly to the column matrix prior to elution using a mini-centrifuge. The quantity and quality of RNA were determined by Nanodrop spectrophotometer analysis. The RNA was then stored at -20 °C until required.

2.3 Complementary DNA (cDNA) synthesis

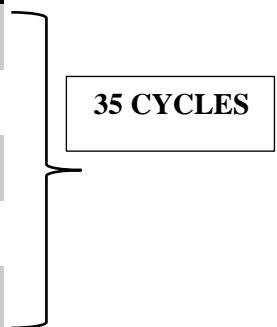
To synthesize cDNA from the RNA, 200 ng of RNA was added to oligo(dT) (0.5 μ l) and the volume was made up to 10 μ l with nuclease-free water. This mixture was heated at 70 °C for 7 minutes in a thermocycler. Thereafter, 0.25 μ l each of reverse transcriptase (AMV-RT) and ribonuclease inhibitor (Rnasin) were added, along with 0.5 μ l (10 mM) deoxynucleotide triphosphates (dNTPs; (Schoenbrunner et al., 2017) and 5 μ l AMV buffer. The volume of the mixture was made up to 20 μ l with the addition of nuclease-free water. All reagents were purchased from Promega. The mixture was placed in a thermocycler for 60 minutes at 42 °C, followed by 5 minutes at 95 °C. The samples were then stored at -20 °C.

2.4 Reverse transcription polymerase chain reaction (RT-PCR)

For this procedure, a master mix containing all reaction components except the cDNA was used. cDNA was prepared as described above. RT-PCR was performed in a reaction volume of 20 μ l (19 μ l master mix and 1 μ l cDNA). The master mix contained 7 μ l H₂O (water for injection), 1 μ l oligonucleotide primers (forward and reverse), and 10 μ l Maxima Hot Start (Thermo Fisher Scientific) or FastGene Optima PCR HotStart ReadyMix (Nippon Genetics), to which 1 μ l of cDNA was added. The solution was placed in the thermocycler (Bioer Genetouch – BTC33BAS) and amplified, using the program outlined in Table 2.2.

Table 1.2. PCR program for RT-PCR.

Program Step	Temperature	Duration
Initial denaturation	95°C	4 minutes
Denaturation	95°C	1 minutes
Annealing	60°C	1 minutes
Extension	72°C	1 minutes
Final synthesis	72°C	10 minutes
Final hold	4°C	N/A



2.4.1 Primers for PCR

The PCR primers that used in this project were previously designed and validated in the lab by other lab members (Table 2.3). All amplicons crossed intron/exon boundaries. All primers were resuspended in nuclease-free water (water for injection) and stored at -20 °C.

Table 2.3. List of primers.

Primer	Sequence (5'-3')	Product size (bp)
OAZ1 Forward	CCAACGACAAGACGAGGATT	164
OAZ1 Reverse	AGCGAACTCCAGGAGAACTG	
SCGB1A1 Forward	AGGACCGGGTATAAGAAGC	279
SCGB1A1 Reverse	TGTAGATGCTCCAGTCTCGG	
SCGB3A1 Forward	AGGACCGGGTATAAGAAGC	230
SCGB3A1 Reverse	TGTAGATGCTCCAGTCTCGG	
CBE1 Forward	GGTCAGAGCTTGAGGTAGCAT	241
CBE1 Reverse	GAGTTGTAACAGCACACTGCA	
TEKT1 Forward	TGGAGCTGTGTCGTCATGTC	198
TEKT1 Reverse	GCATACACAGCACTTCGTCG	
BPIFB1 Forward	CCCTGCCCAATCTAGTGAAA	207
BPIFB1 Reverse	TCACCTCCCCTGTGAGTCG	
BPIFA1 Forward	ATGCCCTCAGCAATGGCCTGC	466
BPIFA1 Reverse	GAGAGGCTGTCCAGAAGACC	
WFDC2 Forward	CCGACAACCTCAAGTGCTG	105
WFDC2 Reverse	CGAGCTGGGGAAAGTTAAT	
SLPI Forward	ATGAAGTCCAGCGGCCTCTT	412
SLPI Reverse	CATATGGCAGGAACTAATCT	
CXCL10 Forward	CCAATTTTGTCCACGTGTTA	190
CXCL10 Reverse	CCTCTGTGTGGTCCATCCTT	
IL6 Forward	CACACAGACAGCCACTCACC	218
IL6 Reverse	TTTCACCAGGCAAGTCTCCT	

2.5 Agarose gel electrophoresis

To analyze the results of the PCR, the DNA was loaded on agarose gels to visualize the amplified bands. For the preparation of the gel, 1–2 gm agarose powder (Seakem LE Agarose, Lonza) was mixed with 1X Tris, acetic acid, EDTA (TAE) buffer to prepare 1–2% gels. Higher percentage gels were used for smaller fragments (Bustin et al., 2015). After adding agarose to the buffer, the solution was heated in a microwave until the agarose dissolved fully. It was then cooled down and 1 µl ethidium bromide was added before the solution was poured into a casting tray. The gel solidified in around 20 minutes and was then placed in a gel tank filled with the TAE buffer, following which electrophoresis was performed. The gel was run at 80 to 90 V for 40 to 50 minutes, and the bands were then visualized under the UV camera in a BioRad ChemiDoc XRS+ System and images were also taken.

2.6 Quantitative polymerase chain reaction (qPCR)

qPCR was used to quantify the expression of the genes listed in Table 2.4, using a master mix with 2X qPCR BIO Probe Blue Mix Luna Universal (New England Biolabs). All TaqMan primers (Thermo Fisher Scientific) were labeled with FAM. A 2X *OAZI* TaqMan probe set labeled with VIC was used as the endogenous control in this experiment. A 10 µl reaction mixture containing 0.5 µl of the template cDNA was used and experiments were performed in triplicate. A 7900 HT Fast Real-Time PCR cycler (Rotor-gene Q 5plex, Qiagen) was used to run 40 cycles of the following program: 95 °C for 15 seconds, 60 °C for 60 seconds, and 95 °C for 15 seconds.

The endogenous control was used to assess the fold-change in the expression of genes of interest, wherein values calculated based on the qPCR were normalized to those of controls. The delta CT ($2^{-\Delta\Delta CT}$) method was used to quantify gene expression (Livak and Schmittgen, 2001). The cycle threshold (CT) refers to the number of cycles required for the fluorescent signals to reach a specified threshold, while the ΔCT value was used to differentiate between the observed CT values of the *OAZI* endogenous control and the genes of interest. Furthermore, the $2^{-\Delta\Delta CT}$ values showed the relative change in the expression of the genes of interest in different samples.

Table 2.4. TaqMan® gene expression assays used for qPCR experiments.

Gene	TaqMan® Gene Expression Assay ID
<i>OAZI</i>	Hs00427923_m1
<i>BPIFA1</i>	Mm00465064_m1
<i>BPIFB1</i>	Mm00600713_m1
<i>TEKT1</i>	Mm00495586_m1
<i>SCGB1A1</i>	Mm00442046_m1
<i>CXCL10</i>	Hs01124251_m1
<i>CXCL1</i>	Hs00605382_m1
<i>IL6</i>	Hs00174131_m1

2.7 Immunostaining and immunofluorescence microscopy of ALI cultures

2.7.1 ALI Culture Sample fixation

Prior to fixation the medium in the basal compartment was aspirated and the apical compartment of each transwell was rinsed with prewarmed HBSS. Then, 300 μ l of 10% formalin was added to the apical side and 700 μ l to the basolateral side. The transwells were incubated at RT for 45–60 minutes, followed by a washing step using phosphate buffered saline (PBS) equilibrated at RT. The samples were then stored at 4 °C in PBS.

2.7.2 Fluorescence immunocytochemistry

The PBS added at the end of the fixation step was removed from each transwell. Then, 300 μ l of blocking buffer (goat serum diluted 1:10 in PBS with 0.5% Triton X) was added and the transwells were placed on a shaker set to 80 rpm for 60 minutes. The blocking buffer was removed from the apical surface and the surface was washed and rinsed again with PBS. Subsequently, a final volume of 300 μ l primary antibody in blocking buffer was added to the apical compartment of each transwell and the solution was allowed to shake at 80 rpm in a cold room for 24 hours. The primary antibodies used in the study are listed in Table 2.5.

Table 2.5. Primary antibodies in immunostaining.

Primary antibody	Dilution	Manufacturer
BPIFA1(Rabbit Ab, polyclonal)	1:400	Non-commercial (Campos et al., 2004)
BPIFB1(Rabbit Ab, polyclonal)	1:300	Produced in lab (Musa et al., 2012)
FOXJ1(Mouse Ab, monoclonal)	1:200	Affymetrix eBioscience (2A5)
MUC5B (Rabbit Ab, polyclonal)	1:300	Santa Cruz Biotechnology (H-300)
Acetyl-α-Tubulin (Rabbit Ab, polyclonal)	1:300	Cell Signaling Technologies (Cat. # 5335S)

Following the overnight incubation, the primary antibody solution was aspirated from the apical surface. The apical and basal transwell compartments were washed again three times with PBS. Then, 300 μ l secondary antibody (Table) in blocking buffer was added to the apical chamber, the transwell was covered with foil to protect it from light, and the solution was allowed to shake at 80 rpm at RT for about 60 minutes.

Table 2.6. Secondary antibodies in immunostaining.

Secondary antibody	Dilution	Manufacturer
Alexa Fluor 568 Goat anti-rabbit Ab. (Red)	1:200	Life technology (Cat. # A11001)
Alexa Fluor 488 Goat anti-mouse Ab. (Green)	1:200	Life technology (Cat. # A11011)

Finally, the secondary antibody solution was removed and the transwell was washed with PBS. The membrane on which the cells were present was cut out carefully and sections were placed on to a glass slide. A single drop of the nuclear stain, DAPI (Vector Laboratories, Inc.) was applied to the cells on the slide and the mixture was incubated at RT for 2 minutes. The slide was covered with a coverslip and sealed with nail polish, followed by a 30-minute incubation to dry the nail polish (Singh et al., 2016). Slides were then refrigerated in sealed boxes to protect from light, until observation under a confocal microscope (FV-1000, Olympus). Images were acquired in the Light Microscope Facility of the Department of Biomedical Science at the University of Sheffield. The ZOE Fluorescent Cell Imager (Bio-Rad) was used for the analysis of infection studies of undifferentiated cells. The software ImageJ-win32 was used to analyze the images.

2.8 Protein analysis

2.8.1 Proteomic data analysis

Proteomic analysis was undertaken using apical washes recovered from differentiated HBEC3-KT cells and primary HBECs as described in Section 2.1.2. A total of 50 μ l of each sample was digested and 18 μ l was injected for 2 hours. The sample was analyzed by nanoflow LC-MS/MS using an Orbitrap Elite (Thermo Fisher; (Barnes et al., 2021)). The initial validation analysis was undertaken by Dr. Mark O. Collins (Department of Biomedical Science, University of Sheffield) Protein group output files generated by MaxQuant were loaded into Perseus version 1.6.10.50. The extracellular compartment database of the Human Protein Atlas, UniProt, and the Pride Archive software were used to identify extracellular proteins. Data analysis to separate extracellular proteins from other proteins was done using Python (v. 3.6.13), a heatmap was generated using the ‘pheatmap’ package of R through the ClustVis web tool (Bioinformatics, Algorithmics and Data Mining Group (BIIT)), and a correlation clustering distance row was applied. A heatmap is a clear way to visually represent protein

abundance in samples. The rows denote proteins and columns denote the samples. A principal component analysis (PCA) was performed using the abundance of proteins identified in each condition, and the results were visualized using the 'ggbiplot' package through the ClustVis web tool (Vu, 2011). To analyze other group data P value less than 0.05. then top 50 were selected.

2.8.2 Human Cytokine Array

The Human Cytokine Array Panel A Kit (R&D Systems) was used to evaluate the secretion of a panel of human cytokines into the apical fluid by cells following infection. The kit is designed to measure 36 different human chemokines and cytokines that play important roles in inflammatory signaling in both the innate and adaptive immune systems. The assay was performed according to the manufacturer's instructions using 500 µl of the apical secretion wash and media. Equal volumes of the apical secretion washes and media were pooled from three different batches of HBEC3-KT and HBE cells to produce the required volume. A pooled mock infected sample from both cell types was used for comparison in these assays. The EZ-ECL Chemiluminescence Detection Kit based on horseradish peroxidase (HRP) was used to detect the cytokines through the visualization of sample-antibody-HRP complexes. For visualization purposes, membranes were inserted in a plastic sleeve and 1 ml each of Reagents 1 and 2 were applied to the membrane. The complexes were exposed to X-ray film for 30 minutes inside a dark room. The film was then developed, washed, and fixed. Subsequently, the manufacturer's instructions were followed to use densitometry to analyze the results. The Image Studio Lite software (LI-COR Biosciences) was used to analyze each dot resulting from pixel density (signal values). The GraphPad Prism 8 software (GraphPad Software, Inc.) was used to plot and visualize data.

2.9 Culture of *Staphylococcus aureus* (*S. aureus*)-GFP

S. aureus strain SH1000, is a laboratory strain derived from *S. aureus* strain NCTC 8325 (Bæk et al., 2013). *S. aureus*-GFP (Boldock et al., 2018) (referred to as *S. aureus*) was provided by the group of Dr. Lynne Prince (Department of Infection, Immunity and Cardiovascular Diseases, University of Sheffield). *S. aureus* was grown on Brain-Heart Infusion (BHI) agar (Sigma-Aldrich) plates overnight at (37 °C). Then, a single bacterial colony was picked, added into BHI culture broth (Sigma-Aldrich), and incubated overnight (37 °C/5% CO₂) in an orbital shaker (200 rpm). Subsequently, the optical density (OD) of 1 ml of the overnight bacterial culture was measured at a wavelength of 600 nm using a spectrophotometer calibrated with 1 ml of uninoculated BHI broth. Following the overnight culture, a sub-culture into 10 ml of

broth was performed to generate log-phase bacterial stocks having an OD 0.7–0.9. Then, the culture was aliquoted into 1 ml tubes and frozen at $-80\text{ }^{\circ}\text{C}$. A schematic representation is given in Figure 2.2.

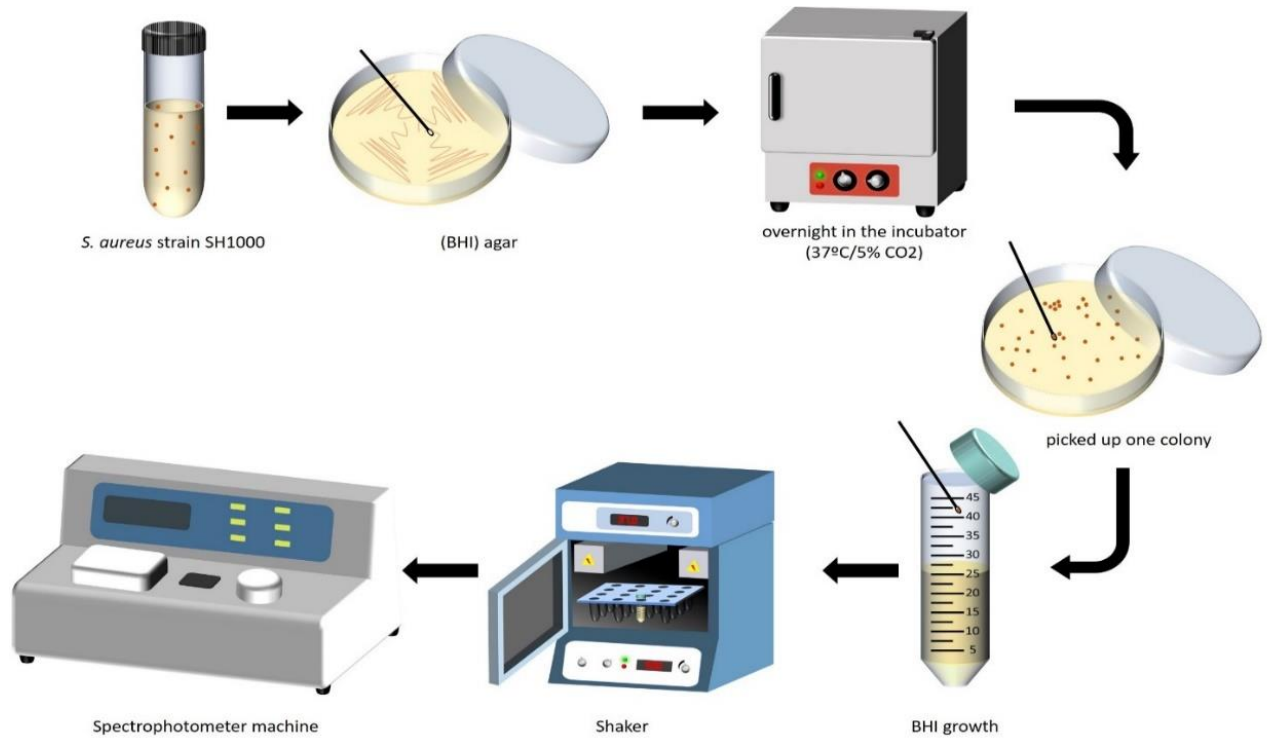


Figure 2.2. Schematic to show the method of culture of *S. aureus*.

S. aureus strain SH1000 was grown on Brain-Heart Infusion (BHI) agar overnight, one single colony was picked up and cultured with (BHI) growth media for overnight in laboratory shaker incubator, and then measured using spectrophotometer.

2.10 Miles Misra protocol for colony forming unit (CFU) count

Serial dilutions of the frozen stock were performed for each fresh stock to evaluate the CFU. 900 μ l PBS was added to defrosted bacterial suspension (100 μ l) and the mixture was vortexed. A 1:10⁶ dilution was serially diluted five times. Dilutions from 10³ -10⁶ were labelled on BHI plates after their division into eight segments. 10 μ l of each dilution was added to each plate after tubes were vortexed, and this step was repeated twice for every tube. Incubation conditions were set at 37°C, and plates were incubated overnight after they were dried. Counting of colonies and subsequent calculation of CFU/ml was performed the next day according to following standards.

1. Viable count was calculated by dividing number of colonies in segment by 3, which would be equal to average CFU divided by 10 μ l.
2. For that dilution, CFU/ml was calculated by multiplication by 100.
3. In dilution, factor would be multiplied by 10^{'segment number'}.

2.11 Infection of cell cultures with *S. aureus*

2.11.1 Undifferentiated cell infection

Undifferentiated (u) HBEC3-KT and HBE cells were seeded and grown to confluence in 24-well plates. These were infected with bacteria for 1 hour with growth medium at different multiplicities of infection (MOIs; 0.01, 0.1, and 1) at 37°C. Subsequently, cells were washed twice with HBSS, and grown for periods of 1, 2, 4, and 24 hours. The culture medium was collected at different time points and samples were serially diluted to obtain viable bacterial counts, while others were spine the bacteria down and frozen. Cells from two wells were lysed using Tri-Reagent for RNA extraction.

2.11.2 Differentiated cell infection

S. aureus was added to the apical surface cells differentiated at the ALI for 1 hour with growth medium; then, cells were washed twice with HBSS. Cells were infected with an MOI of 1 for 2, 4, 8, 16, and 24 hours. Subsequently, washes were taken from the apical surface of the cultures for counting bacteria, and the culture was continued as required. Transwells were washed basolaterally with HBSS to remove excess medium and fixed for approximately 40 minutes in 10% phosphate-buffered formalin (basolateral and apical compartments; see Section 2.7.2). The samples in two transwells were lysed in Tri-Reagent for RNA extraction and two others were washed with 200 μ l of HBSS for protein collection.

2.11.3 Visualization of HBEC3-KT and HBE cells exposed to *S. aureus*

To determine the intensity of *S. aureus* infection in undifferentiated (u) HBEC3-KT and HBE cell cultures, live undifferentiated (u) HBEC3-KT and HBE cells exposed to *S. aureus* were imaged using the ZOE Fluorescent Cell Imager (Bio-Rad) for the periods 1-, 2-, 4- and 24-hours post-infection. Images were taken of four fields on every 24-well plate to define an area for quantification. The mean integrated intensity of the four fields was used to calculate bacterial infection intensity using the ImageJ-win32 application. For quantification, three independent batches of uHBEC3-KT and uHBE cells were examined.

In the same way, differentiated HBECs exposed to *S. aureus* were imaged (see Section 2.7) for the periods 2-, 4-, 8-,16- and 24-hours post-infection. At 40x magnification, images of four fields of each membrane were obtained to determine the quantification area. The mean integrated intensity of the four fields was used to calculate bacterial infection intensity using the ImageJ-win32 application. For quantification, three independent batches of HBECs were analysed.

2.12 Statistics

Statistical analyses were performed where necessary. For RT-qPCR, normalized expression values of individual genes were compared across samples by paired t-test. For multivariate RT-qPCR analysis, one and two-way analysis of variance (ANOVA) were carried out. These analyses were done using GraphPad Prism 8 software (GraphPad Software, Inc.). For statistical analysis of proteomic data, Clustvis web was used, or the individual protein expressions was compared by paired t-test using GraphPad Prism 8. A P-value < 0.05 was considered statistically significant.

CHAPTER 3: Rationalizing a tractable model for human airway using cells grown at the air liquid interface (ALI).

3.1 Introduction

As outlined in the introduction the airway epithelium consists of multiple specialized cell types that generate an efficient innate defensive shield throughout the respiratory tract. Over the years much effort has been made to establish in vitro culture models that can replicate this complex cellular organization.

In 1990, human tracheobronchial cells were used to perform culturing of differentiated cells at the air liquid interface (ALI) (Wu et al., 1990). This study defined a set of conditions that allowed the process of differentiation to occur in the cultures. The development of the mucociliary phenotype was the key characteristic of this technique. In this technique, a surrogate of the human airway was obtained through development of epithelial layer with pseudostratified appearance when the cells were grown at the ALI. The use of this experimental tool has increased over time due to the recognition that the specific organization of the phenotype of the cultures replicates many aspects of the native airway epithelium. Various growth factors such as retinoic acid, epidermal growth factor and insulin were determined to be essential in the development of cilia and differentiation of mucous cells in these airway cell cultures (Lechner et al., 1982, Wu et al., 1985, Randell et al., 2001, O'Boyle et al., 2018). Various protocols with subtle modifications have been developed since the initial establishment of the model (Koo et al., 1999, Ross et al., 2007, Kettle et al., 2010, Dvorak et al., 2011, Villenave et al., 2013, Hiemstra et al., 2019).

The differentiation state of the cultures produced by these different methods has generally been considered to be essentially equal when judged using gene expression analysis and morphological methods. The identification of marker genes that track with the process of differentiation has been confirmed through use of whole genome transcriptional analyses (Ross et al., 2007). This study confirmed that multiple genes such as *MUC5AC*, *MUC5B*, *BPIFA1*, and *BPIFB1* are induced during differentiation. Coupled with analysis of specific protein detection and much more recently developed, single cell RNA sequencing approaches (Choi et al., 2020), it is clear that these genes can be used as markers to confirm the differentiation of specific cells in the cultures.

Primary cells used to perform the ALI culture method (Hiemstra et al., 2018) can be obtained from various sources. They can be isolated directly from patients through resection of tissue or bronchoscopic brushings or biopsies and they can also be obtained through commercial sources. A significant limitation of the use of primary cells obtained from human donors, is

that due to their finite ability to divide in culture, limited number of cells for experimental use can be obtained. However, there are a number of different techniques that can be used to amplify the cells in culture including their treatment with Rho-associated protein kinase inhibition (ROCKi) (Horani et al., 2013), dual SMAD signaling inhibition (Mou et al., 2016), and feeder cells-based expansion of cells, a technique called conditional reprogramming (Butler et al., 2016). Another drawback of the use of primary cells is the marked inter-donor variations that can be seen in responses and cell phenotypes (Longo et al., 2012). However, the most important characteristic of differentiated primary ALI cells is that the cultures are largely representative of the mucociliary airway epithelium found in human airway linings and so it is now generally appreciated that the use of such cultures is warranted for studies of airway biology.

Differentiation and cellular growth within these models can be altered through use of different media or treatments. For example, a recent comparative study of the use of different types of media in the cultures revealed that different expansion of epithelial cells was achieved when they were grown in BGEM or PneumaCult medium along with ROCK inhibitor (Rayner et al., 2019). DAPT (Gerovac et al., 2014) and IL-13 (Seibold, 2018) are two molecules which have shown to modulate cell differentiation, DAPT is a gamma secretases inhibitor to treat abnormal cells in such diseases. This inhibitor downregulates the effects of the NOTCH signaling pathway which is important to increase the production of FOXJ1+ve ciliated cells (Gomi et al., 2015). Th2 cytokine, IL-13 has been shown to increase goblet cells numbers (Turner et al., 2011a, Seibold, 2018). In murine models, IL-13 has been used to increase the development of mucous cell metaplasia. This cytokine is highly involved in the development of diseases of the respiratory system such as cystic fibrosis and during the immune response stage of development of asthma (Tyner et al., 2006, Curran and Cohn, 2010).

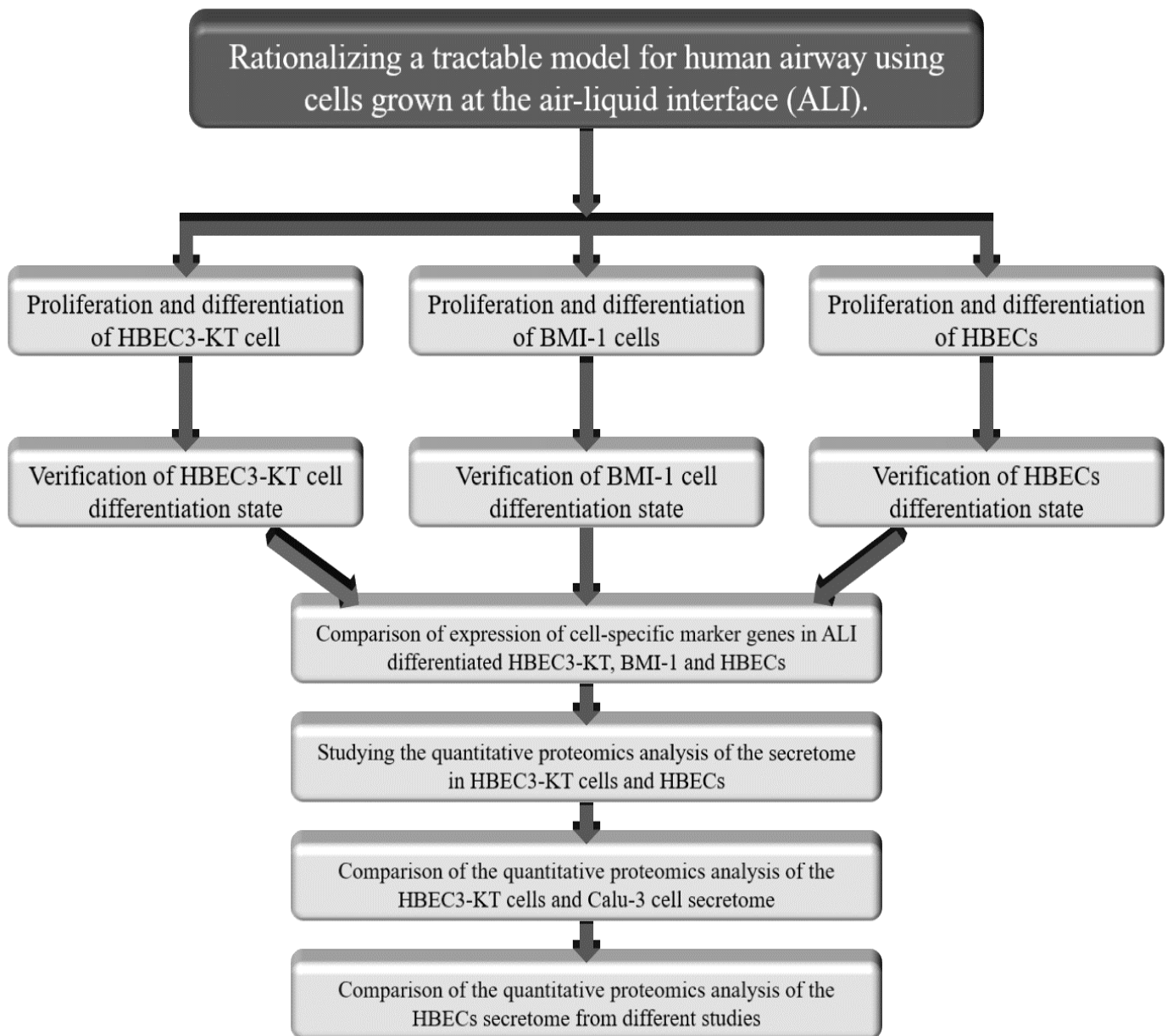
Although, differentiated primary airway cells grown at the ALI are increasingly used in pulmonary studies there is still a place for the use of cell line derived models in pulmonary research. Generally speaking, cell lines become tumorigenic due to several genetic mutations; the influence of these mutations on the retention of specific attributes representing cell type in the tissue of origin is not clear. This is specifically accurate for the genetic expression of airway epithelial genes. For instance, Stewart et al. (2012) reported that the BEAS-2B cell line did not form tight junctions between cells in culture. In contrast, in Calu-3 cells, the staining of β -tubulin implied that cilia were not found, although MUC5AC was identified, suggesting the formation of secretory cells.

In this study, the following two immortalized cell lines have been utilized to research the airway epithelium. HBEC3-KT cells were generated by transfection of hTERT and Cdk4 (Ramirez et al., 2004) and BMI-1 cells were immortalized by transduction with polycomb complex protein BMI-1 (Munye et al., 2017).

3.1.1 Aims:

The main aim of this chapter was to undertake differentiation studies with immortalized airway cell lines in comparison with primary human bronchial epithelial cells to see if they could be used as tractable models for infection studies. To do this the following objectives had to be met:

- 1) To establish and validate cultures of HBEC3-KT cells at an ALI and modulate their phenotype through the addition of IL-13 and DAPT.
- 2) To establish and validate cultures BMI-1 cells at an ALI.
- 3) To directly compare cell line cultures with primary HBECs grown at an ALI.
- 4) To compare protein secretion between differentiated HBEC3-KT cells and HBECs.



Study plan for this chapter.

3.2 Results

3.2.1 Characterization of HBEC3-KT cells

To evaluate the morphology and growth of HBEC3-KT cells, cells were observed in submerged and ALI cultures. Initially, cells were cultured in flasks to expand their numbers. Cells were then cultured in a submerged phase following seeding on transwell membranes. Both collagen-coated and non-collagen-coated transwells were used for culture. Cells were seeded at concentrations of 25,000 per transwell (Figure 3.1) and Keratinocyte-SFM (KSFM) was used in this phase. Epithelial cell islands formed by the establishment of contacts between epithelial cells and their neighboring cells were observed. These appeared elongated, and when grown on plastic, the cells did not readily form a confluent monolayer (Figure 3.1A). Within seven days of seeding onto both coated and non-coated transwells, cells grown in submerged culture produced a confluent monolayer (Figure 3.1 B-C). Subsequently, cells were differentiated at the ALI for 21 days using a Pneumacult™ ALI medium in the basal culture chamber. They were observed under phase contrast microscopy (Figure 3.1F-I). The cellular morphology was similar on day0 but started changing from 14 days of ALI culture (Figure 3.1 F-G). Cell numbers were not counted under the different media conditions.

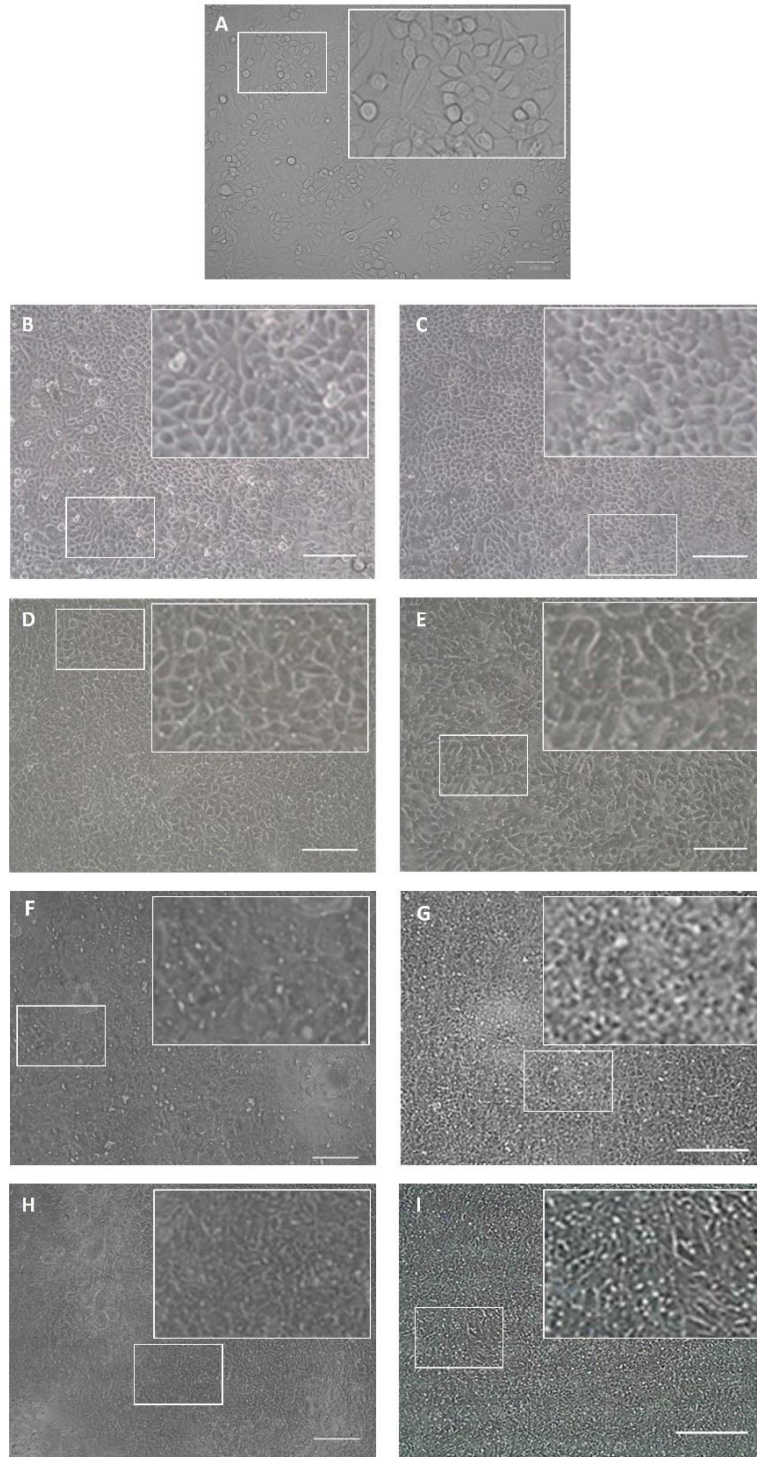


Figure 3.1: Morphological characteristics of HBEC3-KT cells during ALI differentiation on different days.

The images showed difference between the growth and morphology of cells growing in different transwells, provided under the same conditions. (A) Phase contrast images showing HBEC3-KT cells cultured at a submerged phase in traditional culture (Plastic). Scale bar = 100 μm . (B, D, F, and H) show ALI differentiation of the cell cultured in collagen-coated plates on days 0,7,14 and 21 respectively. (C, E, G, and I) show ALI differentiation of the cell cultured in un-coated plates on days 0,7,14, and 21 respectively. Images were captured at 10x magnification Scale bar = 120 μm .

3.2.2 Differentiation of HBEC3-KT cells when grown at the ALI

3.2.2.1 Gene expression by RT-PCR

In order to validate the differentiation of HBEC3-KT cells that were grown at the ALI, expression of a number of epithelial marker genes was analysed during the differentiation phase of cells cultured both on collagen coated and non-collagen coated transwells. RNA was extracted from cells at day 0 (when the cells were confluent but before air lift), day 7, day 14 and day 21 of differentiation and used for RT (endpoint) PCR. Ornithine decarboxylase antizyme 1 (*OAZ1*) is considered as a stable housekeeping gene (De Jonge et al., 2007) and was utilized as a control transcript for all PCRs. As presented in figure 3.2, *OAZ1* was expressed consistently across all cells. *CBE1* and *TEKT1* were used as markers of ciliated cells as they are well recognised as genes associated with motile ciliogenesis (Stead and Kushner, 2016). Both *CBE1* and *TEKT1* were expressed from day 7. *BPIFA1*, *BPIFB1*, *WFDC2*, *SLPI*, *SCGB3A1* and *SCGB1A1* are markers for secretory cells. There was a striking lack of expression of all of these genes in the day 0 undifferentiated cells, with the exception of *SLPI*. The expression of the other secretory genes was clearly seen from day 7, other than *SCGB1A1* which was expressed on day 14. From this analysis it appeared as if collagen pre-coating of the transwells had a limited effect on the gene expression of the different marker genes.

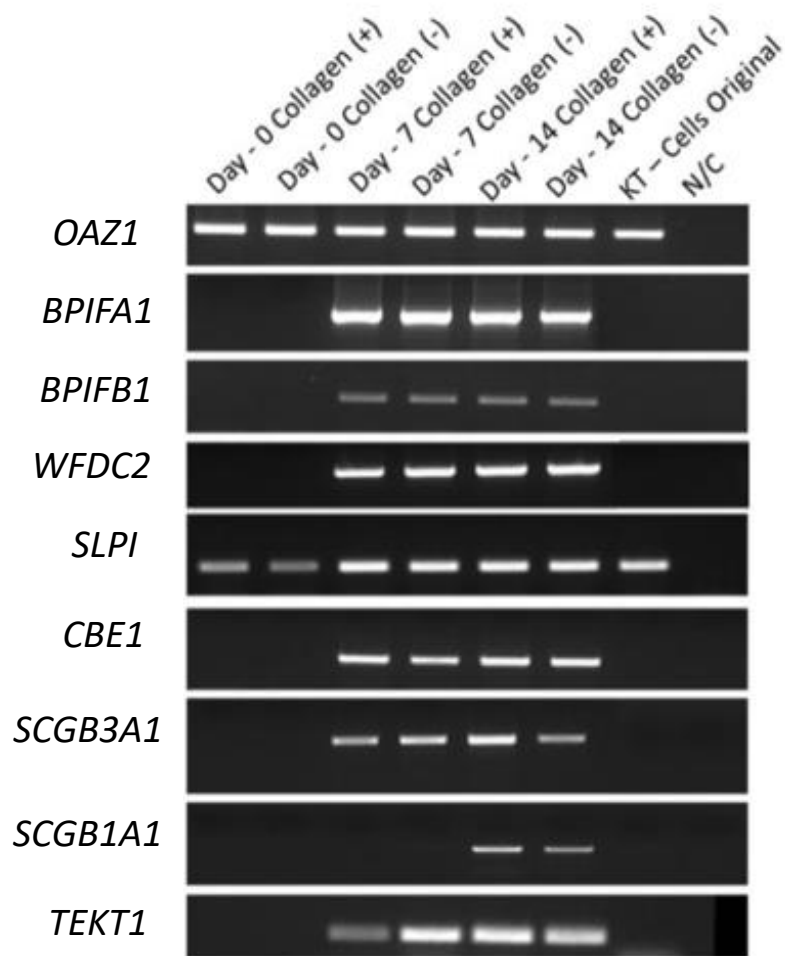


Figure 3.2: RT-PCR of gene expression during ALI differentiation of HBEC3-KT cells. RT-PCR was performed as described using cDNA of samples that were collected on the first, seventh, and fourteenth day of ALI culture. Samples represent the expression of genes in the cell cultured in collagen-coated (collagen+) and uncoated transwells (collagen-). Samples were amplified with primers *OAZ1*, *BPIFA1*, *BPIFB1*, *WFDC2*, *SLP1*, *CBE1*, *SCGB3A1*, *SCGB1A1* and *TEKT1*. This gel represents data from one of three separate replicate experiments. N/C is the negative control without cDNA.

3.2.2.2 Validation of gene expression in differentiating HBEC3-KT cells by RT-qPCR

RT-qPCR was used to quantify *BPIFA1*, *BPIFB1*, and *SCGB1A1* expression as markers for secretory cells and *TEKT1* as a marker for ciliated cells to gain a more quantitative understanding of the level of marker gene expression during cell differentiation. TaqMan primers were used to detect gene expression. Expression was normalised to the *OAZ1* endogenous control in the epithelial cells (explained in detail in the materials and methods chapter section 2.6). The results revealed that the expression of all these genes was undetectable in the undifferentiated condition for day 0 in both absence and presence of collagen samples (the expression was detectable very low level for *SCGB1A1* and *TEKT1* in the absence of collagen). Gene expression significantly increased at day 21 versus day 0 in the transwell membrane in both collagen conditions (Figure 3.3). Nevertheless, the relative fold expression was found to be varying for each gene. *BPIFB1* showed highest fold change on day 21 compared to other markers while the lowest fold change was observed in *TKET1*. This data is consistent with data in Figure 1.11 where *BPIFB1* is the most highly expressed gene and *TEKT1* is the lowest. There was no statistical difference between the two conditions in terms of gene expression at day 21. However, there was variable expression of these genes across the replicates.

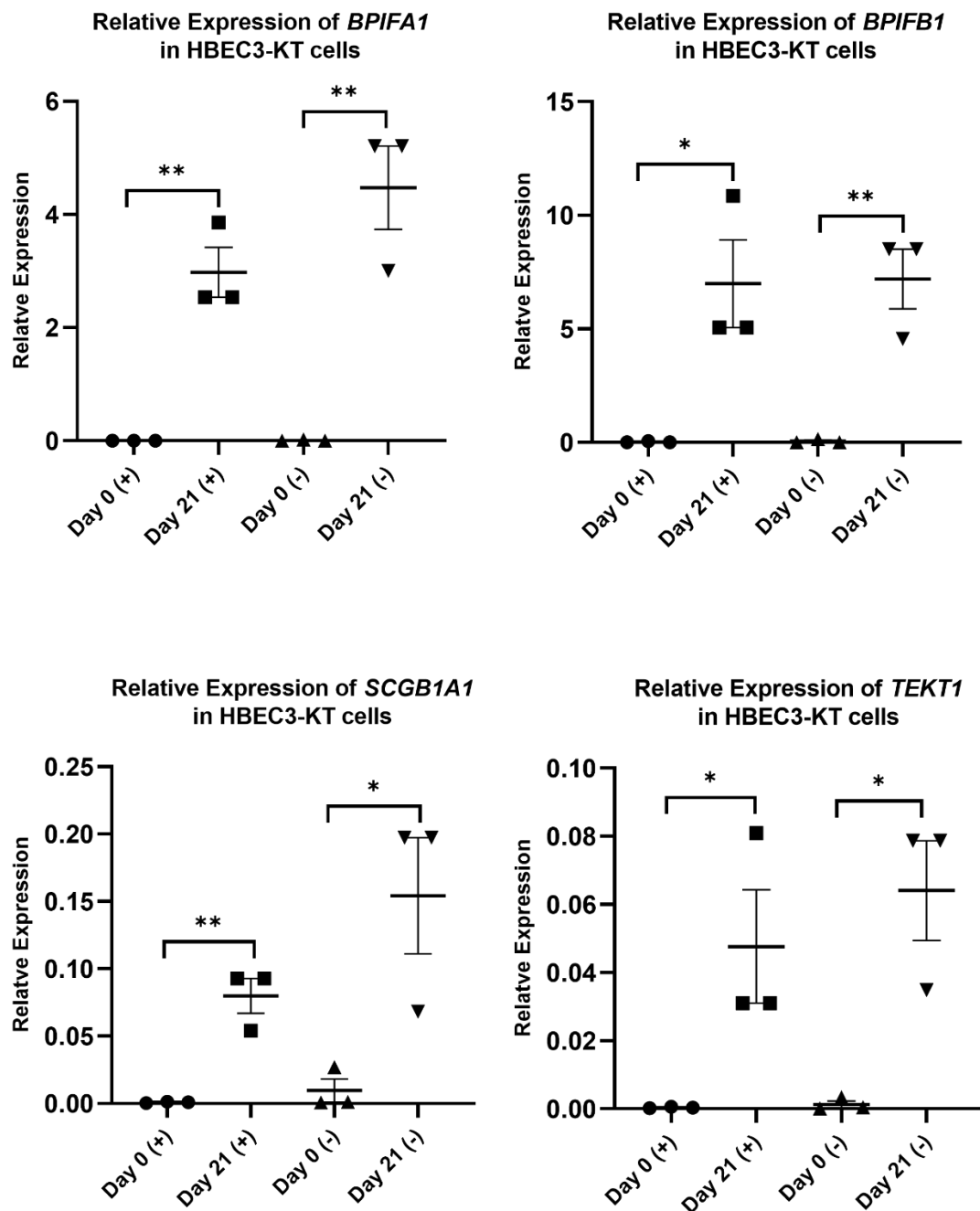


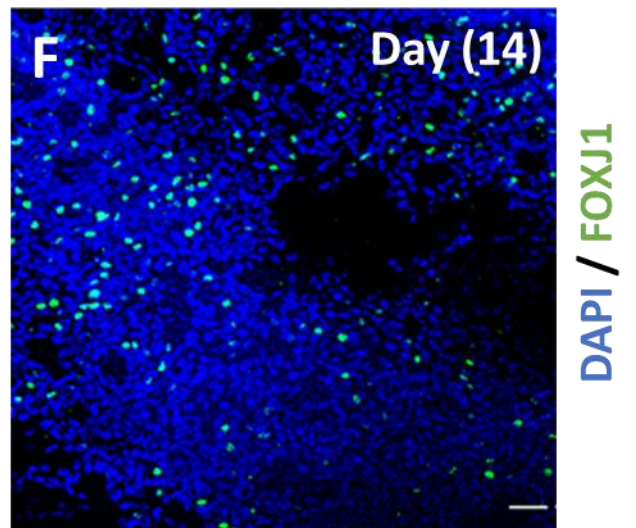
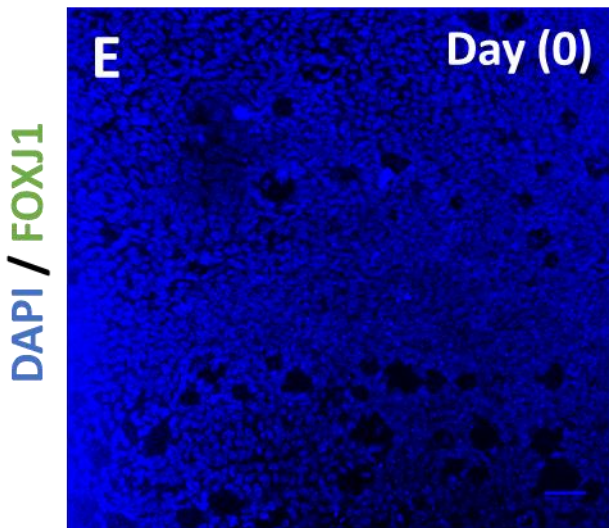
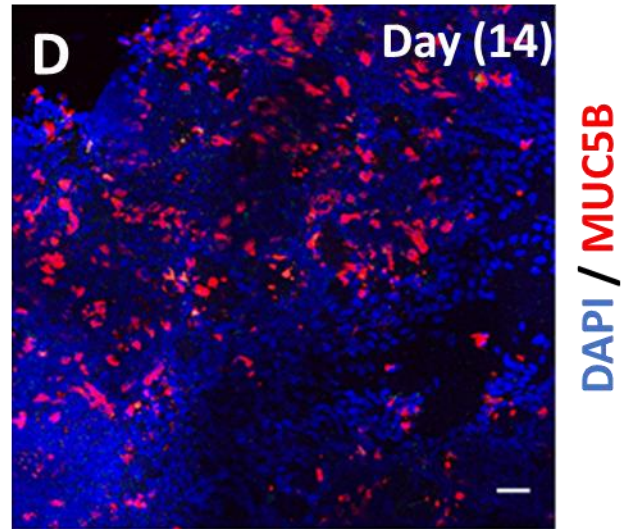
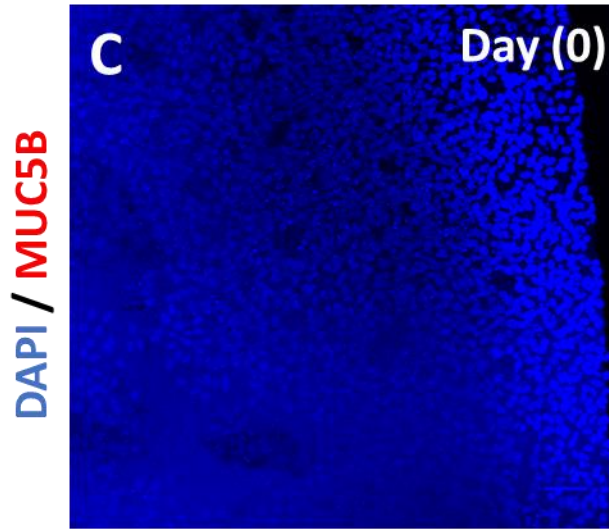
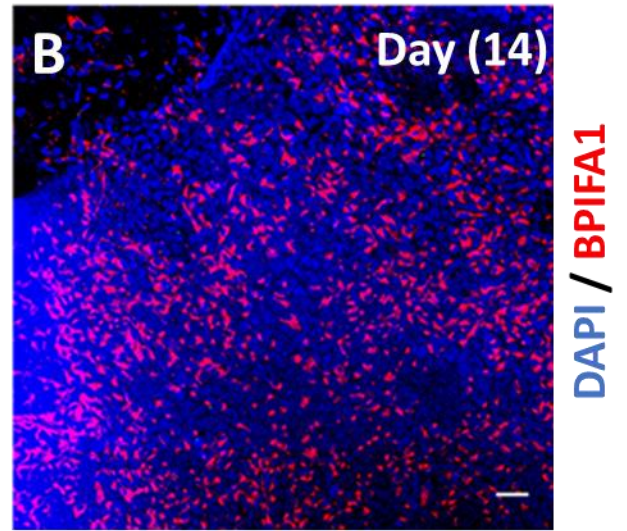
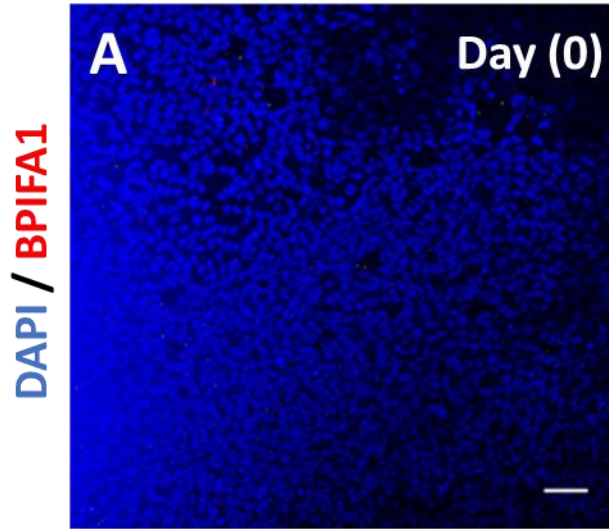
Figure 3.3: RT-qPCR analysis of gene expression during ALI differentiation of HBEC3-KT cells.

Data shown in the bar charts represent average gene expression levels of secretory (*BPIFA1*, *BPIFB1*, and *SCGB1A1*) and ciliated (*TEKT1*) markers in cells grown for 0 and 21 days, plus and minus collagen coating of the transwells. For each gene, the relative expression of mRNA was normalised to *OAZ1* as a control. The fold expression was calculated by comparing the CT values of the genes. Data were analysed using a paired t-test. Error bars: SEM. Analysis was done on 3 independent biological replicates. * $p < 0.05$ and ** $p < 0.01$. (+) or (-) indicate the presence or absence of collagen coating, respectively.

3.2.3 Immunofluorescence microscopy of airway epithelial markers during ALI culture of HBEC3-KT cells

Cells on transwells were stained with antibodies against airway epithelial cell-specific markers at different time points during the ALI differentiation to visualize the specific airway epithelial cells in the cultures. Antibodies against FOXJ1 were used to detect ciliated cells while those against MUC5B and BPIFA1 were used to detect secretory cells. Confocal microscopy was used to visualize the cells after staining. MUC5B, BPIFA1 and FOXJ1 staining was absent in ALI cultured cells on day 0 (Figure 3.4 A, C, and E). However, as shown in Figures 3.4 B and D, the secretory cell markers BPIFA1 and MUC5B were observed on day 14 suggesting the differentiation of a secretory cell population.

Similarly, as can be seen in Figure 3.4 F, the ciliated cell marker FOXJ1 was also visualized on day 14. Figure 3.4 G represents the fluorescence intensity of BPIFA1, MUC5B, and FOXJ1 on day 14 compared to the control on day 0 when there was no mucociliary differentiation. Overall, these results indicate that on day 14, the cells had differentiated from a population of basal cells (airway progenitor cells) to a differentiated population of airway epithelial cells.



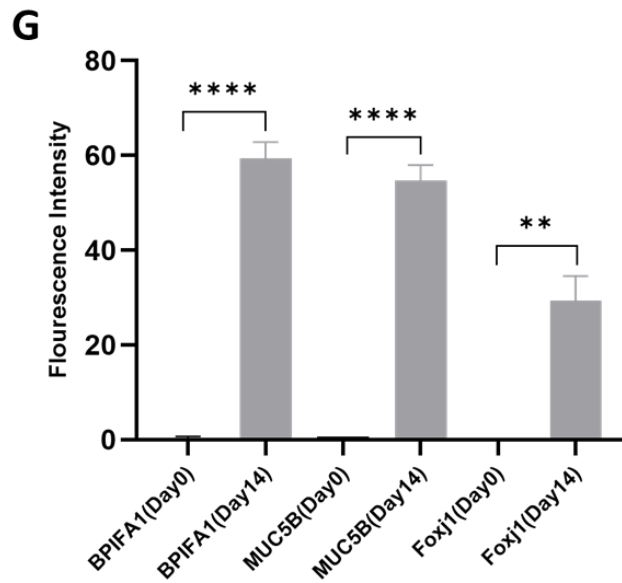


Figure 3.4: Immunofluorescence microscopy of differentiation of secretory and ciliated for HBEC3-KT cells.

Confocal image obtained under Olympus FV1000 confocal microscope (20X) and Fluoview® image analysis system for HBEC3-KT. FOXJ1 antibodies were visualized through staining with Alexa-fluor 488 green stain (secondary). Similarly, antibodies against MUC5B and BPIFA1 were visualized by adding Alexa Fluor 568 red stain secondary antibody to the HBEC3-KT cell cultures. DAPI was used to stain the nuclei (blue). Scale bar = 80 μ m. (G) The intensity of staining was measured in each of 3 replicated experiments. Data were analysed using a paired t-test. Error bars: SEM. ** $p < 0.01$ and **** $p < 0.0001$.

3.2.4 Modulation of HBEC3-KT cells differentiation with DAPT and IL13

As outlined in the introduction, the phenotype of primary airway cells grown at the ALI can be modulated pharmacologically to alter the cellular composition. Therefore, having validated the differentiation capacity of the HBEC3-KT cells when cultured at the ALI, I attempted to modulate the differentiation process by treating them with DAPT and IL-13. In these experiments, cells were treated with 10 μ M DAPT from ALI from day 0 to day 14 of culture. I also treated the HBEC3-KT cells with 10ng/ml IL-13, concentrations used in previous studies (Wilson, 2015). In one set of experiments, I treated cells from ALI day 0 to day 14 and another set of experiments I treated cells from day 7 to day 14 of ALI culture. Both modulators were added to the basolateral media during ALI culture and were changed whenever the basal media was changed.

As shown in Figure 3.5 end point RT-PCR appeared showed that *TEKT1* was more highly expressed on day 14 using DAPT treatment compared to control as shown by the apparent greater band density. Similarly, expression of *BPIFB1* was detected from day 7 and peak expression was observed on day 14. Higher expression of *BPIFB1* appeared to be seen when cells were treated with IL-13 in both treatments.

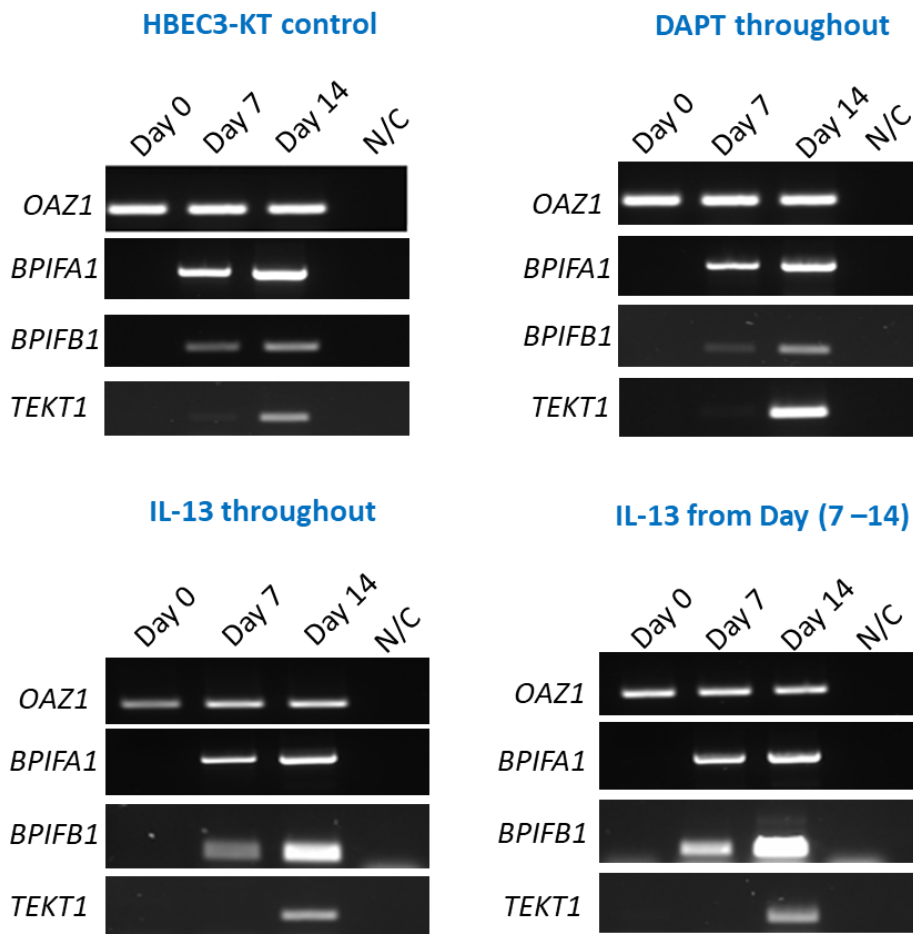


Figure 3.5: Gene expression during ALI differentiation of HBEC3-KT cells treated with DAPT and IL-13.

RT-PCR was undertaken using cDNA of samples that were collected on day 0, 7 and 14 of ALI culture following culture with DAPT or IL-13. The housekeeping gene *OAZ1* was used as a positive control and *BPIFA1* and *BPIFB1* used as markers for secretory cells and *TEKT1* used as a marker for ciliated cells. The figure represents one experiment that was replicated 3 times. All PCR reactions for each gene of interest were undertaken at the same time. N/C is the negative control without cDNA.

Subsequently, I generated quantitative data from these experiments for *BPIFA1*, *BPIFB1*, and *TEKT1* by RT-qPCR with TaqMan primers. Expression was normalised to the *OAZ1* endogenous control. The control cells were grown without any additions to the media. The expression of the markers in the control cells was measured on day 14. It was expected that IL-13 treatment would increase the number of goblet cells by inducing higher expressions of *BPIFA1* and *BPIFB1*, while DAPT treatment would produce more ciliated cells expressing *TEKT1*. My aim was partially achieved. Treatment with DAPT reduced the expression of goblet cell markers *BPIFA1* and *BPIFB1* and increased the expression of the ciliated cell marker, *TKET1*, compared with their expression in control cells. Throughout treatment of IL-13 had an effect completely opposite that of the DAPT treatment. With this treatment, as I expected, the ciliary marker *TKET1* expression was reduced compared with that in control cells. Meanwhile, the expression of *BPIFA1* increased. However, contrary to expectations, the expression of *BPIFB1* in IL-13 throughout treatment was decreased. The late treatment with IL-13 (from day 7 to day 14) had an effect on the expression of all the marker genes similar to that by IL-13 throughout treatment (Figure 3.6). This indicated that the throughout and later treatment of IL-13 resulted in similar gene expression patterns.

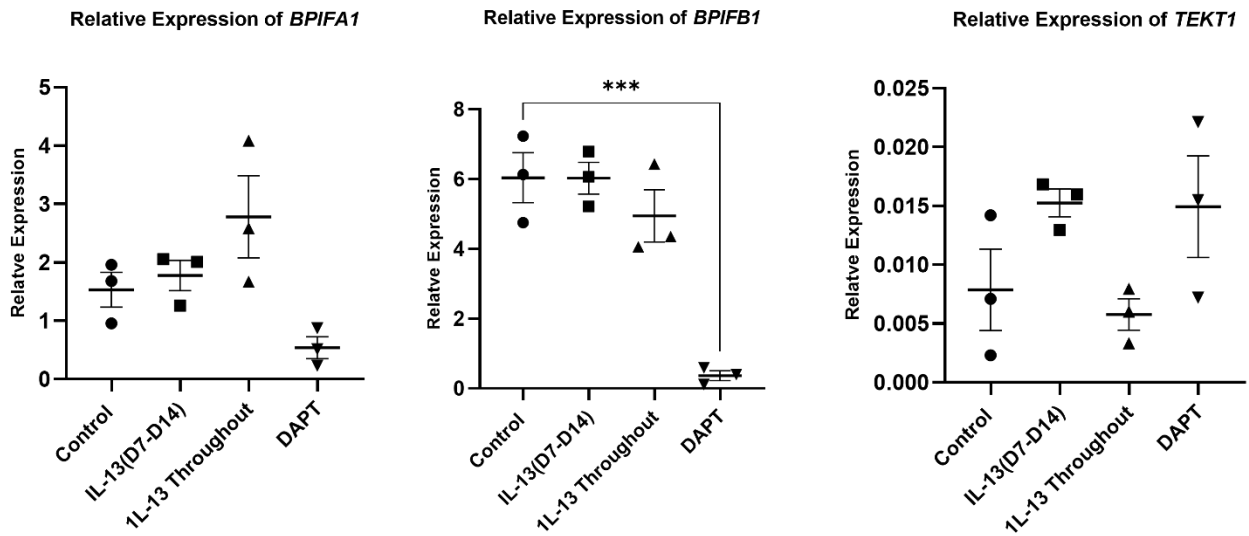


Figure 3.6: RT-qPCR analysis of gene expression during ALI differentiation of HBEC3-KT cells with DAPT and IL-13 treatments on day 14.

The data show levels are plotted along the y-axis and the treatment conditions along the x-axis. The expression of marker genes in the control cells was calculated on day 14. The relative expression of mRNA was normalised to *OAZ1* as a control. The fold expression was calculated by comparing the CT values of the genes. The data were analysed using a one-way ANOVA. Error bars: SEM. Analysis was done on 3 independent biological replicates. *** $p < 0.001$.

3.2.5 Differentiation of BMI-1 cells when grown at the ALI

Having shown that I was able to induce a mucociliary phenotype in the HBEC3-KT cells when they were grown at the ALI, I wanted to examine the ability of a further immortalized human airway cell line, BMI-1 (Munye et al., 2017) to differentiate at the ALI. In these experiments the cells were routinely grown in Pneumacault™ Expand⁺ media to directly compare with the HBEC3-KT cell experiments.

3.2.5.1 Gene expression by RT-PCR

BMI-1 cells were grown on both collagen coated and non-collagen coated transwells in an identical manner to the HBEC3-KT cell. The expression of selected cell-specific markers was examined to validate the differentiation of cells when they were grown at the ALI. RNA was extracted from cells at day 0, day 7, day 14 and day 21 and was initially used for end-point RT-PCR. *OAZ1*, the control gene was essentially equally expressed at all time points (Figure 3.7). BMI-1 cells expressed *BPIFA1*, *SCGB1A1* and *TEKT1* in all samples. This is particularly interesting as these markers were not expected to be expressed in the undifferentiated condition (day 0). *BPIFA1* expression did not appear to change over the time course of differentiation. However, expression of *SCGB1A1* and *TEKT1* appeared to increase over time but were seen prior to differentiation at the ALI. It was not clear to see any effect of the collagen treatment in this PCR data.

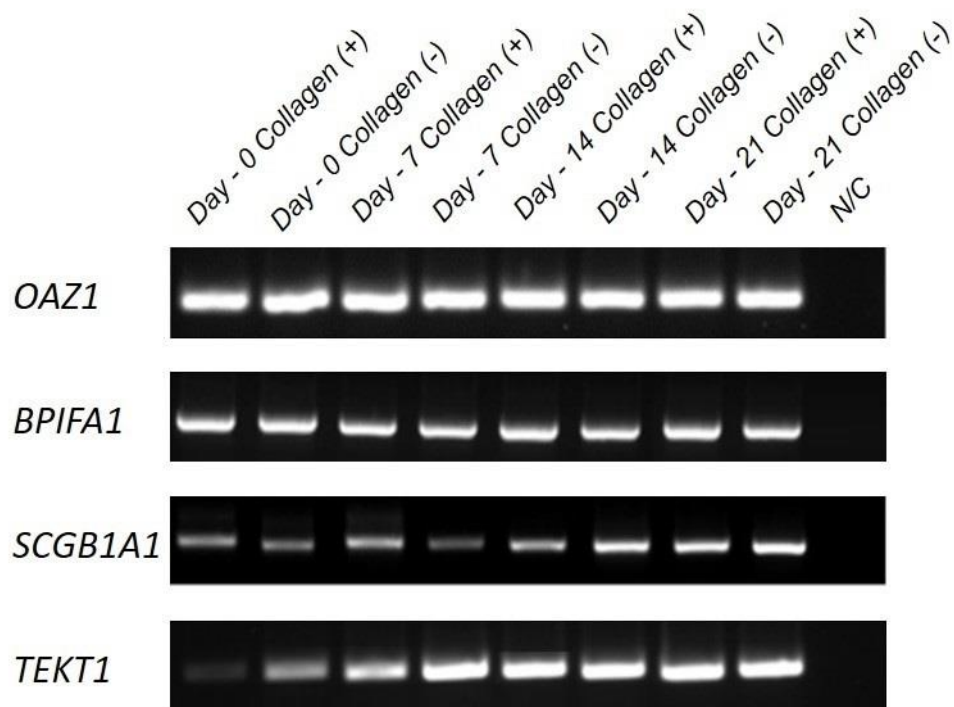


Figure 3.7: RT-PCR of gene expression during ALI differentiation of BMI-1 cells.

RT- Endpoint PCR was performed using cDNA of samples that were collected on day 0, day 7, day 14 and day 21 of ALI culture. Samples represent the expression of genes in the cell cultured in collagen-coated (collagen+) and uncoated transwells (collagen-). Samples were amplified with primers *OAZ1*, *BPIFA1*, *SCGB1A1* and *TEKT1*. The gel represents one experiment that was replicated 3 times. N/C is the negative control without cDNA.

3.2.5.2 Validation of gene expression in BMI-1 cell RNA samples by RT- qPCR

To gain a more quantitative understanding of the level of gene expression during the differentiation of the BMI-1 cells, RT-qPCR was used to measure the expression of *BPIFA1*, *BPIFB1*, *SCGB1A1*, and *TEKT1* using TaqMan primers. Expression was normalised to the *OAZ1* endogenous control. The relative gene expression against the reference gene is shown in Figure 3.8. The expression of the four genes in both the presence and absence of collagen was assessed. The results suggested a similar pattern of expression in *BPIFB1*, *SCGB1A1*, and *TKET1*, as the expression of all three genes was increased in both the conditions (collagen⁺ and collagen⁻) on day 21 in relation to the expression on day 0. There was also no difference between genes on the same day. Nevertheless, the relative expression was found to vary for each gene. The lowest fold change expression (from day 0 to 21) was seen in *TKET1*, which was less than 0.1 for both conditions. This suggests that BMI-1 cells do not ciliate at all upon differentiation. Moreover, the expression of these markers on day 21 in the collagen⁻ condition was higher than that in the collagen⁺ condition. This indicated possible inhibitory role of collagen on the expression of these markers.

There appeared to be a negative correlation between the collagen and *BPIFA1*, as its expression was decreased by \approx 2-fold in collagen-coated transwells. Because of the variation in the data this was not a statistically significant finding.

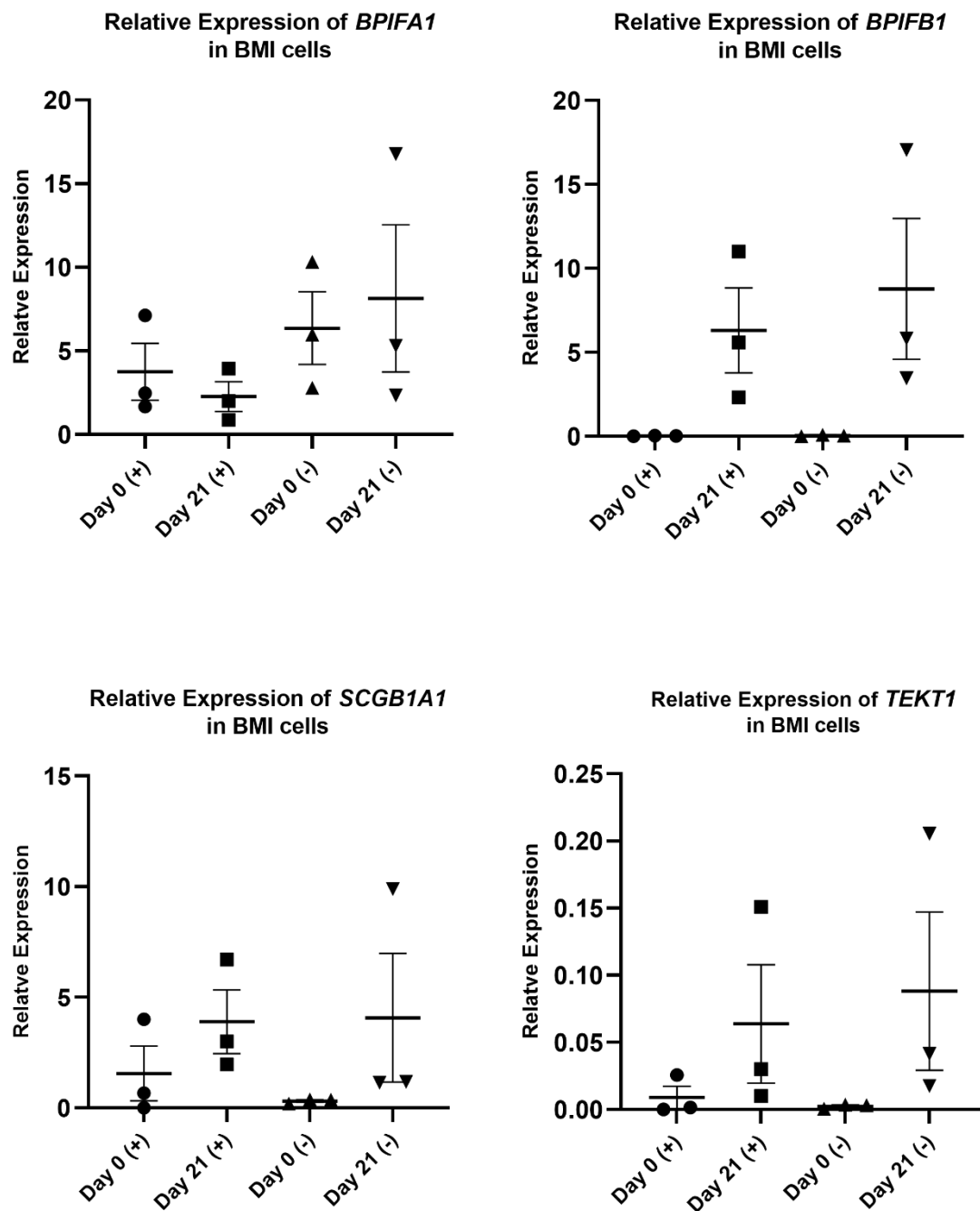
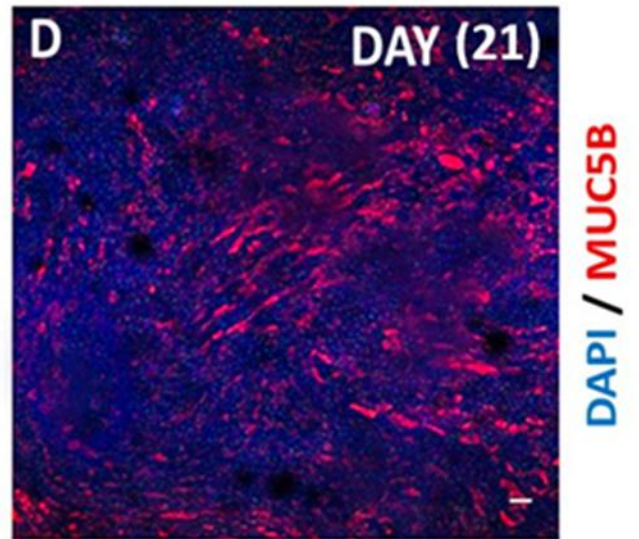
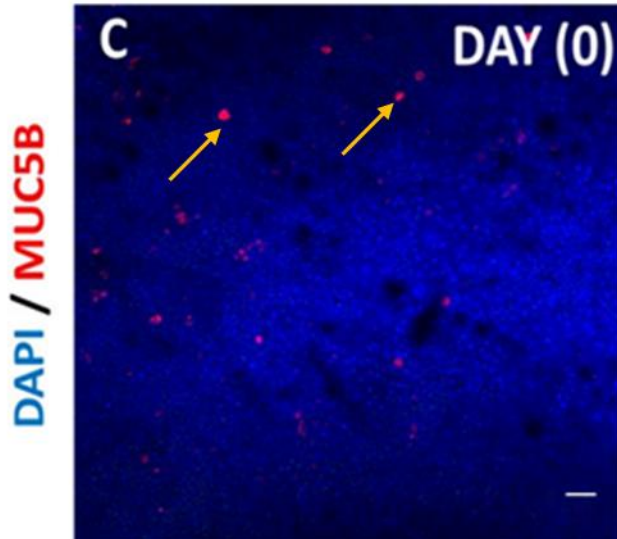
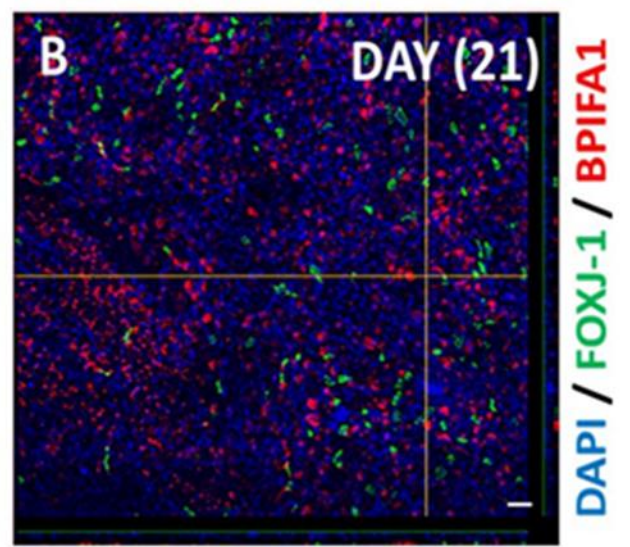
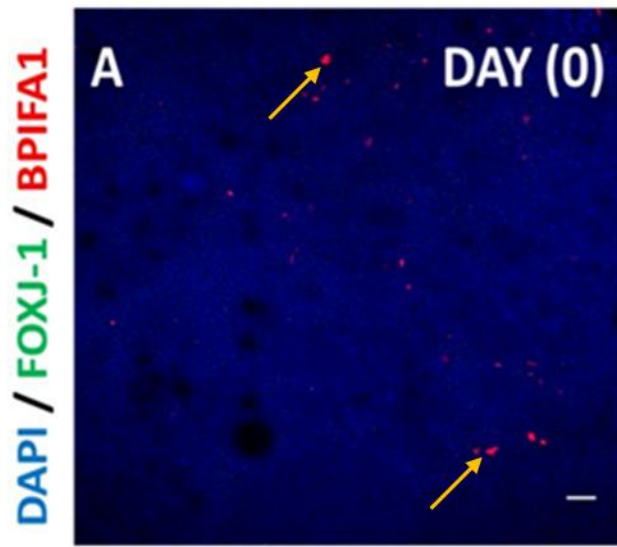


Figure 3.8: RT-qPCR analysis of gene expression during ALI differentiation of BMI-1 cells.

Data show the average expression levels are plotted against the multiple time points (Day 0 and Day 21); the relative expression of mRNA was normalised to *OAZ1* as a control. The fold expression was calculated by comparing the CT values of the genes. Data were analysed using a paired t-test. The Error bars represent SEM. Analysis was done on 3 independent biological replicates. (+) or (-) indicates the presence or absence of a collagen coating.

3.2.6 Immunofluorescence microscopy of airway epithelial markers during ALI culture of BMI-1 cells

Confocal microscopy was used to visualize transwells stained with antibodies against cell type specific markers during ALI differentiation. As shown in Figure 3.9A, on day 0, staining of FOXJ1 was absent but it was present on day 21 (Figure 9B). In contrast, and supporting the PCR data, some limited BPIFA1 staining was seen prior to differentiation at the ALI (Figure 9.A). However, on day 21 the staining was significantly increased (Figure 9B). Similarly, as illustrated in (Figure 3.9 C-D), MUC5B staining was present on day 21 showing the differentiation of a secretory cell population and, similarly to BPIFA1 it was also seen in a few cells prior to differentiation at the ALI (Figure 3.9C). Figure 3.9E, represents the fluorescence intensity of BPIFA1, MUC5B and FOXJ1 staining at day 21 relative to day 0. The staining intensity was assessed in four separate fields from one batch of cells and shows that relative staining levels of BPIFA1, MUC5B and FOXJ1, increases by day 21.



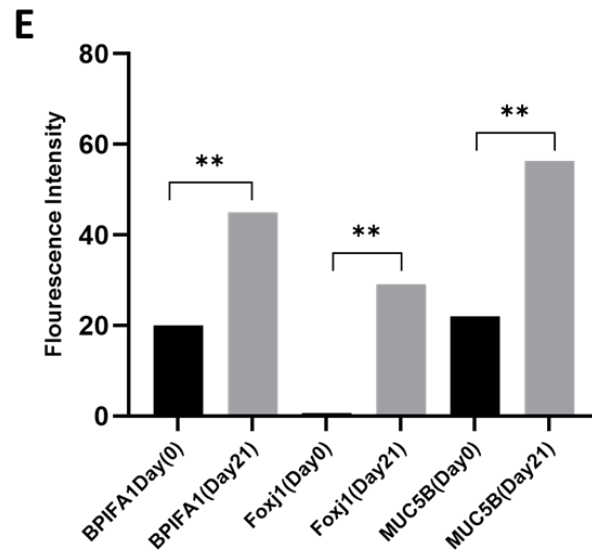


Figure 3.9: Immunofluorescence microscopy reflecting the differentiation of ciliated and secretory BMI-1.

Confocal image obtained under Olympus FV1000 confocal microscope (20X) and Fluoview® image analysis system for BMI-1 cells. FOXJ1 (primary) stained and Alexa-fluor 488 green (secondary), MUC5B and BPIFA1 (primary) stained and Alexa Fluor 568 red (secondary). DAPI was used to stain the nuclei (blue), Scale bar = 80 μ m. (E) The intensity of staining was measured in 4 independent fields. Data were analysed using a paired t-test. Error bars: SEM. ** $p < 0.01$.

3.2.7 Differentiation of HBECs when grown at the ALI

3.2.7.1 Gene expression by RT-PCR

Since I had used two types of immortalized cell lines (HBEC3-KT cells and BMI-1 cells), it was important to compare these cells with human primary cells.

As in the previous studies, primary HBECs (from different donors) were grown at the ALI on both collagen coated and non-collagen coated transwells and the expression of epithelial marker genes were analysed during the differentiation phase. Again, *OAZ1* was used as the endogenous control for all PCRs. As presented in Figure 3.10, *OAZ1* was expressed consistently in all time points during the differentiation of the cells. The single most striking observation to emerge from the data comparison was that HBECs expressed *BPIFA1* and *SCGB1A1* prior to differentiation at the ALI. This was intriguing because these markers were not expected to be expressed in undifferentiated state (day 0) prior to the ALI phase. Over the process of differentiation, the expression of *BPIFA1* and *SCGB1A1* did not seem to be increased. In contrast *TEKT1* expression was not seen in day 0 cells but increased in both collagen and non- collagen from cultures from day 7.

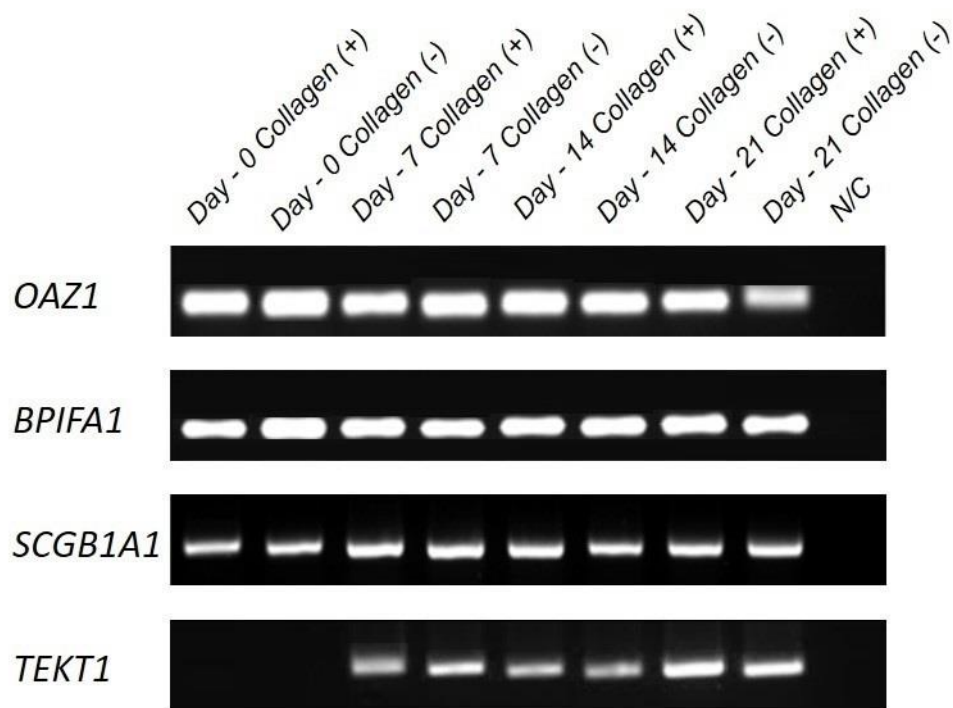


Figure 3.10: RT-PCR of gene expression during ALI differentiation of HBECs.

RT- Endpoint PCR was performed using cDNA of samples that were collected on day 0, day 7, day 14 and day 21 of ALI culture. Samples represent cells cultured in collagen-coated (collagen+) and uncoated transwells (collagen-). Samples were amplified with primers *OAZ1*, *BPIFA1*, *SCGB1A1* and *TEKT1*. This gel represents data from one of 3 separate replicate experiments. N/C is the negative control without cDNA.

3.2.7.2 Validation of gene expression in HBECs RNA samples by RT- qPCR

RT-qPCR was used to measure the expression of *BPIFA1*, *BPIFB1*, *SCGB1A1*, and *TEKT1*, using TaqMan primers to gain a more quantitative understanding of the level of gene expression during differentiation of the primary HBECs. As can be seen in Figure 3.11, the gene expression of all the genes increased from the undifferentiated state on day 0 to the differentiated state on day 21. However, the relative expression was different for each gene. For example, I observed the highest fold change in *SCGB1A1*, which increased about 30-fold from day 0 to day 21. *TKET1* expression was observed to be lower, as it increased less than 1-fold from day 0 to day 21. Similarly, the expression the genes, except that of *BPIFA1*, was observed to increase from day 0 to day 21. However, the relative expression values for each gene were different. *SCGB1A1* showed higher relative expression over time than the other genes. There was no significant increase in the relative expression of *BPIFA1* from day 0 to day 21. In summary, all the marker genes showed higher expression on day 21 in both the absence and presence of collagen coating. However, the fold changes varied for each gene. The exception was observed in *BPIFA1*, which showed no significant difference between day 0 and day 21 in the uncoated transwells.

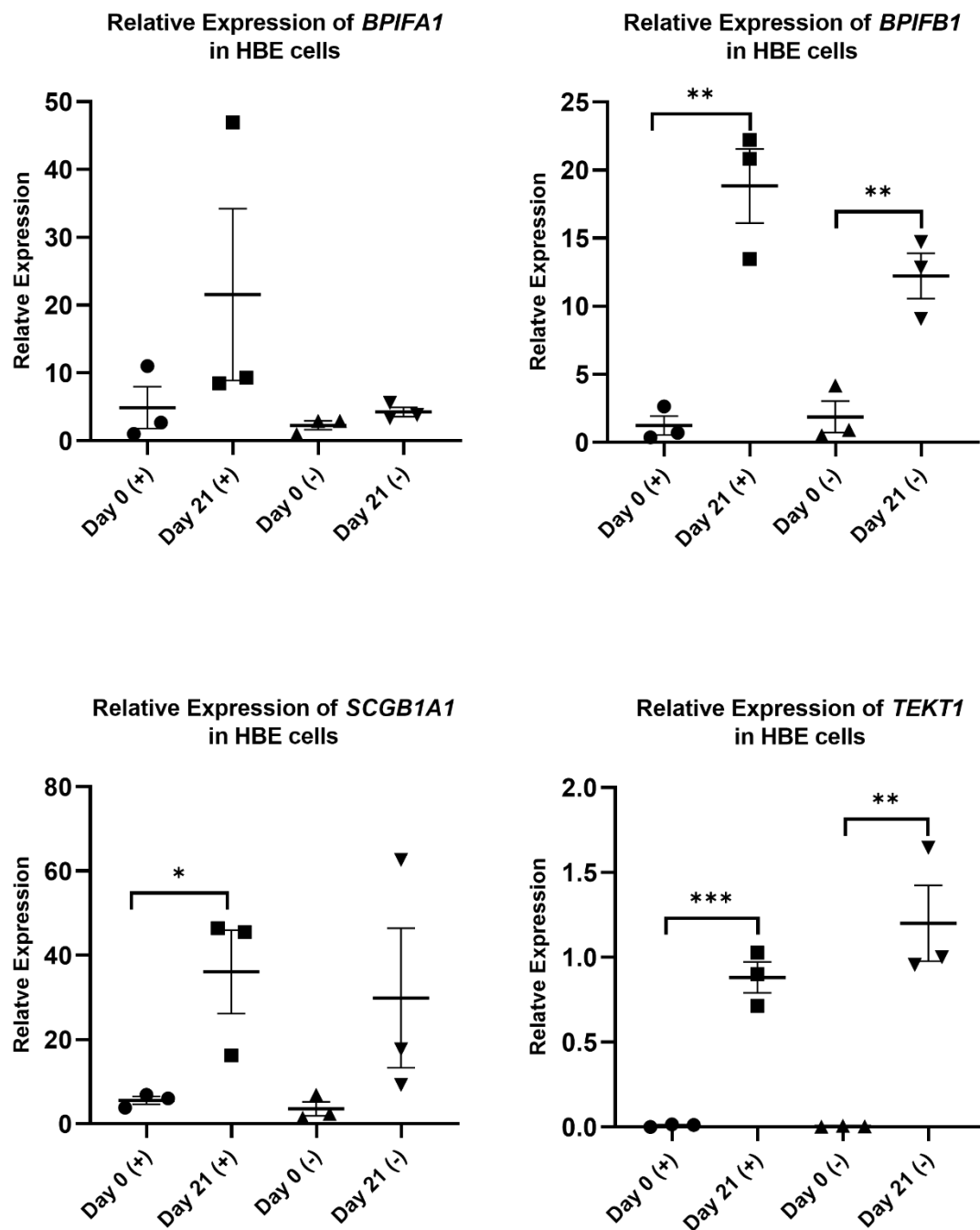


Figure 3.11: RT-qPCR analysis of gene expression during ALI differentiation of HBEs. Data represent the average expression levels are plotted against multiple time points/conditions. For each gene, the relative expression of mRNA was normalised to *OAZ1* as a control. The fold expression was calculated by comparing the CT values of the genes. Data were analyzed using a paired t-test. The error bars represent the SEM. Analysis was done on 3 independent biological replicates using cells from 3 different donors. * $p < 0.05$ and ** $p < 0.01$ and *** $p < 0.001$. (+) or (-) indicate the presence or absence of collagen coating.

3.2.8 Immunofluorescence microscopy of airway epithelial markers during ALI culture of HBECs

Cells were stained with antibodies against FOXJ1 (ciliated cells) and BPIFA1 (secretory cells) at various times during the ALI differentiation. Confocal microscopy was used to observe the cells following labelling.

FOXJ1 staining was absent on day 0, as shown in (Figure 3.12 A) and was present on day 21. In contrast, BPIFA1 expression began to differentiate from the first day, the results of the correlational analysis can be compared to RT-PCR data. However, when compared to day 0, the staining on day 21 was much more substantial. Quantitative data for BPIFA1 and FOXJ1, as can be seen in Figure 3.12C, presented as the fluorescence intensity of the two proteins relative to the first day demonstrates that both proteins increased significantly by day 21. These patterns are markedly different from those observed in HBEC3-KT cells, as HBECs showed more ciliated cells than the HBEC3-KT cells.

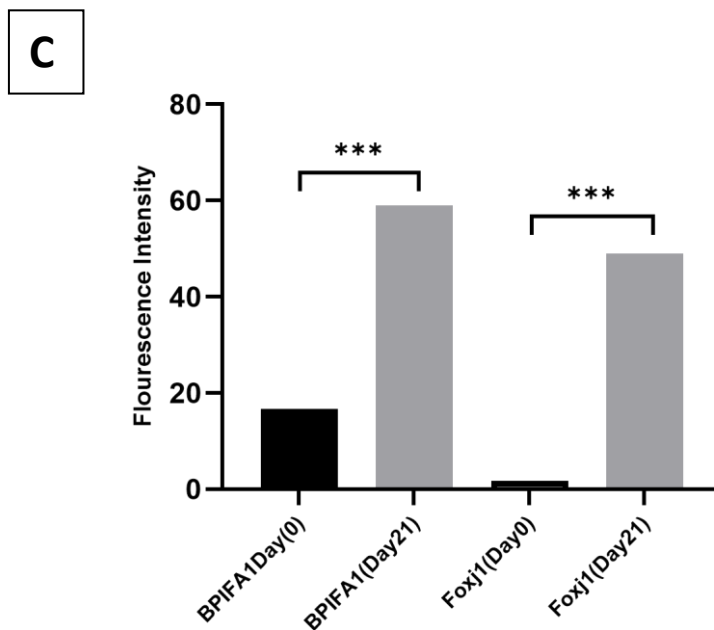
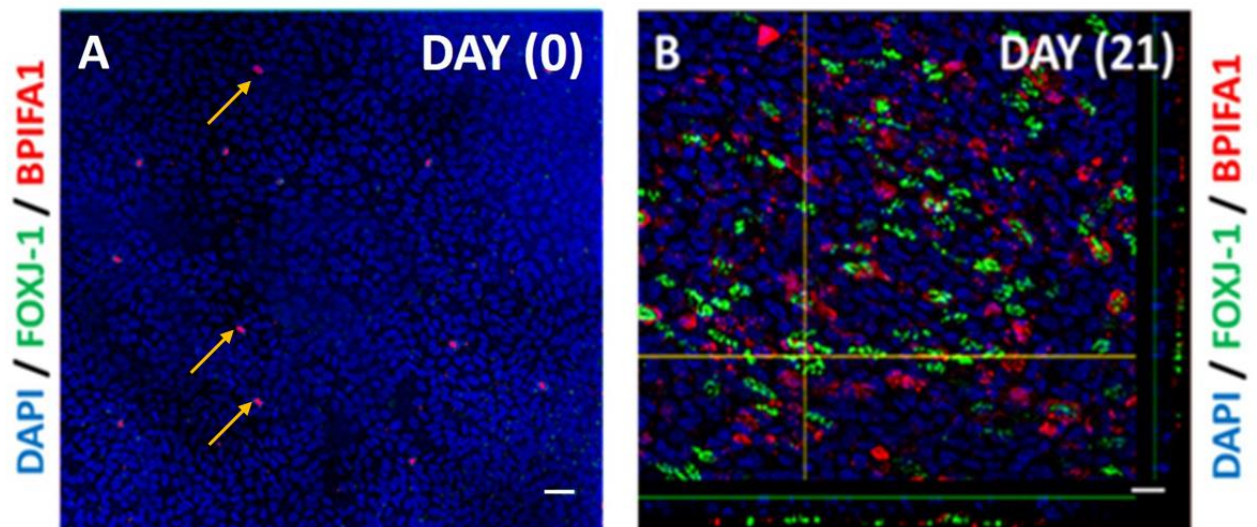


Figure 3.12: Immunofluorescence microscopy reflecting the differentiation of ciliated and secretory HBECS.

Confocal images of HBECS were obtained using the Olympus FV1000 confocal microscope (at 20x magnification for FOXJ1 and BPIFA1) and the Fluoview® image analysis system. The images show FOXJ1 staining (primary) with Alexa Fluor 488 green (secondary) and BPIFA1 staining (primary) with Alexa Fluor 568 red (secondary). DAPI was used to stain the nuclei. Scale bar = 80 μm. (C) The intensity of staining was measured in 4 fields for one donor. Data were analysed using a paired t-test. Error bars = standard error of mean (SEM). **p<0.01 and ***p<0.001.

3.2.9 Comparison of expression of cell-specific marker genes in ALI differentiated HBEC3-KT, BMI-1 and HBEC cells

The above results appeared to show that the expression of the marker genes differed between the three cell types. To investigate the levels of the genes of HBEC3-KT, BMI-1, and HBECs, the RT-qPCR data from the cells grown either with or without collagen on day 21 of ALI culture were further analysed.

The data in Figure 3.13 show the expression of *BPIFA1*, *BPIFB1*, *SCGB1A1*, and *TEKT1* in both the presence and absence of collagen in the transwells. In the absent condition, there was no significant difference in the expression of secretory markers between cell types; however, an increased expression of *SCGB1A1* was observed in the HBECs. Expression of *BPIFA1* was comparable between these cell types irrespective of collagen coating. This scenario was different for *BPIFB1* and *SCGB1A1*; here, the cells were differentiated in the collagen-coated transwell, significantly increasing the expression of these two secretory markers in the HBECs compared to both HBEC3-KT and BMI-1. There was no difference between HBEC3-KT and BMI-1. This indicates that the HBECs were better differentiated to produce secretory cells (goblet and club cells) compared to HBEC3-KT and BMI-1. *TEKT1*, the marker for ciliated cells, was significantly increased in the HBECs compared to both HBEC3-KT and BMI-1 irrespective of collagen presence. In summary, the HBECs expressed all these markers much better than the other two cell types compared here. In terms of gene expression, there was no observable difference between HBEC3-KT and BMI-1.

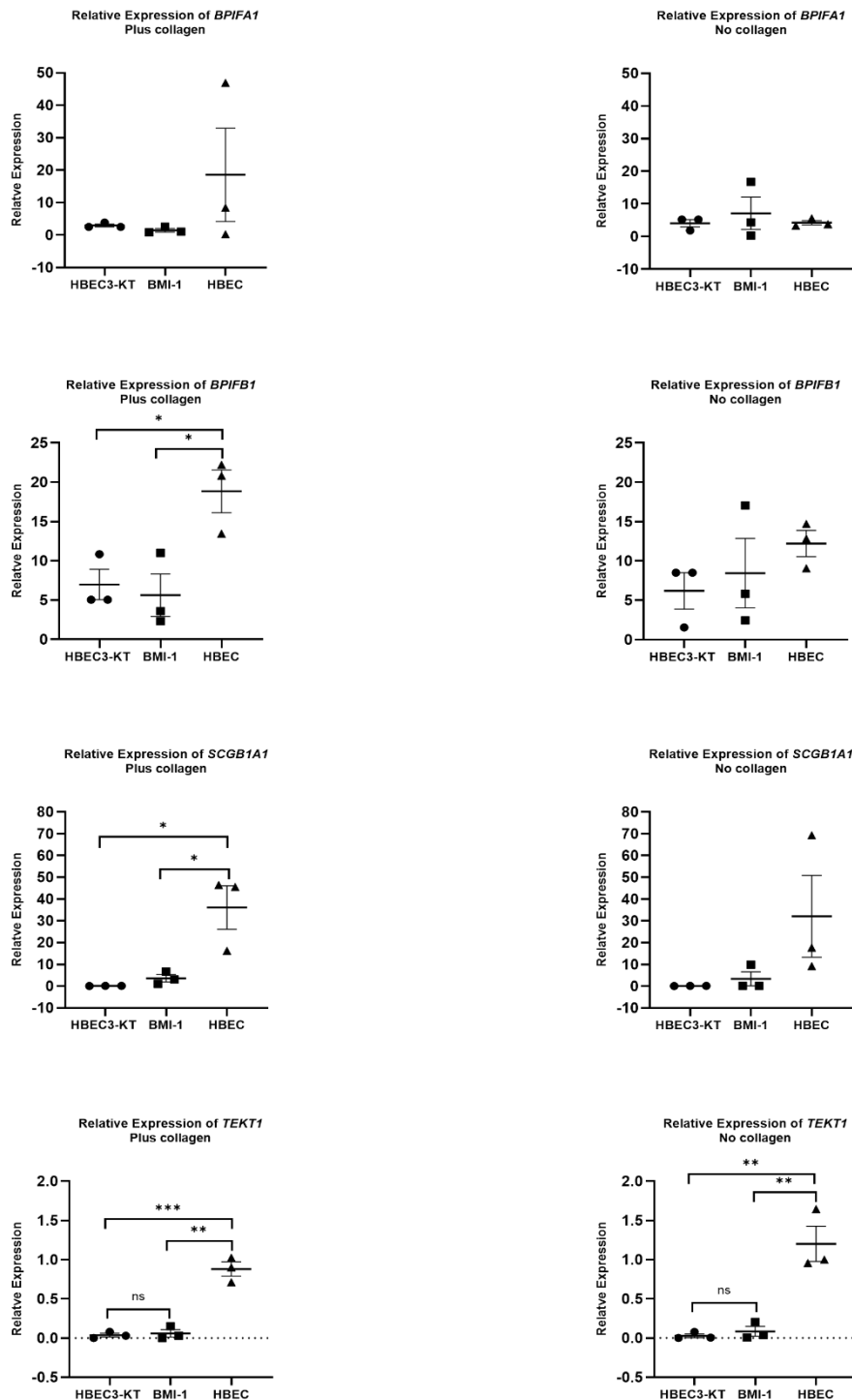


Figure 3.13: RT-qPCR analysis of gene expression during ALI differentiation of HBEC, BMI-1 and HBEC3-KT cells on day 21.

The average expression levels are plotted against the cell type. For each gene, the relative expression of mRNA was normalized to an endogenous *OAZ1* control. A two-way ANOVA was used to analyse the data. Error bars: SEM. Analysis was done on 3 independent biological replicates using cells from 3 different donors for HBECs and 3 batches from BMI-1 and HBEC3-KT cells. * $p < 0.05$, ** $p < 0.01$ and *** $p < 0.001$.

3.2.10 Quantitative proteomics analysis of the secretome in HBEC3-KT cells and HBECs

My previous data suggested that both HBEC3-KT cells and HBECs differentiated when they were cultured at the ALI. To study the consequences of this in more detail a proteomics analysis was conducted to obtain an unbiased view of the similarities and differences in their secretomes. In order to characterise the secretome of HBEC3-KT cells and HBECs in long-term cell cultures by label-free quantitative mass spectrometry, I collected the apical secretions of cells for analysis on day 21 of ALI culture. This sample represented proteins secreted by the cells between 18 and 21 days of culture. All the cell growth experiments were performed using biological triplicates. Four healthy donors provided primary HBECs, and five cultures of HBEC3-KT cells were used. On day 21 following ALI culture, the apical secretions of the cells were collected using 200 μ l of HBSS. A total of 50 μ l of each sample was digested and 18 μ l was injected for 2 hours. The sample was analyzed by nanoflow LC-MS/MS using an Orbitrap Elite.

Principal component analysis (PCA) was used to analyse the quantitative proteomics abundance data in HBEC3-KT cells and HBECs, to better understand the proteome pattern for each condition. PCA provides an optimal visualization of the variables of data. The two major eigenvectors PC1 and PC2 are depicted in Figure 3.14. The secretomes of HBECs form a unique cluster that differs from that of HBEC3-KT cells. Variation between donors, particularly HBEC-01 and HBEC-02, was observed in the data, suggesting that epithelial cells secreted proteins differentially among the donors/experiments. These cells were from healthy male and female donors of various ages and both sexes. In contrast, the HBEC3-KT cell secretome produced a distinct cluster that showed no major variations across samples.

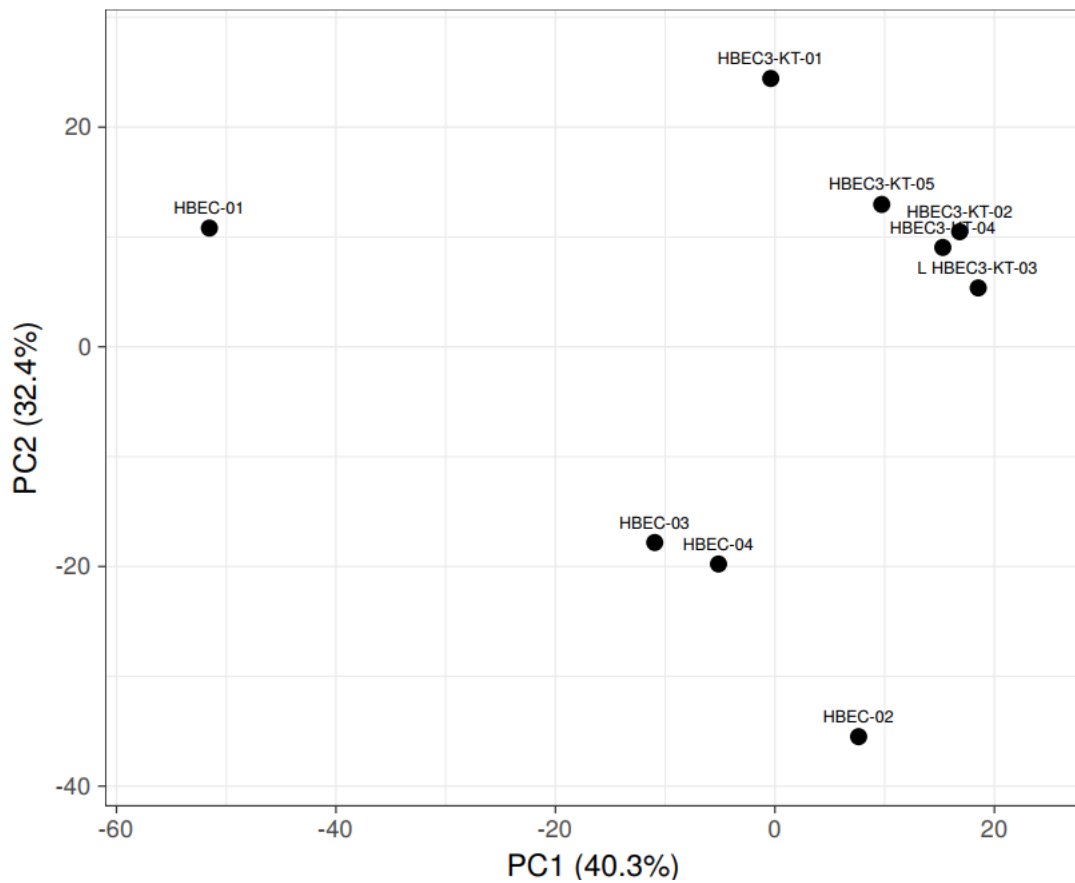


Figure 3.14: PCA of differentiated HBECs and HBEC3-KT cells.

PCA was used to show the relatedness of the samples. Different donors (HBECs) and biological replicates (HBEC3-KT cells) are displayed as circles on the graph. The axis legend shows the proportion associated with each PC. Principal component 1 (PC1) on X-axis shows higher variables (40.13 %) than the principal component 2 (PC2) on the y-axis which counts for 32.4 % of variables.

The analysis of apical secretions of HBECs and HBEC3-KT cells identified a total of 1,186 proteins in all samples (Figure 3.15). I initially visualised the data on a heat map. The heatmap clearly shows differential protein expression in both types of epithelial cells but as expected from the PCA analysis. The hierarchical clustering describes the expression of various secretory protein clusters between two cell types, unsupervised hierarchical clustering grouped the secretions from the two different cell types together. Figure 3.15 clearly shows some differences between the different samples. It shows more red (indicating protein abundance) in HBEC-01 and slightly less in HBEC-02, which likely reflects the amount of protein loaded or differences between the donors. Similarly, there was slightly more red in HBEC3-KT-01 cells compared to the other batches.

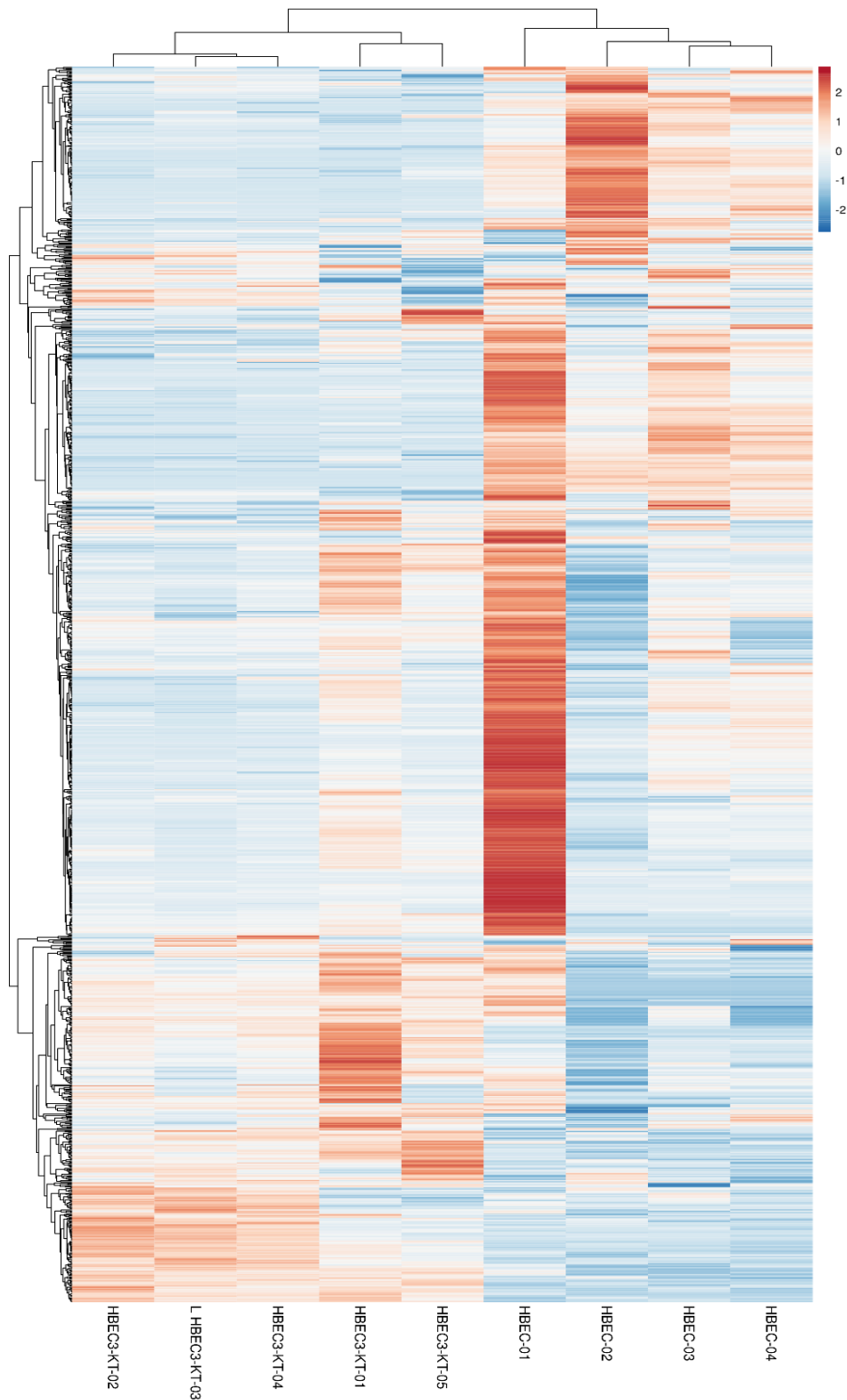


Figure 3.15: Proteomic characterisation of the apical secretome of the human bronchial epithelium in HBEC3-KT cells and HBECs models.

A heatmap of total proteins identified in the apical secretome of HBEC3-KT cells and HBECs on day 21 of ALI is shown. Samples are plotted across X-axis, and Y-axis represents individual protein levels across the samples. Hierarchical clustering refers to the expression of different secretory proteins clusters that are vital for the differentiation of two cell types. The colour bar represents the z-score. The heatmap was generated using the ClustVis web tool.

Figure 3.16 demonstrates the overall differences between HBEC3-KT cells and HBECs secretomes in the form of a volcano plot. The analysis of differences in the secretome of these two cell types identifies fold-change in expression and significant differences between the two groups. Statistically significant differences were determined using the t-test with a permutation-based FDR of 0.05 to correct for multiple hypothesis testing.

The results revealed that proteins including HP (Haptoglobin), CD36 (cluster of differentiation 36), BANF1 (BAF Nuclear Assembly Factor 1), and OLFM4 (Olfactomedin 4) are differentially expressed in HBEC3-KT cells, while HBECs differentially express proteins including as CXCL6 (CXC motif chemokine ligand 6), CEACAM5 (CEA cell adhesion molecule 5), FAM3D (FAM3 Metabolism Regulating Signaling Molecule D), KLK11 (Kallikrein Related Peptidase 11) and MUC5B.

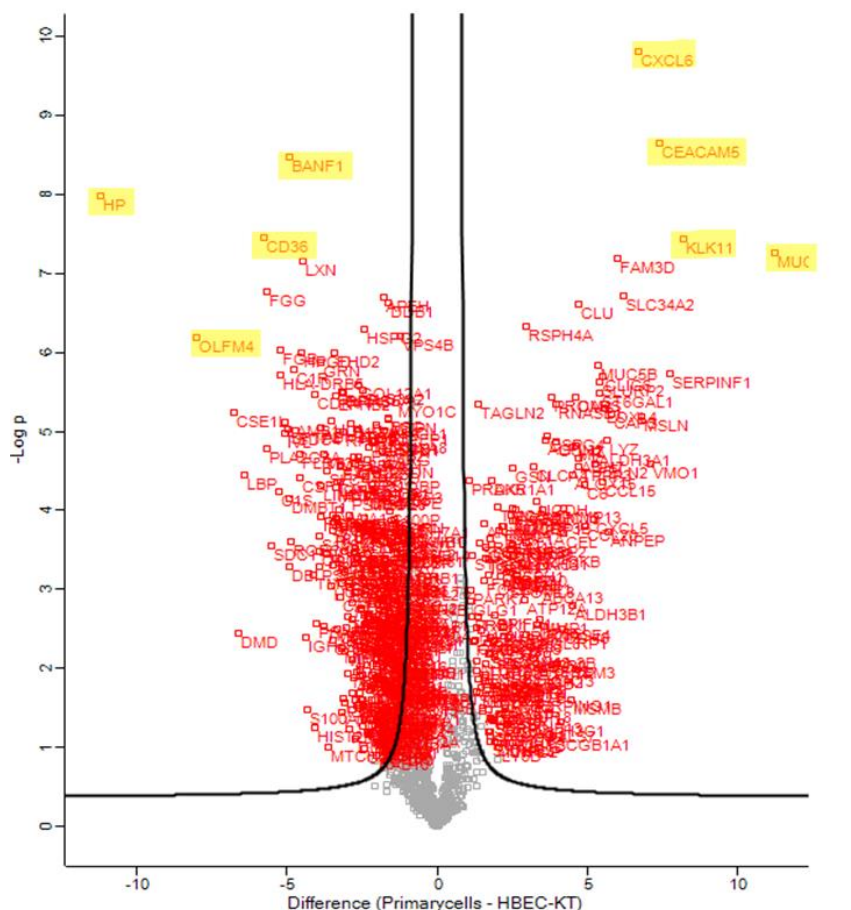


Figure 3.16: Differential analysis of the secretome in HBEC3-KT cells and HBECs.

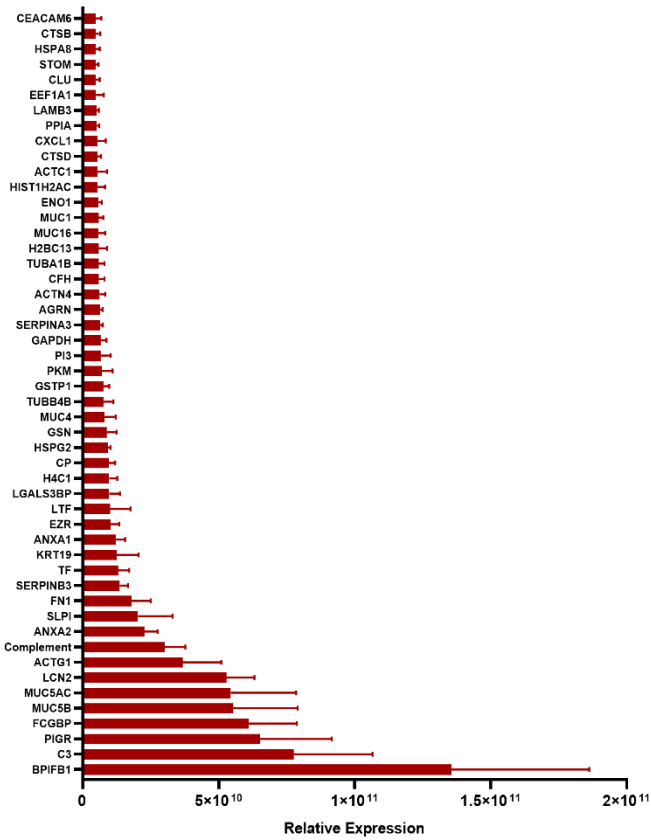
The scatter plot shows the log₂ (intensity) values of the differentially secreted proteins. The dots on the left side indicate greater abundance in HBEC3-KT cells and those on the right side indicate greater abundance in HBECs.

To learn more about the long-term evolution of the two epithelial cell secretomes, the 50 most abundantly secreted proteins at day 21 were compared. Figure 3.17A illustrates the 50 most abundant proteins secreted by HBECs at day 21 following ALI. Some proteins that were highly abundant in the HBECs secretome were secreted at lower levels by HBEC3-KT cells, such as polymeric immunoglobulin receptor (PIGR), mucin-4 (MUC4), IgG Fc-binding protein (FCGBP) and BPI fold-containing family B member 1 (BPIFB1). Some proteins were not found among the 50 most expressed proteins of HBEC3-KT, such as mucin-5B (MUC5B), mucin-5AC (MUC5AC) and antileukoproteinase (SLPI).

Similarly, some proteins that were highly abundant in the HBEC3-KT cells secretome were secreted at lower levels by HBECs, such as complement C3 (C3), lactotransferrin (LFT), basement membrane-specific heparan sulfate proteoglycan core protein (HSPG2) and elafin (P13) (Figure 3.17B). Some proteins were not found among the 50 most secreted proteins of HBECs, such as protein S100-A8 (S100A8), protein S100-A2 (S100A2), Olactomedin4 (OLFM4) and Haptoglobin (HP). I observed that, BPIFA1 was not seen in the top 50 protein list in either cell type but it was seen at lower amounts in both sets of samples.

Figure 3.18 demonstrates the relationships between the abundant proteins in each cell type in the form of a venn diagram using the top 50 most abundant proteins in either sample type. The results show that both types of cells secrete approximately 50% of the proteins differentially. Table 3.1 lists these proteins.

A



B

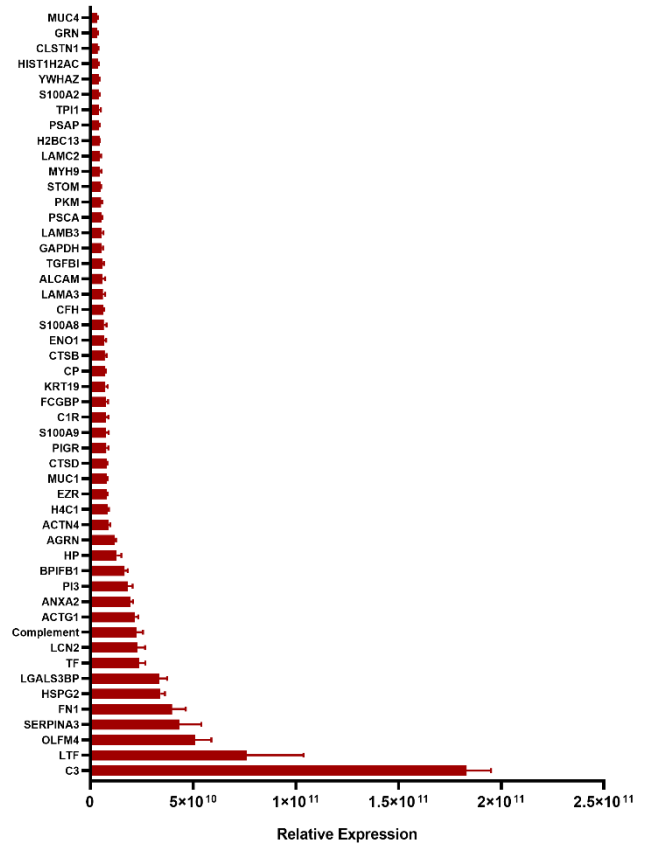


Figure 3.17: Relative abundance of the secretome in HBECs and HBEC3-KT cells.

The 50 most abundant proteins secreted by HBECs (A) and HBEC3-KT cells (B) on Day 21 following ALI are shown. Proteins are designated by their corresponding protein. Error bars = standard error of mean (SEM; n = 4 HBECs) and (SEM; n = 5 HBEC3-KT).

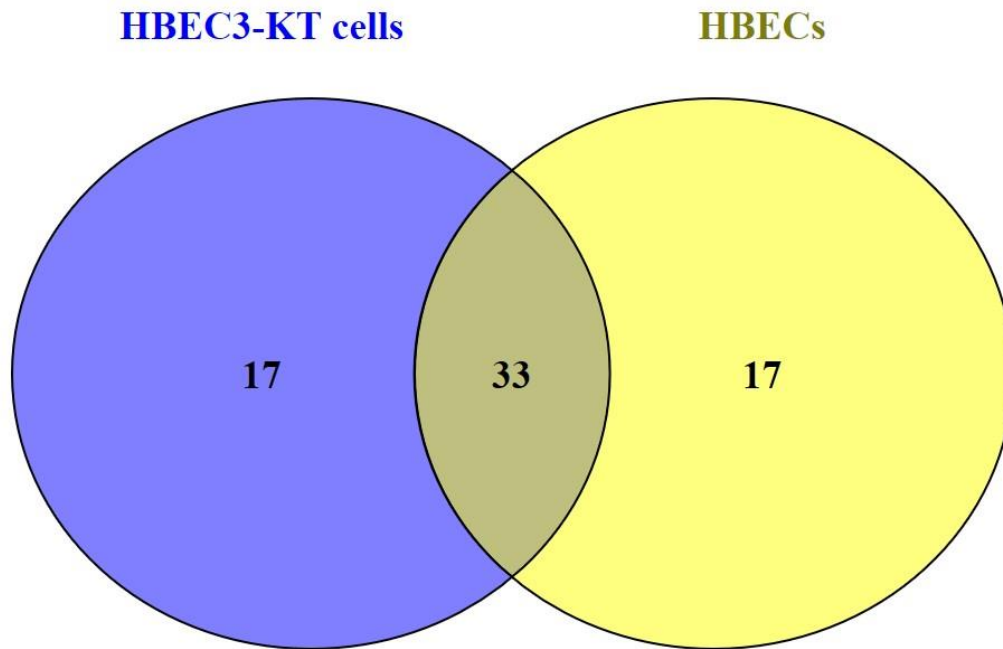


Figure 3.18: Comparison of the HBEC3-KT and HBEC secretomes.

The secreted proteins of HBEC3KT and HBECs at day 21 following ALI were analysed qualitatively. The Venn diagram depicts the top 50 most abundant proteins and the fraction of common proteins.

Table 3.1. Proteins identified in the HBEC3-KT cells and HBECs secretomes at day 21 of ALI. Only the 50 most abundant proteins were considered.

Common (HBEC3-KT and HBEC)	HBEC3-KT	HBEC
C3 - complement C3	OLFM4 – olfactomedin 4	MUC5B – mucin 5B, oligomeric mucus/gel-forming
LTF - lactotransferrin	HP – haptoglobin	MUC5AC – mucin 5AC, oligomeric mucus/gel-forming
SERPINA3 - serpin family A member 3	S100A9 – S100 calcium binding protein A9	SLPI – secretory leukocyte peptidase inhibitor
FN1 – fibronectin 1	CIR – circling	ANXA1 – annexin A1
HSPG2 - heparan sulfate proteoglycan 2	S100A8 – S100 calcium binding protein A8	GSN – gelsolin
LGALS3BP – galectin 3 binding protein	LAMA3 – laminin subunit alpha 3	TUBB4B – tubulin beta 4B class IVb
TF – transferrin	ALCAM – activated leukocyte cell adhesion molecule	GSTP1 – glutathione S-transferase pi 1
LCN2 – lipocalin 2	TGFBI – transforming growth factor beta induced	TUBA1B - tubulin alpha 1b
ACTG1 – actin gamma 1	PSCA – prostate stem cell antigen	MUC16 – mucin 16, cell surface associated
ANXA2 – annexin A2	MYH9 – myosin heavy chain 9	ACTC1 – actin alpha cardiac muscle 1
PI3 – peptidase inhibitor 3	LAMC2 – laminin subunit gamma 2	CXCL1 – C-X-C motif chemokine ligand 1
BPIFB1 – BPI fold containing family B member 1	PSAP – prosaposin	PPIA – peptidylprolyl isomerase A
AGRN – agrinACTN4 – actinin alpha 4	TPI1 – triosephosphate isomerase 1	EEF1A1 – eukaryotic translation elongation factor 1 alpha 1
H4C1 – H4 clustered histone 1	S100A2 – S100 calcium binding protein A2	CLU – clusterin
EZR – ezrin	YWHAZ – tyrosine 3-monooxygenase/tryptophan 5-monooxygenase activation protein zeta	HSPA8 – heat shock protein family A (Hsp70) member 8
MUC1 – mucin 1, cell surface associated	CLSTN1 – calsyntenin 1	CEACAM6 – CEA cell adhesion molecule 6
CTSD – cathepsin D	GRN – granulins precursor	SERPINB3 – serpin family B member 3
PIGR – polymeric immunoglobulin receptor		
FCGBP – Fc gamma binding protein		
KRT19 – keratin 19		
CP – ceruloplasmin		
ACTN4 – actinin alpha 4		
KRT19 – keratin 19		
CTSB – cathepsin B		
ENO1 – enolase 1		
CFH – complement factor H		
GAPDH – glyceraldehyde-3-phosphate dehydrogenase		
LAMB3 – laminin subunit beta 3		
PKM – pyruvate kinase M1/2		
STOM – stomatin		
H2BC13 – H2B clustered histone 13		
HIST1H2AC - histone cluster 1 H2A family member C		
MUC4 – mucin 4, cell surface associated		

Examination of the protein lists identified many intracellular proteins, including those associated with cell debris, cell lysis and perhaps dead cells, among the proteins that were collected from the secretions during the washing steps. Out of all the secretions from the differentiated cells, the extracellular proteins are of the most interest in terms of our work. Therefore, extracellular proteins were selected using The Human Protein Atlas, UniProt and Pride Archive software. The apical secretome of HBECs and HBEC3-KT cells contained 298 extracellular proteins determined in this manner.

Figure 3.19 depicts a heatmap of 100 most abundant extracellular proteins. Warm colours indicate extracellular proteins with a high abundance, with red indicating the highest level, and cool colours indicate the extracellular proteins with the lowest abundance.

The results show more red colour in HBEC-02 and slightly less in HBEC-01, indicating high levels of extracellular proteins in these samples or differences between donors. Similarly, there was slightly more red colour in HBEC5-KT cells compared to other batches. Figure 3.19 only presents the extracellular proteins, while Figure 3.15 represented both intracellular and extracellular proteins. This analysis shows some similarity to that of the whole proteome data set. It also shows BPIFA1 to be differentially expressed in the ALI data sets.

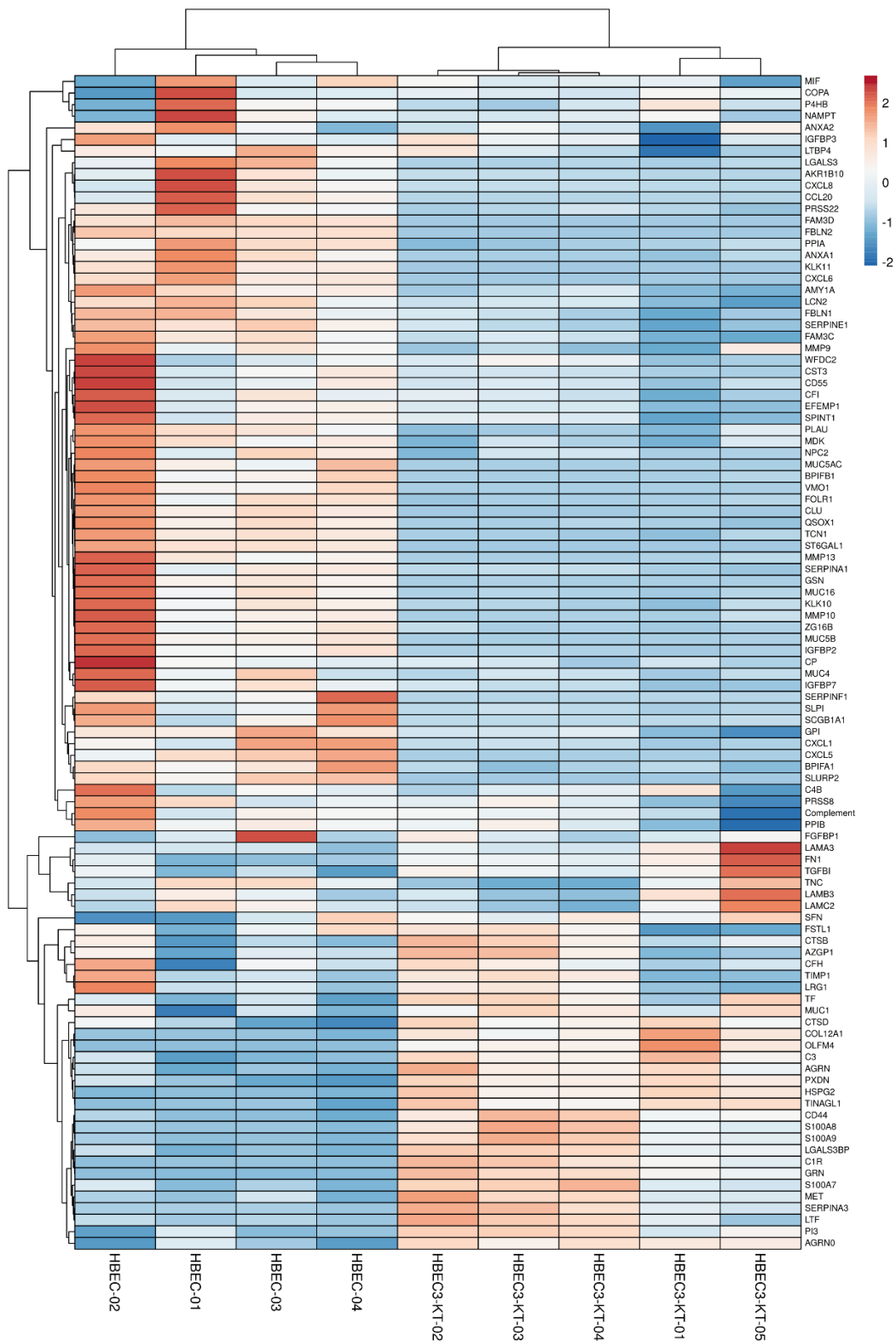


Figure 3.19: Proteomic characterisation of the apical secretome of the human bronchial epithelium in HBEC3-KT cells and HBECs models.

A heatmap of extracellular proteins identified in the apical secretome of HBEC3-KT cells and HBECs at day 21 following ALI is shown. Hierarchical clustering refers to the expression of different extracellular proteins clusters that are vital for the differentiation of two cell types. The colour bar represents the z-score. Red indicates high expression while blue indicates low expression.

To evaluate the similarity of secretions from HBEC3-KT cells and HBECs in ALI cultures, we compared the selected individual proteins in respiratory epithelial cell secretions using HBECs and HBEC3-KT cells. The extracellular proteins identified displayed significantly ($p < 0.05$) altered levels in HBEC3-KT cells and HBECs.

Figure 3.20 shows the evaluation of individual respiratory epithelial cell proteins in HBEC3-KT cells and HBECs. For the most part, the proteins studied had different expression patterns. OLFM4, HP, ITBL1, PXDN, AGRN, and SCPEP1 were the top six proteins that had higher expression in HBEC3-KT cells compared to the primary cells. Moreover, SLPI, LCN2, SCGB1A1, MUC5AC, MUC5B, and BPIFB1 were among the top six proteins secreted at higher levels by HBECs than HBEC3-KT cells. Figure 3.21 shows that significantly differential protein abundance is seen for these proteins ($p < 0.05$).

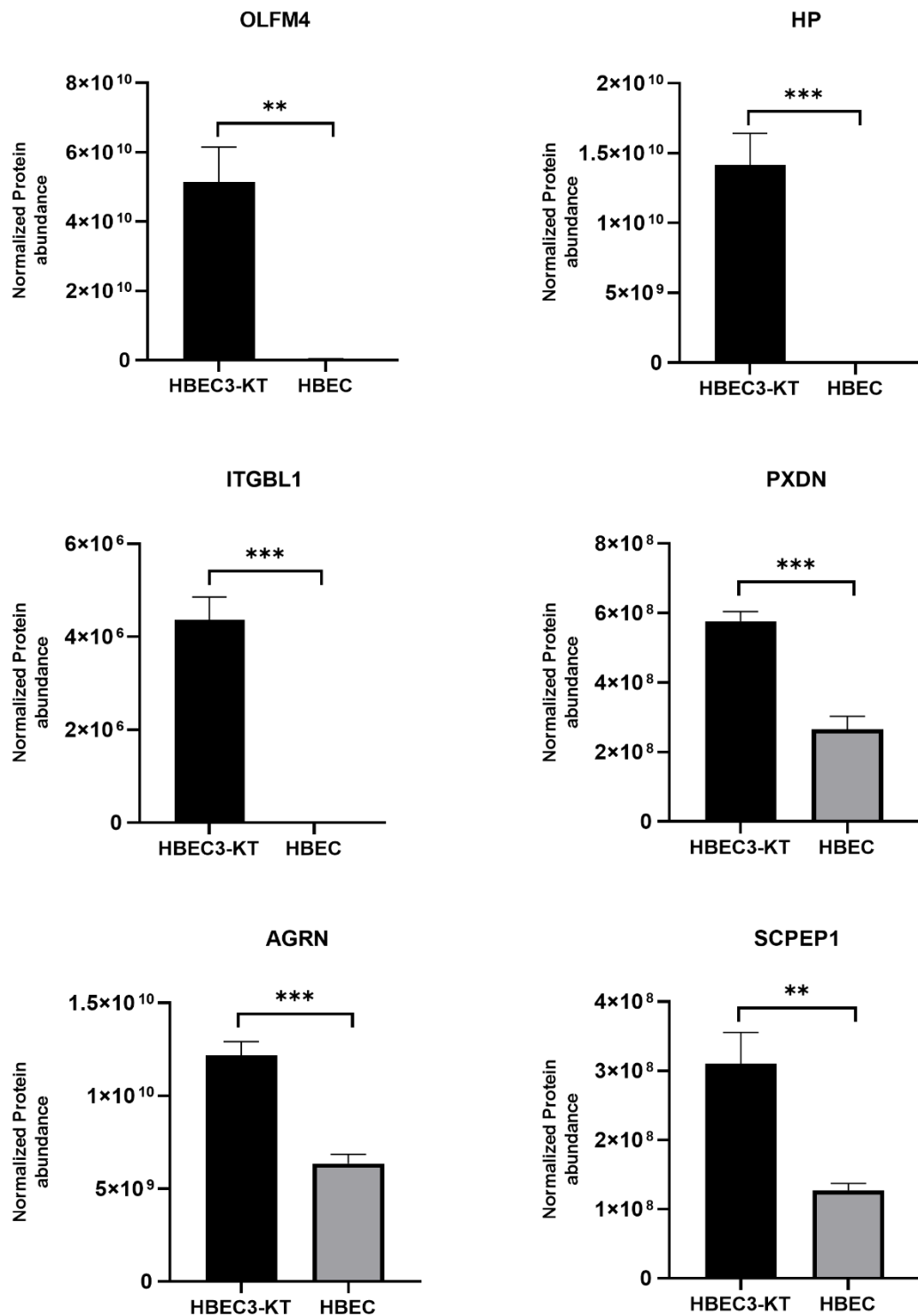


Figure 3.20: Relative abundance of proteins during the ALI differentiation of HBECs and HBEC3-KT cells.

The average expression levels are plotted along the y-axis and cells are plotted along the x-axis, as indicated in the bar chart. A paired t-test was used to analyse the data. Error bars = SEM (n = 4 HBECs) and (n = 5 HBEC3-KT). **p<0.01 and ***p<0.001.

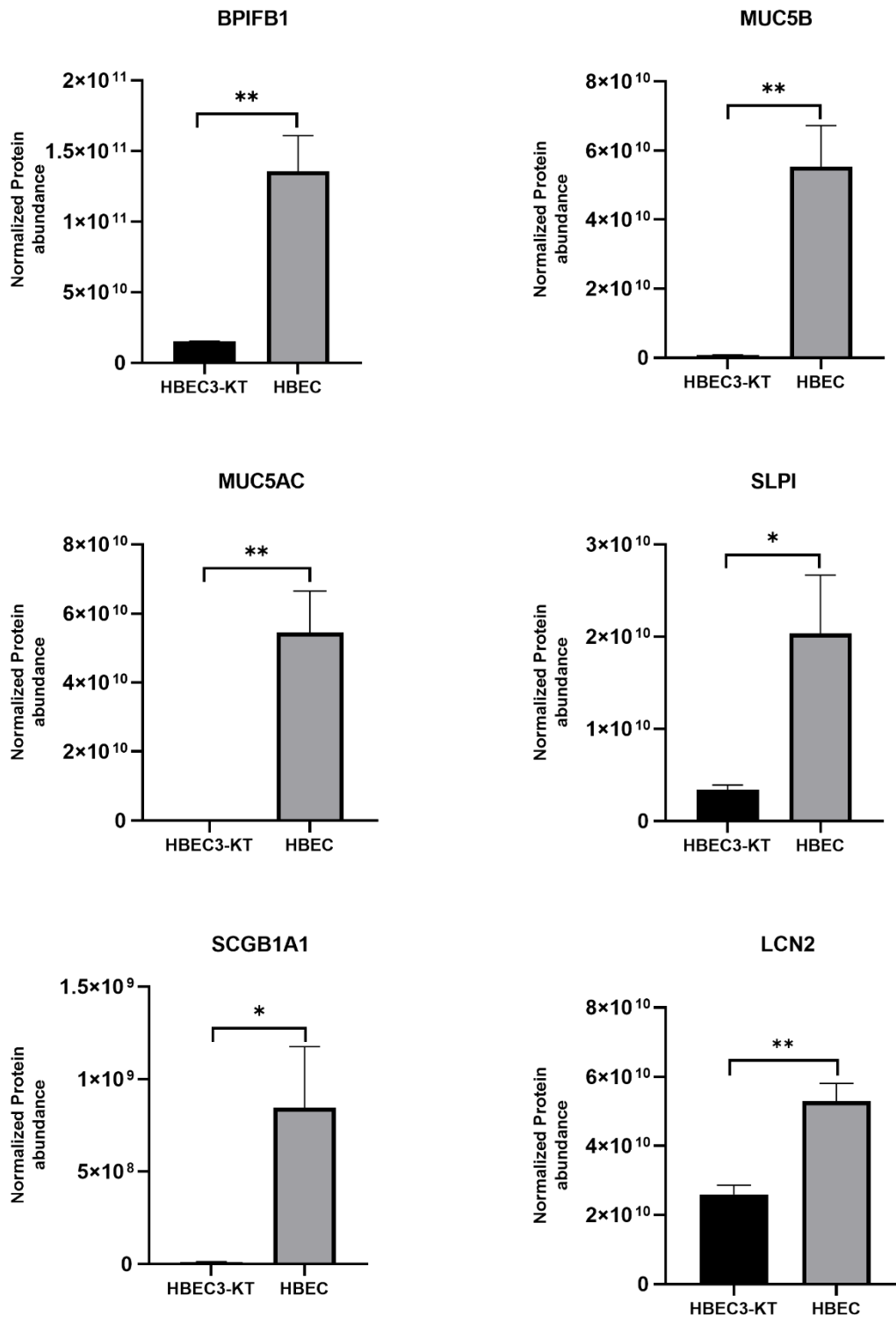


Figure 3.21: Relative abundance of certain innate defence proteins during the ALI differentiation of HBECs and HBEC3-KT cells.

The average expression levels are plotted along the y-axis and cells are plotted along the x-axis, as indicated in the bar chart. A paired t-test was used to analyse the data. Error bars = SEM (n = 4 HBECs) and (n = 5 HBEC3-KT). *p < 0.05 and **p < 0.01.

3.2.11 Comparison of the quantitative proteomics analysis of the HBEC3-KT cells and Calu-3 cell secretome

I also compared the composition of the secreted proteins in HBEC3-KT cells from our analysis with that of Calu-3 cells grown at the ALI and analysed by Sanchez-Guzman et al. (2021) (Figure 3.22). Calu-3 cells are a lung cancer cell line that display epithelial characteristics and have been used as a model of the secretory epithelium (Zhu et al., 2010). Venn diagram depicts the fraction of the top 50 proteins that are common in the secretions from the two cell types. Only 13 proteins OLFM4, C3, PIGR, FCGBP, ENO1, SERPINA3, MUC1, ANXA2, CP, KRT19, YWHAZ, CTSD and LGALS3BP were identified as being within the top 50 most abundant protein in both set of samples (Table 3.2).

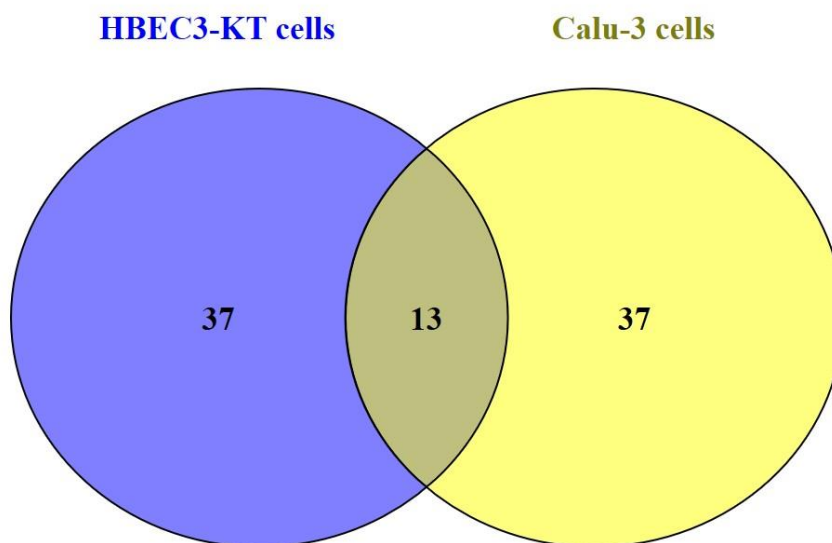


Figure 3.22: Venn diagram showing the percentage of top 50 individual proteins from HBEC3-KT cells and Calu-3 cells that were common to both cell types.

The top 50 most abundant proteins for each cell type were compared using a Venn diagram.

Table 3.2 List of proteins identified in the HBEC3-KT cell and Calu-3 cell secretomes following ALI. Only the 50 most abundant proteins were considered.

Common (Calu-3 and HBEC3-KT cells)	Calu-3 cells	HBEC3-KT cells
OLFM4 – olfactomedin 4	SERPINA1 – serpin family A member 1	FN1 – fibronectin 1
PIGR - polymeric immunoglobulin receptor	RARRES1 – retinoic acid receptor responder 1	BPIFB1 – BPI fold containing family B member 1
FCGBP – Fc gamma binding protein	CFB – complement factor B	AGRN – agrin
SERPINA3 – serpin family A member 3	SPP1 - secreted phosphoprotein 1	ACTN4 – actinin alpha 4
MUC1 – mucin 1, cell surface associated	TCN1 – transcobalamin 1	H4C1 – H4 clustered histone 1
ANXA2 – annexin A2	ACTB – actin beta	S100A9 – S100 calcium binding protein A9
KRT19 – keratin 19	ALB – albumin	LAMA3 – laminin subunit alpha 3
YWHAZ – tyrosine 3-monooxygenase/tryptophan 5-monooxygenase activation protein zeta	GC – GC vitamin D binding protein	ALCAM – activated leukocyte cell adhesion molecule
CTSD – cathepsin D	CTSC – cathepsin C	PSCA – prostate stem cell antigen
C3 - complement C3	KRT8 – keratin 8	LAMC2 – laminin subunit gamma 2
ENO1 – enolase 1	ANXA4 – annexin A4	PKM – pyruvate kinase M1/2
CP – ceruloplasmin	QSOX1 – quiescin sulphydryl oxidase 1	H2BC13 – H2B clustered histone 13
LGALS3BP – galectin 3 binding protein	MUC5B – mucin 5B, oligomeric mucus/gel-forming	MYH9 – myosin heavy chain 9
	LDHA – lactate dehydrogenase A	TPI1 – triosephosphate isomerase 1
	SERPING1 – serpin family G member 1	LTF - lactotransferrin
	H2AC4 – H2A clustered histone 4	HSPG2 – heparan sulfate proteoglycan 2
	KRT14 – keratin 14	TF – transferrin
	RPS27A – ribosomal protein S27a	LCN2 – lipocalin 2
	ALDOA – aldolase, fructose-bisphosphate A	ACTG1 – actin gamma 1
	LYZ – lysozyme	PI3 – peptidase inhibitor 3
	CEACAM7 –CEA cell adhesion molecule 7	Complement
	ACE2 – angiotensin converting enzyme 2	HP – haptoglobin
	ACTC1 – actin alpha cardiac muscle 1	CIR – circling
	DMBT1 – deleted in malignant brain tumors 1	CTSB – cathepsin B
	GSTP1 – glutathione S-transferase pi 1	S100A8 – S100 calcium binding protein A8
	GOLM1 – golgi membrane protein 1	CFH – complement factor H
	LSR – lipolysis stimulated lipoprotein receptor	TGFBI – transforming growth factor beta induced
	H2BC12 – H2B clustered histone 12	GAPDH – glyceraldehyde-3-phosphate dehydrogenase
	TMSB4X – thymosin beta 4 X-linked	LAMB3 – laminin subunit beta 3
	ICAM1 – intercellular adhesion molecule 1	STOM – stomatin
	LDHB – lactate dehydrogenase B	PSAP – prosaposin
	AGR2 – anterior gradient 2, protein disulphide isomerase family member	HIST1H2AC - histone cluster 1 H2A family member C
	TIMP1 – TIMP metallopeptidase inhibitor 1	MUC4 – mucin 4, cell surface associated
	HSPA2 – heat shock protein family A (Hsp70) member 2	GRN – granulin precursor
	MUC5AC – mucin 5AC, oligomeric mucus/gel-forming	CLSTN1 – calystenin 1
	PPIB – peptidylprolyl isomerase B	S100A2 – S100 calcium binding protein A2
	PGK1 – phosphoglycerate kinase 1	EZR – ezrin

3.2.12 Comparison of the quantitative proteomics analysis of HBECs secretomes from different studies

I next wanted to directly compare my data for the HBECs secretome with another HBECs data set. To do this I compared the quantitative proteomic analysis data of the secretome from Touzelet et al. (2020) (A) with my data (B). To compare the composition of the cell secretions from the two studies, the 50 most abundantly secreted proteins were identified after analysing of P value of less than 0.05. The Venn diagram shows the overall number that were common proteins (Figure 3.23). Table 3.3 present the 27 common proteins, BPIFB1, C3, PIGR, FCGBP, MUC5B, MUC5AC, LCN2, ANXA2, SLPI, FNI, SERPINB3, TF, ANXA1, EZR, LTF, LGALS3BP, CP, HSPG2, GSN, MUC4, GSTP1, KRT19, PKM, SERPINA3, MUC16, MUC1, ENO1 and CTSD as well those uniquely present in individual studies. The reasons for the observed dissimilarities may include the use of different donors and ALI media.

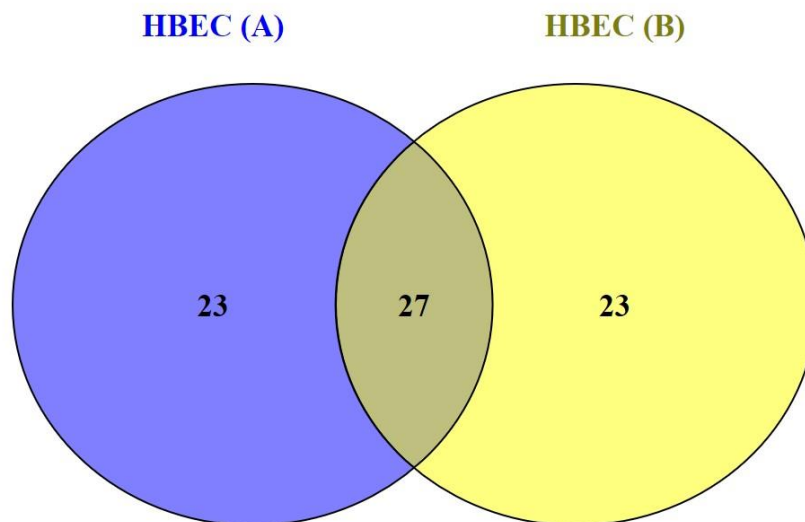


Figure 3.23: Venn diagram showing the distribution of proteins from two ALI secretions highlighting common proteins (HBEC (A) and HBEC (B)).

The top 50 most abundant proteins for each cell type were compared using a Venn diagram.

Table 3.3 List of proteins identified in the HBEC (A) and HBEC (B) secretomes following ALI. Only the 50 most abundant proteins were considered.

Common (HBEC (A) and HBEC (B))	HBEC (A)	HBEC (B)
BPIFB1 – BPI fold containing family B member 1	KRT1 – keratin 1	H4C1 – H4 clustered histone 1
C3 - complement C3	BPIFA1 – BPI fold containing family A member 1	ACTC1 – actin alpha cardiac muscle 1
PIGR - polymeric immunoglobulin receptor	KRT9 – keratin 9	CXCL1 – C-X-C motif chemokine ligand 1
FCGBP – Fc gamma binding protein	KRT10 – keratin 10	HSPA8 – heat shock protein family A (Hsp70) member 8
MUC5B – mucin 5B, oligomeric mucus/gel-forming	CFB – complement factor B	CTSB – cathepsin B
MUC5AC – mucin 5AC, oligomeric mucus/gel-forming	RARRES1 – retinoic acid receptor responder 1	CEACAM6 – CEA cell adhesion molecule 6
LCN2 – lipocalin 2	KRT5 – keratin 5	ACTG1 – actin gamma 1
ANXA2 – annexin A2	SERPINF1 – serpin family F member 1	KRT19 – keratin 19
SLPI – secretory leukocyte peptidase inhibitor	LDHA – lactate dehydrogenase A	TUBB4B – tubulin beta 4B class IVb
FN1 – fibronectin 1	KRT16 – keratin 16	PI3 – peptidase inhibitor 3
SERPINB3 – serpin family B member 3	HIST1H4A - histone cluster 1 H4 family member A	GAPDH – glyceraldehyde-3-phosphate dehydrogenase
TF – transferrin	PGK1 – phosphoglycerate kinase 1	AGRN – agrin
ANXA1 – annexin A1	S100A8 – S100 calcium binding protein A8	ACTN4 – actinin alpha 4
EZR – ezrin	TPI1 – triosephosphate isomerase 1	Complement
LTF - lactotransferrin	DCD – dermcidin	TUBA1B – tubulin alpha 1b
LGALS3BP – galectin 3 binding protein	CIB1 – calcium and integrin binding 1	H2BC13 – H2B clustered histone 13
CP – ceruloplasmin	HIST1H2BI - histone cluster 1 H2B family member 1	HIST1H2AC - histone cluster 1 H2A family member C
GSTP1 – glutathione S-transferase pi 1	HSPA5 – heat shock protein family A (Hsp70) member 5	PPIA peptidylprolyl isomerase A
HSPG2 – heparan sulfate proteoglycan 2	S100A6 – S100 calcium binding protein A6	LAMB3 – laminin subunit beta 3
GSN – gelsolin	SERPINA1 – serpin family A member 1	EEF1A1 – eukaryotic translation elongation factor 1 alpha 1
MUC4 – mucin 4, cell surface associated	CTSC – cathepsin C	CLU clusterin
KRT19 – keratin 19	KRT14 – keratin 14	STOM – stomatin
PKM – pyruvate kinase M1/2	PSCA – prostate stem cell antigen	CFH – complement factor H
SERPINA3 – serpin family A member 3		
MUC16 – mucin 16, cell surface associated		
MUC1 – mucin 1, cell surface associated		
ENO1 – enolase 1		
CTSD – cathepsin D		

3.13 Discussion

In this chapter, studies were undertaken to validate the use of human pulmonary cell line-based models to investigate if they would be suitable for use in functional studies with the human respiratory tract pathogen *S. aureus*. I was particularly interested in cells grown at the ALI to recapitulate the mucociliary morphology of the human respiratory tract. Such models have successfully been applied to conduct studies similar to what I proposed for my research. The *in vitro* models are suitable for the investigation of drug efficacy, bioavailability, and risk assessment. Furthermore, normal and diseases conditions and physiological changes can be effectively studied using human pulmonary cell airway cultures (Hittinger et al. 2017). *In vitro* models are often used in experiments to study biological mechanisms, without the use of human subjects or *in vivo* models, which may cause pain or distress to the subjects or animals. However, the success of such studies depends on the successful creation of tractable cell-based models. The majority of pulmonary cell lines available are unable to differentiate to replicate the phenotype of the native human respiratory tract but a few immortalized cell lines have been established that appear to have the ability to differentiate (Delgado et al., 2011, Miller and Spence, 2017). Therefore, this chapter aimed to determine if it was feasible to reproducibly differentiate immortalized human airway cell lines by growing them at an ALI. I sought to compare these with differentiated HBECs with the ultimate aim of using them as a model for subsequent experiments. For this work, I have used the HBEC3-KT cell line, a human bronchial cell line that was immortalized using hTERT and Cdk4 (Ramirez et al., 2004), and BMI-1 cells that were immortalized by transduction of bronchial epithelial cells with polycomb complex protein BMI-1 (Munye et al., 2017). I directly compared these two cell lines with primary HBECs grown at the ALI. I sought to do this work using immortalized airway cells with a differentiation capacity as I considered that they might represent a more tractable model than the use of primary cells where individual donor variation can be a significant issue (King et al., 2020).

The ALI model of airway cell culture was first described in the 1990s (Wu et al., 1990), and has since been used in multiple studies using multiple variations of culture conditions and media in procedures that have become increasingly more complex. These modifications have allowed modulation by treatment with a range of growth factors such that the cells can be made to adopt different phenotypes (Fulcher et al., 2005, LeSimple et al., 2007, Hackett et al., 2011). ALI culture of airway cells causes cells to differentiate into a pseudostratified epithelium that

mimics the native airway (Ross et al., 2007), and this process is considered to generate a faithful replication of the *in vivo* airway epithelial transcriptome (Dvorak et al., 2011). The results of the study are helpful for our analysis as ALI airway models have a close structural and functional resemblance to the *in vivo* airway epithelium. Further, a study conducted by Hackett et al. (2011), showed the application of asthmatic-derived airway epithelial cultures to study the effect of foreign pathogens and toxins on the asthmatic and non-asthmatic epithelium. It is well established that primary HBECs are multipotent and express markers of a variety of epithelial cells of the human respiratory tract when they are cultured under different conditions (Delgado et al., 2011). They show a multipotent differentiation capacity in ALI cultures where they can differentiate into the secretory, club, goblet, and ciliated cells. These cells have been used in multiple studies and are becoming a standard experimental tool in respiratory biology (Jiang et al., 2018, Hiemstra et al., 2019, Alharbi et al., 2020). The use of the ALI model for my experiments was required to generate the complex phenotype seen in the airway and to allow the investigation of the role of different cells in host defense. Primary airway cells are often cultured in transwells coated with collagen (or other cell-matrix components) as this has been shown to improve cellular growth (Luengen et al., 2020). In my experiments, I compared collagen-coated and non-coated transwells to analyse and confirm the role of collagen in cellular growth or general matrix effects.

3.13.1 The differentiation of HBEC3-KT cells

The HBEC3-KT cell line used in this study has been used in a few studies in the past. One study evaluated the potential of the HBEC3-KT cells to respond to cues from the microenvironment and how this stimulus influences their ability to differentiate into other lung epithelial cell types. One study cultured HBEC3-KT cells both on top of and within a reconstituted basement membrane (Delgado et al., 2011). The results revealed the ability of the cells to differentiate into a number of mature epithelial cell types when they were exposed to this type of environment. In another study, cells were differentiated at the ALI and used for the propagation of three clinical Rhinovirus C isolates (RV-C, RV-C5s3, and RV-C9) (Nakauchi et al., 2019). RV-C selectively infects ciliated cells through the use of CDHR3 as a receptor. SNPs in the gene encoding this protein have shown association with the development of asthma (Rajput et al., 2021).

Following the establishment of the ALI culture, I initially used endpoint RT-PCR to validate the differentiation of the cells using well-established markers of different cell types. *TEKT1* and *CBE1* are markers for ciliated cells. *TEKT1* which encodes the TEKT1 protein is expressed

in the axoneme of the motile cilium and is required for cilia motility (Ryan et al., 2017). *CBE1* is also a known cilia gene. Although its function in airway cilia remains unresolved (Haitchi et al., 2009) it has recently been revealed that Cbe1 localization and expression was seen in the epithelium of the inner medullary collecting duct-3 cells as a model of ciliogenesis during spermiogenesis indicating the importance of the factor in the differentiation of epithelial cells (Pleuger et al., 2019). In ciliated cells of the bronchial epithelium, CBE1 was identified along with the expression of *TEKT1* and *FOXJ1* (Yoshisue et al., 2004). *BPIFA1* and *BPIFB1*, are amongst the most highly expressed genes in differentiated ALI cultures (Ross et al., 2007). This finding is consistent with other studies that have indicated that *BPIFA1* and *BPIFB1* are secreted from human airway cells grown at the ALI (Campos et al., 2004, Bingle et al., 2010). I also investigated other known secretory genes including *WFDC2* and *SLPI* which are expressed in the respiratory tract and are markers for secretory cells (Bingle et al., 2006) as well as the well-studied *SCGB1A1* gene, a marker of club cells (Reynolds et al., 2002). Using these markers enabled me to monitor the process of differentiation in my cultures. The results for the expression profiles of the differentiated HBEC3-KT cells were found to be similar to the study conducted by Ross et al., (2007) (Figure 1.11), suggesting that the gene expression profiles of the differentiated HBEC3-KT cells in my studies were broadly similar to that seen in primary human ALI cells.

RT-qPCR results confirm the differentiation of HBEC3-KT cells by showing mRNA expression of epithelial marker genes during the differentiation phase and all analysis was done on 3 independent biological replicates. The results showed the comparatively weak gene expression for ciliated cell markers in comparison with markers of secretory cells. Positive gene expression was observed in 1st run however, it became weak or say disappeared in the 2nd and 3rd run in the case of ciliated cells. These findings are in line with the research work of (Vaughan et al., 2006), which disclosed that time impacts negatively the expression of ciliated cells in a culture medium i.e., the expression of a gene is decreased over time in this kind of medium. A possible explanation for this could be that cell passage number and possibly slightly different conditions during three experiments might impact the gene expression because the expression also became weak for secretory cell marker genes, *BPIFA1*, *BPIFB1*, and *SCGB1A1*, during the 3rd experiment in comparison to 1st (see Figure 3.3). These results were seen both with and without collagen treatment. The statistical results of the experiments were not found to be normally distributed due to the lack of a sufficient sample size.

Further validation of the cultures was undertaken by IF microscopy. The results confirmed that differentiated cells were present after the passage 14 days. Such observation were consistent n

all three replicates of the study and suggests that whatever was causing the loss of ciliation capacity of the cells was not limiting the secretory differentiation capacity. Again this is consistent with other data using immortalized airway cells where results have shown that cells lacking the cilia formation can differentiate into secretory types of cells (Walters et al., 2013, Peters-Hall et al., 2018, Wang et al., 2019). My initial data suggested that HBEC3-KT cells do have some of the characteristics of primary airway cells differentiated at the ALI but it was important to further validate their potential to be modulated.

3.13.2 Modulation of HBEC3-KT cells differentiation

It is potentially useful to be able to influence the process of mucociliary differentiation *in vitro* using a stimulus to initiate the process. *In vitro* analyses are relatively easy to handle as compared to complicated *in vivo* analyses because *in vivo* involves animal modeling. Several groups have used Taxol and Nocodazole to arrest ciliogenesis by preventing centriole assembly (Vladar and Brody, 2013, Burke et al., 2014). Similarly, DAPT an inhibitor of the Notch signaling pathway is known to increase the number of ciliated cells in primary mTEC cultures (Stubbs et al., 2012, Gerovac et al., 2014, Eenjes et al., 2018). To evaluate whether ciliated cells differentiation could be modulated or not in the cultures, HBEC3-KT cells were treated with DAPT. Previously our lab has applied this treatment to induce ciliated cells in mouse airway cell ALI cultures (Anujan, 2019) and I used the same concentration of DAPT. This treatment was expected to increase the number of ciliated cells and reduce the number of goblet cells. However, it was not clear whether the number of ciliated cells was increased, or the number of secretory cells decreased by this treatment. Further studies are required to resolve this. It may be that the immortalization of the cells prohibits the effect of DAPT in HBEC3-KT cells.

Dysregulation of type 2 cytokine-driven immune response is associated with allergic disorders such as asthma (Wynn, 2015). Type 2 cytokines IL-4 and IL-5 lead to a more severe disease course in asthma patients by activating the effector function of Th2 cells (Cohn et al., 2004, Lambrecht et al., 2019) and recruiting eosinophils (Rosenberg et al., 2013). IL-13 is another type 2 cytokine that induces mucus cells to secrete MUC5AC excessively and decreases ciliated cell amount (Seibold, 2018). Therefore, IL-13 along with other type 2 cytokines are investigated in clinical trials as a potential therapeutic target to restore airway function (Doran et al., 2017). Studies have indicated that the differentiation of IL-13 treated cells is affected by Notch signaling (Gerovac et al., 2016, Seibold, 2018). My data did appear to show an induction of the goblet cell marker *BPIFB1* in the IL-13 treated cells. It was not clear if the

expression of the ciliated cell marker (*TEKT1*) was reduced with IL-13. To quantitative analysis, q-PCR was used. Further, variation in gene expression was also observed with several replicates.

The DAPT-treated HBEC3-KT cells exhibited low expression of ciliated gene markers, while the expression of ciliated cell marker *TEKT1* was not affected during the treatment of HBEC3-KT cells with IL-13. This may be an effect of culturing in the Pneumacult ALI media as other studies were done in BEGM, which may support the formation of higher numbers of ciliated cells (Ross et al., 2007, Bingle et al., 2010). The Notch signaling pathway is stimulated when there is the decision of the ciliated cell's fate in the progenitor cells, while the presence of repressors of secretory cells like DAPT results in the production of lesser secretory cells as compared to ciliated cells (Tsao et al., 2009).

The results following treatment with DAPT showed a few ciliated cells. The reason why DAPT did not work as intended in my study could be due to a number of reasons; either the dosage chosen was inadequate or the duration of treatment to stimulate the cells was insufficient. Furthermore, the HBEC3-KT cells may have lost the capacity to induce a full multiciliated phenotype. Further studies are required to explore this more fully and to reach some solid conclusions.

3.13.3 The differentiation of BMI-1 and HBECs

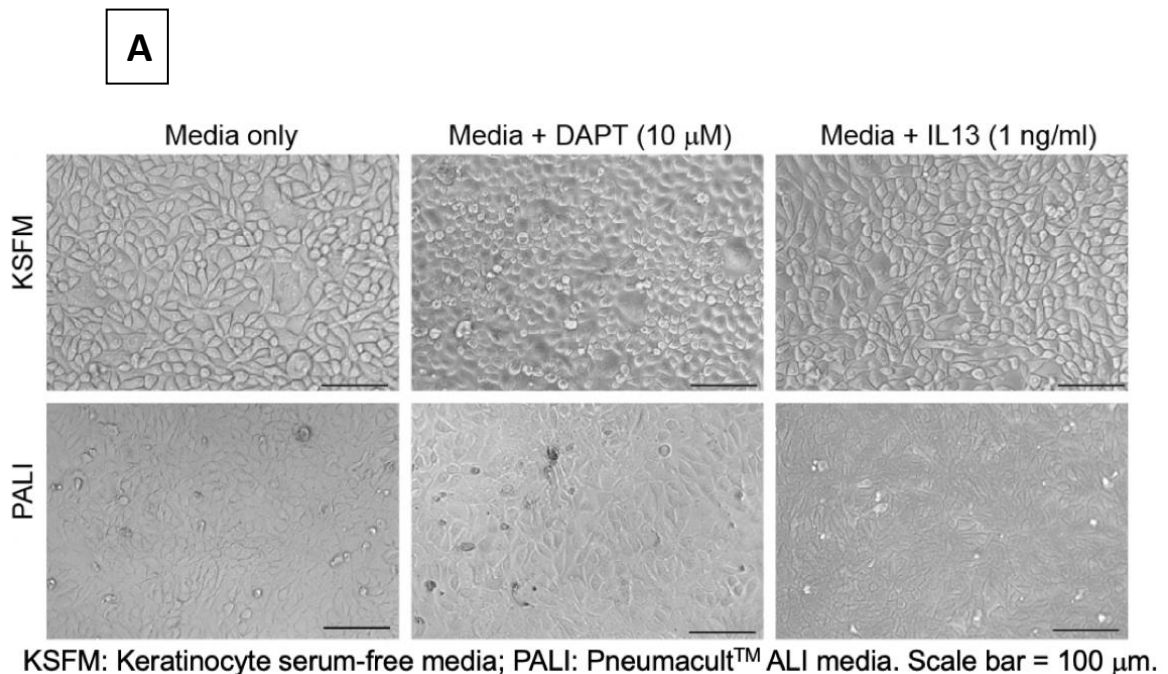
Previous morphologic analysis of the BMI-1/hTERT cells showed that they present as a pseudostratified structure highlighting the presence of two types of cells: ciliated and mucous secretory cells after culturing on ALI for 28 to 35 days (Fulcher et al., 2009). It was found that cultures developed in an abundant quantity of mucous secretory cells within the confluent layer, whereas ciliated cells were observed in very limited quantity although they did increase upon culturing of the cells to 35 days (Fulcher et al., 2009). The exact reason behind the abundance of mucous secretory cells is unknown but is consistent with my data that shows lower levels of ciliated cell markers in the BMI-1 cells.

MUC5B, a secretory cell marker, staining was observed at day 21 showing the differentiation of a secretory cell population. Previous studies have shown that MUC5B and MUC5AC are seen in secretory goblet cells (Rayner et al., 2019).

By directly comparing gene expression in the three different cells types it was clear that expression of differentiated cell markers was highest in the HBECs. This suggest that although both of the immortalized cell lines were able to undergo mucociliary differentiation neither

became as “differentiated” as the primary cells. Whole genome transcriptional analysis would be a tool that could be used to investigate this further.

One of the most striking observations that were seen from the gene expression experiments is that both HBECs and the BMI-1 expressed *BPIFA1* and *SCGB1A1* before differentiation at the ALI. This may be an effect of culturing in the Pneumacult™ Expansion plus media. Unfortunately, I did not directly test this in my study with these two cell lines. Our lab has previously shown that *BPIFA1* and *SCGB1A1* are not expressed in HBECs grown in traditional BGEM-based growth media before differentiation (Bingle et al., 2010). This finding is consistent with transcriptional studies which have shown that using BEGM media does not initiate the expression of differentiation-specific genes before differentiation at the ALI (Ross et al., 2007, Ruiz García et al., 2019). A rational explanation for this early induction of secretory marker genes could be that the growth media influences cell composition (differentiation) in cultures of primary ALI cells. Consistent with this suggestion one of our group members Miraj shown that HBEC3-KT cells grown in submerged cultures of KSFM and Pneumacult ALI media (PALI) begin to express the marker of secretory cell differentiation (Figure 3.24). The analysis suggests that HBEC3-KT cells do not require ALI culture to begin to differentiate.



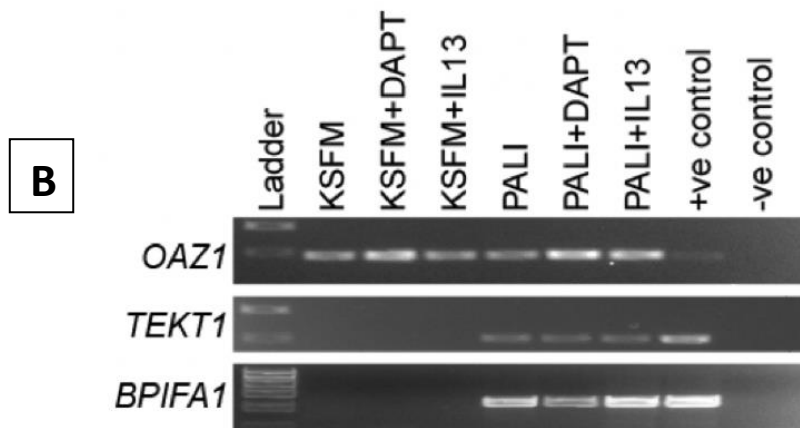


Figure 3.24: (A) HBEC3-KT cells grown in KFSM and PALI media exhibit different phenotypes. (B) HBEC3-KT cells can partially differentiate to both ciliated cells (*TEKT1*-positive) and secretory cells (*BPIFA1*-positive) when cultured under submerged conditions using PALI media, either with or without adding DAPT and IL-13.

Differentiation and expansion media, which contain multiple biological and chemical reagents, are critical for the successful development of primary human cells into completely differentiated pseudostratified epithelium, such media can be purchased from a variety of commercial sellers (Butler et al., 2016). In addition, published research has examined the inclusion of growth-inactivated cells to increase cell life and differentiation potential, when passaging cells exclusively in bronchial epithelial cell growth media, researchers detected and described a loss in cell proliferation and differentiation potential, showing that self-renewal capacities started to be lost after one to two passes (Horani et al., 2013). Another study discovered the benefits of utilising Rho kinase inhibitor and mitotically inactivated feeder cells. The use of this type of media increased the number of primary tracheal airway cells (Butler et al., 2016). The study also described a loss in cell growth and differentiation potential when cells were cultured in BEGM media alone, showing that self-renewal capacities begin to fade. Another group conditionally regulated juvenile cells using Rho kinase inhibitor and conditioned BEGM medium from irradiated inactivated feeder cells, passaging cell 5 to 6 times over 30 days and obtaining significant immune responses in differentiated cells (Hynds et al., 2018b).

3.13.4 Comparison of ALI-differentiated of HBEC3-KT cell and HBEC secretomes

The multiple cell types of the differentiated respiratory epithelium directly secrete proteins on to the epithelial surface. The composition of the secretions of the apical and basolateral epithelial are expected to be different. Mucus is the main secretion from the apical surface of epithelial cells and is a gelatinous and sticky material that lines the nose, throat, lungs, sinuses, and mouth. It forms a layer over the epithelial surface and provides the first line of defense against any invading pathogens and particles at the bronchial level (Zanin et al., 2016). For lung models, the composition and evolution of the apical secretome are important elements to understand. I directly compared the secretomes of the ALI-differentiated HBEC and HBEC3-KT cells with the expectation that they might secrete similar proteins. The analysis of long-term cultures of HBECs and HBEC3-KT cells and their apical secretomes show that the two models do indeed have some similarities.

The secretion of proteins from either cell can be either directly through exocytosis or exosomes. The cellular proteins discussed here belong to both types of secretion in both cell types. Proteins such as MUC5AC, MUC5B, SCGB1A1, and SLPI are well known to be secreted by the HBECs (Jackson et al., 2020, Touzelet et al., 2020), while surprisingly, proteins such as OLFM4 and HP were found to be abundantly secreted in HBEC3-KT cells. Several questions remain unanswered at present about the secretion patterns of these proteins in this type of cell. The finding of an elevated level of OLFM4 (a gut-associated secretory protein) in Calu-3 cells was also reported by Sanchez-Guzman et al., (2021). HP is a protein produced by liver that function is to remove free hemoglobin from blood and helps to neutralize oxidative damage (MacKellar and Vigerust, 2016). Whilst it is mainly produced in liver it has also shown in lung tissue (Naryzhny and Legina, 2021). HP expression is also increased in multiple cancers (Garibay-Cerdenares et al., 2015, Mariño Crespo et al., 2019). Thus, it can be assumed that the over expression of both OLFM4 and HP in HBEC3-KT cells could be attributed to the immortalization of HBEC during the development of this cell line.

HBECs are known to secrete protective proteins as part of the protective barrier of the airway (Jiang, 2018). MUC5B and MUC5AC proteins comprise a major protein component of mucus, and they act as protective physical barriers to both biological and physical damage (Ali et al., 2011, Song et al., 2020). In this regard, these mucins are not the only group of proteins involved in this function, but many other associated proteins including HP and OLFM4 help them in protecting both respiratory and gastrointestinal tracts against bacterial infections (Gersemann

et al., 2012). Therefore, it can be expected that other proteins differentially expressed here in HBEC play a role along with mucins against infection because one of the most important functions of these epithelial cells is to protect the body against infection. On the other hand, previous studies show that HBEC3-KT cells function almost as progenitor basal cells (Delgado et al, 2011), therefore, they express proteins that facilitate their roles to maintain the characteristics of progenitor cells. This characteristic is lost when cells are differentiated into a specific type. Based on the results of previous studies, it can be concluded that proteins that are highly expressed in HBEC3-KT cells such as OLFM4 have their role in maintaining the progenitor cells (Wang et al., 2018b). However, OLFM4 has been shown to be expressed more in a small intestine cell, the Paneth cell, rather than in the airway (Duckworth, 2021).

Sanchez-Guzman et al., (2021) showed that secretions from long-term cultures of NHBE and Calu-3 cells have high similarity, in terms of protein composition. Calu-3 is a human lung adenocarcinoma cell line grown in adherent culture and displays epithelial morphology. The secretions of Calu-3 cells include antimicrobial peptides, a large range of enzymes, and mucins known to be key elements of the mucosal immune system against pathogens and xenobiotics. Relatively similar results were observed for the secretome analysis of the two models of this study in ALI-differentiated of HBEC3-KT cell and HBECs secretomes.

Previous studies have shown that the expression of *BPIFA1* and *BPIFB1* increases gradually during the course of HBEC mucociliary differentiation (Ross et al., 2007). Both genes were expressed in my cultures. However, increased expression of *BPIFA1* during differentiation was not observed in my cultures this suggests that the culture medium used for submerged cultures facilitated the expression of the gene. Furthermore, since the expression of *BPIFA1* was much higher in differentiated HBECs as compared to differentiated HBEC3-KT (Figures 3.3 and 3.12), *BPIFA1* could only be detected in the secretome of HBECs (Figure 3.19).

3.13.5 Variation in this study

In this study, batch-to-batch variation in HBEC3-KT and BMI cells and inter-donor variation in HBECs impacted the results. I noticed changes in the expression of genes specific to the epithelium as well as the production and secretion of proteins. Cells from different donors are known to vary in the viability and growth characteristics in primary cell cultures, leading to unpredictable outcomes (Brachtl et al., 2022). Differences in primary cell culture batches or donors may have several causes. In accordance with my results, previous studies have also demonstrated that different donors can affect results (Mindaye et al., 2017). Different numbers of distinct cell types, such as goblet and secretory cells, may develop in the same batch of cells,

leading to variations in the quantities of airway epithelial markers and proteins generated in each well. Thus, the proteomic analysis of the apical secretomes of HBEC3-KT cells and HBECs may have shown fluctuation across batches or donors due to variations in the composition of epithelial cells. Further variation among the primary HBEC secretome could be attributed to the age, sex and individual genetic background of the donors. Though the genetics of the donors is unknown, many genes including mucins genes are highly polymorphic, and polymorphism has also been detected for other genes such as Clara cell protein 16 (*CC16*) (Fowler et al., 2001, Gribben et al., 2022). Also, a recent report suggested age-dependent structure and function of nasal epithelial cultures where the authors showed variable expression of MUC5AC, MUC5B, Epithelial sodium channels (ENaC), Transmembrane protein 16 (TMEM16A) and CFTR are over-expressed significantly in children as compared to elderly people (Balázs et al., 2022). Such age-dependent gene expression can significantly alter the secretome as we age. Also, secretory proteins tend to alter more in the female smoker as compared to male smokers indicating a gender-based difference in secretome (Kokelj et al., 2021). The study showed a significant alteration of 58 secretory proteins in female compared to 28 secretory proteins in male. Therefore, the sex and age of the subjects have been proven to be important in pulmonary research. Such information should be considered in the future.

3.13.6 Conclusion

In this chapter, the ALI model was used to generate cultures of the immortalised human airway epithelial cells HBEC3-KT and BMI-1 as well as primary HBECs. All cell types are differentiated into the distinct cell types that can be observed in the respiratory tract. However, I observed that different batches yielded somewhat inconsistent results. All three airway epithelial cell types generated a consistent secretory phenotype, which was confirmed by the expression of secretory cell marker genes (*BPIFA1*, *SCGB1A1*), but the two cell lines consistently failed to generate a strong ciliary phenotype. HBEC3-KT cells were treated with DAPT and IL-13 in an attempt to modulate cellular differentiation to more ciliated and mucous phenotypes, respectively. IL-13 treated cells appeared to yield a more goblet cell-rich culture, but the DAPT treatment failed to induce an increased level of ciliogenesis. A proteomics analysis supported the findings that there was a similarity between HBEC3-KT cells and HBEC secretions, but also showed that there were some differences. One of the more significant findings to emerge from my study is that the HBECs remain perhaps a better model for infection studies. My studies demonstrate that the HBEC3-KT cells are not a perfect model for

the airways study because the cells did not have the ciliation level like that seen in HBECs. However, HBEC3-KT cells can be gene-edited and clonally expanded and used for other functional studies. Because of this, I determined to use the line to perform infection experiments, as indicated in the next chapter.

CHAPTER 4: *Staphylococcus aureus* infection in undifferentiated airway cells.

4.1 Introduction

As outlined in the introduction respiratory infections are one of the most prevalent infections in humans, with high mortality and morbidity. In 2015, over 17 million upper respiratory tract infections were reported, while in the same year, lower respiratory tract infections caused over 2.7 million deaths (Korsun et al., 2019). Moreover, a WHO/UNICEF report from 2009 showed that over 1.8 million children under the age of 5 die from pneumonia every year (Mudhune et al., 2009).

Around 30% of humans harbour *S. aureus* as commensal bacteria. However, *S. aureus* can sometimes become pathogenic, and can therefore be characterised as an opportunistic bacterium. *S. aureus* can be isolated from the skin and mucosal surfaces including the respiratory tract and nasopharynx (van Belkum, 2016). Different impacts of this bacteria are observed in different individuals, but it is considered a risk factor for infections because it is found consistently in 20% of individuals and intermittently in 60% of individuals (Albrecht et al., 2015, Kumar et al., 2015). Symptoms associated with *S. aureus* vary from asymptomatic carriers to severe infection. Such variation in symptoms is due in part to the differential response by the host i.e., differences in immune responses against bacterial infection (Montgomery et al., 2014, Greenberg et al., 2018).

As described in the introduction, the airway epithelium is the first line of resistance against both bacterial and viral respiratory pathogens. Its main function is to act as a physical barrier and to activate various innate and adaptive immune responses. The pseudostratified airway epithelium lines the trachea, bronchi, and bronchioles and the ciliated and secretory cells on its surface contribute to the mucociliary apparatus. This epithelium contains a basal cell population located beneath the epithelial surface. As highlighted in Chapter 3 these basal cells have the capacity to differentiate into the multiple cells type found within the epithelium under define tissue culture conditions.

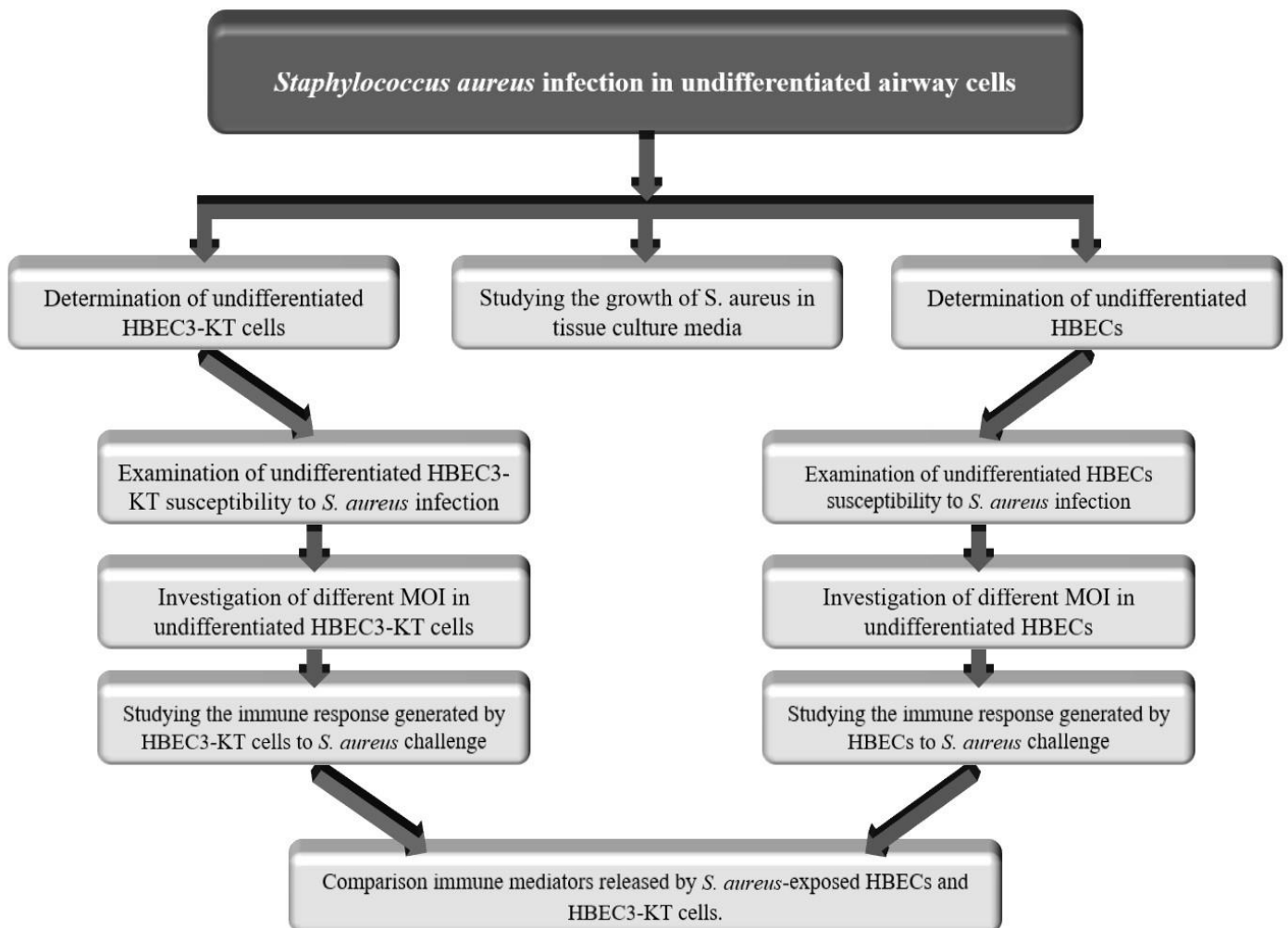
Cell lines are useful for *in vitro* lung research because they are immortalised. These types of cells do not undergo the ageing process and have infinite replication potential; therefore, they are ideal tools for optimisation studies. Such cells are genetic replicas of each other as they are formed through cell division, therefore, no genetic variation should be observed between different cells. However, the disadvantage of using cell lines is that they grow abnormally, and they can show unexpected responses to stimuli. Furthermore, they contain genetic mutations which have made them tumorigenic, therefore, it is not always possible to use them to study

the characteristics of the specific tissue from which they were obtained. As outlined previously, this is particularly the case with lung cells and in Chapter 3, I described aspects of the differentiation of two airway cell lines in direct comparison to primary HBECs.

I have shown that the HBEC3-KT cell line has some limited characteristics of the differentiated airway in submerged culture but that like primary HBECs it can be differentiated in ALI culture. As such when in submerged culture it can be considered having a “basal” cell like phenotype similar to primary HBECs grown in the same manner. Both airway cell lines and undifferentiated HBECs have been used in any studies of bacterial infections (Hasan et al., 2018, Jamieson et al., 2020). ALI culturing of cells is a time-consuming process and therefore I considered that it would be worthwhile to initially study infection of undifferentiated cells prior to working with the more complex ALI cultures.

4.1.1 Aims:

The aim of the experiments reported in this chapter was to establish *S. aureus* infections in airway cells in submerged cell culture. Specifically, I compared infections and cellular responses in undifferentiated HBEC3-KT cells and HBECs infected with *S. aureus* SH1000-GFP.



Study plan for this chapter.

4.2 Results

4.2.1 Growth of *S. aureus* in tissue culture media

In order to determine whether *S. aureus* could be grown in Keratinocyte-SFM (KSFM) and Pneumacault™ Expansion Plus (Ex⁺) media, the bacteria were cultured in suspension in 24-well plates at 1μ. Subsequently, the number of colony-forming units (CFU) was counted in each well. Figure 4.1 illustrates that marked bacterial growth was seen after 4 hours in both KSFM and Pneumacault™ Ex⁺ media. Bacterial numbers significant increased between 2 and 4 hours of growth ($p < 0.0001$). Bacterial growth was significantly faster in Pneumacault™ Ex⁺ media as compared to KSFM ($p < 0.01$). Pneumacault™ Ex⁺ media contains a fraction of human plasma and human plasma is rich in undefined nutrients required for the bacterial growth (90% water, other 10% include nutrient molecules, proteins, ions, wastes and dissolved gases) (Leeman et al., 2018). Hence, it is possible that *S. aureus* is growing faster in Pneumacault™ Ex⁺ media but not in KSFM as KSFM does not contain any human serum or plasma.

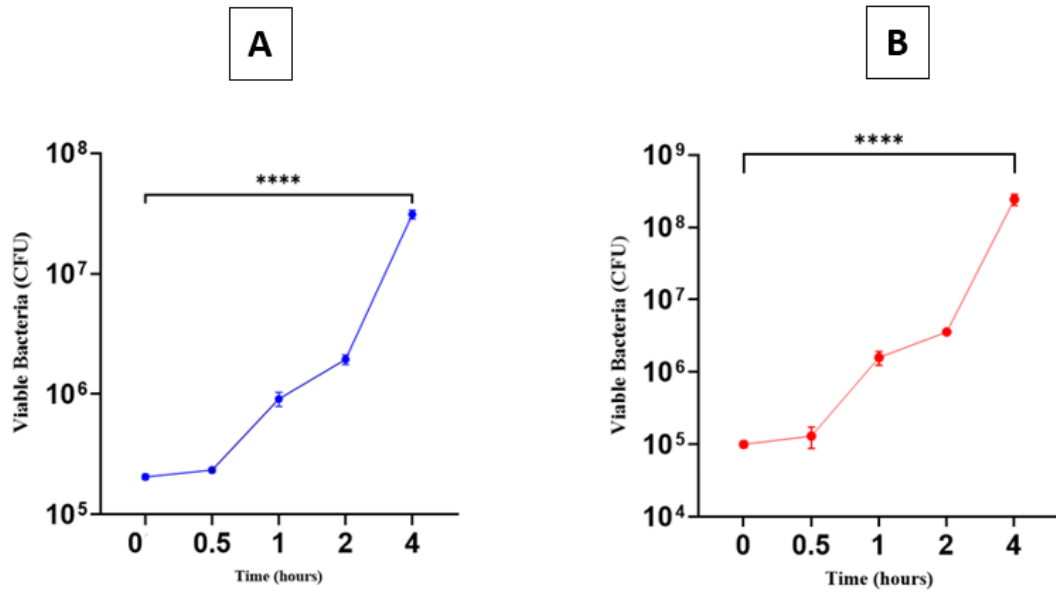


Figure 4.1: Viable Counts of 4 hours *S. aureus* infections in different growth medium. (A) Viable counts were taken at the start, and after 0.5, 1, 2 and 4h of growth in KSFM and (B) Pneumacault™ Ex⁺ media. A one-way ANOVA using time = 0 as the control showed significance at 4 hours. Error bars show SEM. (n=3). ****p<0.0001.

4.2.2 Determination of MOI in undifferentiated HBEC3-KT cells

Undifferentiated HBEC3-KT cells (uHBEC3-KT cells) were cultured on 24 well plates until they were approximately 80% confluent, and cells were initially infected with MOI of 0.01, 0.1 and 1 of *S. aureus* for one hour. After this time, the cultures were washed with HBSS to remove bacteria that were present within the media. The cultures were refed with fresh media and growth continued for periods of 1, 2, 4 and 24 hours (Figure 4.2A).

To obtain a quantitative measurement of the level of bacteria present in cell cultures during the development of infection, viable bacterial counts were conducted as described in detail in the Materials and Methods. As expected, the numbers of bacteria increased with the passage of time. This increase in bacterial cells was evident in all three MOI doses. As was expected the CFU increased more when the initial MOI was higher when compared those that resulted from lower MOIs.

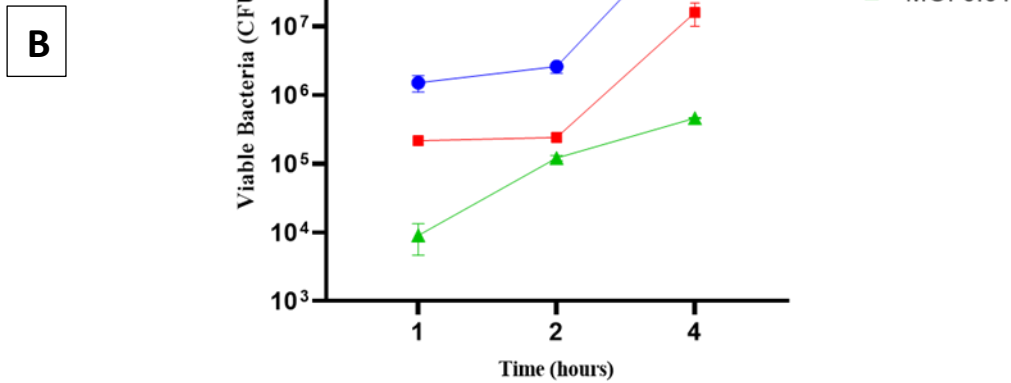
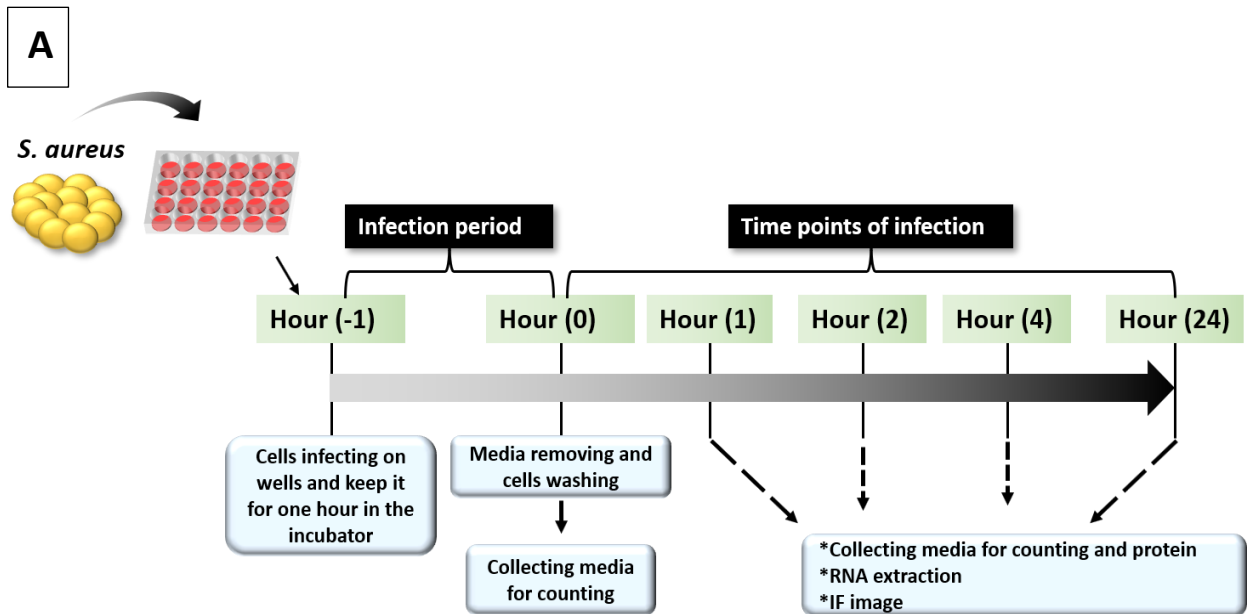


Figure 4.2: Viable Counts of *S. aureus* infections in uHBEC3-KT cells.

(A) Timeline of infection and at regular intervals, samples were taken for viable counting of *S. aureus*, cytokine arrays study and transcriptional. (B) Viable counts were taken at t 1h, 2h and 4h of short-term infections and are displayed as means and SEM. (n=3).

4.2.3 Establishing infections in uHBEC3-KT cells

To visualise the infection of HBEC3-KT cells with *S. aureus*, cells were seeded at 25,000 cells per well in 24-well plates. At approximately 80% confluence, the cells were infected with *S. aureus* strain SH1000-GFP at different MOIs (1, 0.1 and 0.01) for 1, 2, 4 and 24 hours. After washing of cells with HBSS, a ZOE Fluorescent Cell Imager microscopy was used to examine the level of infection. This was performed to analyse the bacteria associated with host cells, not freely living bacteria in the media.

Figures 4.3, 4.4 and 4.5 reveal that there was a gradual increase in the amount of infection. Consistent with the bacterial count data from above, for all three MOIs, at the 1-hour time point only very small amounts of green fluorescence was seen in the infected cells. Similarly, by 2-hours the number of GFP bacteria increased compared to the first hour and by 4 hours there appeared to be more bacteria (as illustrated by green fluorescence) in all wells. By 24 hours, the number of bacteria was markedly increased for all MOIs as the green fluorescence is very evident after 24 hours of the cellular growth when essentially all cells appear to be infected.

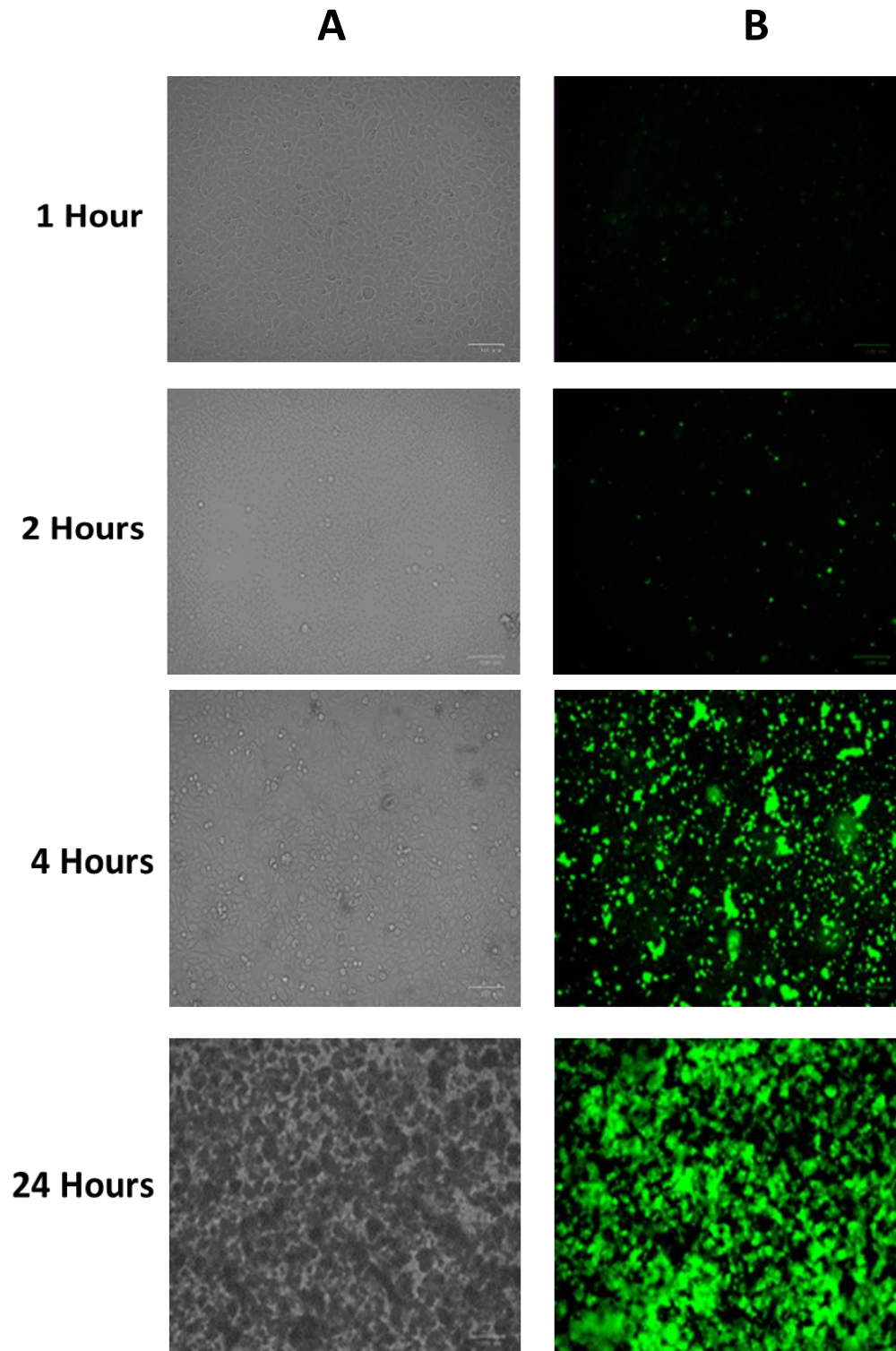


Figure 4.3: Infection uHBEC3-KT cells with *S. aureus* at MOI (1). uHBEC3-KT were infected with *s. aureus* at an MOI of (1) for 1,2,4 and 24 hours. (A) illustrates brightfield images. (B) Green fluorescence demonstrates the presence of bacteria. Images are representative of n=3 independent infections. Scale bar = 100 μ m.

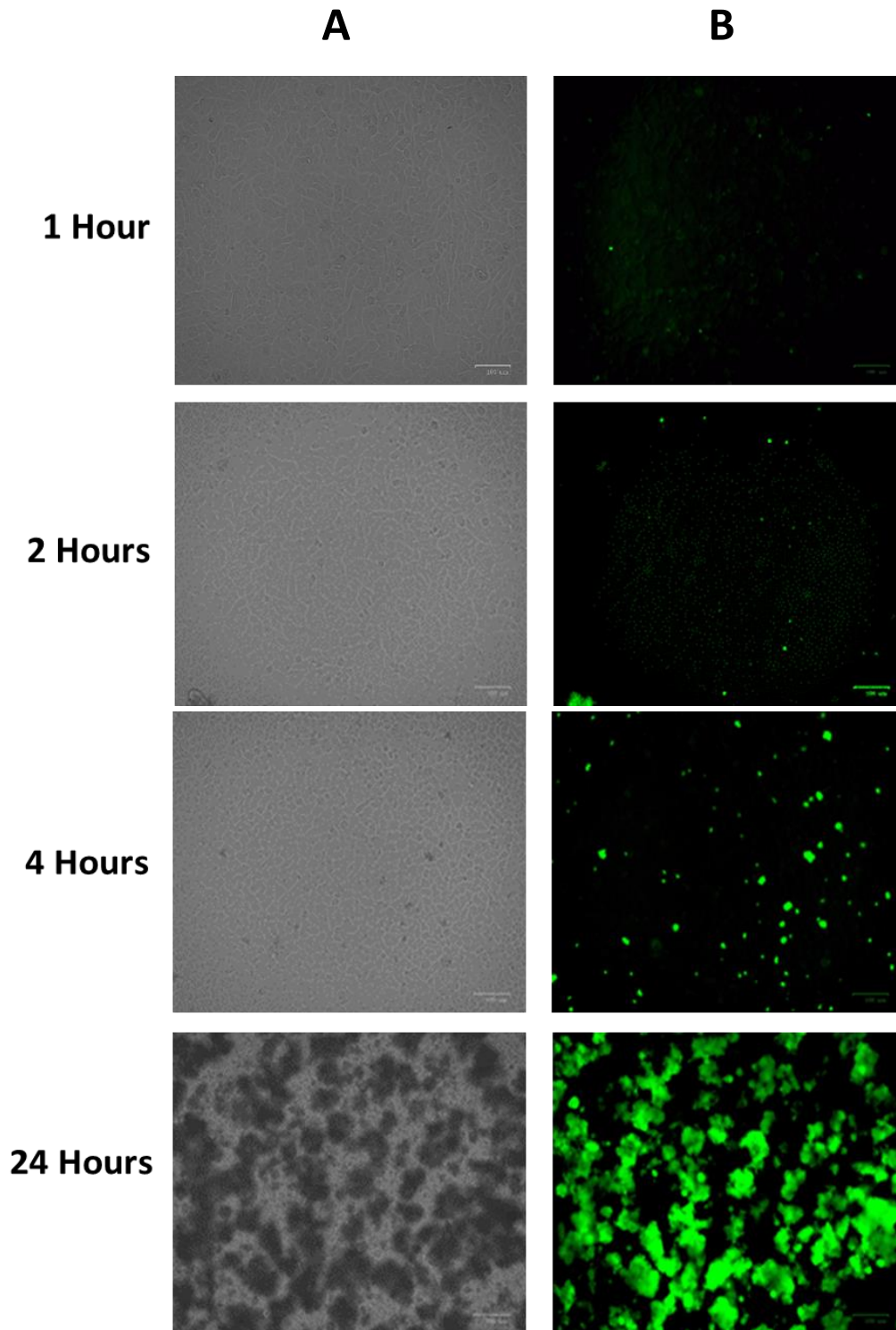


Figure 4.4: Infection uHBEC3-KT cells with *S. aureus* at MOI (0.1). uHBEC3-KT were infected with *s. aureus* at an MOI of (0.1) for 1,2,4 and 24 hours. (A) illustrates brightfield images. (B) Green fluorescence demonstrates the presence of bacteria. Images are representative of n=3 independent infections. Scale bar = 100 μ m.

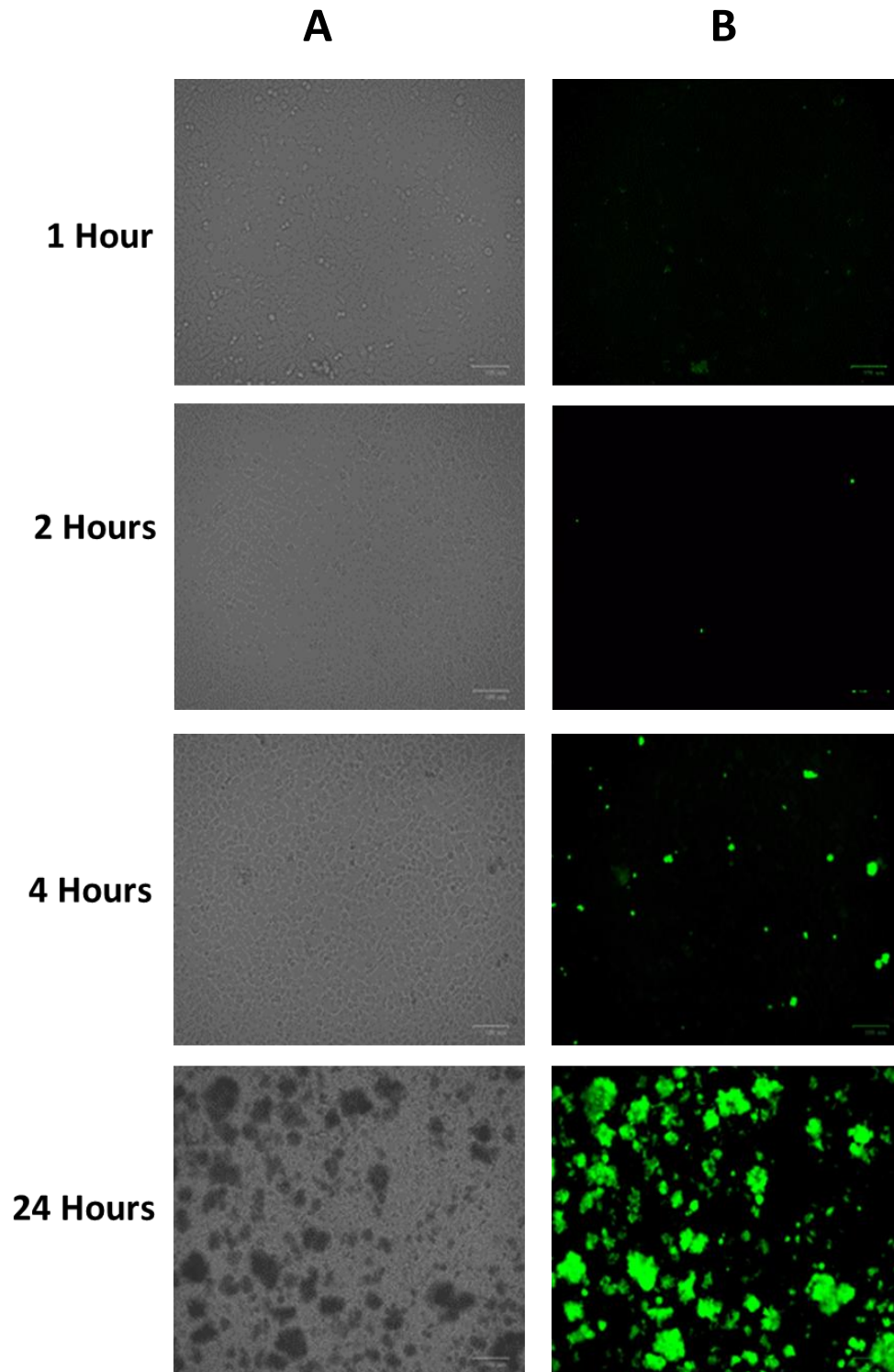
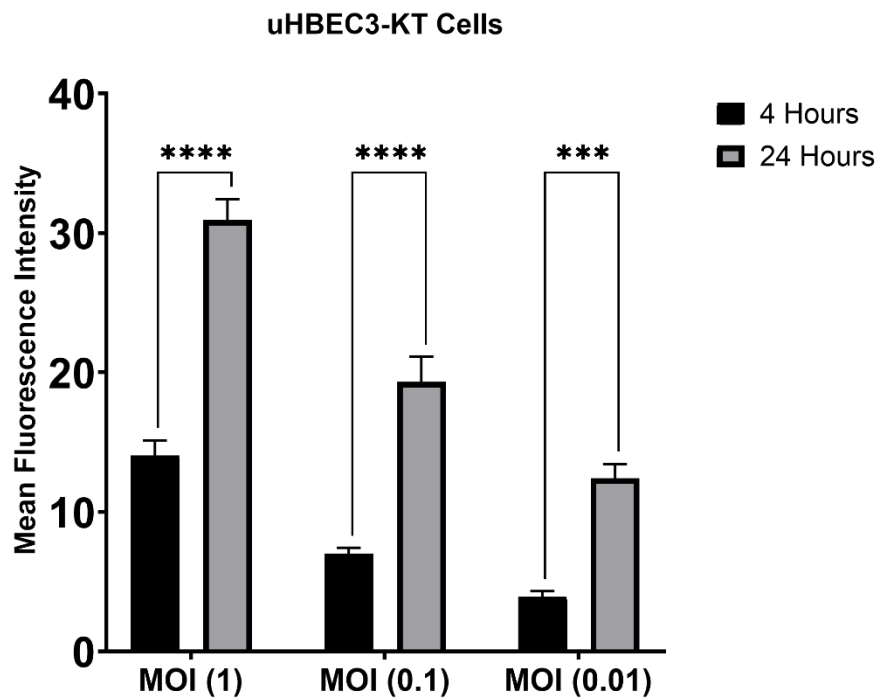


Figure 4.5: Infection uHBEC3-KT cells with *S. aureus* at MOI (0.01).

uHBEC3-KT were infected with *S. aureus* at an MOI of (0.01) for 1,2,4 and 24 hours. (A) illustrates brightfield images. (B) Green fluorescence demonstrates the presence of bacteria. Images are representative of n=3 independent infections. Scale bar = 100 μ m.

I next used a quantitative approach to measure the level of bacterial infection in the cultures. For this, the infection intensity was measured in four random fields in each of three separate experiments. As illustrated in Figure 4.6A the comparison between different samples loaded with different MOIs. In all cases significant increases in bacterial level (as judged by GFP intensity) were seen after 4 hours. As illustrated in Figure 4.6B, the mean fluorescence intensity is increased when higher MOI was used for infection at four different time intervals; 1,2,4 and 24 h. Moreover, the mean fluorescence intensity was also increased with passage of time of infection.

A



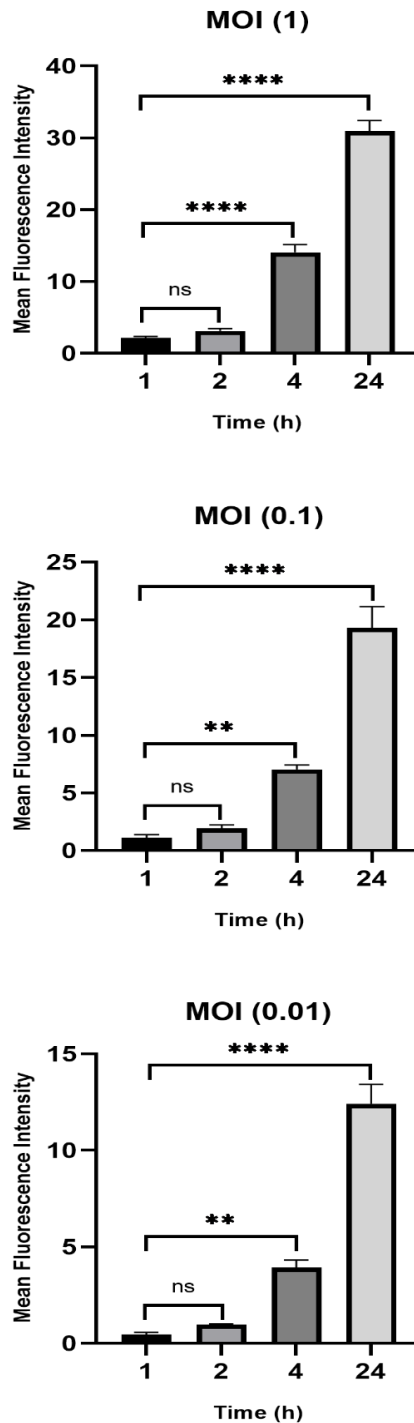
B

Figure 4.6: Comparison of mean fluorescence intensity of GFP in uHBEC3-KT cells infected with *S. aureus* at different MOIs.

(A) MOIs of 0.01, 0.1 and 1 were used for comparison between 4 and 24 hours. Data were analysed using a paired t-test. (B) Different MOIs (0.01, 0.1 and 1) were used for infections of uHBEC3-KT cells for periods of 1, 2, 4 and 24 hours. Data were analysed using A one-way ANOVA test. The intensity of infection was measured in 4 fields in each of 3 replicated experiments. Images obtained under the ZOE Fluorescent Cell Imager. Fluorescence intensity was measured through processing with using ImageJ-win32 and intensities were compared. Error bars: SEM. * $p < 0.05$; ** $p < 0.01$ and **** $p < 0.0001$.

4.2.4 Responses of uHBEC3-KT cells infected with *S. aureus*

4.2.4.1 Induction of host cell gene expression

In order to investigate the inflammatory gene responses to the infection of uHBEC3-KT cells with *S. aureus*, RNA was extracted from cells at multiple time points (1, 2 and 4 hours) during infection at different MOIs. (1, 0.1 and 0.01) and used for RT (endpoint) PCR. *OAZ1* is a stable housekeeping gene and was utilized as a PCR reaction control. It would be expected that cell viability would be decreased as MOIs would be increased in culture media. We used primers against *CXCL10* and *IL6* to compare their mRNA expression across the time points of infection (Figure 4.7). The pro-inflammatory cytokines IL-6 and CXCL10 were chosen because they are produced by respiratory cells (Al Mubarak et al., 2018, Callahan et al., 2021). *OAZ1* was expressed essentially equally across all samples. The data shows that both *CXCL10* and *IL6* were expressed at all times of infection for all three different of MOIs. There was a suggestion that both genes were induced in a time and dose dependent manner. Neither gene was expressed in the uninfected samples. The results of the RT-PCR showed that expression of both *IL6* and *CXCL10* increased with time (i.e., their expression was much higher after hour 3 as compared to their expression after hour 1) (Figure 4.7). This trend can be observed for both genes. Furthermore, the highest expression of both genes was observed when the maximum dose of infection (i.e., an MOI of 1 versus an MOI of 0.1 and 0.01). This is worth noting because such trends were not observed for *OAZ1*, which was used as a loading control in this experiment.

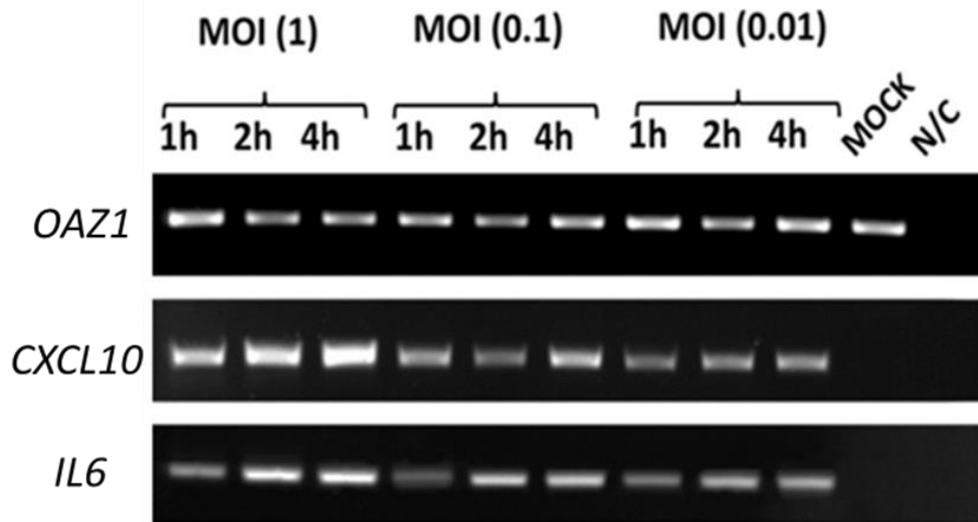


Figure 4.7: RT-PCR of gene expression during the infection of uHBEC3-KT with *S. aureus*.

RT- Endpoint PCR was performed as described using cDNA of samples collected at 1, 2 and 4 hours of infection. Samples were amplified with primers *OAZ1*, *CXCL10* and *IL6*. This gel represents data from one of 3 separate replicate experiments. MOCK indicates a sample of uninfected cells; MOI refers to multiplicities of infection and N/C is the negative control without cDNA.

To further confirm the validity of the endpoint-PCR data, TaqMan RT-qPCR using was used to generate quantitative data on the expression of *CXCL10* and *IL6* as an indication for the expression of pro-inflammatory genes. *CXCL10* and *IL6* expression levels increased in uHBEC3-KT cells infected with *S. aureus* at an MOI of 1, 0.1 and 0.01 when compared to the relevant control (Figure 4.8 A and B).

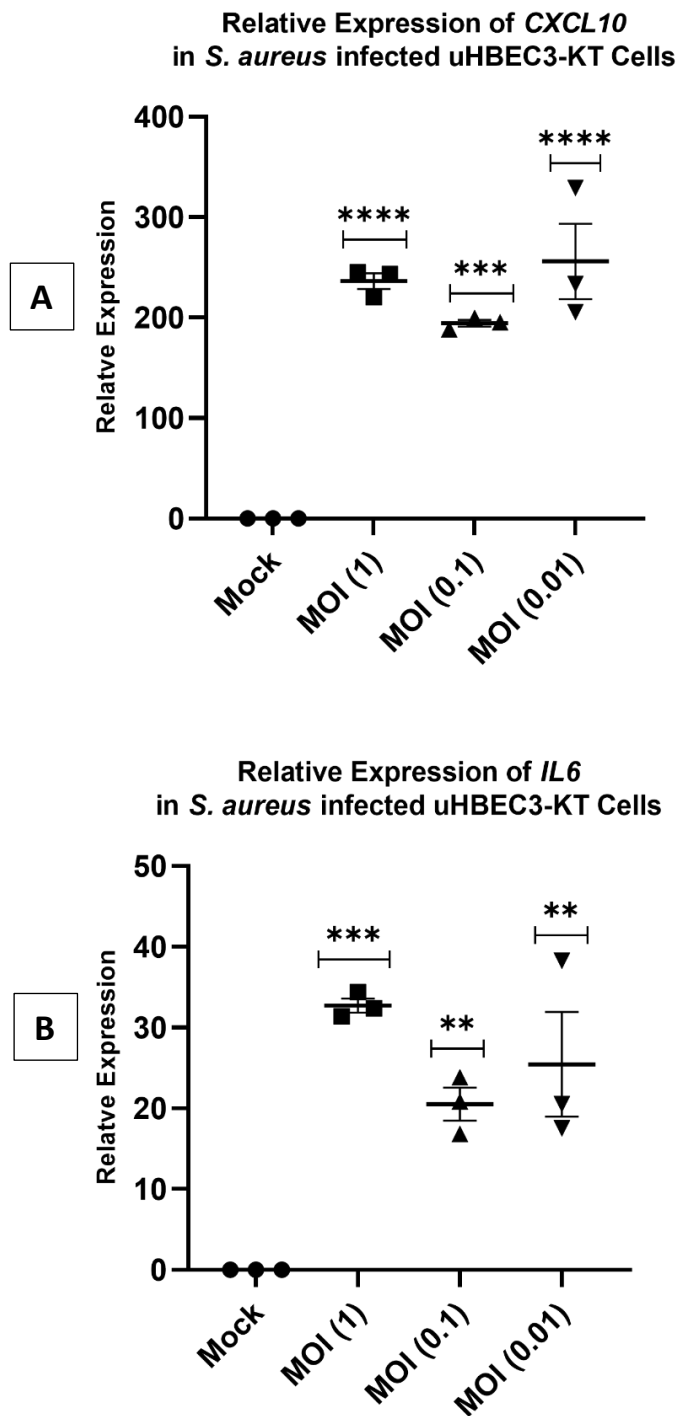


Figure 4.8: Comparison of *CXCL10* and *IL6* in uHBEC3-KT cells infected with three different MOIs of *S. aureus*.

qPCR was used to obtain quantitative data utilizing primers against *CXCL10* (A) and *IL6* (B) in samples from uHBEC3-KT cells infected with different MOIs of *S. aureus* for 4 hours. The relative expression of mRNA was normalised to *OAZ1* as a control. The fold expression was calculated by comparing the CT values of the genes. Data were analysed using A one-way ANOVA test. Error bars: SEM. Analysis was performed on 3 independent biological replicates. ** $p < 0.01$, *** $p < 0.001$ and **** $p < 0.0001$.

4.2.5 Cytokine and chemokine production by *S. aureus* exposed uHBEC3-KT cells

To learn more about how the cells reacted to the infections, a protein secretion study was conducted at an early infection time point. 4 hours after infection at MOI 1, conditioned medium was taken from the cells, along with control medium from mock infected wells and the secretion of inflammatory cytokines and chemokines was measured using Human Cytokine Array Panel A as described in the Materials and Methods section (2.8.2). Due to the volume of media needed for the assay, media was combined from 3 different experiments. For all samples, the array experiment was performed at the same time and results were obtained from exposures at the same length of time to ensure accurate results.

Control uHBEC3-KT conditioned medium gave strong signals for Serine protease inhibitor-1 (SerpinE1) and migration inhibitory factor (MIF) and weak signals for C-X-C motif chemokine 12 (CXCL12)/ Stromal Cell-derived factor 1 (SDF-1), IL-1 α /IL-1F1 and IL-18/IL-1FA (Figure 4.9 A). Infection reduced the SerpinE1 signal but had no effect on MIF (Figure 4.9 B). Densitometry analysis indicated a modest increase in CXCL12/SDF-1, IL-1 α /IL-1F1 and IL-18/IL-1FA. What is striking about the figures in this graph is a strong signal for IL-6 (Figure 4.10). It is important to note that because these are the results of a single experiment (albeit with samples pooled from a number of experiments), their reproducibility cannot be determined. The changes in cytokine secretion in uHBEC3-KT cells was compared between mock cells and infected with *S. aureus* for 4 hours. The results revealed that significant differences were observed in Serpin E1/PAI-1 as this factor is seen at reduced level in infected as compared to mock cells. The level of Serpin E1/PAI-1 was reduced from 12000 to 7000 mean pixel density. Smaller reductions have also been observed for IL-18/IL-1FA (from 2500 to 1800 mean pixel density) and IL-1alpha/IL-1F1 (800 to 200 mean pixel density). On the other hand, levels of IL-6 and CXCL-12/SDF-1 were increased in response to the bacterial infection as they were not seen in mock cells but are significantly secreted in infected cells. Finally, MIF was not affected by infection as it remained the same both in mock and infected cells.

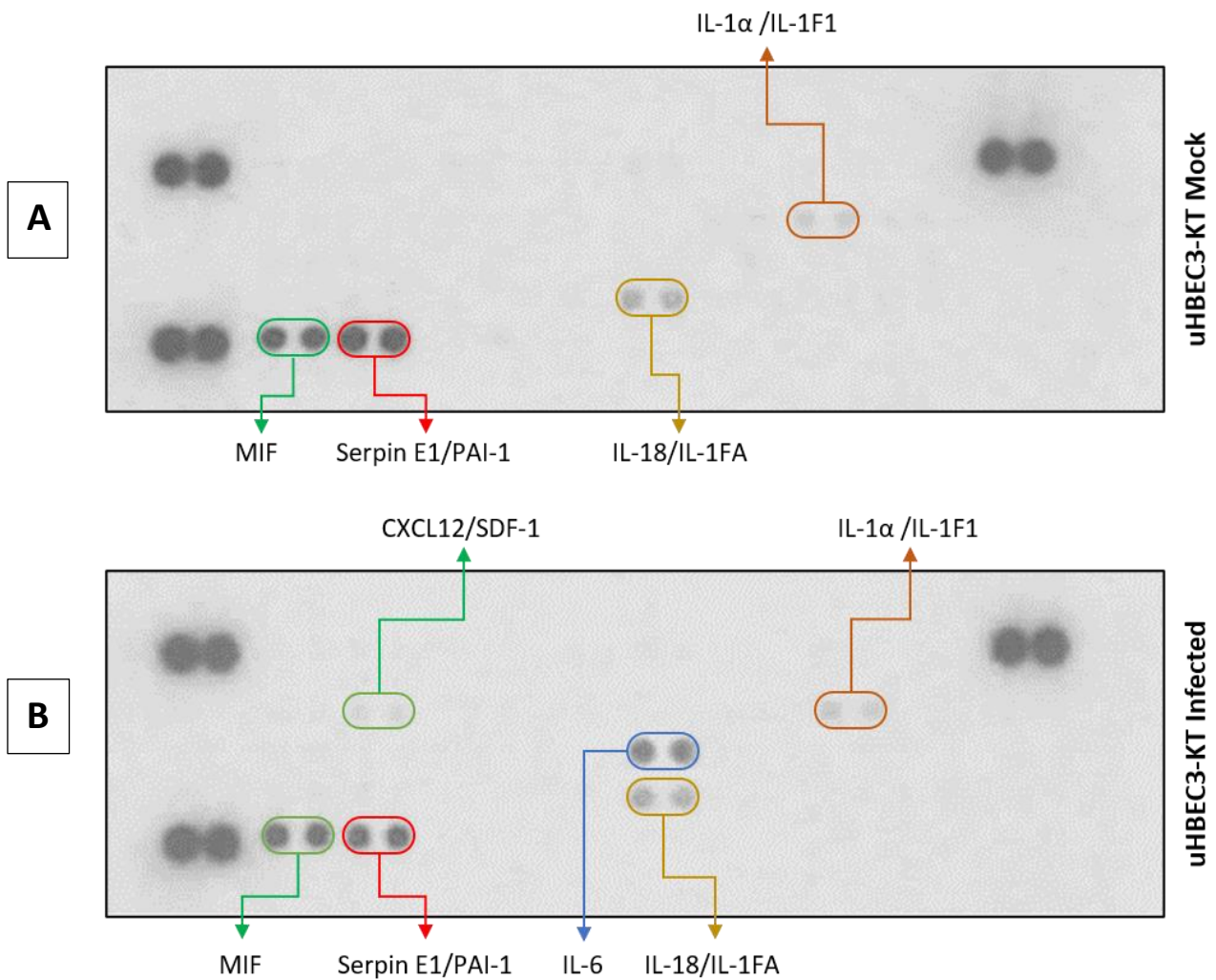


Figure 4.9: Cytokine Array from uHBEC3-KT cells with *S. aureus* for 4 hours. Conditioned medium of uHBEC3-KT were pooled and used for analysis. At 4 hours post-challenge, immune mediators produced by cells exposed to *S. aureus* (MOI-1). Panel (A) represents the secretion of immune mediators of mock cells (uninfected cells). Panel (B) represents the secretion of immune mediators of infected uHBEC3-KT. Cells were analysed by cytokine array analysis. (The blot is representative of n=3).

Change in cytokine and chemokine expression in uHBEC3-KT cells infected with *S. aureus* for 4hours

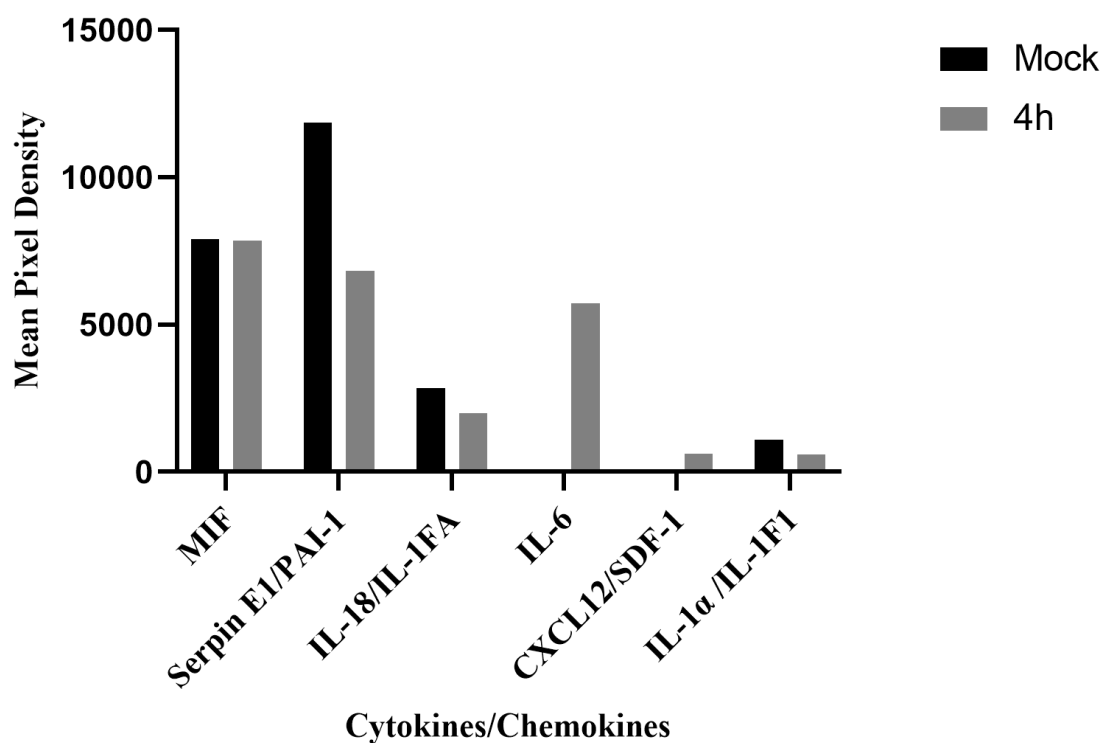


Figure 4.10: Comparison of immune mediators released by *S. aureus*-exposed for 4 hours uHBEC3-KT cells (MOI-1).

Results of the human Cytokine Array assay, illustrating levels of signaling molecules released by uHBEC3-KT exposed to *S. aureus* 4 hours post-infection as compared to those released from mock cells. The pixel density was calculated through processing with using The Image Studio Lite software (LI-COR Biosciences). Media from 3 individual uHBEC3-KT batches were pooled.

4.2.5 Determination of MOI in undifferentiated HBECs

Having undertaken infections in the uHBEC3-KT cell I wanted to directly compare them to the responses of undifferentiated primary uHBECs to *S. aureus* infections. As outlined in chapter 3, uHBECs represent a basal cell population with limited phenotypic similarity to the mucociliary epithelium. For these experiments, cells were cultured on 24 well plates in a manner similar to the uHBEC3-KT cells. They were initially infected with *S. aureus* for one hour. After this time cells were washed, and media was replaced with fresh media. MOIs of 0.01, 0.1 and 1 were used for periods of 1, 2, 4 and 24 hours (Figure 4.11A).

I next performed viable bacterial counts to quantify the bacteria present in the cultures during infection development. The number of viable bacteria had increased significantly by hour 4 for all three MOIs (1, 0.1, and 0.01; Figure 4.11B). As expected, the results showed that the CFU values were higher when the MOI used was high. For instance, the CFU value at MOI 1 was 10^7 as compared to 10^7 at MOI 0.01. In contrast, uHBEC3-KT cells showed similar CFU at MOI 1 to that of uHBEC; however, the CFU at MOI 0.1 and 0.01 was much lower for the uHBEC3-KT cells. For example, the CFU of the uHBEC3-KT cells at MOI 0.01 was close to 10^7 (Figure 4.2B).

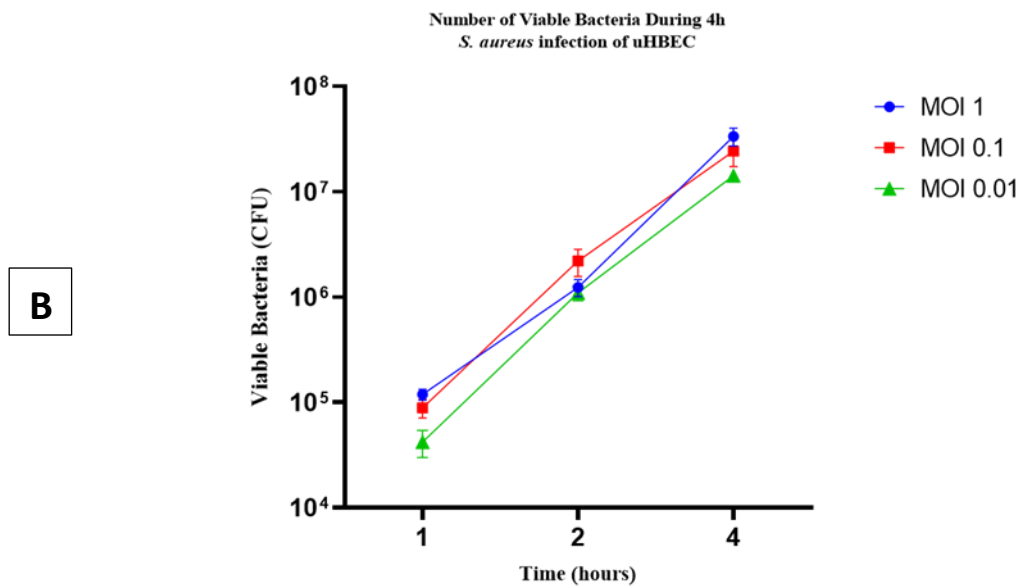
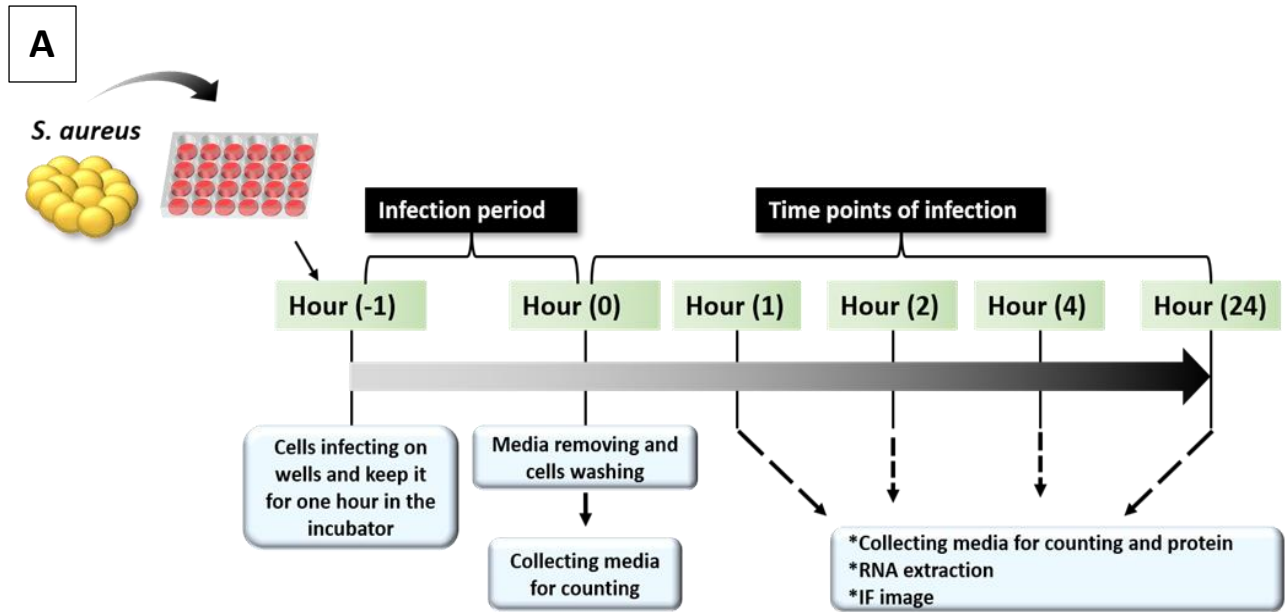


Figure 4.11: Viable Counts of *S. aureus* infections in uHBECs.

(A) Timeline of infection for viable counting of *S. aureus*, cytokine arrays study and transcriptional investigations. (B) Viable counts were taken at the 1h, 2h and 4h of short-term infections performed using uHBECs. (n=3). Error bars show SEM.

4.2.6 Establishing infections in uHBECs

To establish uHBECs infections with *S. aureus* and to determine an appropriate dosage for future research, uHBECs were grown on 24-well plates with 30,000 cells per well. At roughly 80% confluence cells were infected with *S. aureus* at various MOIs of 1, 0.1, and 0.01 for 1, 2, 4 and 24 hours. ZOE Fluorescent Cell Imager microscopy was used to evaluate the amount of infection after the cells were washed. This was done to look at bacteria that are associated with host cells rather than free-living in the medium.

Figures 4.12, 4.13, and 4.14 demonstrate that the amount of infection gradually increased. At the 1-hour time point, cells at all three MOIs were confluent, with only modest green fluorescence in the infected cells. The number of bacteria (as seen by green fluorescence) in the wells had increased after 4 hours. By 24 hours, the quantity of bacteria had increased for all three MOIs, with MOI 1 having the most dramatic cell death at 24 hours. In this experiment, the increased infection level was investigated using fluorescence signal and it has shown that no such signal was present at the start, and it was highest after 4 hours.

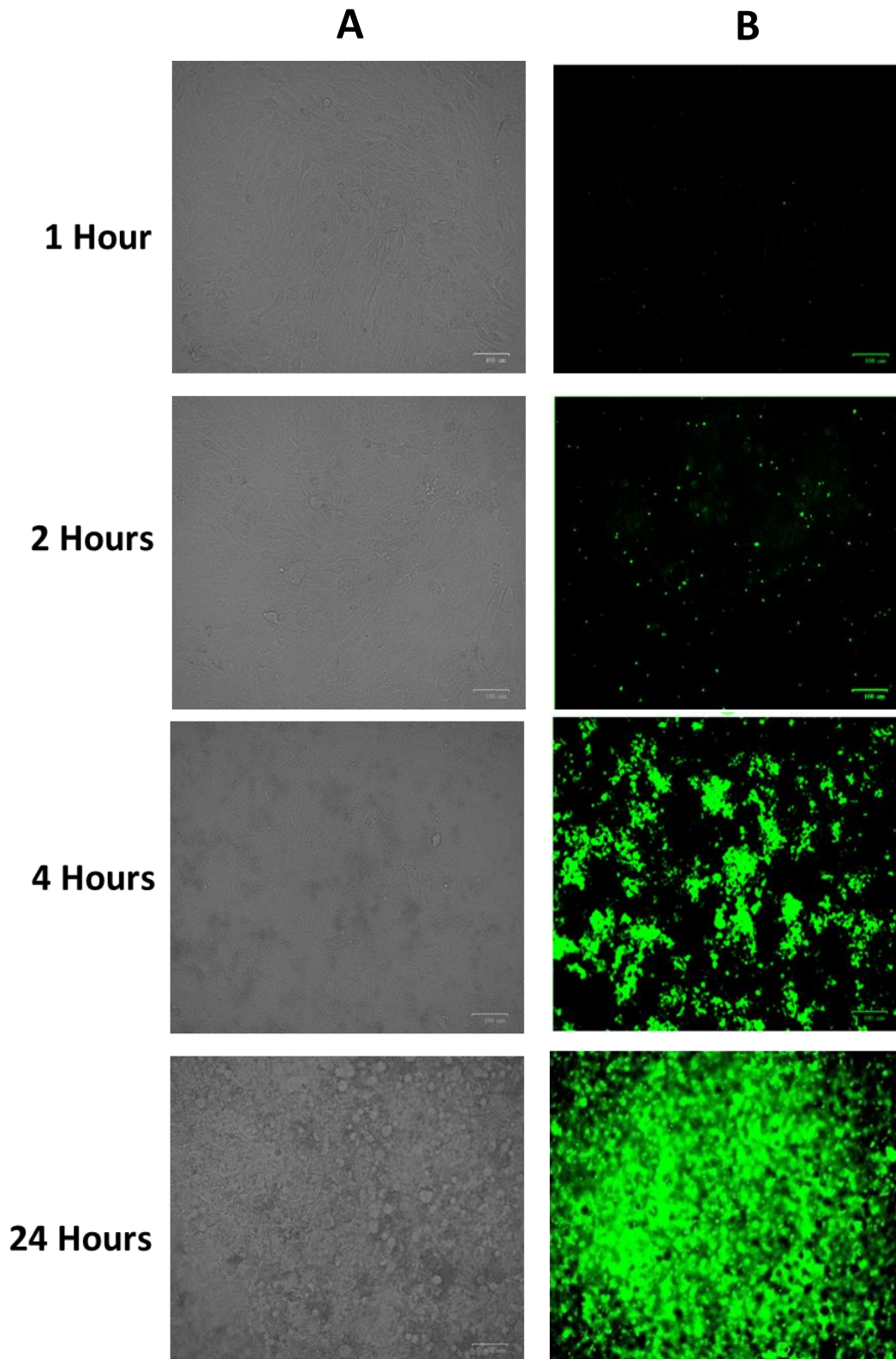


Figure 4.12: Infection uHBEC with *S. aureus* at MOI (1).

uHBEC were infected with *s. aureus* at an MOI of (1) for 1 ,2,4 and 24 hours. (A) illustrates brightfield wells as no green fluorescence. (B) Green fluorescence demonstrates the presence of bacteria. Images are representative of 3 independent infections. Scale bar = 100 μ m.

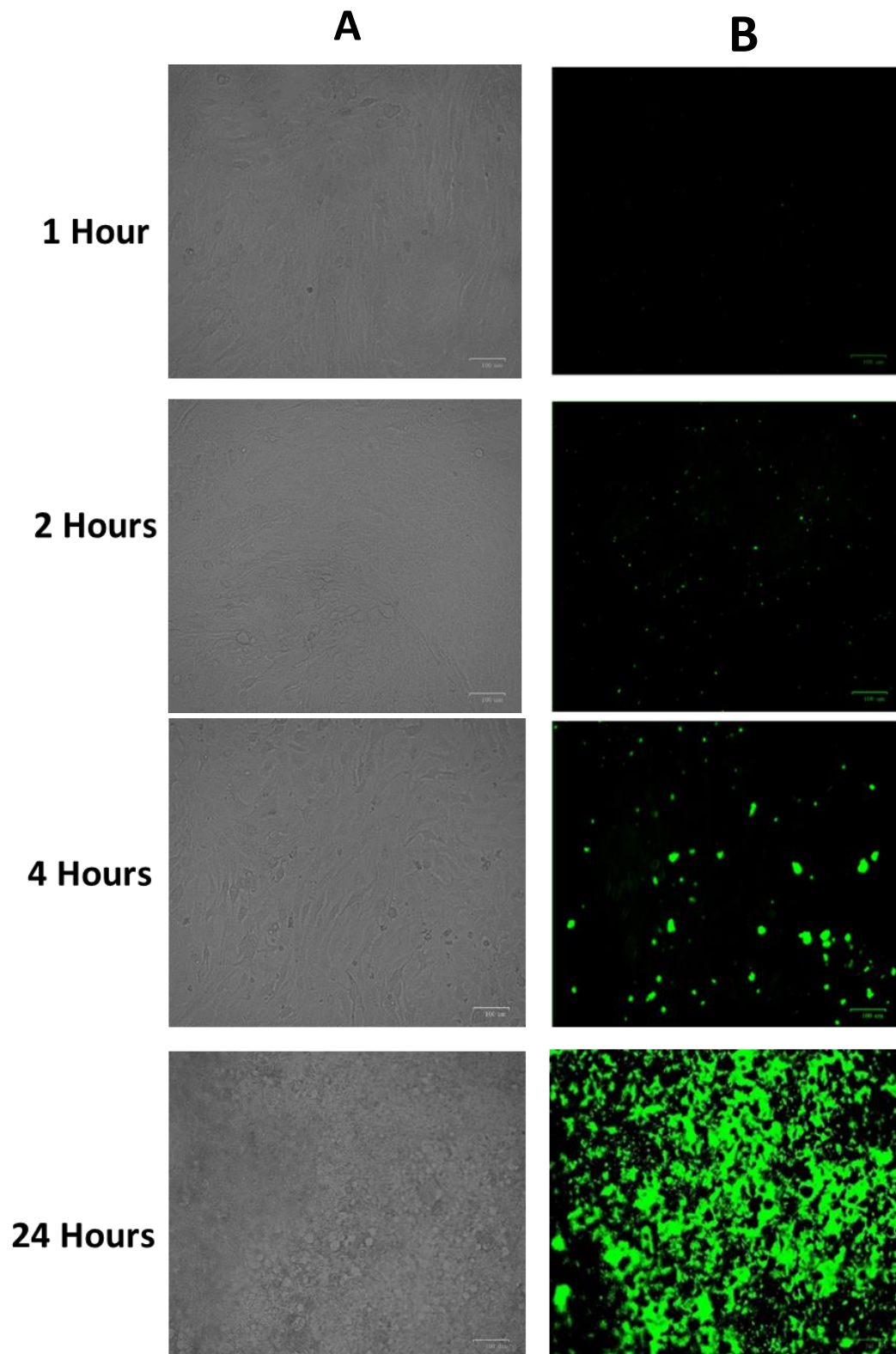


Figure 4.13: Infection uHBEC with *S. aureus* at MOI (0.1).

uHBEC were infected with *s. aureus* at an MOI of (0.1) for 1 ,2,4 and 24 hours. (A) illustrates Brightfield wells as no green fluorescence. (B) Green fluorescence demonstrates the presence of bacteria. Images are representative of 3 independent infections. Scale bar = 100 μ m.

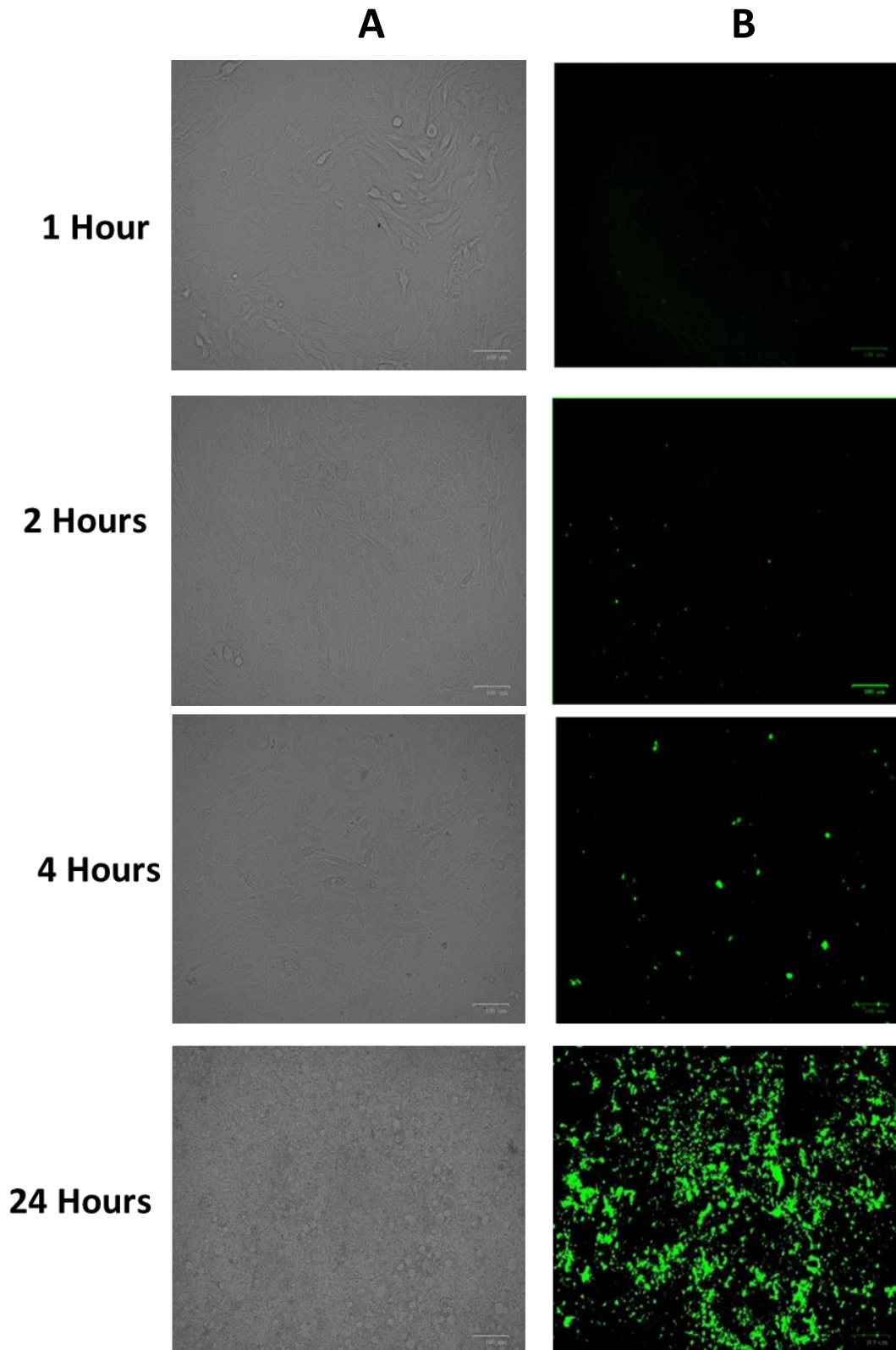
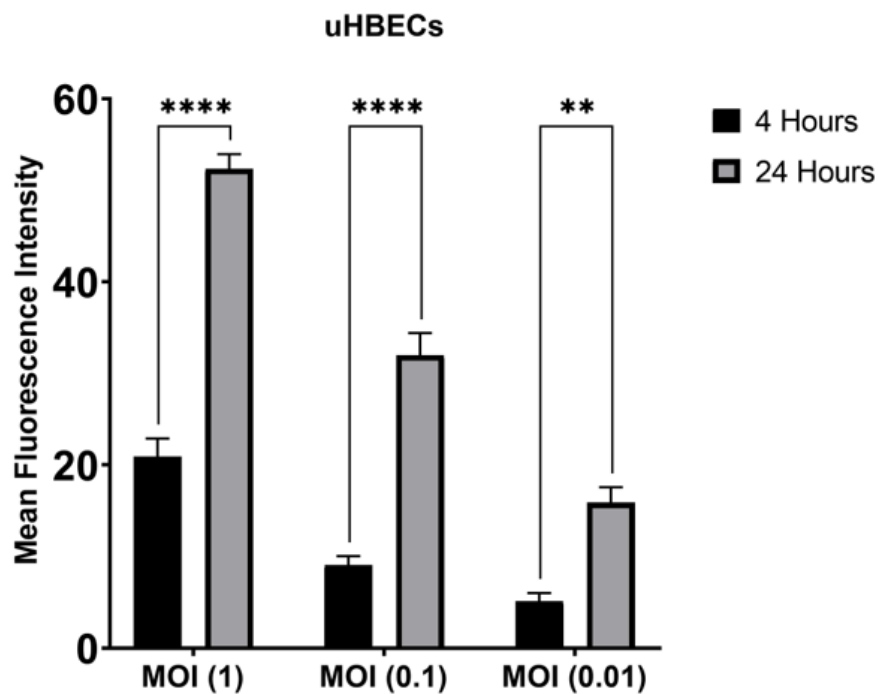


Figure 4.14: Infection uHBEC with *S. aureus* at MOI (0.01).

uHBEC were infected with *s. aureus* at an MOI of (0.01) for 1 ,2,4 and 24 hours. (A) illustrates brightfield images (B) Green fluorescence demonstrates the presence of bacteria. Images are representative of 3 independent infections. Scale bar = 100 μ m.

To quantify the number of bacteria in the infections, I quantitated GFP intensity in three separate studies, by assessing four image fields. Figure 4.15A shows the comparison between different samples loaded with different MOIs. In all cases significant increases in bacterial level (as judged by GFP intensity) were seen after 4 hours. These results are similar to those observed in uHBEC3-KT cells as significant fluorescence intensity is observed in both types of cells only after 4 hours. As illustrated in Figure 4.15B, the mean fluorescence intensity is increased when higher MOI was used for infection at four different time intervals; 1,2,4 and 24 h. Moreover, the mean fluorescence intensity was also increased with passage of time of infection.

A



B

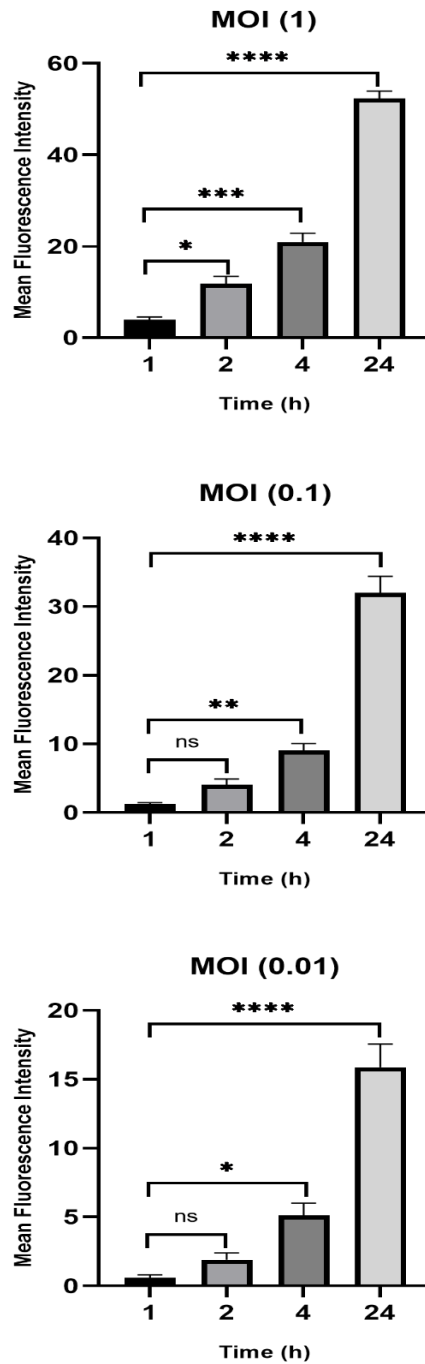


Figure 4.15: Comparison of mean fluorescence intensity in uHBEC exposed to *s. aureus* at three different MOIs.

(A) MOIs of 0.01, 0.1 and 1 were used for comparison between 4 and 24 hours. Data were analysed using a paired t-test. (B) Different MOIs (0.01, 0.1 and 1) were used for infections of uHBECs for periods of 1, 2, 4 and 24 hours. Data were analysed using A one-way ANOVA test. The intensity of infection was measured in 4 fields in each of 3 donors. Images obtained under the ZOE Fluorescent Cell Imager. Fluorescence intensity was measured through processing with using ImageJ-win32 and intensities were compared subsequently to obtain the results. Error bars: SEM. *p<0.05; **p<0.01, ***p<0.001 and ****p<0.0001.

Next, I directly compared the differential quantitated intensity in uHBEC and uHBEC-KT cells. For this, the infection intensity was measured in period of 4 and 24 hours. This analysis provided the evidence of cellular response when these two types of cells are infected by *S. aureus*.

The results shown in figure 4.16 the comparison between uHBEC3-KT cells and uHBECs when they subjected to bacterial infection. Mean fluorescence intensity was higher for uHBECs as compared to uHBEC3-KT cells at all time points post infection and doses of infection. The figure 4.16A shows comparative cellular response after 4 hours while figure 4.16B shows responses after 24 hours. It can be observed that fluorescence is maximum for both types of cells when higher dose of infection i.e., MOI 1 was used as compared to lower doses of infection. Furthermore, fluorescence intensity was increased over the time as maximum mean fluorescence intensity after 4 hours of infection is 21 while it was increased to 53 after 24 hours post infection. These results suggest that uHBECs show higher response to bacterial infection compared to uHBEC3-KT cells while the bacterial cell population (judged by fluorescence intensity) was increased with incubation time after infection and with higher infection dose.

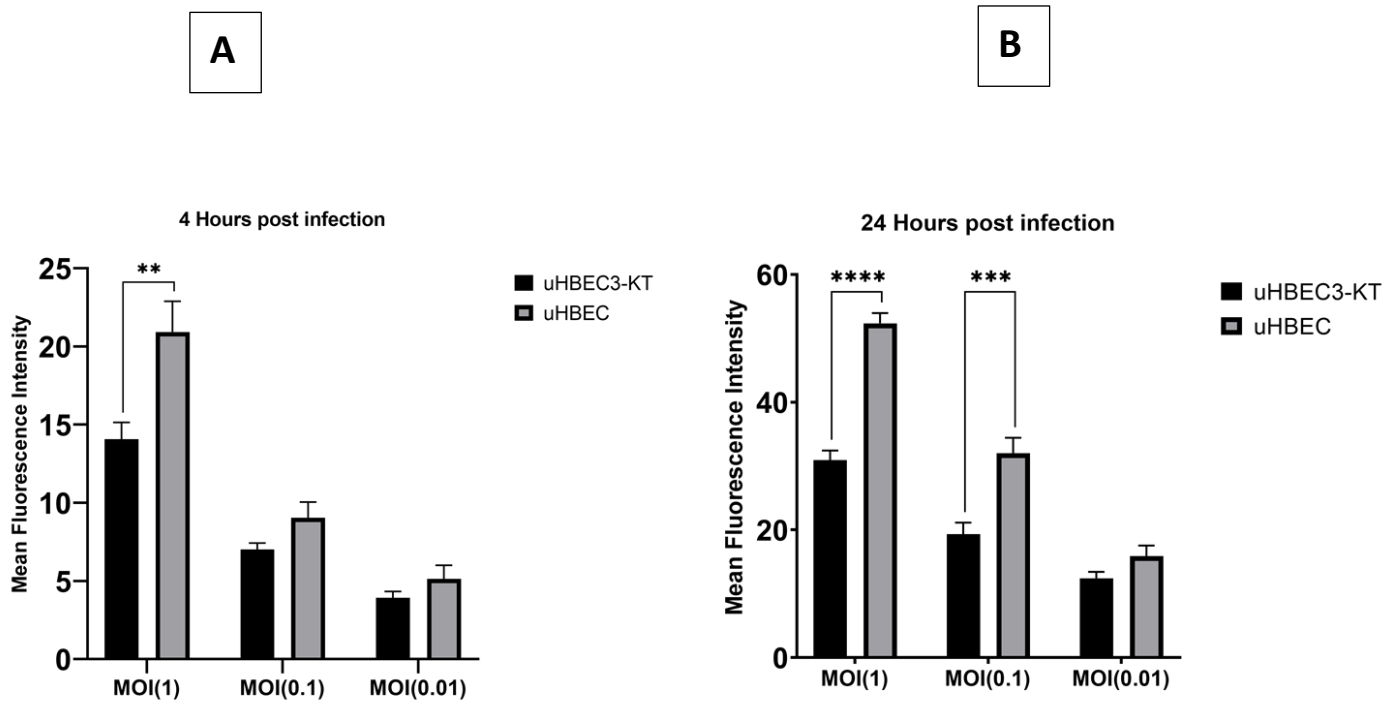


Figure 4.16: Comparison of mean fluorescence intensity in uHBECs and uHBEC3-KT cells exposed to *S. aureus* at different MOIs.

(A) MOIs of 0.01, 0.1 and 1 were used for comparison between uHBECs and uHBEC3-KT cells at 4 hours post infection. (B) MOIs of 0.01, 0.1 and 1 were used for comparison between uHBECs and uHBEC3-KT cells at 24 hours post infection. Data were analysed using a paired t- test. Error bars: SEM (n=3). **p<0.01, ***p<0.001 and ****p<0.0001.

4.2.7 Determination infection of uHBECs with *S. aureus*

4.2.7.1 Validation of host cell gene expression

In order to investigate the inflammatory gene responses to the infection of uHBECs with *S. aureus*, cells were grown in 24-well plates seeded at 30,000 cells per well. To focus on the early cell responses, RNA was collected from cells at 1, 2, and 4 hours after infection with *S. aureus* at MOIs of 0.01, 0.1, and 1 and utilized for RT (endpoint) PCR. *OAZ1* was used as the loading control since it is a stable housekeeping gene, as shown in Figure (4.17). To assess mRNA expression across time periods of infection, I utilized primers against *CXCL10* and *IL6*. The findings revealed that *CXCL10* and *IL6* expression could be identified at all stages of infection and at all three MOIs. It appeared that *CXCL10* was increased with passage of time especially when MOI is of 0.1 and 0.01 while similar concentration of *CXCL10* was observed at different time points when MOI was of 1. On the other hand, no clear difference was observed for *IL6* at different time points at any of MOIs.

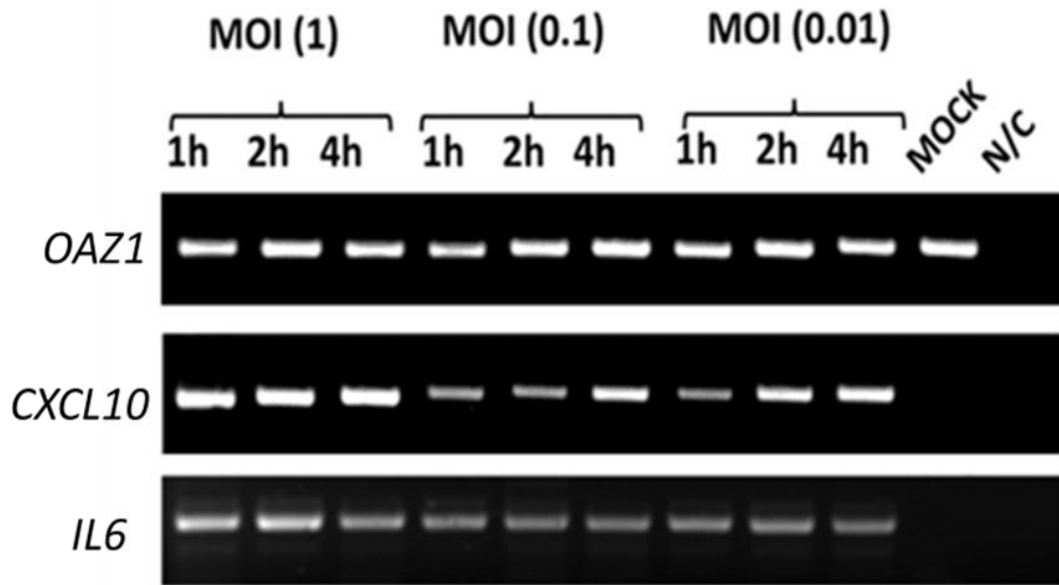


Figure 4.17: RT-PCR of gene expression during infection of uHBECs with *S. aureus*. RT- Endpoint PCR was performed as described using cDNA of samples collected at 1, 2 and 4 hours of infection. Samples were amplified with primers *OAZ1*, *CXCL10* and *IL6*. This gel represents data from one of 3 separate replicate experiments. MOCK indicates sample of uninfected cells, and N/C is the negative control without cDNA.

mRNA transcripts of *CXCL10* and *IL6* were assessed in the same sample using TaqMan RT-qPCR (Figure 4.18). *CXCL10* expression was increased in uHBECs infected with *S. aureus* at MOIs of 1, 0.1 and 0.01 in comparison to the relevant control, with statistical significance being seen for MOI 1 (Figure 4.18 A). mRNA expression of *IL6* was similar across different MOI and was increased when compared to the mock control. However, a high variation was seen in the results possibly due to inter-donor variations.

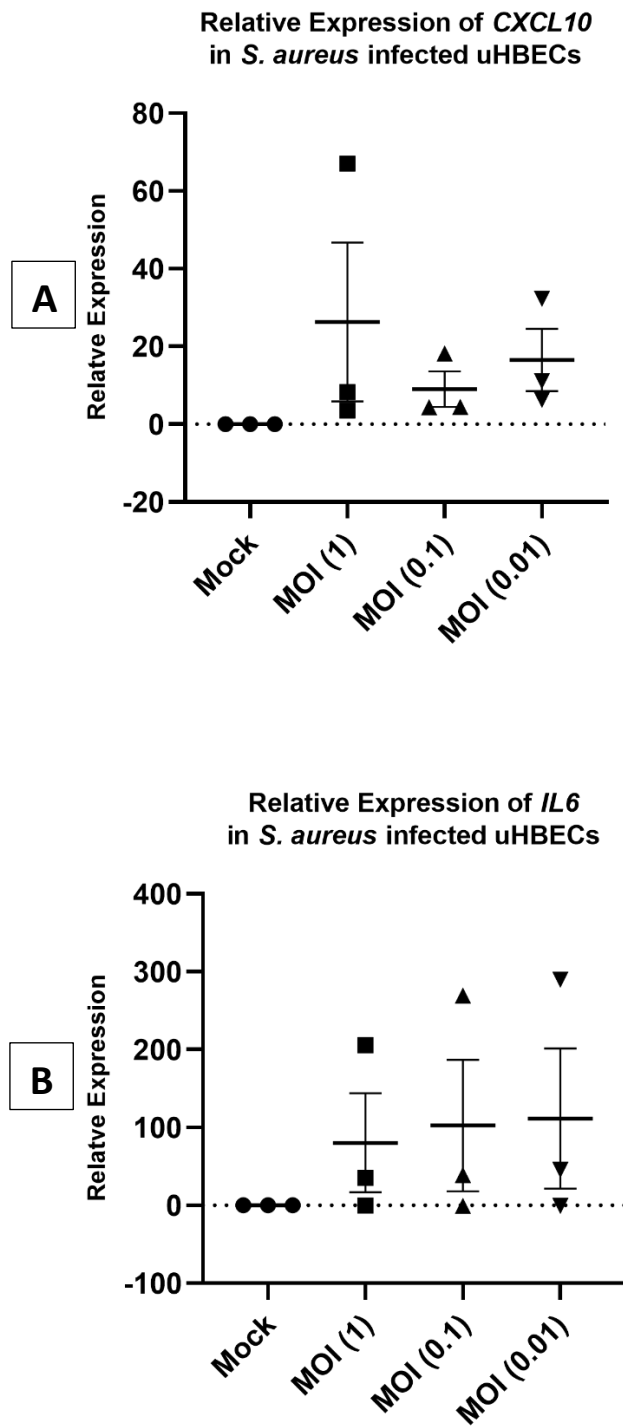


Figure 4.18: Comparison of *CXCL10* and *IL6* in uHBEC infected with three doses for 4 hours of *S. aureus*.

qPCR was used to obtain quantitative data utilizing primers against *CXCL10* (A) and *IL6* (B) in samples from uHBEC infected with *S. aureus* for 4 hours. The relative expression of mRNA was normalised to *OAZ1* as a control. The fold expression was calculated by comparing the CT values of the genes. Data were analysed using A one-way ANOVA test. Error bars: SEM. Analysis was done on 3 independent biological replicates with cells isolated from 3 different donors.

4.2.8 Cytokine and chemokine production by *S. aureus* exposed uHBEC

To learn more about how the uHBECs reacted to the infections, an identical protein secretion study was conducted as for the HBEC3-KT cells. 4 hours after infection at MOI 1, conditioned medium was taken from the cells, along with control medium from mock infected wells and the secretion of inflammatory cytokines and chemokines was measured using the Human Cytokine Array Panel A. The studies were all conducted under identical conditions and the same amount of time of exposure was used in each experiment.

Control uHBECs conditioned medium demonstrated the presence of strong signals for SerpinE1 and CXCL12/SDF with a weak signal for MIF, IL-1 α /IL-1F1, IL-13 and IL-18/IL-1FA (Figure 4.19 A). Infected uHBECs had similar levels of CXCL12/SDF but a reduced signal for SerpinE1 (Figure 4.19 B). Densitometry analysis indicated small increases in CD40 Ligand/TNFSF5, IL-1 α /IL-1F1 and IL-18/IL-1FA (Figure 4.20), a larger increase in IL-8 and induction of IL-1ra/IL-1F3. It is important to note that because these are the results of a single experiment with media combined from multiple experiments, their reproducibility cannot be determined. As shown in Figure 4.20, the levels of different cytokines and chemokines in uHBEC are compared in mock cells and infected *S. aureus* after four hours. The results show that most significant decrease in secretion was observed in Serpin E1/PAI-1 as it is reduced from 10000 mean pixel density to almost 100 mean pixel density. Small level reduction was also observed for CXCL-12/SDF-1. On the other hand, levels of IL-1ra/IL-1F3, MIF, IL-18/IL-1FA, IL-1alpha/IL-1F1 and IL-13 were increased significantly in infected cells as compared to the mock cells.

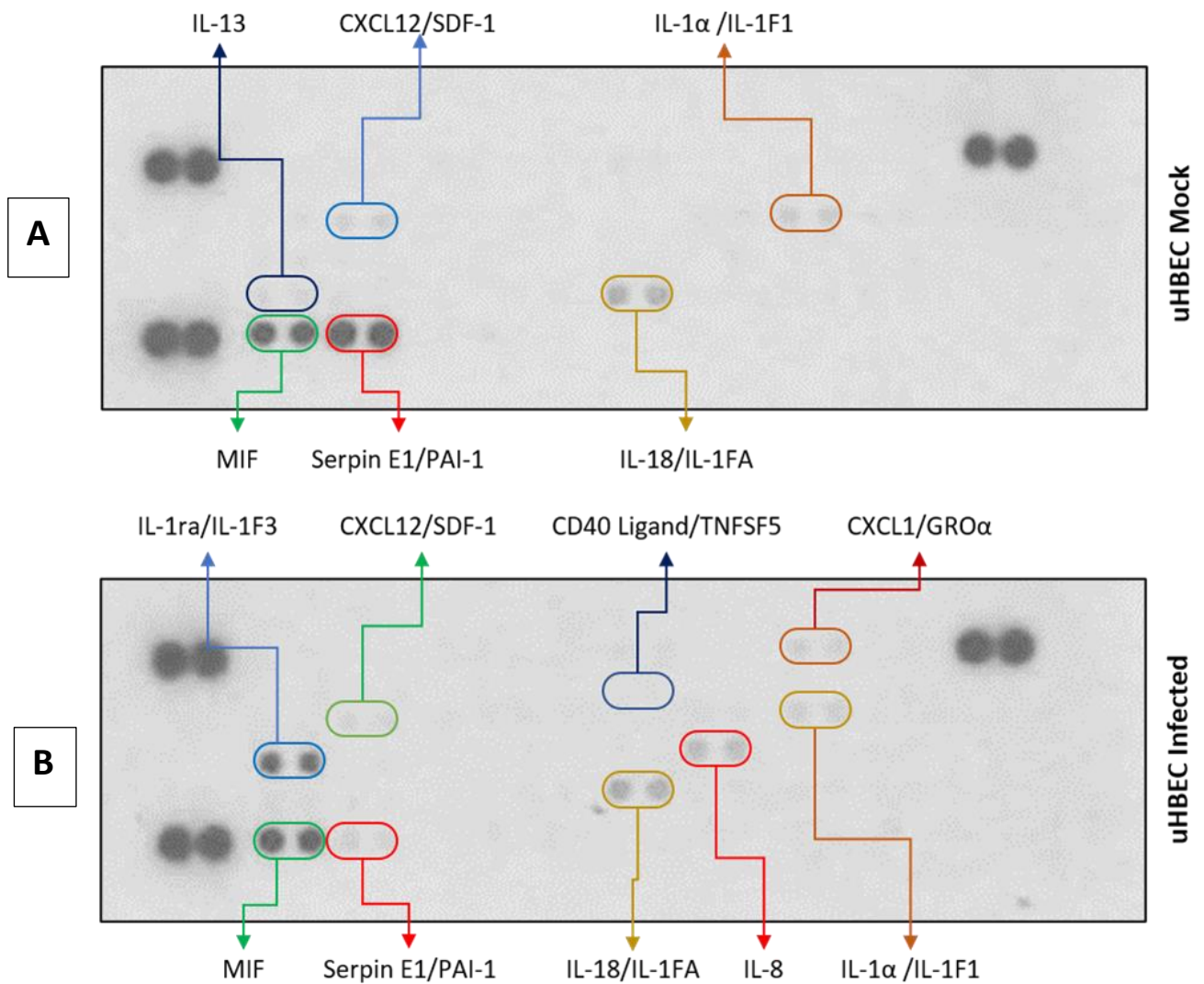


Figure 4.19: Cytokine Array from uHBECs with *S. aureus* for 4 hours.

Conditioned medium of uHBECs 4 hours post-infection was pooled for study of immune mediators produced by cells exposed to *S. aureus* (MOI-1) and MOCK cells (uninfected cells).

Panel (A) represents the secretion of immune mediators of mock cells. Panel (B) represents the secretion of immune mediators of infected uHBECs. (The blot is representative of n=3).

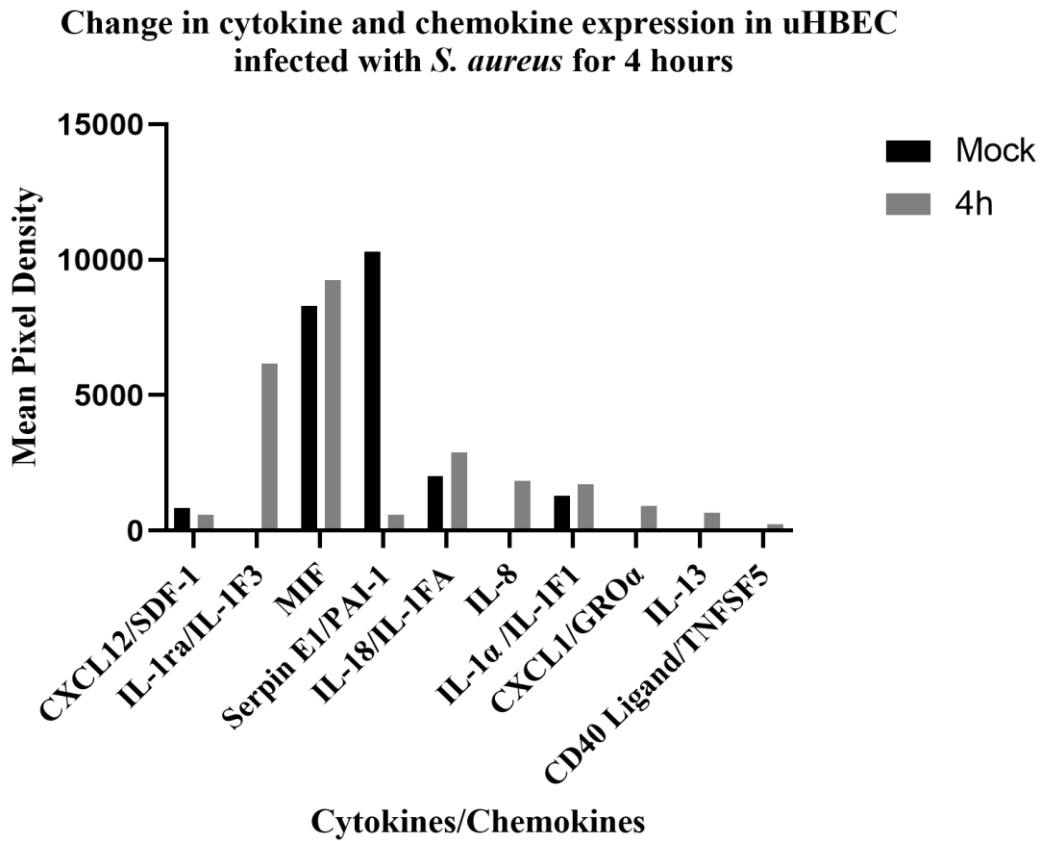


Figure 4.20: Comparison of immune mediators released by *S. aureus*-exposed for 4 hours uHBECs (MOI-1).

Results of the human Cytokine Array assay, illustrating a generation of immune response released by uHBECs exposed to *S. aureus* (MOI-1) alongside mock cells 4 hours post-challenge. The levels of signaling molecules released by MOCK-exposed uHBECs were used as the basal levels. The pixel density was calculated through processing with using The Image Studio Lite software (LI-COR Biosciences).

4.2.9 Comparison of the cytokine and chemokine production by *S. aureus* exposed uHBEC3-KT cells and uHBECs

I next directly compared the differential secretion of chemokines and cytokines in uHBEC and uHBEC-KT cells. This analysis provided evidence of cellular response when these two types of cells were infected by *S. aureus*.

As illustrated in Figure 4.21, uHBEC3-KT conditioned medium demonstrated the presence of high levels of SerpinE1 and IL-6 with lower levels of MIF, IL-1 α /IL-1F1, CXCL1/GRO α , CD40 Ligand/TNFSF5 and IL-8. IL-18/IL-1FA protein expression was similar between uHBEC3-KT and uHBECs whereas uHBECs had reduced signals for SerpinE1 and IL-6. Densitometry analysis indicated significant level for IL-1ra/IL-1F3, MIF and IL-8. There was also a small increase in CD40 Ligand/TNFSF5 and CXCL1/GRO α protein expression. It is crucial to note that because these are the results of a single experiment, their reproducibility cannot be determined.

Change in cytokine and chemokine expression in uHBEC3-KT and uHBE cells infected with *S. aureus* for 4 hours

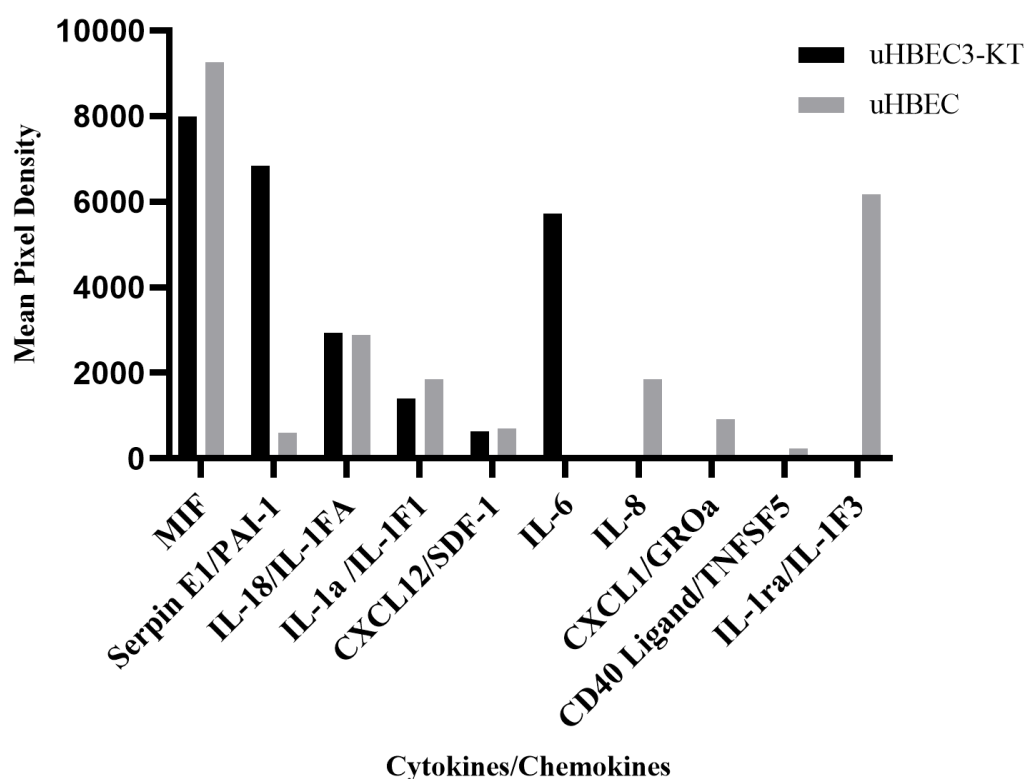


Figure 4.21: Comparison of immune mediators released by *S. aureus*-exposed for 4 hours uHBECs and uHBEC3-KT cells (MOI-1).

The results have shown comparison of types of molecules and their levels released from uHBEC and uHBEC3-KT cells. Gray bars are showing levels (mean pixel density) of cytokines/chemokines released uHBEC while black bars are showing levels of cytokines/chemokines released from uHBEC3-KT. The pixel density was calculated through processing with using The Image Studio Lite software (LI-COR Biosciences).

4.10 Discussion

One of the most common pathogens of the respiratory tract *S. aureus*, is known to colonize the tract first before being internalized. Therefore, its interaction with respiratory cells is very a important first step to the pathogenic infection. Many previous studies have been conducted to investigate the interaction between primary respiratory cells and this pathogen where it has been shown that the bacteria bind with cells before entering the cells and causing apoptosis of the infected cells (Da Silva et al., 2004). *In vitro* studies of human respiratory cells are dependent on either primary cells or cell lines. In this chapter I evaluated whether two types of undifferentiated human respiratory epithelial cells, HBEC3-KT and primary HBECs would show similar responses when exposed to *S. aureus* infection. As highlighted in chapter 3 the undifferentiated cells used here have characteristics of basal respiratory cells. Both HBECs and HBEC3-KT are human bronchial epithelial cells, and therefore might be expected to respond in a similar manner to perform functions related to the human respiratory system (Kaisani et al., 2014). Previous studies have shown that bacterial infection induce differential responses in respiratory cell lines and primary airway cells (Palma Medina et al., 2020). Therefore, the use of primary cells *in vitro* for cellular responses to the bacterial infection are more beneficial than use of cell lines as they would provide a closer approximation of natural bacterial-host interactions. Initially I confirmed that *S. aureus* grew in both types of culture media in the absence of cells. Both types of media have basic nutrients which are needed by the animal cells to grow, including amino acids, ions, salts, vitamins and carbohydrates (Leeman et al., 2018). It was important to determine how bacteria would grow in these two media. The most obvious finding to emerge from this analysis was the higher growth rate in Pneumacault™ Ex⁺ media evidenced by a higher CFU. A possible explanation for this could be that the fraction of human plasma present in this media could be a good source of nutrition to promote growth of *S. aureus*. Most of the nutritional component of this media are undefined, but it can be concluded that human plasma in Pneumacault™ Ex⁺ media is the major cause of increased *S. aureus* growth compared to KSFM. KSFM is a serum free media, but it contains bovine pituitary extract rather than any human serum component.

As shown in Chapter 3 the ALI culture system allows for differentiation of cells to replicate the complex cellular organisation seen in the airways but as it is a complicated culture system, I expected that undifferentiated cells grown on plastic might provide a helpful model to establish initial infections with *S. aureus*. Thus, I studied the response to *S. aureus* infection in HBEC3-KT cell line alongside primary HBECs. In this regard, the study included different

doses of *S. aureus* infection because it has been observed in previously studies that primary respiratory cell show differential responses to different bacterial doses (Hillyer et al., 2018, Lin et al., 2021). The study has revealed that in both types of cells, the dose of infection is directly proportional to bacterial proliferation, although, the trend was for different levels of bacterial growth in the two types of cells. Both types of cells have been investigated for their responses to the bacterial infection over time and as expected, cellular responses increased with passage of time. I also evaluated the differential cellular responses at molecular level and synthesis and secretion of different molecules in response to the bacterial infection were investigated in both types of cells. Previous research had indicated that different respiratory cells show different types of cellular response to the same type of infection i.e., *S. aureus* (Moreilhon et al., 2005). For this purpose, the differential transcription of some factors involved in immune responses of cells were investigated. The arrays from infected cells shoed that CXCL10 was reduced as compared to mock cells. Such results are consistent with previous studies showing that *S. aureus* infection leads to a downregulation of IP-10 cytokine (Li et al., 2017) which is direct interactor with CXCL10 during the inflammation mechanism (Liu et al., 2011). Therefore, inhibition of CXCL10 results in disruption of activation of T and B cells as this cytokine binds on CXCR3 to activate these cells. The bacterial cells are able to reduce this factor to evade the immune reaction from host body.

As expected infection levels increased over time and both cell types expressed greater MOIs at 24 hours compared to one-hour post-infection. Wilden et al. (2020) investigated the effect of *S. aureus* on small colony variants on cell immune response during a subsequent *in vitro* infection and report a similar increase in the rate of infection. The difference in MOI is vital to assist in understanding how bacterial infection progresses in the respiratory system. Wilden et al. (2020) observed a significant impact on the regulation of pro-inflammatory factors, which led to a synergistic effect on cell intrinsic innate immune response. However, the observed cytopathic effect in the presence of pathogens did not result from increased pathogen load. Abnormalities that affect immune cells such as T lymphocytes are highly likely to cause immunosuppression. Ben-Moshe et al. (2019) reports that the different ways that immune cells respond to infection allow them to establish a coordinated and complex protection to the body. Thus, bacterial infection could cause the expression of different types of immunological factors. My study used epithelial cells alone. It was shown that uHBEC3-KT cells are highly vulnerable to infection, with bacterial colonies increasing rapidly within 1 hour and multiplying further in 4 hours. Longer time point resulted in the cultures being overgrown with bacteria.

The pro-inflammatory cytokines produced in respiratory cells following *S. aureus* include IL-6 and CXCL10. CXCL10 is associated with mobilisation and activation of neutrophils, pulmonary oedema, and bronchoconstriction. IL-6 is known to be involved in the induction of acute-phase proteins that have protective and regenerative roles.

uHBEC3-KT and HBECs express the genes *CXCL10* and *IL6*, as part of the immune response to *S. aureus* infection. CXCL10 plays a role in immune response and disease progression and thus, has potential therapeutic implications (Liu et al., 2011). Similarly, the involvement of IL-6 in inducing acute-phase proteins provides both protective and regenerative roles. Differential expression of *CXCL10* and *IL6* was shown to depend on MOI concentration. The findings are significant in disease monitoring and prevention since immunomodulating, and pro-inflammatory cytokines and chemokines are produced and released by host cells in response to pathogen invasion of the body. When pathogens such as *S. aureus* stimulate immune cells, inducible cytokines and chemokines are produced. These proteins are part of the host defence system, and their absence can cause deleterious effects for the host. The pathophysiology of bacterial sepsis results from innate immunity mediated by monocytes. Pro-inflammatory cytokines produced during septic shock include IL-6, IL-1 β and TNF- α while anti-inflammatory cytokines include IL-10 (Schulte et al., 2013). Numerous studies show that respiratory cells produce systemic cytokine responses when they are infected by *S. aureus* (Fournier and Philpott, 2005).

Although these respiratory cells can secrete a wide variety of cytokines and chemokines in response to pathogenic infections, such release is not observed in every type of infection, and the synthesis and release of specific factors may depend on the type of infection. Duan et al. (2021) report variations in cytokine formation in different cell lines are clinically beneficial since they indicate differences in the rate of bacterial infection and secretion of inflammatory mediators depending on the type of immune cells. While some immune cells are adapted to mounting a quick response, others are slower (Moreno-Villanueva et al., 2018). For instance, while innate immunity is responsible for a quick response, the slow adaptive immunity is stronger and results in memory cells, which confer future protection to such antigens.

The mechanism by which cytokine synthesis is induced following bacterial infection involves recognition of *S. aureus* by TLR-2. The main biomolecules involved in bacterial recognition by host cells include bacterial cell wall teichoic acid linked to lipoteichoic acid and peptidoglycan. Lipoteichoic acid has been demonstrated in previous studies to induce the

synthesis and release of chemoattractant and cytokines such as IL-6, IL-8, IL-10, IL-12, IL-1 β and TNF- α (Liu et al., 2001). The potential downstream factors involved in host cell activation by bacterial infection include TGF- α , EGFR, P38/TACE, and NF- κ B (Providence et al., 2008), while intermediates in these pathways include mitogen activated protein (MAP) kinases and secondary messengers.

Further characterisation of the molecules induced by *S. aureus* infection in uHBEC3-KT and uHBECs was performed using a cytokine array. I only used a single time point of bacterial exposure for this study, 4 hours. The results for the uHBEC3-KT cell line showed that the expression of IL-6 and CXCL12/SDF1 was increased in infected cells compared to control cells, while expression of Serpin E1/PAI-1, IL-18/IL-1FA, and IL-1 α /IL-1F1 was increased in control cells (mock) compared to infected cells. Providence et al. (2008) noted that the reduced level of PAI-1, a serine protease inhibitor, can be explained by its role in wound healing. Its levels are only increased in cultured epithelial cells when wound-like insults are applied, but in this study, no wounding condition was used, rather cell death was increased in the cultures. Therefore, cells infected with the bacterial agent had reduced expression of PAI-1. The levels of IL-18/IL-1FA were decreased in infected uHBEC3-KT cells following infection. Previous studies have found that IL-18/IL-1FA levels are increased in response to viral infections such as human rhinovirus (Rajan et al., 2014) rather than bacterial infection. Such infections induce neutrophils to release more granule contents and activate neutrophilic inflammation. Similar trends were observed for both IL-18 and IL-1 and previous studies have shown both are dependent on viral entry and caspase-1 cleavage (Piper et al., 2013). Therefore, it can be expected that these two cytokines are interrelated, and their regulation is correlated. For the same reason, upon bacterial infection, the levels of both factors were decreased compared to non-infected cells.

The cytokine array performed on infected uHBECs resulted in differential expression profiles of inflammatory cytokines. Some had the same trend as in uHBEC3-KT cells, likely because both cell types are of a similar origin and retain many similar characteristics. However, these trends differ from those in other respiratory cell lines showing selective expression of cytokines, and chemokines, depending on the exposure to pathogens. Upon infection, uHBEC3-KT cells had lower expression of SerpinE1 while the expression of MIF remained constant in infection and uninfected stages. IL-6, an important cytokine in the activation of lymphocytes, synthesis of acute-phase polypeptides, and differentiation of B lymphocytes,

increased significantly upon infection by *S. aureus*. These results are similar to the findings of Ben-Moshe et al. (2019), who noted that *S. aureus* induces the increased production of CXCL8 and IL-6. Other inflammatory mediators that increased modestly upon infection included IL-1 α /IL-1F1, CXCL12/SD, and IL-18/IL-1FA. On its part, uHBEC control showed a strong signal for SerpinE1 and CXCL12/SDF and weak expression of MIF, IL-13 and IL-18 compared to infected cells.

Although this study demonstrates that infection rate varies across time and gene expression in uHBEC3-KT, a few limitations should be noted. Firstly, the reproducibility of these results is a concern as they are from a single experimental time point (albeit with pooled experimental samples). More data could have been gathered by the use of ELISA analysis across a wider time series and at different MOIs. Varying the time point for the cytokines analysis would be useful in determining the exact duration of response among the different immune cells, although perhaps longer time points could not have been studied in the undifferentiated cells. uHBEC showed that the expression of IL-1ra/IL-1F3, MIF, IL-18/IL-1FA, IL-8, IL-13 and CXCL1/GRO α were increased after 4 hours of infection compared to control cells. On the other hand, Serpin E1/PAI-1 was decreased in infected uHBEC compared to control cells. The differences in expression of these factors between the two cell types is probably a result of their genetic and morphological differences. uHBEC3-KT cells are artificially generated by over expression of transforming factors while uHBEC cells are primary in nature, so they are more 'natural' cells. Such differences in the production and activation of different cytokines and chemokines can explain the differences in use of drugs to treat *S. aureus* infection (Cavaillon, 2003). Such comparisons between cell types helps to reveal how different cell types can be utilised in research.

In conclusion, I have shown that uHBEC3-KT and HBECs are readily infected by *S. aureus* in submerged culture. Both cell types are overcome by infection after 4 hours of infection and this may be a limitation in their use for studies of this nature. Both cell types show similar trends to infection by *S. aureus*, but some differences are noted. These differences may be the result of changes to HBEC3-KT induced by immortalisation and changes in cellular phenotype may have resulted in changes in their immune responses. Some cytokines were equally expressed by both cell types while others were differentially expressed. Therefore, it can be suggested that the two types of respiratory epithelial cells have different expression patterns of cytokines and chemokines. These differences would likely result in changes in their responses

to bacterial or other pathogenic infections. This, together with the lack of inflammatory reactions, indicated that uHBECs and HBEC3-KT cells were not a good representation of the human airway epithelium as the model must be able to tolerate infection and evoke the complicated responses observed in the human airway. This implies that a more accurate model of the airway epithelium is needed to properly build an infection model. Therefore, studies needed to be carried out in order to establish the infection in differentiated HBECs.

CHAPTER 5: *Staphylococcus aureus* infection in differentiated primary human bronchial epithelial cells.

5.1 Introduction

The respiratory tract is lined by a pseudostratified epithelium from the nose to terminal bronchioles. This epithelium is first line of defence of the lung against external stress and includes multiple cell types including: basal, club, goblet and multiciliated cells that contribute to its function. The ALI differentiation process results in the development of a modelled mucociliary phenotype, which replicate these cell types and secretes multiple proteins from the apical surface that form part of an intrinsic defensive shield. As described in Chapters 3 and 4, ALI cells are considered to provide a good *in vitro* model of the respiratory epithelium and thus may be a more representative tool to study the interaction of pathogens compared to cell lines in submerged culture (Schwarze et al., 1997, Hiemstra et al., 2019). At the ALI, cells become tightly packed, develop functional tight junctions and a pseudostratified appearance. It is considered that the increased cell densities observed in these cultures, as well as the multiple innate defence proteins that they release into the apical secretions by the specific cell types, will play a role in protecting the underlying epithelium from infections. In the previous chapter, I described and studied the infection of undifferentiated HBECs and HBEC3-KT cells with *S. aureus*, and in this chapter, I built on these results to establish infection in ALI-differentiated HBECs.

As previously mentioned, *S. aureus* causes an impressive array of infections. It has been linked to the development of chronic upper airway inflammatory illness, such as chronic rhinosinusitis with nasal polyps. *S. aureus* and its enterotoxins disrupt tissue inflammation at multiple levels, including structural cells, as well as the innate and adaptive immune systems. It is assumed that the surface components of staphylococcal cells interact with complementary components on the eukaryotic host cell membranes to establish effective colonization (Derycke et al., 2010). The adherence of bacteria is aided by eukaryotic surface glycoproteins and proteoglycans found on apical mucous membranes.

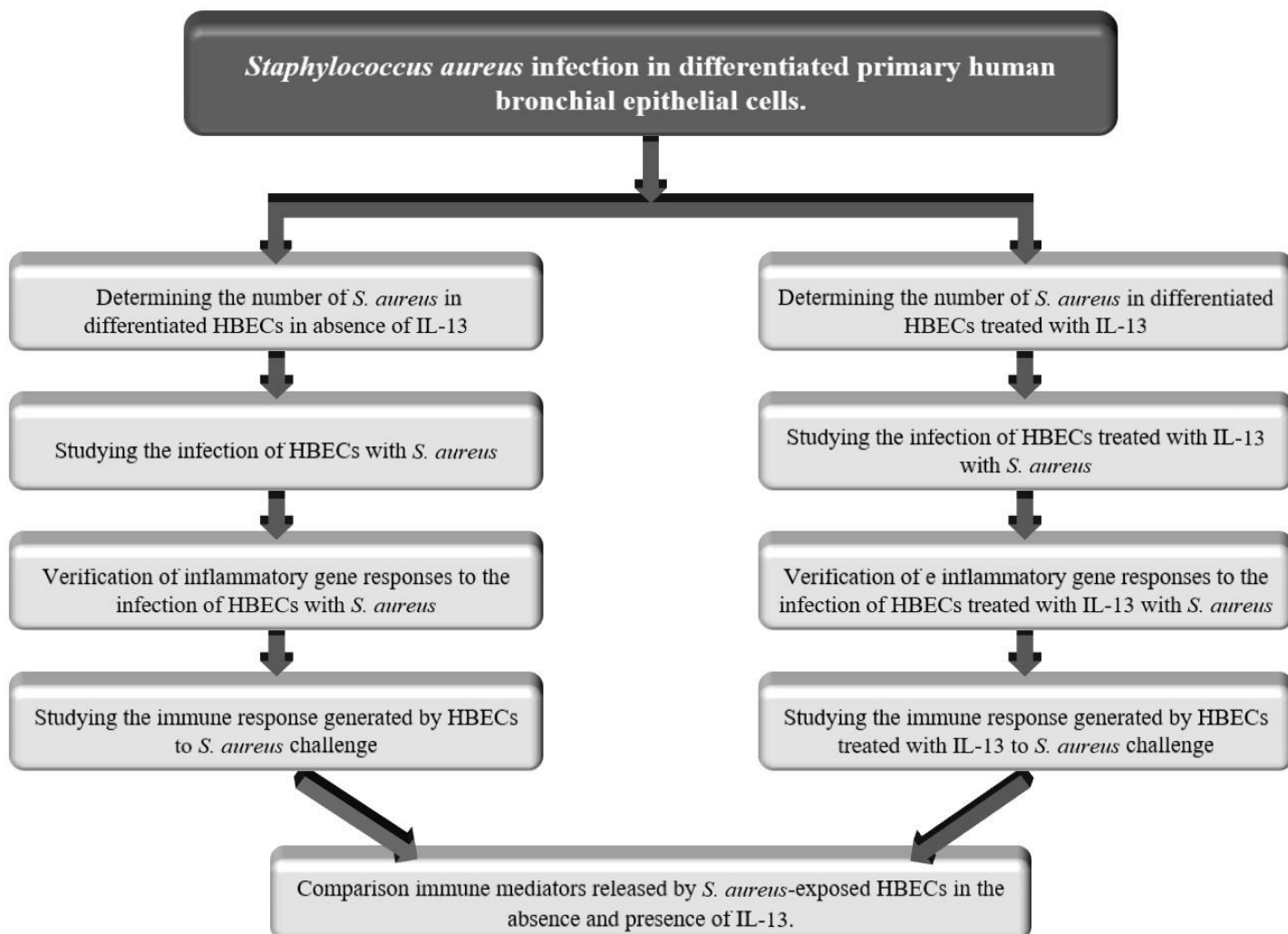
In vitro studies have revealed that *S. aureus* infections activate signalling pathways in airway epithelial cells, resulting in NF- κ B activation and IL-8 production (Da Silva et al., 2004). The activation of the expression of IL-8 is unaffected by the intact bacteria's adhesion properties, suggesting that secreted and/or shed components of the bacteria can cause the airway cells to respond. The host-pathogen interaction of *S. aureus* has been studied for short time periods, so these studies do not provide a clear understanding, but these provide little information of the pathophysiology of *S. aureus*-induced respiratory disease. Furthermore, the balance between the virulence factors of *S. aureus* and host defence molecules, as well as different effects of *S.*

aureus on the rectitude of airway cells have not been examined at several concentrations (Eichstaedt et al., 2009).

5.1.1 Aims:

ALI differentiated airway epithelial models are an attractive system to investigate the initial response to infection with *S. aureus* and the aims of the experiments reported in this section were:

- 1) To establish and characterize *S. aureus* infections in differentiated HBECs and study the effects of infection on cell responses in ALI culture cells.
- 2) To compare and characterize *S. aureus* infections between differentiated HBECs in the absence and presence of IL-13.
- 3) To compare the responses to *S. aureus* infections in differentiated and undifferentiated HBECs.



Study plan for this chapter.

5.2 Results

5.2.1 Determining the number of *S. aureus* in differentiated HBECs

To acquire a quantitative assessment of the levels of bacteria present in cultures as an infection developed, each transwell was seeded with 30,000 HBECs. On day 28 when cells were shown to be differentiated as outlined in chapter 3, they were infected with *S. aureus* for one hour. Subsequently, bacteria in media were removed from the apical surfaces, and the cells were washed with HBSS to remove excess media and non-cell associated bacteria. ALI cultures were fed with fresh media in the apical compartment. In this study an MOI of 1 was used for periods of 2, 4, 8, 16 and 24 hours (Figure 5.1A).

HBECs were grown at the ALI, and the number of bacteria was assessed as described in the Materials and Methods. Bacteria were measured for up to 16 hours after infection. Viable bacterial numbers increased significantly between 4 and 8 hours and continued to grow rapidly by 16 hours (Figure 5.1B). Although not counted, bacteria would have continued to increase to 24 hours.

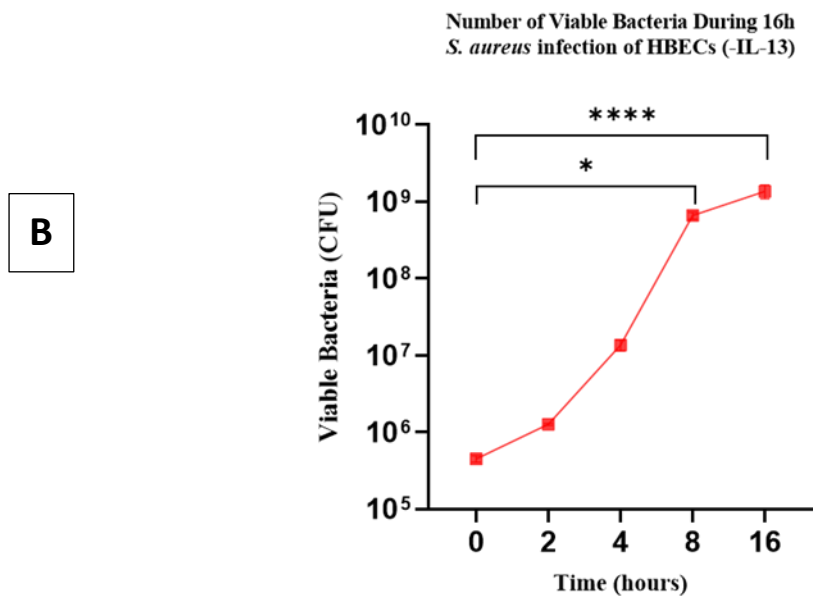
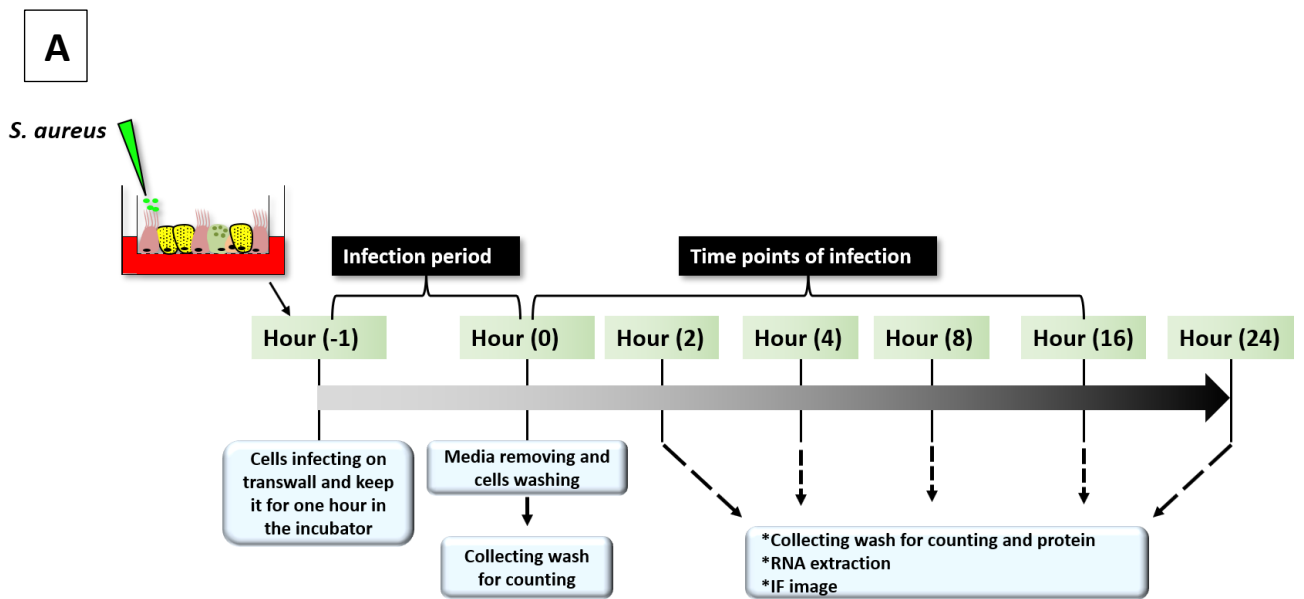


Figure 5.1: Viable counts of *S. aureus* infections in differentiated HBECs.

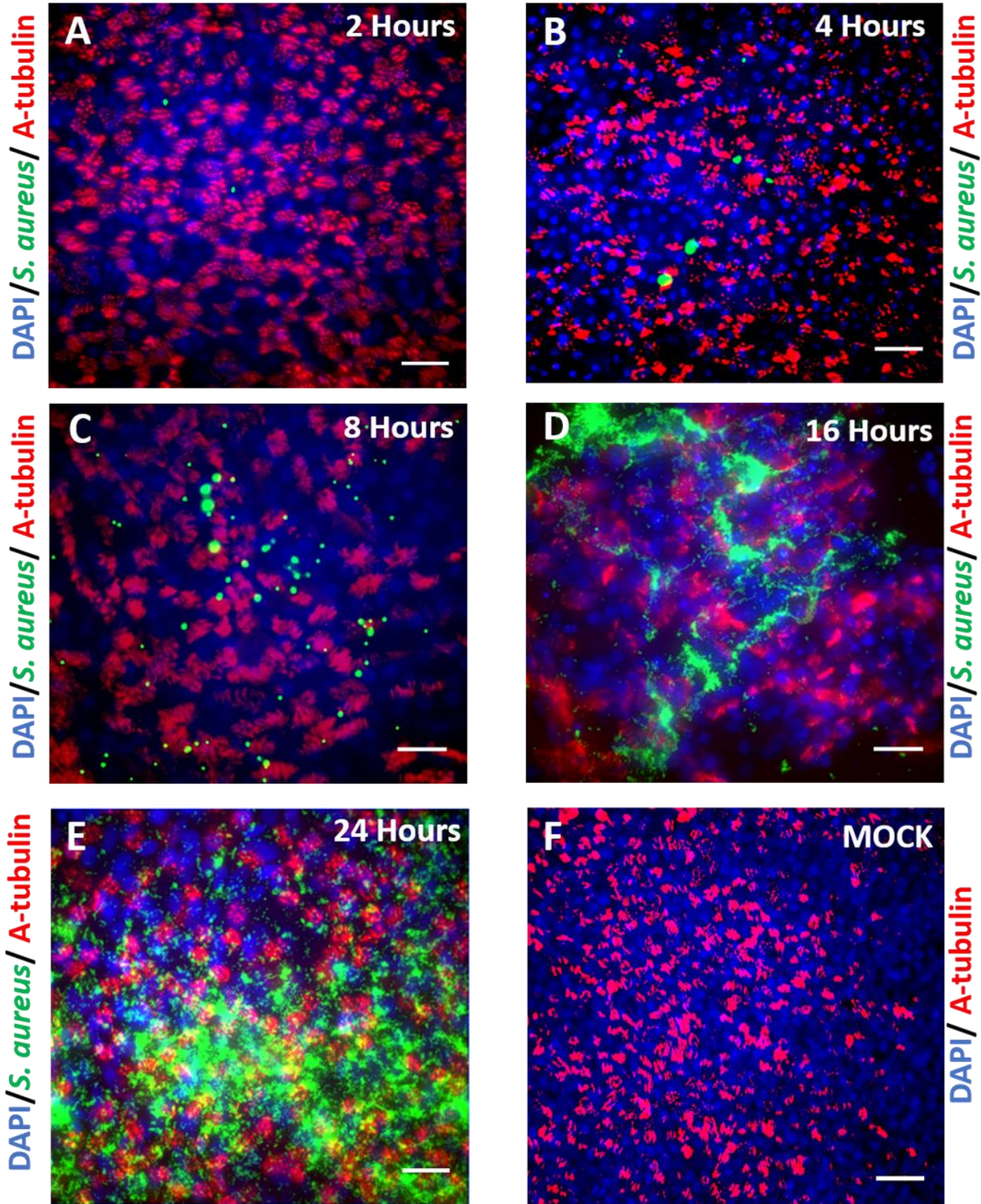
(A) Timeline of infection. At regular intervals, samples were taken for viable counting of *S. aureus*, protein study and transcriptional information. (B) Viable bacterial counts were taken at 0, 2, 4, 8 and 16 hours of short-term infections using differentiated HBECs. A one-way ANOVA using time (0) as the control showed significant values by 8 and 16 hours. Analysis was done on 3 independent biological replicates with cells isolated from 3 different donors. Error bars are too small to see. * $p < 0.1$ and **** $p < 0.0001$.

5.2.2 Infection of differentiated HBECs with *S. aureus*

To determine whether we could infect differentiated HBECs with *S. aureus* and then evaluate the role of secretions from the surface on the infection process, HBECs were seeded at 30,000 cells per transwell. On day 28 of ALI culture, the cells were infected with *S. aureus* strain SH1000-GFP at an MOI of 1 for 2, 4, 8, 16 and 24 hours. To remove excess media, the transwells were washed twice in HBSS. Cell cultures were fixed and stained with antibodies against acetylated alpha-tubulin (a ciliated cell marker), in order to visualize the differentiated airway epithelial cells in the cultures. Confocal microscopy was used to examine the level of infection by assessing GFP as a surrogate marker for *S. aureus* abundance.

Figure 5.2 reveals that there was a gradual increase in the amount of bacterial infection. At the 2-hour time point, the cells showed very small amounts of green fluorescence (*S. aureus*) associated with the cells. Between 8 and 16 hours, there were many more bacteria (as illustrated by green fluorescence) in all cultures, between these times the bacteria appeared to dissipate in the cultures and gave the appearance that they were within the cells. By 24 hours, the number of bacteria had increased markedly. These results indicate that at least some *S. aureus* infected ciliated cells, as shown by the yellow co-localisation in Figure 5.2E at 16 hours, but that early infection was not in ciliated cells (Figure 5.2 C and D). Moreover, these results suggest that green fluorescence (and *S. aureus*) continue to increase, and cell infection grows in the cultures over time. As expected, the uninfected controls showed no green fluorescence (Figure 5.2F).

To determine the amount of bacterial infection in the cultures, I employed a quantitative methodology. In each of three repeated studies, the infection intensity was assessed in four fields from each experiment. As illustrated in Figure 5.2G, the fluorescence intensity was initially low at 2 and 4 hours. However, the mean fluorescence then increased significantly from 8 to 24 hours. Notably, these findings confirm the suggestion from the imaging that the intensity of fluorescence continued to increase with time.



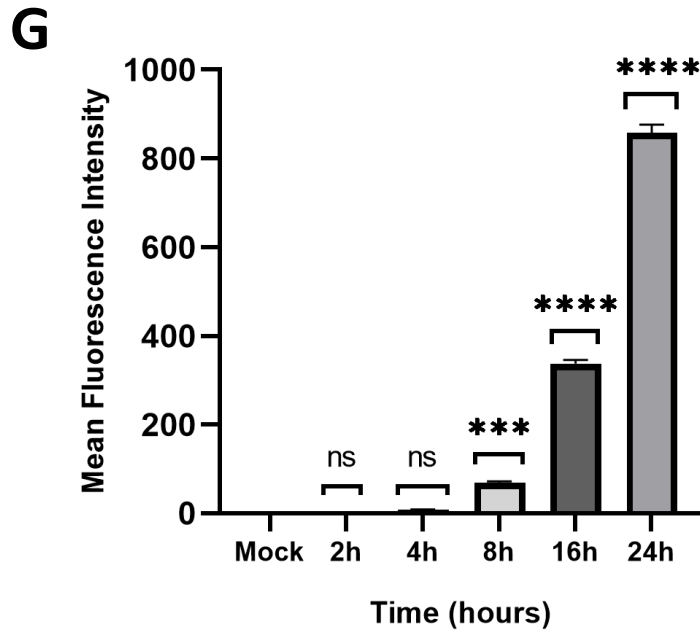


Figure 5.2: Immunofluorescence quantitation in differentiated HBEC infected with *S. aureus*.

IF image obtained with an Olympus FV1000 confocal microscope (40X) and Fluoview® image analysis system for infected HBECs. HBECs were infected with *S. aureus* at an MOI of 1 for 2, 4, 8, 16 and 24 hours. Cells were stained with acetylated alpha-tubulin (primary) and Alexa Fluor 568 red (secondary) and DAPI was used to stain the nuclei (blue). Green fluorescence demonstrates the presence of bacteria. Images are representative of n=3 infections from different donors. Scale bar = 50 µm. (G) The intensity of staining was measured in 4 fields in each of 3 replicated experiments. Data were analysed using A one-way ANOVA. Error bars: SEM. ***p<0.001 and ****p<0.0001.

5.2.3 Response of differentiated HBECs infected with *S. aureus*

5.2.3.1 induction of host cell gene expression

In order to investigate inflammatory gene responses to the infection of differentiated HBECs with *S. aureus*, RNA was extracted from cells at multiple time points (2, 4, 8 and 16 hours) of infection at an MOI of 1 and used for RT (endpoint). For the loading control, PCR. As before *OAZ1* was used as a control for all PCRs, as shown in Figure 5.3. Similarly, to the work in chapter 4 we employed primers against *CXCL10* and *IL6* as two pro-inflammatory cytokines generated by respiratory cells. In summary, these results show that *CXCL10* and *IL6* expression could be seen to be induced at all time points of infection (Figure 5.3). There was particularly weak expression in the mock infected samples of both genes.

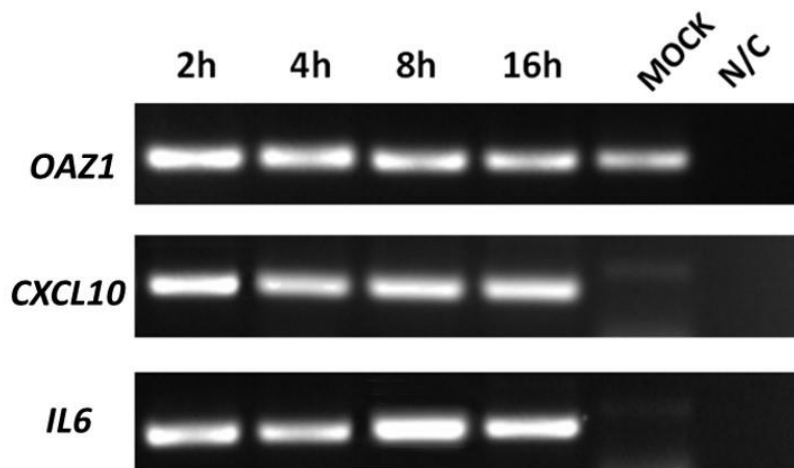


Figure 5.3: Comparison of expression of *CXCL10* and *IL6* after infection.

RT- Endpoint PCR was performed as described using cDNA of samples collected at 2, 4, 8 and 16 hours of infection. Samples were amplified with primers *OAZ1*, *CXCL10* and *IL6*. The image is representative of 3 experiments performed using cells from 3 different donors. MOCK indicates a sample that was uninfected, and N/C is the negative without cDNA.

To quantitatively measure the mRNA transcript levels *IL6*, *CXCL1* and *CXCL10* I utilised RT-qPCR with TaqMan primers as described in Chapter 4. Figure 5.4 shows the gene expression data for *IL6*, *CXCL10* and *CXCL1*.

Figure 5.4 displays that expression of all three gene was increased during *S. aureus* infections. However, it is expression levels decreased post infection at 16h time point. The results demonstrated that *IL6* levels were particularly low at the start of infection and increased with time. The highest level was recorded at 8 hours post infection. However, interestingly, its level decreased at 16 hours post-infection. The expression level of *CXCL10* peaked at 2 hours of infection. Followed by a decrease in longer duration of infection. *CXCL1* for the first two time points but increased significantly after 8 hours of infection, but similar to *CXCL10* its level then slightly decreased at longer infection time point. Variation was present within the data sample since cells from different donors were utilised. This therefore limited the statistical significance within the dataset.

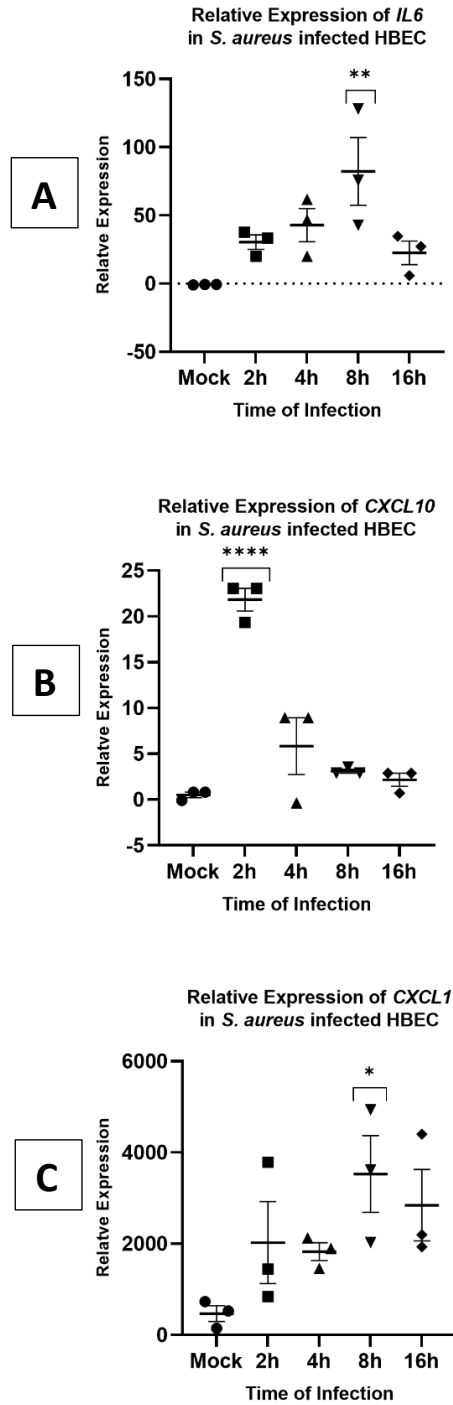


Figure 5.4: Comparison of *IL6*, *CXCL10* and *CXCL1* in differentiated HBECs infected with *S. aureus*.

qPCR was used to obtain quantitative data utilizing primers against *IL6* (A), *CXCL10* (B) and *CXCL1*(C) in samples from HBECs infected with *S. aureus* for 16 hours. The relative expression of mRNA was normalised to *OAZ1* as a control. The fold expression was calculated by comparing the CT values of the genes. Data were analysed using a one-way ANOVA. Error bars: SEM. * $p < 0.05$, ** $p < 0.01$ and **** $p < 0.0001$. Analysis was performed on 3 independent biological replicates isolated from 3 different donors.

5.2.4 Cytokine and chemokine production by *S. aureus* exposed differentiated HBECs

Apical secretion washes were collected from the cells infected with *S. aureus* at an MOI 1, and the synthesis of inflammatory cytokines and chemokines was measured using the Human Cytokine Array Panel A to determine the immune response to bacterial challenge in pooled samples from different experiments. For all samples, the experiment was performed at the same time, and results were obtained for the same length of time to ensure the accuracy of the results. The control HBECs apical secretion wash showed high concentration of SerpinE1, G-CSF, GM-CSF and ICAM-1/CD54 and very weak signals compared to the levels of other pro-inflammatory cytokines such as IL-6 (Figure 5.5).

SerpinE1 levels decreased after infection as compared to their level in mock cells. Similarly, granulocyte colony stimulating factor (G-CSF), granulocyte-macrophage colony-stimulating factor (GM-CSF) and intercellular adhesion molecule 1 (ICAM-1)/cluster of differentiation 54 (CD54) levels decreased following the infection as compared to their expression levels in mock cells. On the other hand, secretion levels of IL-6, IL-8/IL-1FA and IF-1beta/IL-1F2 increased with time following infection—they were not detected at the start of infection and were only detected after 16 hours of infection (Figure 5.5). Moreover, densitometry analysis confirmed the production of IL-18/IL-1FA, IL-1 α /IL-1F1 and IF-1 β /IL-1F2 after 16 hours of infection, whereas secretion of these factors was not detected either in mock cells or infected cells before 16 hours (Figure 5.6). Furthermore, this analysis confirmed the increased gradual secretion of CXCL-1/growth-related oncogene alpha (GRO α), with low-level secretion detected in mock cells and a steady increase following *S. aureus* infection. Moreover, the levels of MIF, Serpin E1/PAI-1, G-CSF, ICAM-1/CD54 were first decreased after infection up to 8 hours and after 16 hours their level were increased. Secretion of IL-8 was very peculiar because it decreased after infection of *S. aureus* for up to 8 hours and increased after 16 hours of infection. However, the most significant change in this regard was the secretion of GM-CSF, which was not detected at all after infection but was present in mock cells. In contrast, the secretion of IL-6, which was detected at all after infection but was not detected in mock cells (Figure 5.6).

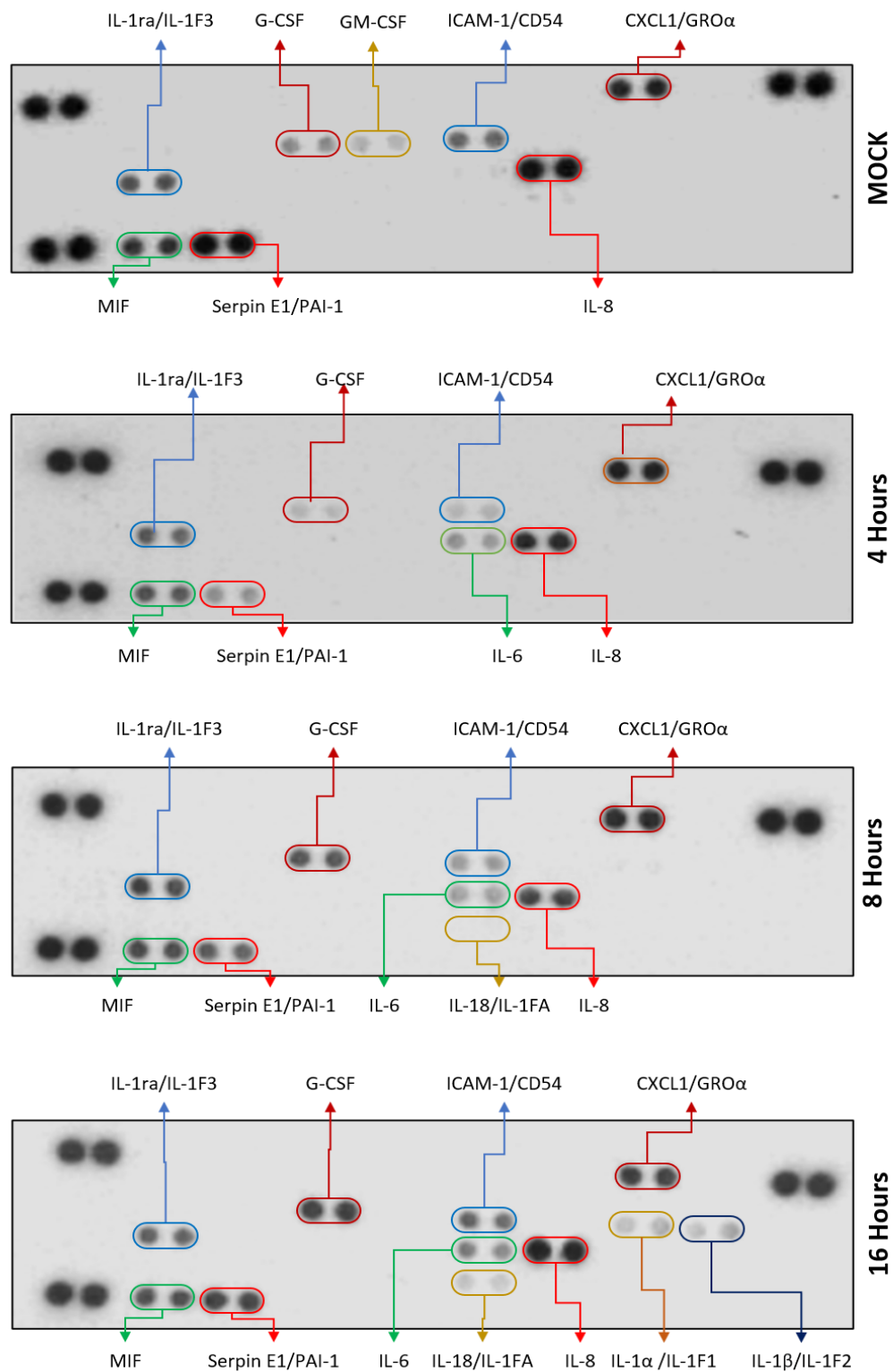


Figure 5.5: Cytokine secretion from HBECs infected with *S. aureus*.

Immune mediators were detected in apical secretion washes of HBECs exposed to *S. aureus* (MOI of 1) and MOCK challenged cells. Panel 1 is showing the secretions of mock cells as they are not infected while panels 2,3 and 4 are representing the secretions of infected as 4-, 8-, and 16-hours post-infection, respectively. (The blot is representative of n=3).

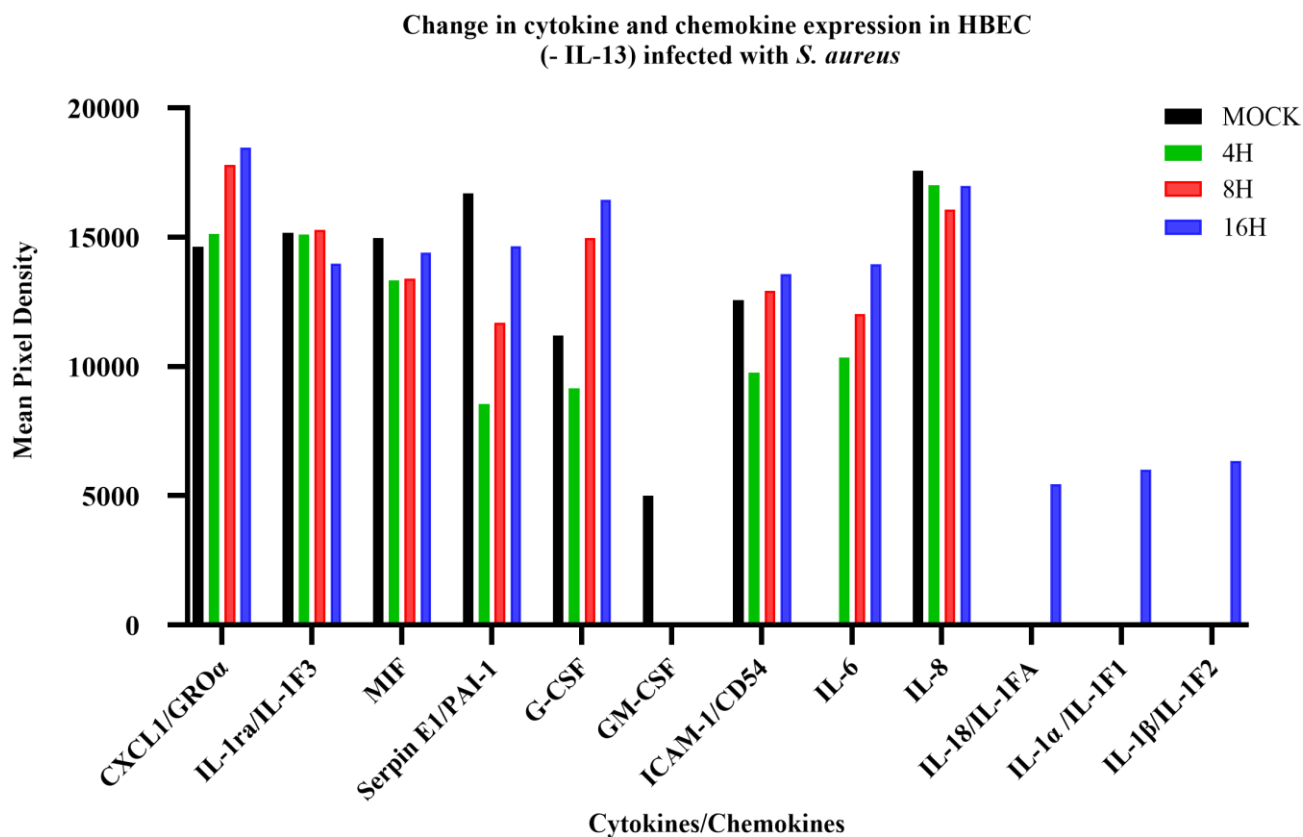


Figure 5.6: Densitometry analysis of cytokine array from HBECs infected with *S. aureus*.

Results of the Human Cytokine Array assay, illustrating levels of signalling molecules released by HBECs exposed to *S. aureus* alongside mock after 4-, 8- and 16-hours post-challenge. The pixel density was calculated through The Image Studio Lite software (LI-COR Biosciences).

Subsequently, I directly compared the differential secretions of various chemokines and cytokines in uHBEC and HBEC cells regarding *S. aureus* infection for mock cells which act as negative control because they were not infected with bacteria and 4 hours. This analysis provided evidence of a cellular response when these two types of cells were infected by *S. aureus*.

Figure 5.7A illustrates the comparison between the chemokine and cytokine secretions of mock uHBECs and mock HBECs. IL-13, CXCL12/SDF-1, IL-1 α /IL-1F1 and IL-18/IL-1FA were detected in the uHBECs. In contrast, IL-1ra/IL-1F3, G-CSF, GM-CSF, ICAM-1/CD54, CXCL1/GRO α and IL-8 were detected only in HBECs. The presence of signals of MIF and Serpin E1/PAI-1 were significantly increased in HBECs compared to uHBECs.

Figure 5.7B compares the presence of chemokine signals and cytokine secretions in uHBECs and HBECs infected with *S. aureus* after four hours. The signals of IL-1ra/IL-1F3, CXCL1/GRO α , MIF, Serpin E1/PAI-1 and IL-8 were increased when we observed them in differentiated HBECs infected with *S. aureus*. However, the secretions of CXCL-12/SDF-1, CD40 Ligand/TNFSFS, IL-18/IL-1FA and IL-1 α /IL-1F1 were detected only in the infected uHBECs. In contrast, cytokine/chemokine array analysis showed that G-CSF, ICAM-1/CD54 and IL-6 were detected only in infected HBECs, and these were completely absent in uHBECs.

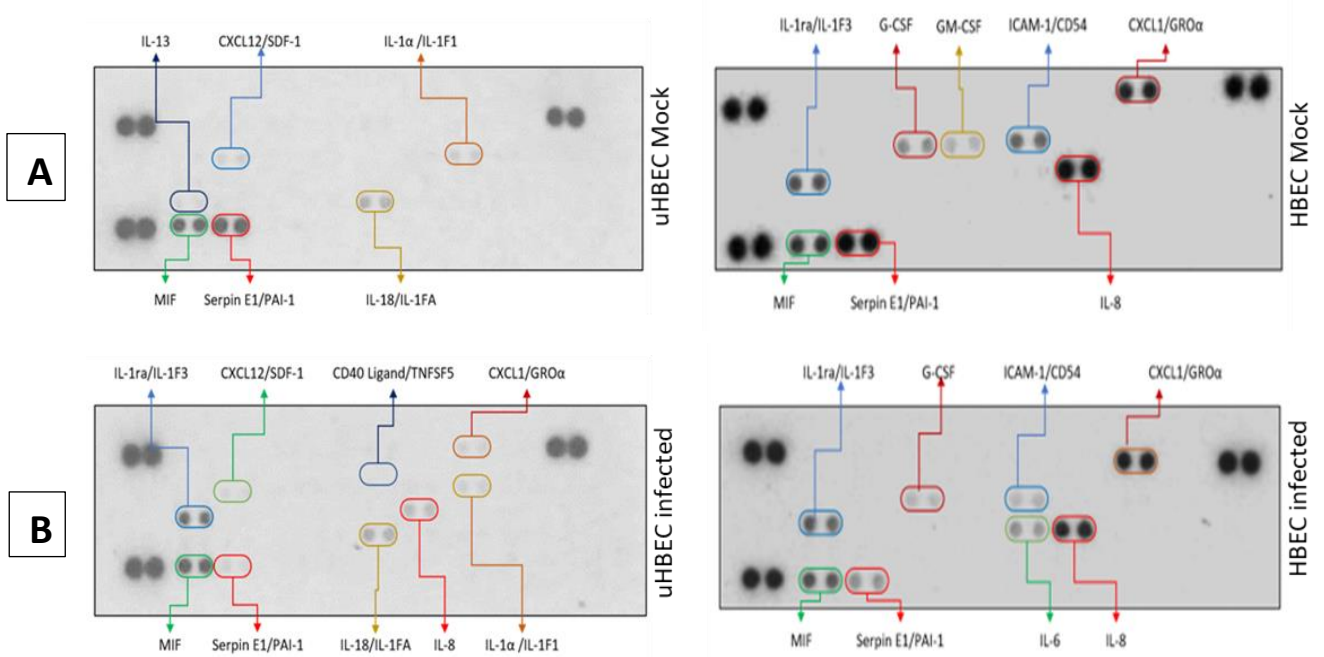


Figure 5.7: Cytokine secretion from uHBECs and HBECs infected with *S. aureus* as compared to mock cells.

At 4 hours post challenge, immune mediators were detected in apical secretion washes of HBECs and conditioned medium of uHBECs exposed to *S. aureus* (MOI of 1) and MOCK challenged cells. (A) mock cells without infection and (B) cells with infection.

5.2.5 Determining *S. aureus* numbers in differentiated HBECs in the presence of IL-13

Having undertaken infections in the differentiated HBECs, I next undertook infections in HBECs treated with IL-13, which as described in chapter 3 was expected to increase the number of goblet cells and the mucociliary phenotype. Following the treatment of HBECs with 10 ng/ml IL-13 during culture. On day 28, infections with an MOI of 1 were used and cells were then washed following media removal from the apical surfaces and bacterial counts undertaken after incubation of 2, 4, 8, 16 and 24 hours (Figure 5.8A).

Viable bacterial counts were performed to analyse bacterial numbers in cell cultures following infection. Bacteria were observed to increase after 4 hours and significantly increase after 8 and 16 hours of infection (Figure 5.8B).

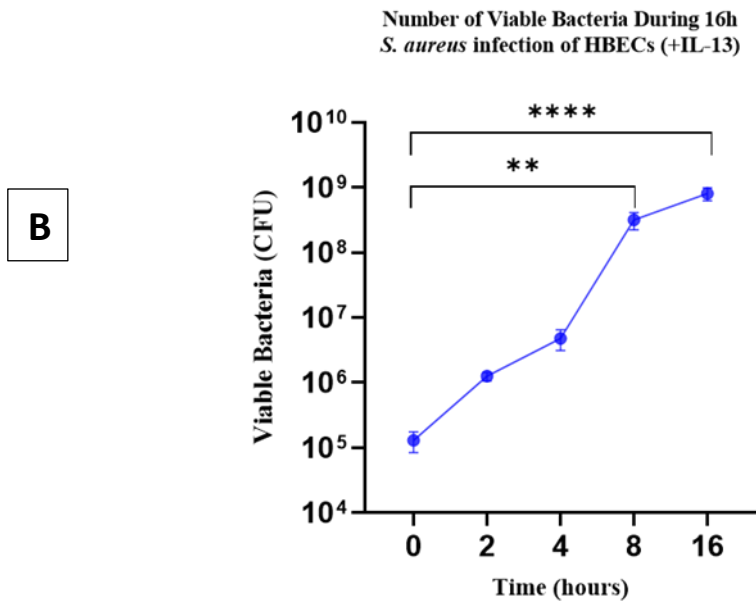
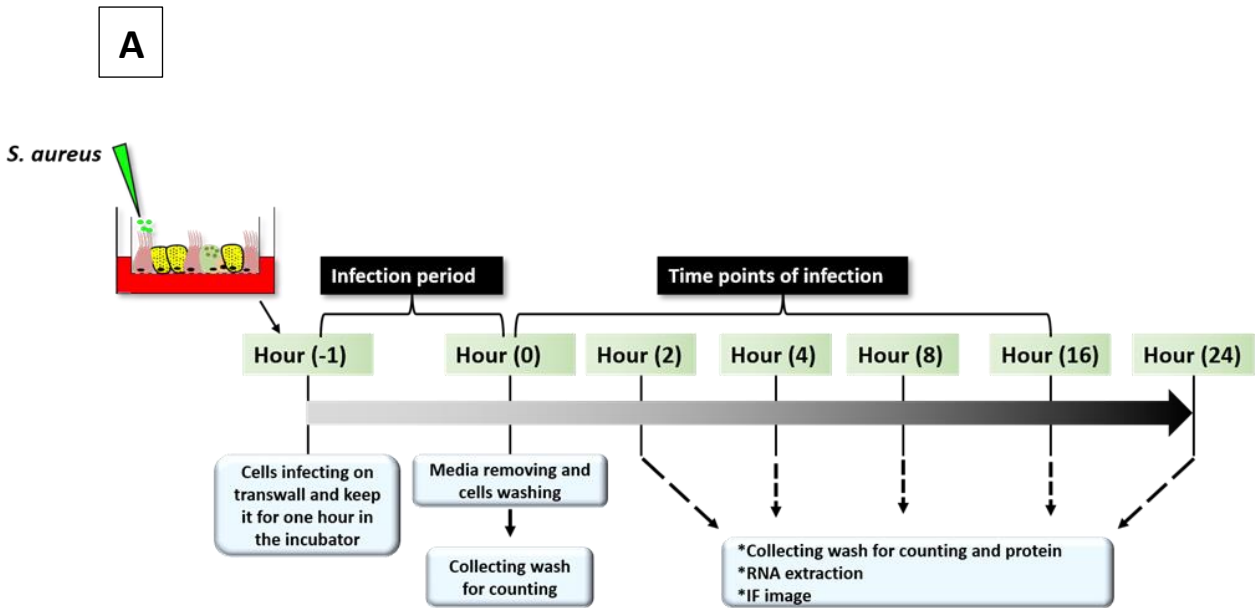


Figure 5.8: Viable counts of *S. aureus* infections in differentiated HBECs in the presence of IL-13.

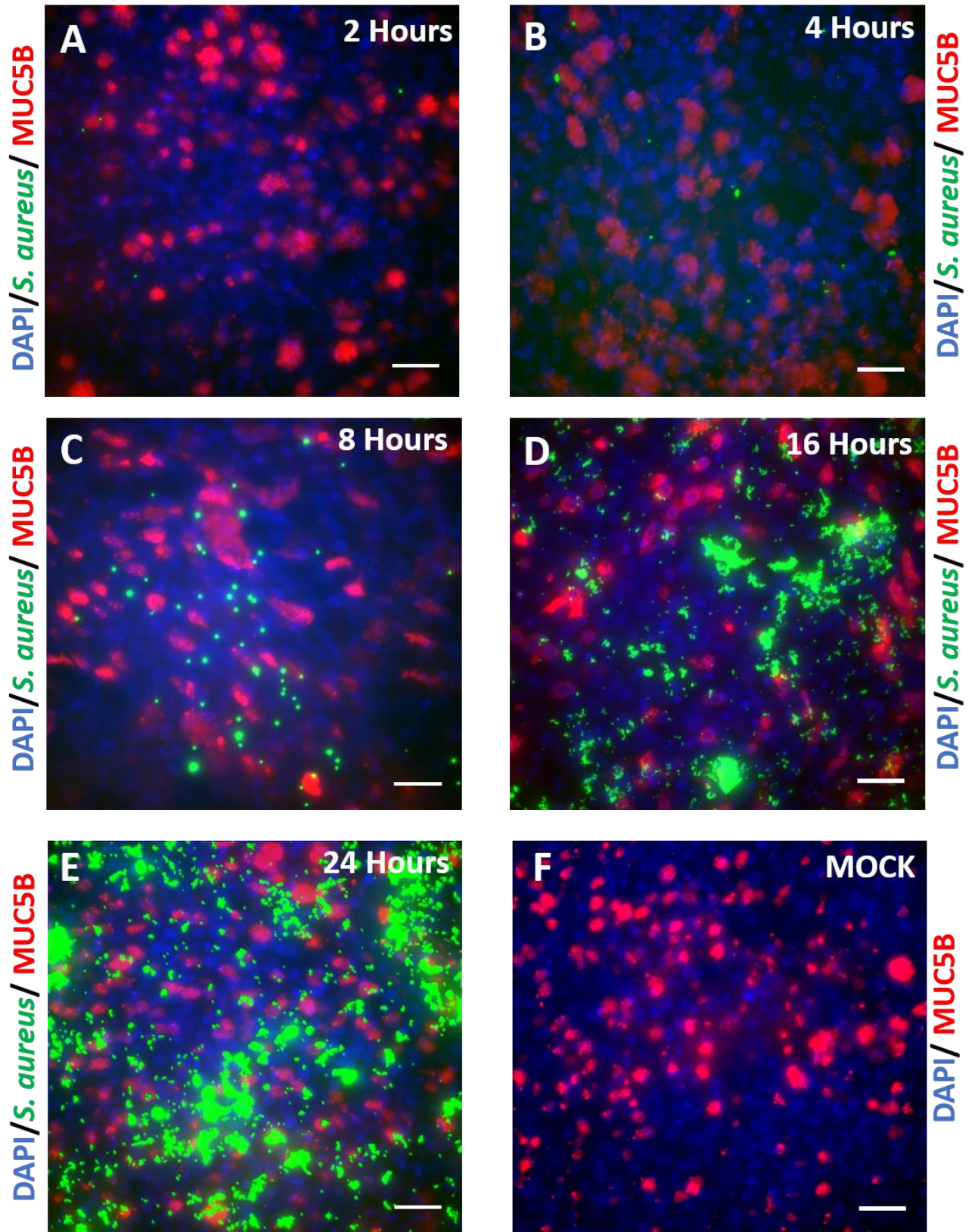
(A) Timeline of infection. At regular intervals, samples were taken for viable counting of *S. aureus*, protein study and transcriptional information. (B) Viable bacterial counts were taken at 0, 2, 4, 8 and 16 hours of short-term infections using differentiated HBECs. A one-way ANOVA using time (0) as the control showed significant values by 8 and 16 hours. Analysis was done on 3 independent biological replicates with cells isolated from 3 different donors. Error bars show SEM. ** $p < 0.01$ and **** $p < 0.0001$.

5.2.6 Infection of differentiated HBECs with *S. aureus* in the presence of IL-13

To gain better knowledge of the effects of IL-13 treatment of HBECs prior to *S. aureus* infection I visualized the bacteria in cultures of differentiated airway epithelial cells co-stained with MUC5B as a marker of goblet cells were labelled with stained antibodies at ALI differentiation. The level of infection was examined via confocal microscopy.

The results revealed that the infection level gradually increased as shown by green *S. aureus* (Figure 5.9). After two hours of infection, a small amount of green fluorescence was observed, indicating that the infection level was very low. In all the transwells, the fluorescence increased, indicating higher numbers of bacteria, and as expected was highest after 24 hours of infection. Overall, these results indicate that *S. aureus* that as infection increased it was not clear that the bacteria infected goblet cells as there was no clear co-localization of MUC5B and bacteria. As expected, no infection was recorded in the control (mock) (Figure 5.9F).

I next used a quantitative approach to measure the level of bacterial infection. For this work, the intensity of infection was measured in four fields in each of 3 replicated experiments. The data showed there was no significant difference in bacteria between 2 and 4 hours. The mean fluorescence then increased significantly up to 24 hours (Figure 5.9G).



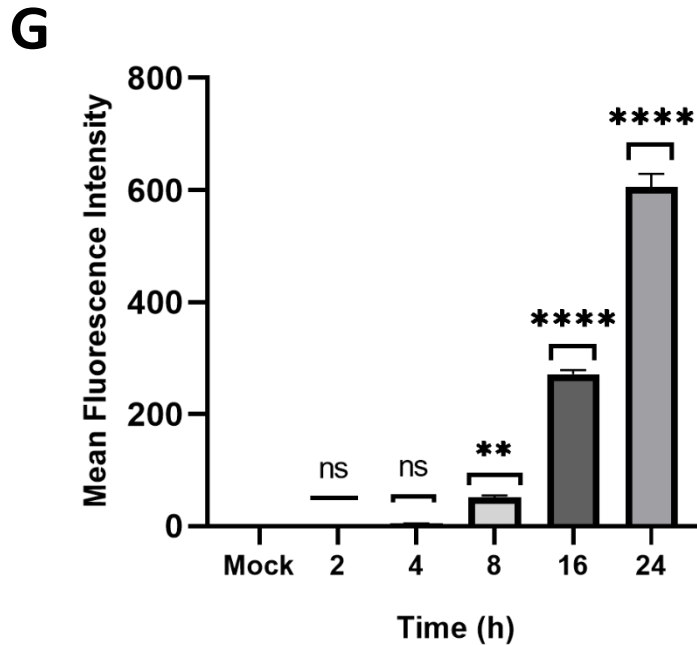


Figure 5.9: Immunofluorescence microscopy of HBECs differentiated in the presence of IL-13 infected with *S. aureus*.

Confocal image obtained with an Olympus FV1000 confocal microscope (40X) and Fluoview® image analysis system for HBECs. HBECs were infected with *S. aureus* at an MOI of 1 for 2, 4, 8, 16 and 24 hours. MUC5B (primary) stained, Alexa Fluor 568 red (secondary) stained, and DAPI was used to stain nuclei (blue). Green fluorescence demonstrates the presence of bacteria (images are representative of n=3 infections from 3 different donors). Scale bar = 50 μ m. (G) The intensity of staining was measured in 4 fields in each of 3 replicated experiments. Data were analysed using a one-way ANOVA. Error bars: SEM. **p<0.01 and ****p<0.0001.

5.2.7 Determination infection of HBECs with *S. aureus* in the presence of IL-13

5.2.7.1 Validation of host cell gene expression

I next investigate inflammatory gene responses in the IL-13 treated differentiated HBECs infected with *S. aureus*. RNA was extracted from cells at multiple time points (2, 4, 8 and 16 hours) of infection at an MOI of 1 and used for RT-PCR. *OAZ1* was used as a control gene, PCR. As before was used as a control for all PCRs (Figure 5.10). Primers against *IL6* and *CXCL10* were used to assess mRNA levels at different post-infection time points. In summary, these results showed that similar levels of induction of these genes was observed at all different time points following infection (Figure 5.10) compared to that seen in the mock infected samples.

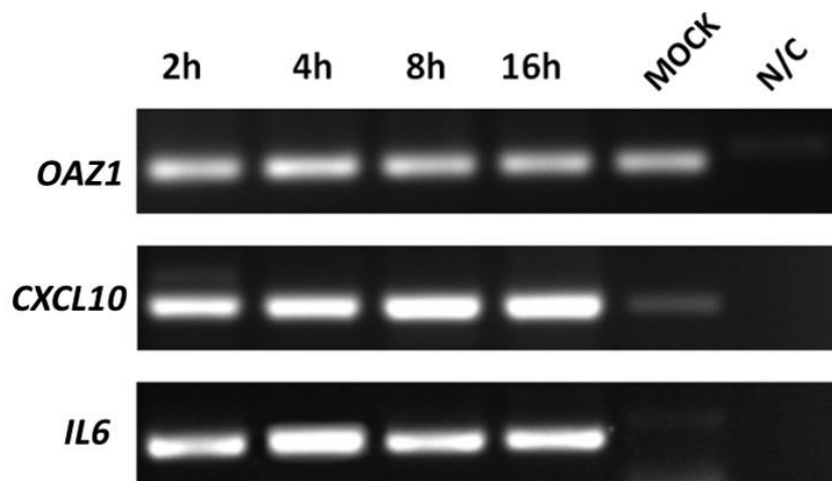


Figure 5.10: Comparison of gene expression in early time points in the presence of IL-13 using *CXCL10* and *IL6*.

RT-Endpoint PCR was performed as described using cDNA of samples that were collected at 2, 4, 8 and 16 hours of infection. Samples were amplified with primers *OAZ1*, *CXCL10* and *IL6*. The gel is representative one of 3 independent experiments. MOCK indicates an uninfected sample, and N/C is the negative control without cDNA.

To acquire a better quantitative understanding of IL-13's impact on cells, RT-qPCR was performed using TaqMan primers for pro-inflammatory cytokines. Figure 5.11 shows the quantitative analysis of the expression levels of *IL6*, *CXCL1* and *CXCL10*.

The results confirmed that all three genes, *IL6*, *CXCL1* and *CXCL10* increased at 4- and 16-hours post infection in the presence of IL-13. However, differences were found at their highest concentration because *IL6* was observed in its highest amount at 4 hours post-infection time, whereas *CXCL1* and *CXCL10* were at their highest concentrations at 16 hours post infection. *IL6* was also present in a negligible amount in mock cells, whereas *CXCL1* was detected in slightly higher concentrations even prior to infection. Finally, the changes in *CXCL1* expression were the most rapid compared to the rate of increase in *IL6* and *CXCL10*. It should be noted here that there was significant variation among the three experiments in the different donors. Furthermore, when the results of infection of differentiated HBECs in the presence of IL-13 was compared with that in absence of this cytokine, some significant differences were observed such as *IL6* and *CXCL1* highest expression point in absence of IL-13 was observed at 8 hours post infection. On the other hand, highest level of *CXCL10* was observed at 2 hours post infection time.

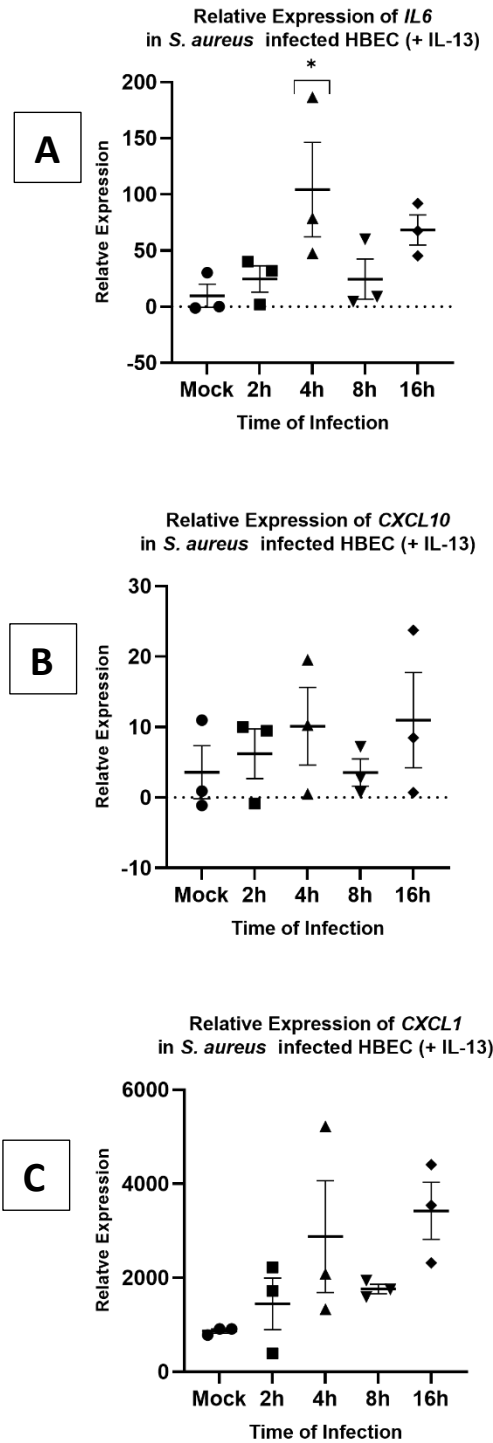


Figure 5.11: Comparison of *CXCL10*, *CXCL1* and *IL6* in IL-13 treated differentiated HBECs infected with *S. aureus*.

qPCR was used to obtain quantitative data utilizing primers against *IL6* (A), *CXCL10* (B) and *CXCL1* (C) in samples from HBECs infected with *S. aureus*. The relative expression of mRNA was normalised to *OAZ1* as a control. The fold expression was calculated by comparing the CT values of the genes. Data were analysed using a one-way ANOVA. Analysis was carried out on 3 independent biological replicates from 3 different donors. Error bars: SEM. * $p < 0.05$; ** $p < 0.01$ and *** $p < 0.001$.

5.2.8 Cytokine and chemokine production by IL-13 treated differentiated HBECs infected with *S. aureus*

To gain a better quantitative knowledge of IL-13's influence on infected HBECs, cell apical secretion washes were collected from the infected cells at cells and the production of inflammatory cytokines and chemokines was evaluated using the Human Cytokine Array Panel A at MOI of 1. To achieve reliable findings, the experiments were performed at the same time for all samples, and the imaging results were acquired for the same amount of time.

Figures 5.12 and 5.13 show the cytokine array analysis on changes in cytokines secreted from apical surfaces from HBECs infected with *S. aureus* in the presence of IL-13, revealing that CXCL1/GRO alpha increased following infection as compared to its level in mock cells. Similarly, the levels of IL-8, G-CSF, Serpin E1/PAI-1, ICAM-1/CD54, IL-1ra/IL-1F3 and IL-1alpha/IL-1F1 gradually increased following bacterial infection. On the other hand, CXCL-12/CDF-1, IL-18/IL-1FA, and IL-1alpha/IL-1F1 were only secreted when cells were infected with bacteria. However, the concentration of these factors following infection was observed at low levels, whereas those of IL-6 and MIF were found to be at a very high level and were only present following infection. Furthermore, cytokines such as IL-21 were only produced after 16 hours of infection. On the other hand, densitometry analysis showed related but not identical results, with IL-21, GM-CSF and IL-1beta/IL-1F2 only being expressed after 16 hours of bacterial infection in the presence of IL-13 (Figure 5.13). Moreover, other cytokines, including CXCL-12/SDF-1, IL-18/IL-1F1, IL-1alpha/IL-1F1, MIF, IL-6 and CXCL-11/1-TAC were only secreted in cells when they were infected with bacteria and were absent in mock cells. Interestingly, CXCL-11/1-TAC was absent after 16 hours of infection as well. Finally, cytokines such as IL-8 and CXCL-1/GRO alpha gradually increased following infection, although their basal level expression was present in mock cell secretions.

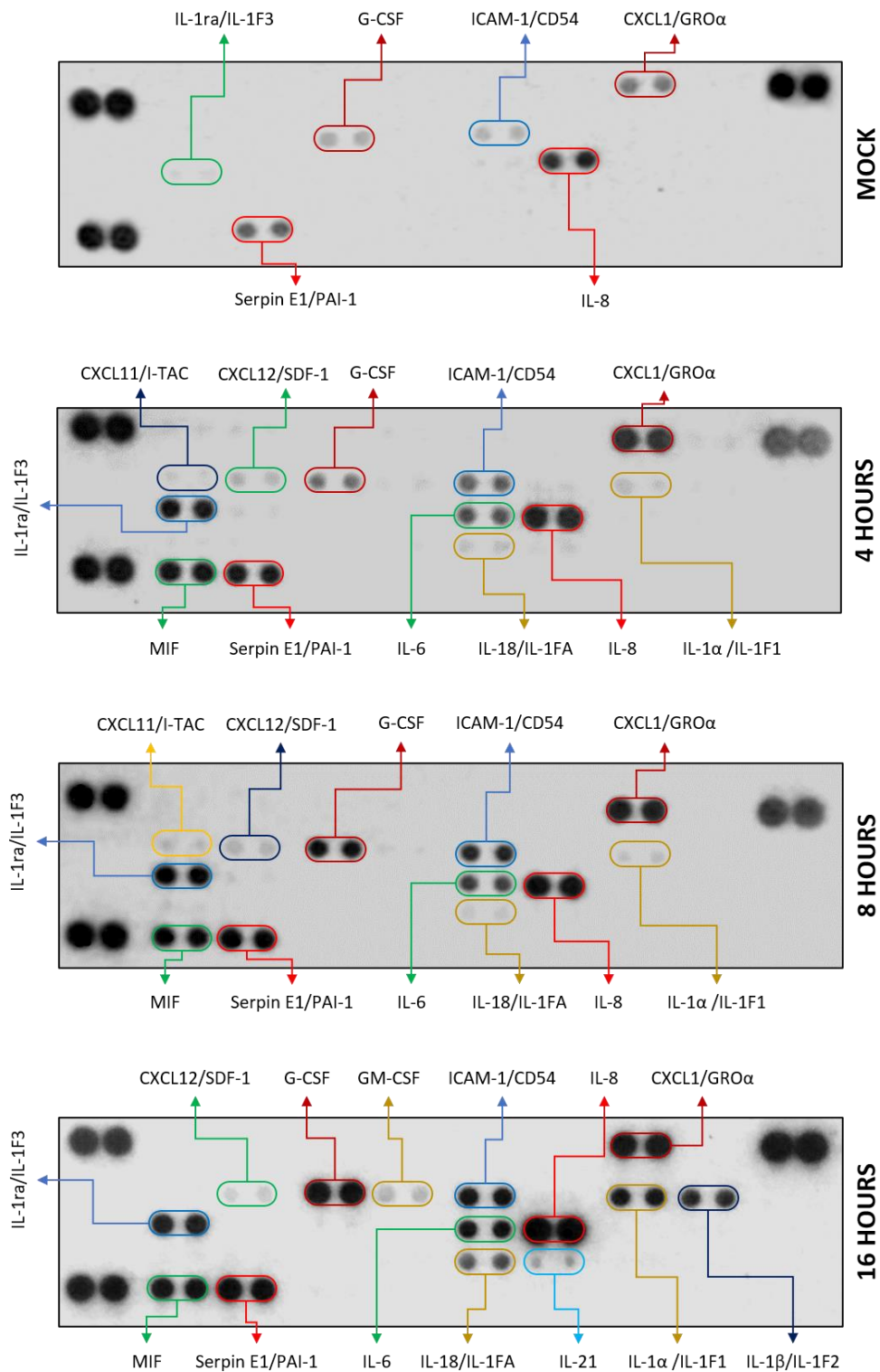


Figure 5.12: Cytokine array from IL-13 treated HBECs infected with *S. aureus*.

Apical secretion washes of HBECs were pooled and used for analysis, immune mediators were produced by cells exposed to *S. aureus* (MOI-1) and MOCK challenged cells. Panel 1 is showing the secretions of mock cells as they are not infected while panels 2,3 and 4 are representing the secretions of infected as 4-, 8-, and 16-hours post-infection, respectively. (The blot is representative of n=3).

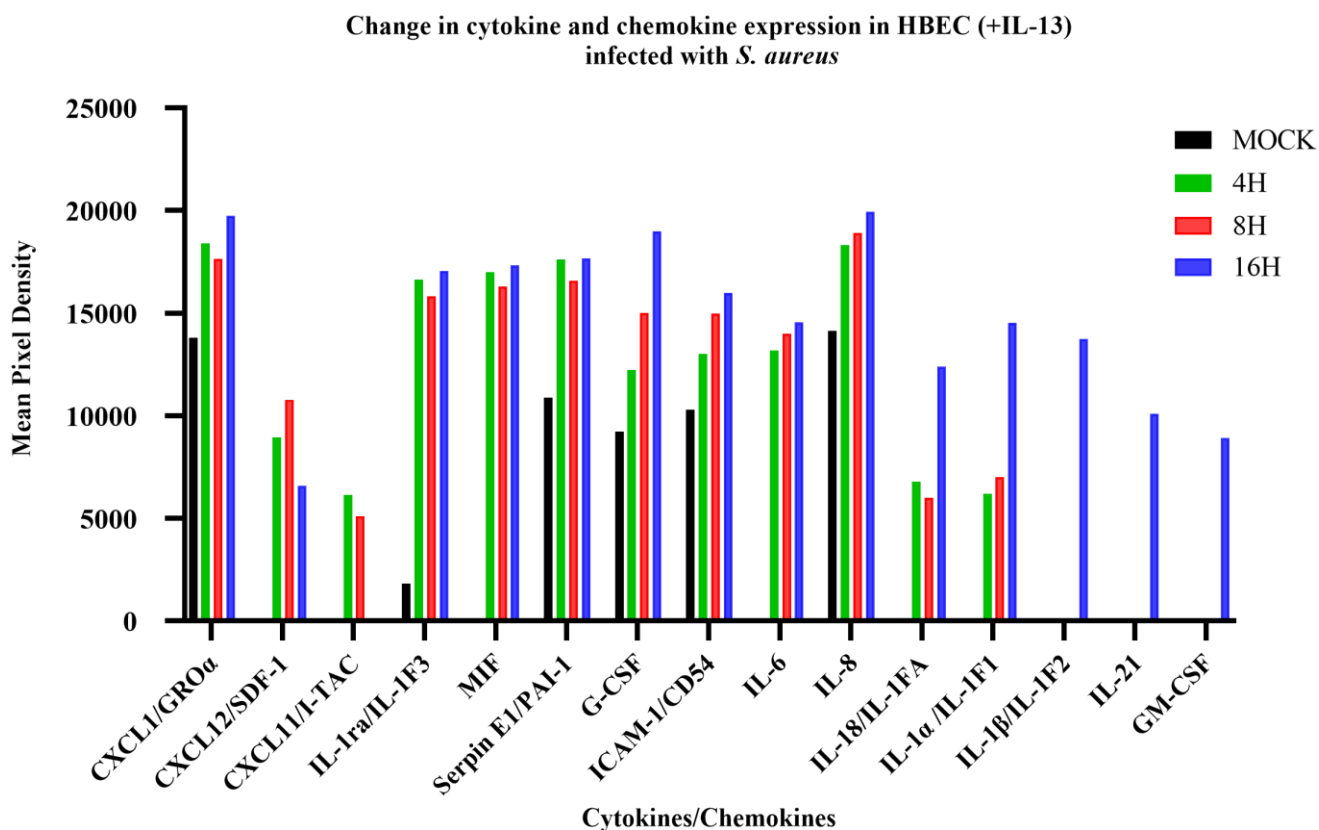


Figure 5.13: Densitometry analysis performed on cytokine array from IL-13 treated HBECs infected with *S. aureus*.

Results of a Human Cytokine Array assay, illustrating levels of signalling molecules released by HBECs exposed to *S. aureus* alongside mock 4-, 8- and 16-hours post-challenge. The pixel density was calculated through The Image Studio Lite software (LI-COR Biosciences).

Overall, the results have revealed that the presence of IL-13 lead to the differential expression of different cytokines and chemokines. Although, all the factors are present both in presence and absence of IL-13, the levels were different in both cases. The differences can be explained based on modifications in the cellular signalling cascades which are resulted from the presence of IL-13. However, it is important to note that these results are somewhat limited because levels were measured based on a single array experiment, although the assays were performed using pooled samples. Therefore, further repetition of experiments and then taking mean values would provide more repeatable results.

5.2.9 Comparison of the infection of differentiated HBECs with *S. aureus* in absence and presence of IL-13

To evaluate the cell response to the *S. aureus* infection in the presence or absence of IL-13 treatment, I directly compared the viable bacteria numbers in the two sets of experiments. The results show that viable bacterial counts were modestly lower in IL-13 treated HBECs as compared to the infection undertaken in cells cultured in the absence of IL-13 (Figure 5.14).

I also compared levels of cytokines and chemokines secreted from differentiated HBECs in the absence and presence of IL-13. For this I compared the immune response of epithelial cells to *S. aureus* infection for 16 hours. The results were compared with those of mock cells which act as negative control because they were not infected with bacteria. As illustrated in Figure 5.15, the densitometry analysis results show the production of cytokines and chemokines by HBECs cultured either in the presence or absence of IL-13 treatment before infection with *S. aureus*. The cells without treatment IL-13 demonstrated the presence of a high concentration of factors such as GM-CSF, IL-8, Serpin E1/PAI-1 and IL-1ra/IL-1F3, which were not detected in the presence of IL-13. In contrast, the secretion levels of IL-18/IL-1FA and IL-6 were very high in the presence of IL-13 compared to the absence of IL-13, where no signals of these factors were detected. Furthermore, the level of G-CSF, ICAM-1/CD-54n and CXCL1/GRO α factors was slightly higher in the absence of IL-13 compared to their levels in the presence of IL-13. However, the MIF signal was highly significant in the absence of IL-13 compared to the presence of IL-13. These results for mock cells can be used as a reference so that the results of experimental cells can be compared with them.

As illustrated in Figure 5.16, the concentrations of GM-CSF, IL-21 and CXCL12/SDF-1 were high in the presence of IL-13, while no signals were detected in the absence of IL-13. The secretion levels of CXCL1/GRO α , IL1ra/IL-1F3, MIF, Serpin E1/PAI-1, G-CSF, ICAM-1/CD54, IL-6 and IL-8 were detected slightly higher in the presence of IL-13 compared to their levels in the absence of IL-13. Treatment with IL-13 affected the secretion of IL-18/IL-1FA, IL-1 α /IL-1F1 and IL-1btea/IL-1F-2 a great deal because their levels were significantly higher after treatment with IL-13 compared to without treatment.

In summary, the results suggested that the expression of most of the cytokines and chemokines was higher than in the presence of IL-13. Such pattern was clearly noted in densitometry analyses of differentiated HBEC cells as compared to mock cells, as they have shown differential expression of these factors upon the bacterial infection in the presence and absence

of IL-13. These results are very interesting as CFUs were higher in the absence of IL-13 while host cells have shown increased expression of different cytokines and chemokines in the presence of IL-13. However, it is important to note that because these are the results of a single experiment, their reproducibility cannot be determined.

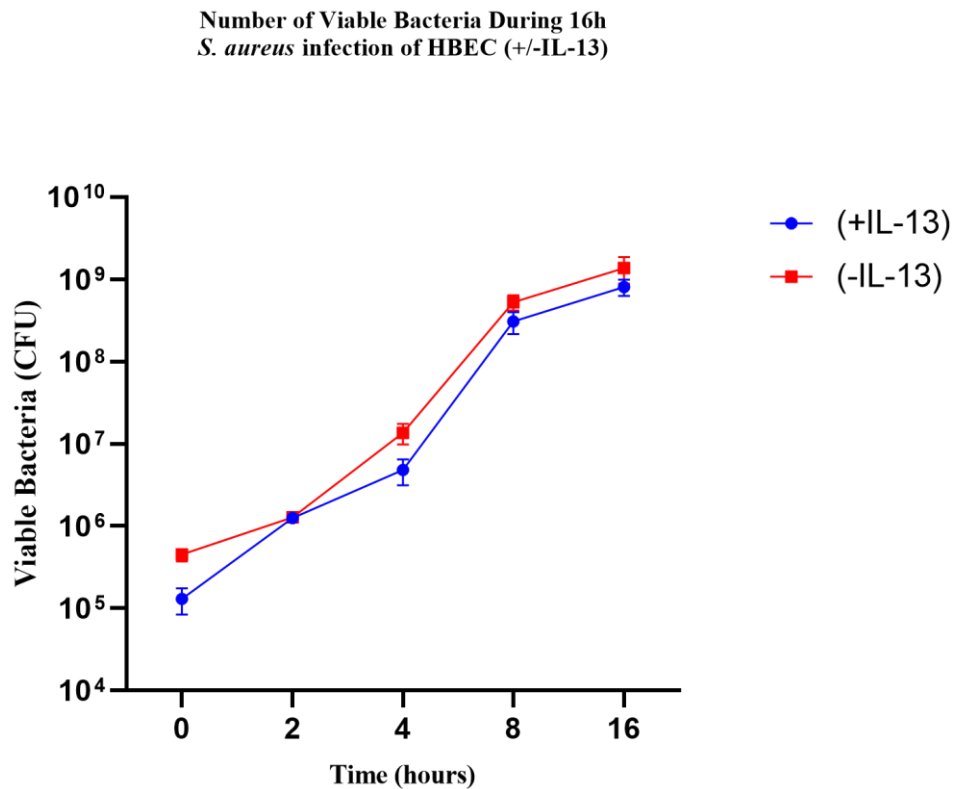


Figure 5.14: Comparison of viable counts of *S. aureus* during infections on differentiated HBECs in absence and presence of IL-13.

Viable counts were taken at 0, 2, 4, 8 and 16 hours of infections performed on differentiated HBECs. in absence and presence of IL-13. (n=3). Error bars show SEM.

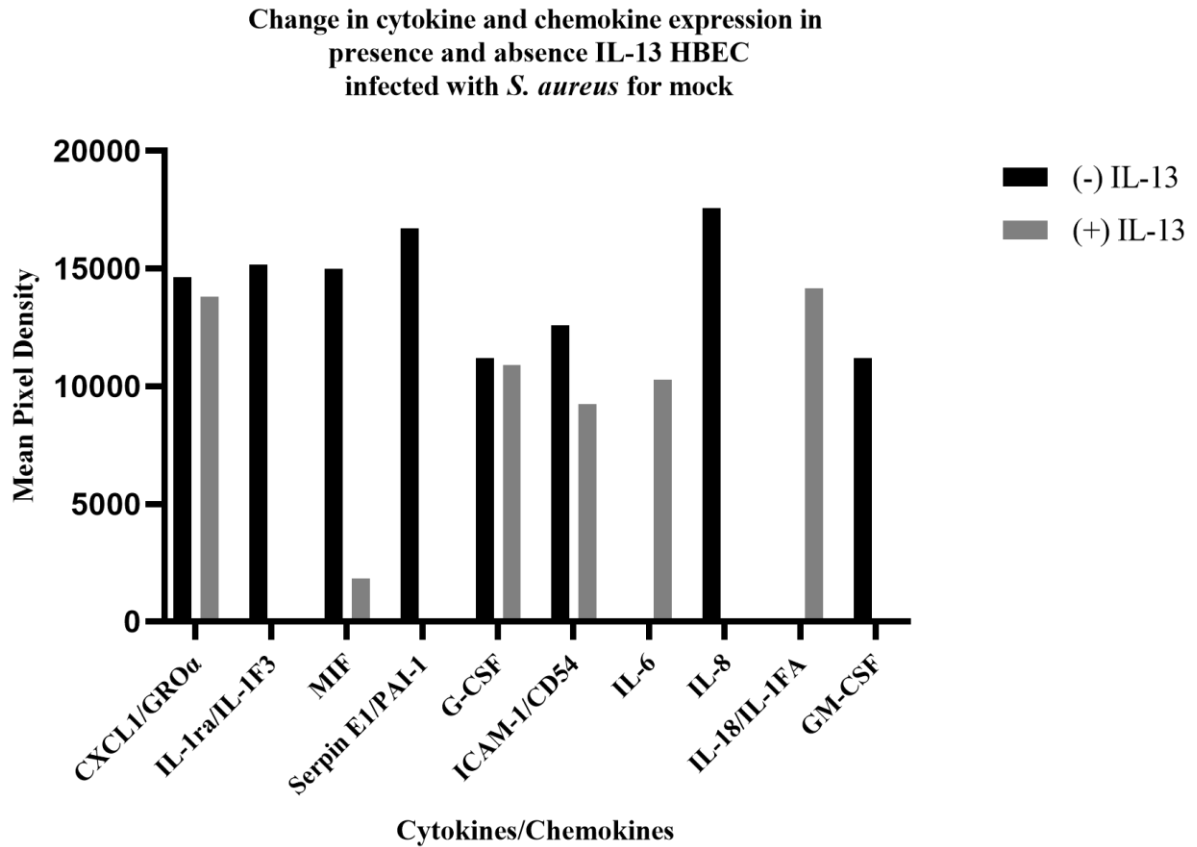


Figure 5.15: Comparison of immune mediators released by HBECs in the absence and presence of IL-13 (MOI-1).

Results of the Human Cytokine Array assays, illustrating levels of signalling molecules released by HBECs grown in the presence or absence of IL-13. The pixel density was calculated through The Image Studio Lite software (LI-COR Biosciences).

Change in cytokine and chemokine expression in Presence and absence IL-13 HBEC infected with *S. aureus* for 16 hours

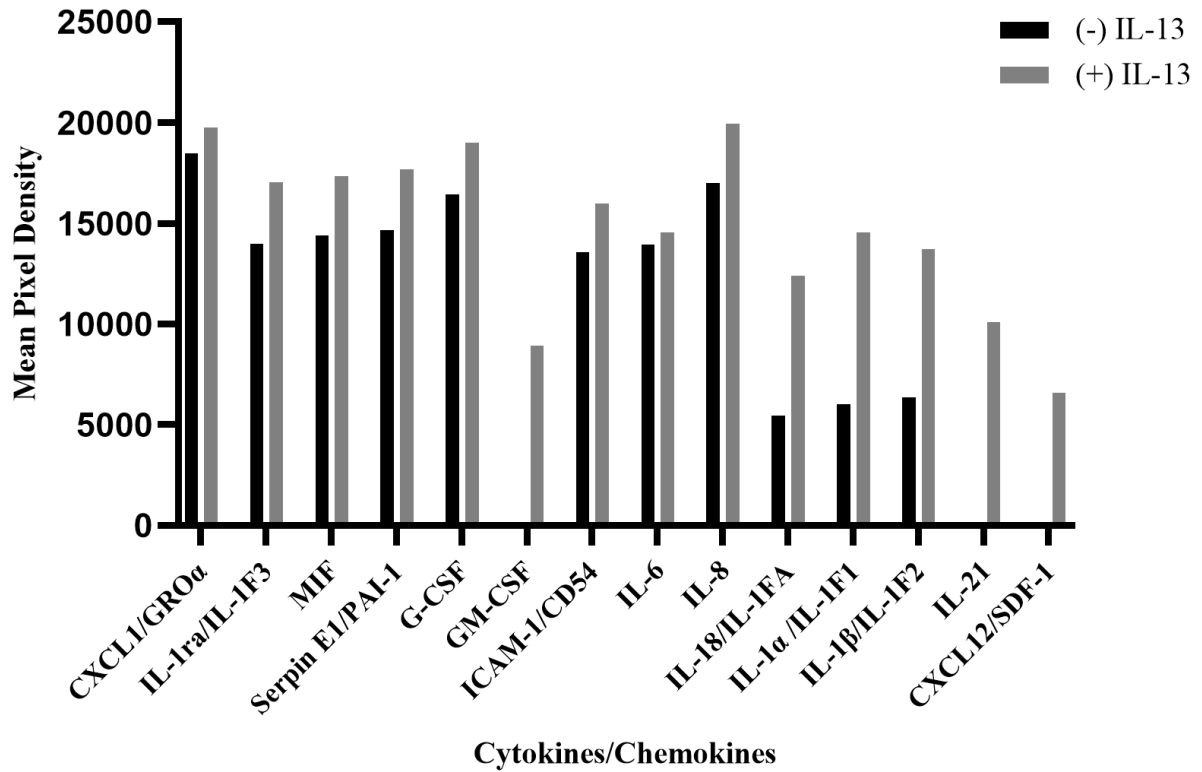


Figure 5.16: Comparison of immune mediators released by *S. aureus*-exposed for 16 hours HBECs in the absence and presence of IL-13 (MOI-1).

Results of the Human Cytokine Array assay, illustrating levels of signalling molecules released by HBECs exposed to *S. aureus* after 16 hours post-challenge. The pixel density was calculated through The Image Studio Lite software (LI-COR Biosciences).

5.10 Discussion

In this chapter I aimed to establish and characterize infection models using *S. aureus* in ALI-differentiated HBECs as they represent the airway epithelium *in vivo* more faithfully. As detailed in Chapter 3. The ALI-cultivated cells are more complex than those cultured in submerged conditions as a result of the differentiation process that leads to the establishment of a mucociliary phenotype and mucus secretion. This process should allow the cells to respond to foreign material (infections) in a more complicated manner that is more like what is seen *in vivo*. This complexity, I hypothesized, would help cells survive infection and provide a more faithful depiction of the human airway. I also wished to determine whether cultures grown in the presence of IL-13, so as to take on a more mucoid phenotype, would be differentially sensitive to infection.

As previously outlined human tracheobronchial epithelial cells or human bronchial epithelial cells (HBECs) can be used as a model system for *S. aureus* infections. These cells are maintained in traditional monolayer culture and have a “basal” cell like phenotype. Before experimentation, these cells are differentiated into pseudostratified epithelium using ALI (Davis et al., 2015), which generates a complex culture including non-ciliated goblet, ciliated and basal cells. Multiple of studies, have been used to compare the phenotypes of both types of cells (i.e., differentiated, and undifferentiated cells) (Ross et al., 2007, Martinez-Anton et al., 2013, Jackson et al., 2020).

IL-13 is a well-known Th2-type cytokine, the level of which is increased in many respiratory diseases (Seibold, 2018). It is known to increase the secretion of MUC5AC and intracellular oxidant stress (Alevy et al., 2012, Jackson et al., 2020, Siddiqui et al., 2021). In this way, it contributes to the secretion of the main gel-forming mucins from the epithelial cells of the respiratory tract. Studies have shown that when epithelial cells are induced with IL-13, a higher amount of MUC5AC is released, the numbers of epithelial cells secreting MUC5AC are increased, and oxidant activity is increased (Jaguin et al., 2013, Dickinson et al., 2016). My study describes a comparison of *S. aureus* infection and subsequent secretions from differential epithelial cells (i.e., HBECs with and without IL-13). My research with undifferentiated HBECs (described in Chapter 4) demonstrated that these cells can be infected. However, it is not clear that they adequately represented the cellular phenotype seen in the native airway. They became infected in an uncontrolled manner possibly as a result of bacterial growth in the media of the submerged cultures compared to the growth on the cell surface of the ALI cells.

This finding was in part likely due to these cells' inability to build adequate innate defence mechanisms to counteract the infection.

The studies in this chapter with differentiated cells were exposed to bacterial infections at a single MOI of 1. The complexity of the ALI culture system meant that only a limited number of wells could be generated from each donor and so only one MOI was used. Therefore, a comparative study was not conducted with different MOIs. As expected, the number of viable bacterial increased in differentiated epithelial cells both in the presence and absence of IL-13. Unlike in the undifferentiated cell experiments viable cells were seen in cultures up to 24 hours post infection. The viability of the infected cells, as viewed by their gross morphology, did not appear to differ in either in presence or absence of IL-13. When the extent of the infection, in the form of fluorescence intensity, was compared in both cases, the infection level increased more in epithelial cells grown in the absence of IL-13 compared to being in the presence of IL-13 (mean fluorescence intensity of 900 vs 600 after 24 hours). This difference can be explained based on immune system activation in the presence of IL-13, which decreases the infection level as compared to the absence of IL-13 (Figure 5.2G, and 5.8G). This hypothesis can be supported based on the roles played by IL-13 in previous studies. One such study demonstrated that IL-13 is involved in a reduction of illness and infection level of the syncytial virus in primary respiratory cells of the mouse (Zhou et al., 2006). This cytokine functions by regulating STAT1 induction and increasing IFN gamma secretion. Therefore, it is expected that IL-13 could play a similar role here in the presence of bacterial infection in the respiratory cells. A study by Jackson et al. (2020) indicated that IL-13 adjusts the state of secretory expression in airway epithelial cells. Chronic IL-13 reduces innate defence while inducing interferon signalling in cells that are ciliated. The reprogramming of IL-13 results in pathologic mucus that reduces the frequency of ciliary beating. This may have implication for bacterial infections. This is because the ciliary beating is crucial to keep the pathogenic bacteria from infecting the epithelium. Cilia form a physical layer that prevents bacteria from reaching the epithelial cells (Bustamante-Marin and Ostrowski, 2017). The beating makes sure that the mucus containing particle matter and pathogens is directed back towards the throat from where it is excreted (Fahy and Dickey, 2010).

The next series of experiments in this study were based on a comparison of the cellular response following *S. aureus* infection. This cellular response was measured in the form of changes in the expression level of two cytokines *CXCL10* and *IL6*. The results revealed that the levels of both factors increased in response to infection as compared to their levels without infection

(i.e., mock cells). Furthermore, the levels of both of these factors increased immediately after the infection and remained stable afterwards (i.e., their expression levels remained high from one-hour post infection until 16 hours). Comparing both types of analyses, the expression level of these factors in epithelial cells both in the presence and absence of IL-13 was similar; hence, both cell types exhibited similar immunological responses when infected by the bacterial strains. The mechanism of increased levels of IL-6 and CXCL-10 in response to such infection could involve the cascade in which cAMP levels are increased. In this regard, the interaction of the bacterial cells with HBECs might be based on specific glycosylation patterns on the surface of these host cells (Taylor et al., 1993). In another related study, an increased level of IL-6 was associated with higher cAMP concentrations when HBECs and another two types of airway epithelial cells were induced by CyaA (Bianchi et al., 2021). To confirm this hypothesis, further investigations would be required in which HBEC cells are exposed to *S. aureus*, and their cAMP levels are measured.

The differential response of cells in the presence and absence of IL-13 to bacterial infection was also measured by using qPCR to determine the expression levels of *IL6*, *CXCL1* and *CXCL10*. These genes are pro-inflammatory cytokines and chemokines involved in the immune system fight against bacterial infection through related but different mechanisms. They are produced by M1-like macrophages and subsequently cause type-1 inflammation (Vogel et al., 2014). On the other hand, IL-13 is produced by M2-like macrophages, and it is expected that when IL-13 is present, epithelial cells would, therefore, release the anti-inflammatory cytokines, and pro-inflammatory cytokine secretion would decrease (Tarique et al., 2015). However, my data did not demonstrate such a direct decrease in pro-inflammatory cytokines in the presence of IL-13 as compared to its absence during bacterial infection. Different release patterns of these cytokines and chemokines in both cases were observed, but these factors were not found to decrease. Such results could be explained based on the infections of *S. aureus* because the effects of IL-13 may be pathogenic specific. Hence, it would be interesting to perform a similar experiment to test the effect of IL-13 on changes in the expression in these factors if differentiated epithelial cells are infected with other bacterial species or other pathogens.

I found differential levels of various cytokines in my cytokine array analysis. For instance, according to cytokine array analysis, G-CSF, Serpin E1, GM-CSF and ICAM-1/CD54 levels decreased when epithelial cells were infected with the bacterial cells without IL-13 presence. However, the levels of all of these factors in the presence of IL-13 gradually increased when

epithelial cells were infected with *S. aureus*. Such contrasting results could be explained based on the pro-inflammatory roles of these factors. However, other cytokines, such as IL-6 showed a modest increase in the absence of IL-13 compared to the presence of IL-13. However, most of the cytokines and chemokines were higher in the mock cells in the absence of IL-13, confirming that inflammation was induced in epithelial cells upon bacterial infection even in the absence of IL-13. On the other hand, densitometry analyses showed some differences in the results, such as no detection of GM-CSF in any of the infected cells in the absence of IL-13, whereas it was detected in the uninfected cells. This type of difference might be explained based on variations in the detection efficiency of the techniques, or a sub-optimal methodology followed during the experiment. Furthermore, some previous studies showed that HBECs obtained from various sources demonstrated different types of responses when infected with potential pathogens. For instance, these cells are vulnerable to Influenza A virus infections, and one study showed that cells obtained from different donors express various types of proteins in response to influenza infection (Mindaye et al., 2017). The levels of both pro-viral and anti-viral proteins released by these host cells vary depending on the type of source of these cells.

The infection of HBECs with *S. aureus* in the presence and absence of IL-13 resulted in the production of cytokines (CXCL-10, CXCL-1, and IL-6) at different time points after the bacterial infection (Parkunan et al., 2016). In this regard, some of these cytokines are produced immediately after infection because they are directly regulated by IL-13 and bacterial infection. Such cytokines include IL-8, IL-1ra/IL-1F3, ICAM-1/CD54 and CXCL-1/GRO alpha, and their concentration increased with time. On the other hand, other cytokines such as IL-21, GM-CSF and IL-1beta/IL-1F2 were only expressed after 16 hours of the bacterial infection. Such delayed expression of these cytokines may be the result of their gene induction by other cytokines mentioned above, the expressions of which are gradually increased. Based on such results, it can be stated that bacterial infection of differentiated epithelial cells such as HBEC results in the activation of immunological reactions related to inflammation so that they can counter the infection both in the presence and absence of IL-13. However, the presence of this cytokine along with infection is involved in relatively differential pathways, with different sets of cytokines showing differential expression. The cytokines including IL-1 beta, IL-6, IL-8 and TNF-alpha are known to be associated with inflammation-related responses of epithelial respiratory cells due to parasitic infection (Gillette et al., 2013); therefore, their observed increase in this study in response to bacterial infection confirms the inflammation-based host cell response.

Similar findings were revealed in a study by Ansari et al. (2019). In their study, there was an increase in the level of various cytokines such as IL-1F3, IL-8 and CXCL-1/GRO alpha due to regulation by bacterial infection and IL-13. Therefore, it can be suggested that bacterial infection of differentiated epithelial cells results in the activation of immunological reactions related to inflammation so that they can counter the infection both in the presence and absence of IL-13. However, it is important to note that the presence of this cytokine along with infection is involved in differential pathways, with different sets of cytokines showing differential expression.

In summary, this chapter described a comparison of epithelial cell reaction to bacterial infection when they had been differentiated at the ALI in the presence or absence of IL-13. The cells secreted various cytokines and altered their levels in the presence of this cytokine as compared to when it is absent. There were some apparent contradictions in the results that could be minimized through more optimized protocols for the experimentation of cytokine arrays and densitometry analyses. It is evident that infected ALI cells could be grown longer than undifferentiated cells. They produced different cytokines in the mock situation compared to undifferentiated cells. They showed subtle differences in infection and response comparing IL-13 treated cells with untreated cells. Furthermore, future studies should be broader based in which more pathogens are included, such as other bacterial strains or even other pathogens, and then cellular responses should be noted because some of the human cellular responses can be pathogenic specific. In this regard, other respiratory pathogens, such as pneumococcal species, could be included. Finally, it is important to conduct further work to define the precise mechanism through which IL-13 influences the host immune cells to counteract this mechanism. In this context, the receptors and factors involved in the two processes could be assessed so that a more detailed mechanism can be provided.

CHAPTER 6: General discussion.

For functional studies of the human respiratory system, multiple different types of models have been used. As such experimentation cannot be performed on human subjects due to ethical considerations, therefore, alternative models including *in vivo* models and *in vitro* analyses have been used. *In vivo* models use many animals whose respiratory system is very similar to that of humans. However, ethical issues and pain caused by the use of experiments to animals also limits the use of such models as well. Therefore, *in vitro* models have been used extensively in respiratory biology. However, the use of most respiratory cell lines is limited by their inability to differentiate (Miller and Spence, 2017) and their failure to take on the phenotype of the airways. Therefore, my study was designed to investigate the culture of immortalized respiratory cell lines grown at an ALI and directly compare the results with those from differentiated primary HBECs, the model that is increasingly being seen as the gold standard. I had considered that such cell line models would prove to be an alternative to the use of primary HBECs. I used two respiratory cell lines originally derived from HBECs. HBEC3-KT cells which have been immortalized with Cdk4 and hTERT and BMI-1 cells that were produced by over expression of BMI-1 (Munye et al., 2017). The overall purpose of these experiments was to establish if these two cells' lines could be grown to be truly representative of respiratory cells. For this purpose, the ALI technique was used because this culture method is known to allow the differentiation of airway cells into a pseudostratified epithelium similar to that seen in the human respiratory tract (Wang et al., 2019b, Hiemstra et al., 2019).

In my initial studies ALI differentiation was undertaken with cells grown on transwells either collagen treated, or non-collagen treated. The purpose of this experiment was to investigate the differential differentiation of respiratory cells in these two conditions as it has been reported in the literature that such coatings mimic the basement membrane and facilitate differentiation. The differentiation process was initially evaluated through use of endpoint PCR with multiple cell type specific markers of different differentiated cells including *TEKT1* (ciliated cells) and *BPIFA1*, *BPIFB1* and *SCGB1A1* (secretory cells). Overall the expression of these genes in all three cell types confirmed that these cultures exhibited gene expression induction similar that previously reported for primary human ALI cells (Ross et al., 2007). When I more directly compared the expression levels of different markers in the different cultures during ALI exposure the results showed that ciliated cell gene expression was relatively weak compared to that of secretory cells gene expression. Indeed, the expression of these markers was less in the two cell lines compared to that seen in the primary HBECs. A similar pattern was observed by Vaughan et al., 2006, who concluded that ciliated cells development was relatively inhibited

(Vaughan et al., 2006). Moreover, Dvorak et al., (2011) validated that cilia-related genes have lower expression in ALI cultures in comparison to secretory and brushed cell genes. I was able to study the spatial distribution of FOXJ1 (a ciliated cell marker), through the use of IF microscopy. These results showed that ciliated cells detected through FOXJ1 staining were not found in undifferentiated cells, but they were present in differentiated epithelial cells. It appeared as if there was less FOXJ1 in the cell line ALI cells compared to in the primary HBECs, although I did not formally quantitate this. Previous studies have also made such observation with the differentiation process being shown to produce limited evidence of ciliated cell differentiation (Fulcher et al., 2009). I attempted to induce the differentiation of ciliated cells using DAPT treatment. DAPT is an inhibitor of Notch signalling, and has been used to induce the differentiation of ciliated cells (Gerovac et al., 2014). Unexpectedly, I was not able to demonstrate ciliated cell numbers increased in response to DAPT induction. The inability to produce ciliated cells following such treatment might be explained because either the dosage used was too low or that too short a duration of induction was used (Wang et al., 2019a). Alternatively, it is also possible that HBEC3-KT cells may have lost the ability to differentiate more ciliated cells following DAPT treatment. Similar results have been shown when other “immortalised” airway cells have been differentiated at the ALI suggesting the effect may be due to the process of transformation. The basis for this could be studied by investigating genome wide transcriptional data from the three cell types when they are undergoing ALI mediated differentiation.

Another interesting result from the differentiation studies was the observation of expression of the secretory cell markers *BPIFA1* and *SCGB1A1* in both BMI-1 and HBEC cells before their differentiation at the ALI. Many studies have shown that secretory genes are not seen pre-ALI induction when cells are cultured in the “traditional” BEGM (Ross et al., 2007). It seems reasonable to assume that culturing the cells in Pneumacault™ Expansion Plus media prior to differentiation may be responsible for the induction of secretory cell markers. However, I did not directly test this during the current study. However, previous work in our lab has not observed high expression of these genes in HBECs when they were grown in BGEM based growth media (Bingle et al., 2006). It can be suggested that growth media used in this study has induced the early expression of these genes (Lin et al, 2021).

Although all three ALI cell cultures appeared to show some level of mucociliary differentiation it was unclear if these differentiated cells would produce similar types of secretions. For instance, mucus associated proteins are one of the most important components of these

secretions and these can be secreted in the form of exomes or by exocytosis (Piper et al., 2013). I applied an unbiased proteomic technique to directly compare the secretomes of differentiated HBEC3-KT cells and primary HBECs. My results showed that many of the proteins secreted by the two cell types were common, but a number were not. Amongst those expressed differentially were many host defence and mucus proteins including MUC5AC, MUC5B, SCGB1A1 and SLPI and these were found to be much more highly secreted from HBECs compared to HBEC3-KT cells. Whereas proteins such as HP and OLMF4 were much more highly secreted by HBEC3-KT cells. Along with the higher differential expression of ciliated cell markers in HBECs these differences in secretory protein production also further suggest that ALI differentiated HBEC3-KT cells are not a faithful surrogate model for a fully differentiated airway epithelium. For this reason, the majority of my infection studies were undertaken in primary HBECs rather than in the immortalized cell lines. This was a departure from my original experimental plans that was dictated by my results.

A central aim of my thesis was to investigate the initial infection of airway epithelial cells with *S. aureus* as it was hypothesised that such studies could identify both host and pathogen genes required for the initial stages of airway infection. I initially undertook to investigate the differences between undifferentiated and differentiated cells and how they responded when they were infected with *S. aureus*. As HBECs and HBEC3-KT cells are both human respiratory cells with a similar origin, it was expected that they would respond in a similar manner to this bacterial pathogen. These two cell types are routinely grown in different media when they are in submerged (routine) culture. So, prior to my infection study I studied bacterial growth in these different media. Bacteria showed different growth responses to different types of media. Bacterial growth was much higher in Pneumacault™ Expansion Plus media as compared to that in Keratinocyte-SFM media. This difference could possibly be explained by differences in the content of the two types of media. Pneumacault™ Expansion Plus media contains human serum which probably supports bacterial growth more effectively as compared to the media which lacks this component.

There were significant differences in the way in which undifferentiated and differentiated cells responded to *S. aureus* infection. Bacterial growth was more marked in submerged cultures of undifferentiated cells. This is probably due to a combination of two factors. Infection occurring both within the cells and in the overlying media, and the fact that the undifferentiated cells produce less innate defence proteins. Previous studies have shown that the rate of infection can be higher for undifferentiated cells, therefore, bacteria can grow there at higher rates as compared

to their growth rates in differentiated cells (Liu et al. 2011). Furthermore, studies have indicated that bacterial infection in respiratory system results in release of pro-inflammatory cytokines such as IL-6 and CXCL10 (Ben-Moshe et al. 2019). Gene expression data showed that a number of inflammatory mediators were induced in the infected undifferentiated cells but the cytokines array data shows that these cells did not produce significant levels of proinflammatory cytokines. It may be that the time point chosen for this analysis was not optimal for seeing a strong signal, but it seems likely that these cells are lacking key host defence proteins to allow them to mount a significant defence against *S. aureus* infection.

The last phase of the study was focused on interactions between differentiated host cells and bacterial infections. These differentiated ALI cells were expected to respond more like *in vivo* cells. My data shown that these cells were able to mount a more robust defence against *S. aureus* infection. I could also show that in the uninfected state these cells secreted a more cytokines and chemokines even without infection but following infection they appeared to mount a greater induction. There were also some differences in the response of cells differentiated in the presence IL-13. This cytokine is known to be increased in response to infection of respiratory cells (Stier et al., 2016, Morrison et al., 2022). Previous studies have shown that when epithelial respiratory cells are exposed to IL-13, they increase the secretions of MUC5AC (Dickinson et al., 2016) and other HPDs (e.g. LL37, CCL20 and lysozyme) (Zuyderduyn et al., 2011, Wang et al., 2022), such an induction is not observed in the undifferentiated cells treated with IL-13, which may contribute to making them more vulnerable to infections.

Overall, my study has suggested that ALI differentiated respiratory epithelial cells can be representatives of *in vivo* cells and are a better model that the use of undifferentiated cells in submerged tissue culture. Furthermore, when such cells are exposed to infections with *S. aureus*, they respond in a more robust manner compared to cells in submerged culture. therefore, they provide a good model for investigation of different types of respiratory infections and diseases.

6.1 Strengths and Weaknesses

My study has allowed me to show that HBEC3-KT cells (and perhaps other immortalized airway cells) are not as good as primary cells in respect to their ability to fully differentiate when grown at the ALI and that perhaps they do not faithfully recapitulate the mucociliary epithelium of the human airways *in vitro*. My work has shown that differentiated HBEC3-KT cells do not fully ciliate when grown at the ALI and fail to secrete a number of key proteins expected to be produced by the native mucociliary epithelium. This may limit use of such cells as a model of the native human respiratory epithelium.

This thesis has provided insight into establishment of *S. aureus* infections in both differentiated and undifferentiated airway cells. It has shown that differentiated ALI HBEC cultures are a robust model that can be used for these types of studies. This model allows researchers to start asking questions about the specific aspects of this process and would allow an investigation of what happens when inflammatory cells are added to the model.

On a less positive note, my data also showed a very varied expression level of different markers among different donors of the primary cells and between different replicates of the cell lines. Another limiting factor for the use of the HBEC3-KT cells was the fact that they failed to ciliate in a manner seen in primary HBECs, even when they were treated with DAPT. They also did not respond as expected to IL-13 treatment. These observations may also limit the use of this cell line as a surrogate for the human airway.

Another limitation of the study was that I did not examine any strain-specific responses in my infection study. I used a single laboratory isolate of *S. aureus*. To obtain more robust results, it would have been necessary to examine several strains of *S. aureus* and ultimately study clinical isolates.

6.2 Future Directions

My study leaves open a significant number of potential further studies.

It would be possible to increase the robustness of this model by identifying and quantifying immune responses with the help of additional techniques. Enzyme-linked immunosorbent assay (ELISA) and Cytometric Bead Arrays could be used to gain more quantitative data on the production of inflammatory molecules at different time points and across more infection MOIs. Such quantitative techniques would be helpful to look at responses to infection with different strains of *S. aureus*.

Genome wide transcriptional approaches could be applied to study gene expression both during the differentiation process, when the cell lines could be compared in detail, and also during infections when induction of a wide range of genes could be investigated. It would be informative to see how the transcriptional data from the two cell types compares.

I could also investigate primary virulence factors responsible for such infections through the use of mutant strains of *S. aureus*. Many mutant *S. aureus* strains could be investigated in a systematic manner to see how specific genes in the bacteria alter the primary host response.

Finally, both host and pathogen factors could be examined through genetic engineering approaches such as gene silencing or gene knock down for selected genes in both the pathogen or in host epithelial cells. Our laboratory has already generated multiple gene edited mutant HBEC3-KT cell lines.

Appendix 1 – List of cytokines and chemokines

C5a	IL-4	IL-27
CD40 Ligand	IL-5	IL-32 alpha
G-CSF	IL-6	CXCL10/IP-10
GM-CSF	IL-8	CXCL11/I-TAC
CXCL1/GRO alpha	IL-10	CCL2/MCP-1
CCL1/I-309	IL-12 p70	MIF
ICAM-1	IL-13	MIP-1 alpha/MIP-1 beta
IFN-gamma	IL-16	CCL5/RANTES
IL-1 alpha	IL-17	CXCL12/SDF-1
IL-1 beta	IL-17E	Serpin E1/PAI-1
IL-1ra	IL-18	TNF-alpha
IL-2	IL-21	TREM-1

Appendix 2 – List of the top 100 extracellular proteins.

GENE	HBEC3-KT-01	HBEC3-KT-02	HBEC3-KT-03	HBEC3-KT-04	HBEC3-KT-05	HBEC-02	HBEC-03	HBEC-04	HBEC-05
BPIFB1	1.57E+10	1.53E+10	1.53E+10	1.47E+10	2.24E+10	8.73E+10	2.00E+11	1.04E+11	1.51E+11
LCN2	1.8E+10	2.64E+10	2.89E+10	3.03E+10	1.1E+10	6.24E+10	5.4E+10	5.68E+10	3.84E+10
C3	2.52E+11	2.26E+11	1.80E+11	1.80E+11	1.78E+11	4.65E+10	1.16E+11	6.94E+10	7.88E+10
MUC5AC	15647000	8353200	12617000	12221000	29908000	4.09E+10	7.98E+10	2.81E+10	6.91E+10
MUC5B	9.65E+08	6.94E+08	7.8E+08	7.16E+08	1.48E+09	3.9E+10	9.02E+10	4.18E+10	5.05E+10
ANXA2	1.47E+10	1.87E+10	2.16E+10	1.89E+10	2.27E+10	2.82E+10	2.43E+10	2.17E+10	1.65E+10
Complement	2.12E+10	2.81E+10	2.66E+10	2.56E+10	1.05E+10	2.25E+10	4.05E+10	2.95E+10	2.84E+10
ANXA1	2.01E+09	2.75E+09	2.97E+09	2.79E+09	3.51E+09	1.69E+10	1.05E+10	1.23E+10	9.3E+09
FN1	3.92E+10	3.3E+10	3.26E+10	2.8E+10	6.56E+10	1.22E+10	2.83E+10	1.47E+10	1.64E+10
PI3	1.01E+10	2.18E+10	2.19E+10	2.12E+10	1.62E+10	1.18E+10	3.29E+09	5.49E+09	6.17E+09
TF	1.27E+10	2.76E+10	2.76E+10	2.24E+10	2.82E+10	1.04E+10	1.75E+10	1.53E+10	8.69E+09
HSPG2	3.82E+10	4.02E+10	2.93E+10	2.98E+10	3.3E+10	9.77E+09	8.96E+09	1.02E+10	7.79E+09
CP	7.29E+09	7.88E+09	7.41E+09	6.65E+09	6.91E+09	8.88E+09	1.31E+10	8.31E+09	7.97E+09
GSN	1.03E+09	1.04E+09	1.12E+09	1.04E+09	9.5E+08	6.75E+09	1.41E+10	8.18E+09	6.65E+09
SERPINA3	2.28E+10	6.62E+10	6.29E+10	5.08E+10	1.46E+10	6.64E+09	7.03E+09	7.03E+09	4.91E+09
LGALS3BP	2.37E+10	4.07E+10	3.98E+10	3.86E+10	2.49E+10	6.56E+09	1.53E+10	1E+10	7.27E+09
SLPI	1.98E+09	3.39E+09	4.55E+09	3.61E+09	2.9E+09	6.39E+09	3.1E+10	1.28E+10	3.12E+10
PPIA	2.58E+09	2.15E+09	2.37E+09	2.49E+09	2.79E+09	6.35E+09	4.17E+09	5.23E+09	5.13E+09
LAMB3	6.52E+09	4.86E+09	4.05E+09	3.94E+09	8.2E+09	6.13E+09	4.59E+09	5.39E+09	4.15E+09
LAMC2	4.88E+09	3.92E+09	3.47E+09	3.08E+09	7.12E+09	5.98E+09	3.72E+09	5.19E+09	4.04E+09
MUC4	2.53E+09	2.99E+09	4.11E+09	3.62E+09	3.4E+09	5.98E+09	1.28E+10	9.74E+09	3.57E+09
CTSD	8.7E+09	8.66E+09	7.35E+09	7.59E+09	7.24E+09	5.68E+09	7.21E+09	4.62E+09	4.06E+09
AGRN	1.26E+10	1.41E+10	1.11E+10	1.09E+10	9.81E+09	5.45E+09	7.67E+09	6.59E+09	5.68E+09
TNC	3.81E+09	2.72E+09	2.34E+09	2.35E+09	5.31E+09	4.96E+09	3.18E+09	4.92E+09	3.73E+09
LTF	4.75E+10	1.37E+11	1.17E+11	1.07E+11	3.84E+09	4.58E+09	1.91E+10	1.33E+10	3.45E+09
LAMA3	6.53E+09	5.36E+09	4.35E+09	4.35E+09	9.95E+09	4.42E+09	4.24E+09	4.32E+09	3.3E+09
MUC1	6.29E+09	7.36E+09	9E+09	8.14E+09	8.81E+09	3.95E+09	8.07E+09	6.19E+09	5.09E+09
MUC16	5.87E+08	8.83E+08	1.05E+09	9.77E+08	1.02E+09	3.77E+09	9.3E+09	5.83E+09	4.39E+09
CLU	1.69E+08	1.1E+08	1.15E+08	1.15E+08	1.37E+08	3.73E+09	6.75E+09	4.95E+09	4.02E+09
CFH	4.96E+09	7.65E+09	6.9E+09	6.12E+09	5.5E+09	3.52E+09	8.38E+09	6.43E+09	5.29E+09
LGALS3	6.77E+08	7.35E+08	7.19E+08	7.8E+08	8.17E+08	3.51E+09	1.51E+09	3.11E+09	1.73E+09
CTSB	4.76E+09	8.89E+09	8.45E+09	7.11E+09	6.02E+09	3.2E+09	7.13E+09	4.77E+09	3.99E+09
QSOX1	8.85E+08	8.5E+08	9.13E+08	1.02E+09	6.31E+08	3.04E+09	5.31E+09	3.93E+09	3.16E+09
TGFBI	5.57E+09	5.63E+09	5.08E+09	4.52E+09	8.36E+09	3.02E+09	5.04E+09	3.93E+09	2.41E+09
KLK11	2392800	5227800	4189600	6290800	5728700	2.79E+09	1.86E+09	1.63E+09	1.61E+09
P4HB	1.69E+09	8.6E+08	7.48E+08	9.9E+08	9.15E+08	2.45E+09	5.51E+08	1.45E+09	1.39E+09
CXCL8	46446000	91473000	88620000	1.01E+08	52628000	2.36E+09	1.9E+08	1.15E+09	8.59E+08
IGFBP7	4.47E+08	1.22E+09	1.01E+09	9.97E+08	5.62E+08	2.22E+09	5.35E+09	3.34E+09	2.01E+09
EFEMP1	1.47E+09	2.23E+09	2.18E+09	2.19E+09	1.52E+09	2.2E+09	4.92E+09	3.04E+09	3.08E+09
MMP9	8.02E+08	1.18E+09	1.51E+09	1.09E+09	2.78E+09	2.13E+09	4.05E+09	2.98E+09	2.45E+09
CST3	9.46E+08	1.47E+09	1.49E+09	1.42E+09	9.5E+08	1.71E+09	6.5E+09	2.93E+09	3.62E+09
IGFBP2	1.09E+08	2.47E+08	2.65E+08	2.45E+08	2.57E+08	1.68E+09	4.31E+09	1.83E+09	2.49E+09
CXCL1	4.95E+08	1.24E+09	1.34E+09	1.19E+09	7.38E+08	1.57E+09	4.25E+09	7.82E+09	7.87E+09

SERPINE1	6.1E+08	9.88E+08	8.98E+08	8.29E+08	7.76E+08	1.54E+09	1.78E+09	1.71E+09	1.37E+09
IGFBP3	1E+09	1.74E+09	1.55E+09	1.51E+09	1.45E+09	1.48E+09	1.94E+09	1.53E+09	1.47E+09
SERPINA1	4.22E+08	6.58E+08	7.26E+08	7E+08	2.99E+08	1.47E+09	4.57E+09	2.54E+09	2.47E+09
TIMP1	1.24E+09	2.28E+09	2.45E+09	2.25E+09	1.31E+09	1.46E+09	2.78E+09	1.58E+09	1.35E+09
FBLN1	2.49E+08	5.97E+08	5.22E+08	4.35E+08	4.16E+08	1.3E+09	1.28E+09	1.01E+09	7.33E+08
MMP10	1.96E+08	1.81E+08	2.49E+08	2.21E+08	4.33E+08	1.28E+09	3.38E+09	1.58E+09	1.68E+09
C4B	3.04E+09	1.1E+09	1.78E+09	1.98E+09	2.57E+08	1.27E+09	4.61E+09	2.44E+09	1.83E+09
WFDC2	7.26E+08	2.48E+09	4.33E+09	3.2E+09	1.11E+09	1.2E+09	9.57E+09	2.36E+09	3.64E+09
SERPINF1	0	10258000	0	8063200	0	1.07E+09	3.24E+09	1.95E+09	5.2E+09
GPI	6.73E+08	8.04E+08	8.25E+08	8.88E+08	5.29E+08	1.07E+09	1.12E+09	1.33E+09	1.14E+09
CXCL6	0	0	0	0	0	9.98E+08	7.21E+08	5.95E+08	6.31E+08
LRG1	7.34E+08	1.64E+09	1.75E+09	1.5E+09	6.27E+08	9.65E+08	2.43E+09	1.15E+09	7.24E+08
S100A8	4.5E+09	6.83E+09	9.64E+09	8.86E+09	3.34E+09	9.2E+08	1.39E+09	1.07E+09	5E+08
PPIB	6.87E+08	8.95E+08	9.69E+08	8.19E+08	5.13E+08	9.09E+08	1.16E+09	9.88E+08	9.19E+08
TINAGL1	2.25E+09	2.47E+09	1.8E+09	1.8E+09	2.27E+09	8.43E+08	7.87E+08	8.66E+08	5.51E+08
KLK10	1.04E+08	2.64E+08	2.48E+08	2.02E+08	3.25E+08	7.85E+08	1.85E+09	1.11E+09	9.54E+08
VMO1	0	0	0	0	0	7.45E+08	1.65E+09	6.93E+08	1.16E+09
FAM3D	0	0	0	0	0	7.42E+08	5.85E+08	6.47E+08	5.71E+08
S100A9	4.95E+09	8.41E+09	1.07E+10	9.58E+09	4.32E+09	7.37E+08	1.6E+09	9.58E+08	4.34E+08
AZGP1	8.27E+08	2.13E+09	2.11E+09	1.67E+09	9.54E+08	6.97E+08	1.62E+09	1.31E+09	1.11E+09
PRSS22	1.76E+08	1.56E+08	1.78E+08	2.07E+08	1.32E+08	6.82E+08	4.29E+08	3.68E+08	3.41E+08
SPINT1	4.39E+08	7.39E+08	7.58E+08	7.09E+08	5.07E+08	6.53E+08	1.32E+09	9.3E+08	9.07E+08
PLAU	1.42E+08	1.62E+08	1.96E+08	2.07E+08	3.63E+08	6.47E+08	8.4E+08	6E+08	4.63E+08
ZG16B	3.22E+08	4.08E+08	3.43E+08	3.5E+08	3.62E+08	6.47E+08	1.31E+09	7.76E+08	8.67E+08
AGRN0	9.31E+08	1.05E+09	8.59E+08	1.01E+09	8.91E+08	6.38E+08	2.2E+08	4.24E+08	2.45E+08
SFN	8.53E+08	8.79E+08	8.06E+08	9.34E+08	1E+09	6.18E+08	6.07E+08	7.73E+08	1.01E+09
FOLR1	1.98E+08	1.77E+08	2.1E+08	2.09E+08	2.37E+08	5.83E+08	1.23E+09	9.23E+08	8.9E+08
CD55	3.74E+08	5.51E+08	6.64E+08	5.7E+08	5.44E+08	5.73E+08	1.85E+09	8.05E+08	1.07E+09
NAMPT	2.71E+08	1.65E+08	1.71E+08	2.03E+08	1.12E+08	5.5E+08	76162000	2.95E+08	1.98E+08
CXCL5	0	0	0	0	0	5.48E+08	2.77E+08	6.2E+08	7.18E+08
MIF	3.45E+08	3.86E+08	3.12E+08	3.39E+08	1.96E+08	5.4E+08	2.07E+08	3.27E+08	4.74E+08
FGFBP1	5.27E+08	6.49E+08	5.36E+08	4.66E+08	6.15E+08	5.38E+08	4.43E+08	8.68E+08	4.75E+08
FSTL1	4.6E+08	9.72E+08	1.01E+09	8.81E+08	5.08E+08	5.23E+08	8.98E+08	8.07E+08	1.02E+09
FAM3C	1.47E+08	2.53E+08	3.1E+08	2.55E+08	1.31E+08	4.99E+08	6.66E+08	5.41E+08	4.01E+08
BPIFA1	1.82E+08	1.8E+08	79103000	1.52E+08	64191000	4.85E+08	6.78E+08	5.94E+08	8.8E+08
MMP13	16356000	14054000	14693000	12291000	54113000	4.74E+08	9E+08	3.37E+08	3.95E+08
COL12A1	2.55E+09	1.85E+09	1.35E+09	1.64E+09	1.83E+09	4.71E+08	4.54E+08	4.65E+08	3.07E+08
C1R	5.9E+09	1.04E+10	9.74E+09	7.75E+09	3.99E+09	4.7E+08	3.13E+08	4.45E+08	3.14E+08
CFI	2.38E+08	5.25E+08	4.67E+08	4.03E+08	3.4E+08	4.65E+08	1.09E+09	7.4E+08	5.37E+08
TCN1	23352000	70749000	68316000	53534000	96298000	4.54E+08	7.17E+08	5.02E+08	4.55E+08
AKR1B10	44487000	58043000	59527000	51356000	47585000	4.28E+08	1.18E+08	2.4E+08	1.46E+08
CCL20	0	0	0	0	0	4.14E+08	55924000	2.27E+08	1.67E+08
CD44	1.06E+09	1.34E+09	1.77E+09	1.64E+09	1.12E+09	3.94E+08	5.61E+08	3.93E+08	2.65E+08
PRSS8	2.06E+08	2.88E+08	3.33E+08	2.75E+08	1.52E+08	3.8E+08	4.36E+08	2.48E+08	3.01E+08
AMY1A	41033000	69777000	1.1E+08	1.64E+08	14859000	3.65E+08	4.78E+08	2.76E+08	2.97E+08
FBLN2	0	0	0	0	0	3.41E+08	3.74E+08	3.11E+08	3.16E+08

OLFM4	8.16E+10	3.9E+10	4.29E+10	4.23E+10	4.94E+10	3.32E+08	5.89E+08	2.71E+08	1.05E+08
ST6GAL1	0	0	0	0	0	3.24E+08	4.67E+08	3.34E+08	2.95E+08
S100A7	1.56E+09	3.69E+09	3.77E+09	4.2E+09	1.1E+09	3.23E+08	1.49E+09	7.53E+08	1.78E+08
GRN	2.75E+09	4.36E+09	3.84E+09	3.7E+09	2.23E+09	3.15E+08	4.1E+08	3.23E+08	2.68E+08
COPA	1.51E+08	1.21E+08	96886000	79426000	1.26E+08	3.11E+08	0	93379000	1.03E+08
MET	3.85E+08	6.64E+08	5.78E+08	5.81E+08	3.81E+08	2.93E+08	3.2E+08	3.65E+08	2.61E+08
PXDN	6.23E+08	6.28E+08	5.21E+08	5.32E+08	5.39E+08	2.88E+08	3.6E+08	2.22E+08	1.92E+08
LTBP4	1.27E+08	3.13E+08	2.41E+08	2.14E+08	2.05E+08	2.74E+08	3.05E+08	3.67E+08	2.93E+08
SLURP2	0	0	0	0	0	2.67E+08	4.06E+08	4.44E+08	4.64E+08
NPC2	90043000	0	1.88E+08	1.64E+08	1.01E+08	2.49E+08	8.71E+08	6.55E+08	5.05E+08
MDK	95701000	99953000	1.43E+08	1.25E+08	1.59E+08	2.43E+08	3.05E+08	1.94E+08	2.22E+08
SCGB1A1	6303100	19684000	0	10173000	32422000	0	1.28E+09	6.55E+08	1.45E+09

References

- ABDULMANNAN, F., ANDREW, P., WEILI, L., ELEWOSI, T. G. V., ROMA, N. R., FATMA, F., SUAAD, D., YAZAN, R., YASSER, S. & J, A. J. 2018. Modulation of innate and adaptive immune responses by arabinoxylans. *Journal of Food Biochemistry*, 42, e12473.
- AGRAWAL, A., GINDODIYA, A., DEO, K., KASHIKAR, S., FULZELE, P. & KHATIB, N. 2021. A comparative analysis of the Spanish Flu 1918 and COVID-19 pandemics. *The Open Public Health Journal*, 14.
- AHN, D. S., PARKER, D., PLANET, P. J., NIETO, P. A., BUENO, S. M. & PRINCE, A. 2014. Secretion of IL-16 through TNFR1 and calpain-caspase signaling contributes to MRSA pneumonia. *Mucosal Immunol*, 7, 1366-74.
- AKIL, N. & MUHLEBACH, M. S. 2018. Biology and management of methicillin resistant Staphylococcus aureus in cystic fibrosis. *Pediatric pulmonology*, 53, S64-S74.
- AL MUBARAK, R., ROBERTS, N., MASON, R. J., ALPER, S. & CHU, H. W. 2018. Comparison of pro-and anti-inflammatory responses in paired human primary airway epithelial cells and alveolar macrophages. *Respiratory research*, 19, 1-14.
- ALBRECHT, V. S., LIMBAGO, B. M., MORAN, G. J., KRISHNADASAN, A., GORWITZ, R. J., MCDUGAL, L. K. & TALAN, D. A. 2015. Staphylococcus aureus colonization and strain type at various body sites among patients with a closed abscess and uninfected controls at US emergency departments. *Journal of clinical microbiology*, 53, 3478-3484.
- ALEVY, Y. G., PATEL, A. C., ROMERO, A. G., PATEL, D. A., TUCKER, J., ROSWIT, W. T., MILLER, C. A., HEIER, R. F., BYERS, D. E. & BRETT, T. J. 2012. IL-13-induced airway mucus production is attenuated by MAPK13 inhibition. *The Journal of clinical investigation*, 122, 4555-4568.
- ALHARBI, Z., CHOWDHURY, M. M. K., BINGLE, L. & BINGLE, C. 2020. Air liquid interface (ALI)-grown immortalized human cell lines: a promising tractable model for human airway. *Eur Respiratory Soc*.
- ALI, M., LILLEHOJ, E. P., PARK, Y., KYO, Y. & KIM, K. C. 2011. Analysis of the proteome of human airway epithelial secretions. *Proteome science*, 9, 1-10.
- ALYSANDRATOS, K.-D., HERRIGES, M. J. & KOTTON, D. N. 2021. Epithelial stem and progenitor cells in lung repair and regeneration. *Annual Review of Physiology*, 83, 529-550.
- AMINI, S.-E., GOUYER, V., PORTAL, C., GOTTRAND, F. & DESSEYN, J.-L. 2019. Muc5b is mainly expressed and sialylated in the nasal olfactory epithelium whereas Muc5ac is exclusively expressed and fucosylated in the nasal respiratory epithelium. *Histochemistry and Cell Biology*, 152, 167-174.
- ANNUNZIATO, F., ROMAGNANI, C. & ROMAGNANI, S. 2015. The 3 major types of innate and adaptive cell-mediated effector immunity. *Journal of Allergy and Clinical Immunology*, 135, 626-635.
- ANUJAN, P. 2019. *Functional analysis of novel protein, PIERCE1, in motile ciliogenesis*. University of Sheffield.
- ARIFUZZAMAN, M., MOBLEY, Y. R., CHOI, H. W., BIST, P., SALINAS, C. A., BROWN, Z. D., CHEN, S. L., STAATS, H. F. & ABRAHAM, S. N. 2019. MRGPR-mediated activation of local mast cells clears cutaneous bacterial infection and protects against reinfection. *Science advances*, 5, eaav0216.
- ARMENTROUT, E. I., LIU, G. Y. & MARTINS, G. A. 2020. T Cell Immunity and the Quest for Protective Vaccines against Staphylococcus aureus Infection. *Microorganisms*, 8, 1936.
- ARNELLOS, A. & KEIJZER, F. 2019. Bodily complexity: Integrated multicellular organizations for contraction-based motility. *Frontiers in physiology*, 1268.
- ARORA, S., DEV, K., AGARWAL, B., DAS, P. & SYED, M. A. 2018. Macrophages: Their role, activation and polarization in pulmonary diseases. *Immunobiology*, 223, 383-396.

- ASKARIAN, F., WAGNER, T., JOHANNESSEN, M. & NIZET, V. 2018. Staphylococcus aureus modulation of innate immune responses through Toll-like (TLR),(NOD)-like (NLR) and C-type lectin (CLR) receptors. *FEMS microbiology reviews*, 42, 656-671.
- BACHERT, C., GEVAERT, P., HOWARTH, P., HOLTAPPELS, G., VAN CAUWENBERGE, P. & JOHANSSON, S. 2003. IgE to Staphylococcus aureus enterotoxins in serum is related to severity of asthma. *Journal of Allergy and Clinical Immunology*, 111, 1131-1132.
- BACHERT, C., HUMBERT, M., HANANIA, N. A., ZHANG, N., HOLGATE, S., BUHL, R. & BRÖKER, B. M. 2020. Staphylococcus aureus and its IgE-inducing enterotoxins in asthma: current knowledge. *European Respiratory Journal*, 55.
- BÆK, K. T., FREES, D., RENZONI, A., BARRAS, C., RODRIGUEZ, N., MANZANO, C. & KELLEY, W. L. 2013. Genetic variation in the Staphylococcus aureus 8325 strain lineage revealed by whole-genome sequencing. *PLoS One*, 8, e77122.
- BALASUBRAMANIAN, D., OHNECK, E. A., CHAPMAN, J., WEISS, A., KIM, M. K., REYES-ROBLES, T., ZHONG, J., SHAW, L. N., LUN, D. S., UEBERHEIDE, B., SHOPSIN, B. & TORRES, V. J. 2016. Staphylococcus aureus Coordinates Leukocidin Expression and Pathogenesis by Sensing Metabolic Fluxes via RpiRc. *mBio*, 7.
- BALÁZS, A., MILLAR-BÜCHNER, P., MÜLLEDER, M., FARZTDINOV, V., SZYRWIEL, L., ADDANTE, A., KUPPE, A., RUBIL, T., DRESCHER, M. & SEIDEL, K. 2022. Age-Related Differences in Structure and Function of Nasal Epithelial Cultures From Healthy Children and Elderly People. *Frontiers in immunology*, 13.
- BALDASSI, D., GABOLD, B. & MERKEL, O. 2021. Air-liquid interface cultures of the healthy and diseased human respiratory tract: promises, challenges and future directions. *Adv Nanobiomed Res*, 1.
- BARAC, A., ONG, D. S., JOVANCEVIC, L., PERIC, A., SURDA, P., TOMIC SPIRIC, V. & RUBINO, S. 2018. Fungi-induced upper and lower respiratory tract allergic diseases: one entity. *Frontiers in microbiology*, 9, 583.
- BARDOEL, B., VOS, R., BOUMAN, T., AERTS, P., BESTEBROER, J., HUIZINGA, E., BRONDIJK, T., VAN STRIJP, J. & DE HAAS, C. 2012. Evasion of Toll-like receptor 2 activation by staphylococcal superantigen-like protein 3. *Journal of molecular medicine*, 90, 1109-1120.
- BARKAUSKAS, C. E., CRONCE, M. J., RACKLEY, C. R., BOWIE, E. J., KEENE, D. R., STRIPP, B. R., RANDELL, S. H., NOBLE, P. W. & HOGAN, B. L. 2013. Type 2 alveolar cells are stem cells in adult lung. *The Journal of clinical investigation*, 123, 3025-3036.
- BARNES, C., ENGLISH, D., BRODERICK, M., COLLINS, M. & COWLEY, S. M. 2021. Proximity-dependent biotin identification (BioID) reveals a dynamic LSD1-CoREST interactome during embryonic stem cell differentiation. *Molecular Omics*.
- BASIL, M. C., KATZEN, J., ENGLER, A. E., GUO, M., HERRIGES, M. J., KATHIRIYA, J. J., WINDMUELLER, R., YSASI, A. B., ZACHARIAS, W. J. & CHAPMAN, H. A. 2020. The cellular and physiological basis for lung repair and regeneration: past, present, and future. *Cell Stem Cell*, 26, 482-502.
- BAUER, M., WEIS, S., NETEA, M. G. & WETZKER, R. 2018. Remembering pathogen dose: long-term adaptation in innate immunity. *Trends in immunology*, 39, 438-445.
- BEKEREDJIAN-DING, I., INAMURA, S., GIESE, T., MOLL, H., ENDRES, S., SING, A., ZÄHRINGER, U. & HARTMANN, G. 2007. Staphylococcus aureus protein A triggers T cell-independent B cell proliferation by sensitizing B cells for TLR2 ligands. *J Immunol*, 178, 2803-12.
- BEN-MOSHE, N. B., HEN-AVIVI, S., LEVITIN, N., YEHEZKEL, D., OOSTING, M., JOOSTEN, L. A., NETEA, M. G. & AVRAHAM, R. 2019. Predicting bacterial infection outcomes using single cell RNA-sequencing analysis of human immune cells. *Nature communications*, 10, 1-16.
- BERKESTEDT, I., HERWALD, H., LJUNGGREN, L., NELSON, A. & BODELSSON, M. 2010. Elevated plasma levels of antimicrobial polypeptides in patients with severe sepsis. *Journal of innate immunity*, 2, 478-482.
- BESTEBROER, J., DE HAAS, C. J. & VAN STRIJP, J. A. 2010. How microorganisms avoid phagocyte attraction. *FEMS microbiology reviews*, 34, 395-414.

- BIANCHI, M., SIVARAJAN, R., WALLEES, T., HACKENBERG, S. & STEINKE, M. 2021. Susceptibility of primary human airway epithelial cells to Bordetella pertussis adenylate cyclase toxin in two- and three-dimensional culture conditions. *Innate Immunity*, 27, 89-98.
- BIEBER, K. & AUTENRIETH, S. E. 2020. Dendritic cell development in infection. *Mol Immunol*, 121, 111-117.
- BINGLE, C. D., WILSON, K., LUNN, H., BARNES, F. A., HIGH, A. S., WALLACE, W. A., RASSL, D., CAMPOS, M. A., RIBEIRO, M., BINGLE, L. J. H. & BIOLOGY, C. 2010. Human LPLUNC1 is a secreted product of goblet cells and minor glands of the respiratory and upper aerodigestive tracts. 133, 505-515.
- BINGLE, L., CROSS, S. S., HIGH, A. S., WALLACE, W. A., RASSL, D., YUAN, G., HELLSTROM, I., CAMPOS, M. A. & BINGLE, C. D. 2006. WFDC2 (HE4): a potential role in the innate immunity of the oral cavity and respiratory tract and the development of adenocarcinomas of the lung. *Respir Res*, 7, 61.
- BLACK, R. E., COUSENS, S., JOHNSON, H. L., LAWN, J. E., RUDAN, I., BASSANI, D. G., JHA, P., CAMPBELL, H., WALKER, C. F., CIBULSKIS, R., EISELE, T., LIU, L. & MATHERS, C. 2010. Global, regional, and national causes of child mortality in 2008: a systematic analysis. *Lancet*, 375, 1969-87.
- BOERS, J. E., AMBERGEN, A. W. & THUNNISSEN, F. B. 1998. Number and proliferation of basal and parabasal cells in normal human airway epithelium. *American journal of respiratory and critical care medicine*, 157, 2000-2006.
- BOLDOCK, E., SUREWAARD, B. G., SHAMARINA, D., NA, M., FEI, Y., ALI, A., WILLIAMS, A., POLLITT, E. J., SZKUTA, P. & MORRIS, P. 2018. Human skin commensals augment Staphylococcus aureus pathogenesis. *Nature microbiology*, 3, 881-890.
- BONSER, L. R. & ERLE, D. J. 2017. Airway mucus and asthma: the role of MUC5AC and MUC5B. *Journal of clinical medicine*, 6, 112.
- BOONPIYATHAD, T., SÖZENER, Z. C., SATITSUKSANO, P. & AKDIS, C. A. Immunologic mechanisms in asthma. *Seminars in immunology*, 2019. Elsevier, 101333.
- BORSINI, A., DI BENEDETTO, M. G., GIACOBBE, J. & PARIANTE, C. M. 2020. Pro-And anti-inflammatory properties of interleukin in vitro: relevance for major depression and human hippocampal neurogenesis. *International Journal of Neuropsychopharmacology*, 23, 738-750.
- BOSCH, L., DE HAAN, J. J., BASTEMEIJER, M., VAN DER BURG, J., VAN DER WORP, E., WESSELING, M., VIOLA, M., ODILLE, C., EL AZZOZI, H. & PASTERKAMP, G. 2021. The transverse aortic constriction heart failure animal model: a systematic review and meta-analysis. *Heart failure reviews*, 26, 1515-1524.
- BRACHTL, G., POUPARDIN, R., HOCHMANN, S., RANINGER, A., JÜRCHOTT, K., STREITZ, M., SCHLICKEISER, S., OELLER, M., WOLF, M. & SCHALLMOSER, K. 2022. Batch Effects during Human Bone Marrow Stromal Cell Propagation Prevail Donor Variation and Culture Duration: Impact on Genotype, Phenotype and Function. *Cells*, 11, 946.
- BRUBAKER, S. W., BONHAM, K. S., ZANONI, I. & KAGAN, J. C. J. A. R. O. I. 2015. Innate immune pattern recognition: a cell biological perspective. 33, 257-290.
- BURKE, M. C., LI, F.-Q., CYGE, B., ARASHIRO, T., BRECHBUHL, H. M., CHEN, X., SILLER, S. S., WEISS, M. A., O'CONNELL, C. B. & LOVE, D. J. J. C. B. 2014. Chibby promotes ciliary vesicle formation and basal body docking during airway cell differentiation. 207, 123-137.
- BUSTAMANTE-MARIN, X. M. & OSTROWSKI, L. E. 2017. Cilia and mucociliary clearance. *Cold Spring Harbor perspectives in biology*, 9, a028241.
- BUSTIN, S., DHILLON, H. S., KIRVELL, S., GREENWOOD, C., PARKER, M., SHIPLEY, G. L. & NOLAN, T. J. C. C. 2015. Variability of the reverse transcription step: practical implications. 61, 202-212.
- BUTLER, C. R., HYND, R. E., GOWERS, K. H., LEE, D. D. H., BROWN, J. M., CROWLEY, C., TEIXEIRA, V. H., SMITH, C. M., URBANI, L. & HAMILTON, N. J. 2016. Rapid expansion of human epithelial

- stem cells suitable for airway tissue engineering. *American journal of respiratory and critical care medicine*, 194, 156-168.
- BUTTON, B., CAI, L. H., EHRE, C., KESIMER, M., HILL, D. B., SHEEHAN, J. K., BOUCHER, R. C. & RUBINSTEIN, M. 2012. A periciliary brush promotes the lung health by separating the mucus layer from airway epithelia. *Science*, 337, 937-41.
- CALLAGHAN, P. J., FERRICK, B., RYBAKOVSKY, E., THOMAS, S. & MULLIN, J. M. 2020. Epithelial barrier function properties of the 16HBE14o-human bronchial epithelial cell culture model. *Bioscience reports*, 40.
- CALLAHAN, V., HAWKS, S., CRAWFORD, M. A., LEHMAN, C. W., MORRISON, H. A., IVESTER, H. M., AKHRYMUK, I., BOGHDEH, N., FLOR, R., FINKIELSTEIN, C. V., ALLEN, I. C., WEGER-LUCARELLI, J., DUGGAL, N., HUGHES, M. A. & KEHN-HALL, K. 2021. The Pro-Inflammatory Chemokines CXCL9, CXCL10 and CXCL11 Are Upregulated Following SARS-CoV-2 Infection in an AKT-Dependent Manner. *Viruses*, 13.
- CAMPOS, M. A., ABREU, A. R., NLEND, M. C., COBAS, M. A., CONNER, G. E. & WHITNEY, P. L. 2004. Purification and characterization of PLUNC from human tracheobronchial secretions. *Am J Respir Cell Mol Biol*, 30, 184-92.
- CARSETTI, R., ZAFFINA, S., PIANO MORTARI, E., TERRERI, S., CORRENTE, F., CAPPONI, C., PALOMBA, P., MIRABELLA, M., CASCIOLI, S. & PALANGE, P. 2020. Different innate and adaptive immune responses to SARS-CoV-2 infection of asymptomatic, mild, and severe cases. *Frontiers in immunology*, 11, 3365.
- CAVAILLON, J.-M. 2003. Proinflammatory and anti-inflammatory cytokines as mediators of Gram-negative sepsis. *Cytokines and chemokines in infectious diseases handbook*. Springer.
- CHEN, G., KORFHAGEN, T. R., XU, Y., KITZMILLER, J., WERT, S. E., MAEDA, Y., GREGORIEFF, A., CLEVERS, H. & WHITSETT, J. A. 2009. SPDEF is required for mouse pulmonary goblet cell differentiation and regulates a network of genes associated with mucus production. *J Clin Invest*, 119, 2914-24.
- CHEN, Q., YANG, Y., PAN, Y., SHEN, L., ZHANG, Y., ZHENG, F., SHU, Q. & FANG, X. 2022. Human Neutrophil Defensins Disrupt Liver Interendothelial Junctions and Aggravate Sepsis. *Mediators of inflammation*, 2022.
- CHEUNG, G. Y. C., BAE, J. S. & OTTO, M. 2021. Pathogenicity and virulence of *Staphylococcus aureus*. *Virulence*, 12, 547-569.
- CHOI, J. R., YONG, K. W., CHOI, J. Y. & COWIE, A. C. 2020. Single-cell RNA sequencing and its combination with protein and DNA analyses. *Cells*, 9, 1130.
- CLAESSON-WELSH, L., DEJANA, E. & MCDONALD, D. M. 2021. Permeability of the endothelial barrier: identifying and reconciling controversies. *Trends in molecular medicine*, 27, 314-331.
- COHN, L., ELIAS, J. A. & CHUPP, G. L. 2004. Asthma: mechanisms of disease persistence and progression. *Annu. Rev. Immunol.*, 22, 789-815.
- COLE, B. B., SMITH, R. W., JENKINS, K. M., GRAHAM, B. B., REYNOLDS, P. R. & REYNOLDS, S. D. 2010. Tracheal basal cells: a facultative progenitor cell pool. *The American journal of pathology*, 177, 362-376.
- CONG, J. & WEI, H. 2019. Natural Killer Cells in the Lungs. *Front Immunol*, 10, 1416.
- COOK, P. C. & MACDONALD, A. S. 2016. Dendritic cells in lung immunopathology. *Semin Immunopathol*, 38, 449-60.
- CRAVEN, R. R., GAO, X., ALLEN, I. C., GRIS, D., BUBECK WARDENBURG, J., MCELVANIA-TEKIPPE, E., TING, J. P. & DUNCAN, J. A. 2009. *Staphylococcus aureus* alpha-hemolysin activates the NLRP3-inflammasome in human and mouse monocytic cells. *PLoS One*, 4, e7446.
- CRUZ, A. R., BENTLAGE, A. E., BLONK, R., DE HAAS, C. J., AERTS, P. C., SCHEEPMAKER, L. M., BOUWMEESTER, I. G., LUX, A., VAN STRIJP, J. A. & NIMMERJAHN, F. 2022. Staphylococcal protein A inhibits IgG-mediated phagocytosis by blocking the interaction of IgGs with FcγRs and FcRn.

- CURRAN, D. R. & COHN, L. 2010. Advances in mucous cell metaplasia: a plug for mucus as a therapeutic focus in chronic airway disease. *American journal of respiratory cell and molecular biology*, 42, 268-275.
- DA SILVA, M. C., ZAHM, J.-M., GRAS, D., BAJOLET, O., ABELY, M., HINNRSKY, J., MILLIOT, M., DE ASSIS, M. C., HOLOGNE, C. & BONNET, N. 2004. Dynamic interaction between airway epithelial cells and *Staphylococcus aureus*. *American Journal of Physiology-Lung Cellular and Molecular Physiology*, 287, L543-L551.
- DAVIS, A. S., CHERTOW, D. S., MOYER, J. E., SUZICH, J., SANDOUK, A., DORWARD, D. W., LOGUN, C., SHELHAMER, J. H. & TAUBENBERGER, J. K. 2015. Validation of normal human bronchial epithelial cells as a model for influenza A infections in human distal trachea. *Journal of Histochemistry & Cytochemistry*, 63, 312-328.
- DAVIS, J. D. & WYPYCH, T. P. 2021. Cellular and functional heterogeneity of the airway epithelium. *Mucosal Immunology*, 1-13.
- DE JONGE, H. J., FEHRMANN, R. S., DE BONT, E. S., HOFSTRA, R. M., GERBENS, F., KAMPS, W. A., DE VRIES, E. G., VAN DER ZEE, A. G., TE MEERMAN, G. J. & TER ELST, A. J. P. O. 2007. Evidence based selection of housekeeping genes. 2, e898.
- DE VOR, L., ROOIJAKKERS, S. H. & VAN STRIJP, J. A. 2020. Staphylococci evade the innate immune response by disarming neutrophils and forming biofilms. *FEBS letters*, 594, 2556-2569.
- DEAN, C. H. & SNELGROVE, R. J. 2018. New rules for club development: new insights into human small airway epithelial club cell ontogeny and function. American Thoracic Society.
- DELAVERIS, C. S., WEBSTER, E. R., BANIK, S. M., BOXER, S. G. & BERTOZZI, C. R. 2020. Membrane-tethered mucin-like polypeptides sterically inhibit binding and slow fusion kinetics of influenza A virus. *Proceedings of the National Academy of Sciences*, 117, 12643-12650.
- DELEO, F. R., OTTO, M., KREISWIRTH, B. N. & CHAMBERS, H. F. 2010. Community-associated methicillin-resistant *Staphylococcus aureus*. *Lancet*, 375, 1557-68.
- DELGADO, O., KAISANI, A. A., SPINOLA, M., XIE, X.-J., BATTEN, K. G., MINNA, J. D., WRIGHT, W. E. & SHAY, J. W. 2011. Multipotent capacity of immortalized human bronchial epithelial cells. *PloS one*, 6, e22023.
- DEPLANCHE, M., MOUHALI, N., NGUYEN, M. T., CAUTY, C., EZAN, F., DIOT, A., RAULIN, L., DUTERTRE, S., LANGOUET, S., LEGEMBRE, P., TAIEB, F., OTTO, M., LAURENT, F., GÖTZ, F., LE LOIR, Y. & BERKOVA, N. 2019. *Staphylococcus aureus* induces DNA damage in host cell. *Sci Rep*, 9, 7694.
- DERYCKE, L., PÉREZ-NOVO, C., VAN CROMBRUGGEN, K., CORRIVEAU, M.-N. & BACHERT, C. 2010. *Staphylococcus aureus* and chronic airway disease. *World Allergy Organization Journal*, 3, 223-228.
- DICKINSON, J. D., ALEVY, Y., MALVIN, N. P., PATEL, K. K., GUNSTEN, S. P., HOLTZMAN, M. J., STAPPENBECK, T. S. & BRODY, S. L. 2016. IL13 activates autophagy to regulate secretion in airway epithelial cells. *Autophagy*, 12, 397-409.
- DIVYAKOLU, S., CHIKKALA, R., RATNAKAR, K. S. & SRITHARAN, V. 2019. Hemolysins of *Staphylococcus aureus*—An update on their biology, role in pathogenesis and as targets for anti-virulence therapy. *Advances in Infectious Diseases*, 9, 80-104.
- DOMÍNGUEZ-ANDRÉS, J., JOOSTEN, L. A. & NETEA, M. G. 2019. Induction of innate immune memory: the role of cellular metabolism. *Current opinion in immunology*, 56, 10-16.
- DORAN, E., CAI, F., HOLWEG, C. T. J., WONG, K., BRUMM, J. & ARRON, J. R. 2017. Interleukin-13 in Asthma and Other Eosinophilic Disorders. *Front Med (Lausanne)*, 4, 139.
- DUAN, W., CEN, Y., LIN, C., OUYANG, H., DU, K., KUMAR, A., WANG, B., AVOLIO, J., GRASEMANN, H. & MORAES, T. J. 2021. Inflammatory epithelial cytokines after in vitro respiratory syncytial viral infection are associated with reduced lung function. *ERJ open research*, 7.
- DUCKWORTH, C. A. 2021. Identifying key regulators of the intestinal stem cell niche. *Biochemical Society Transactions*, 49, 2163-2176.

- DVORAK, A., TILLEY, A. E., SHAYKHIEV, R., WANG, R. & CRYSTAL, R. G. 2011. Do airway epithelium air-liquid cultures represent the in vivo airway epithelium transcriptome? *American journal of respiratory cell and molecular biology*, 44, 465-473.
- EENJES, E., MERTENS, T. C., BUSCOP-VAN KEMPEN, M. J., VAN WIJCK, Y., TAUBE, C., ROTTIER, R. J. & HIEMSTRA, P. S. 2018. A novel method for expansion and differentiation of mouse tracheal epithelial cells in culture. *Scientific reports*, 8, 1-12.
- EICHSTAEDT, S., GÄBLER, K., BELOW, S., MÜLLER, C., KOHLER, C., ENGELMANN, S., HILDEBRANDT, P., VÖLKER, U., HECKER, M. & HILDEBRANDT, J.-P. 2009. Effects of Staphylococcus aureus-hemolysin A on calcium signalling in immortalized human airway epithelial cells. *Cell calcium*, 45, 165-176.
- ELKHATIB, W. F., HAIR, P. S., NYALWIDHE, J. O. & CUNNION, K. M. 2015. New potential role of serum apolipoprotein E mediated by its binding to clumping factor A during Staphylococcus aureus invasive infections to humans. *J Med Microbiol*, 64, 335-343.
- ETTER, D., CORTI, S., SPIRIG, S., CERNELA, N., STEPHAN, R. & JOHLER, S. 2020. Staphylococcus aureus population structure and genomic profiles in asymptomatic carriers in Switzerland. *Frontiers in Microbiology*, 11, 1289.
- EVAVOLD, C. L. & KAGAN, J. C. 2018. How Inflammasomes Inform Adaptive Immunity. *J Mol Biol*, 430, 217-237.
- FAHY, J. V. & DICKEY, B. F. 2010. Airway mucus function and dysfunction. *New England journal of medicine*, 363, 2233-2247.
- FALUGI, F., KIM, H. K., MISSIAKAS, D. M. & SCHNEEWIND, O. 2013. Role of protein A in the evasion of host adaptive immune responses by Staphylococcus aureus. *mBio*, 4, e00575-13.
- FARAGE, M. & MAIBACH, H. 2006. The vulva: anatomy, physiology, and pathology. New York, NY: Informa Healthcare USA. Inc.
- FARNSWORTH, C. W., SCHOTT, E. M., JENSEN, S. E., ZUKOSKI, J., BENVIE, A. M., REFAAI, M. A., KATES, S. L., SCHWARZ, E. M., ZUSCIK, M. J. & GILL, S. R. 2017. Adaptive upregulation of clumping factor A (ClfA) by Staphylococcus aureus in the obese, type 2 diabetic host mediates increased virulence. *Infection and immunity*, 85, e01005-16.
- FAVOINO, E., PRETE, M., CATAACCHIO, G., RUSCITTI, P., NAVARINI, L., GIACOMELLI, R. & PEROSA, F. 2021. Working and safety profiles of JAK/STAT signaling inhibitors. Are these small molecules also smart? *Autoimmunity Reviews*, 20, 102750.
- FEYRTER, F. 1954. Argyrophilia of bright cell system in bronchial tree in man. *Zeitschrift für mikroskopisch-anatomische Forschung*, 61, 73-81.
- FIRACATIVE, C. 2020. Invasive fungal disease in humans: are we aware of the real impact? *Memórias do Instituto Oswaldo Cruz*, 115.
- FLANNAGAN, R. S., HEIT, B. & HEINRICHS, D. E. 2015. Antimicrobial mechanisms of macrophages and the immune evasion strategies of Staphylococcus aureus. *Pathogens*, 4, 826-868.
- FLANNAGAN, R. S., HEIT, B. & HEINRICHS, D. E. 2016. Intracellular replication of Staphylococcus aureus in mature phagolysosomes in macrophages precedes host cell death, and bacterial escape and dissemination. *Cellular microbiology*, 18, 514-535.
- FOSTER, T. J. 2016. The remarkably multifunctional fibronectin binding proteins of Staphylococcus aureus. *Eur J Clin Microbiol Infect Dis*, 35, 1923-1931.
- FOURNIER, B. & PHILPOTT, D. J. 2005. Recognition of Staphylococcus aureus by the innate immune system. *Clinical microbiology reviews*, 18, 521-540.
- FOWLER, J., VINALL, L. & SWALLOW, D. 2001. Polymorphism of the human muc genes. *Frontiers in Bioscience-Landmark*, 6, 1207-1215.
- FOX, P. G., SCHIAVETTI, F., RAPPUOLI, R., MCLOUGHLIN, R. M. & BAGNOLI, F. 2021. Staphylococcal Protein A Induces Leukocyte Necrosis by Complexing with Human Immunoglobulins. *Mbio*, 12, e00899-21.
- FULCHER, M. L., GABRIEL, S., BURNS, K. A., YANKASKAS, J. R. & RANDELL, S. H. 2005. Well-differentiated human airway epithelial cell cultures. *Human cell culture protocols*. Springer.

- FULCHER, M. L., GABRIEL, S. E., OLSEN, J. C., TATREAU, J. R., GENTZSCH, M., LIVANOS, E., SAAVEDRA, M. T., SALMON, P. & RANDELL, S. H. 2009. Novel human bronchial epithelial cell lines for cystic fibrosis research. *American Journal of Physiology-Lung Cellular and Molecular Physiology*, 296, L82-L91.
- GANDHI, N. A., PIROZZI, G. & GRAHAM, N. M. 2017. Commonality of the IL-4/IL-13 pathway in atopic diseases. *Expert review of clinical immunology*, 13, 425-437.
- GANJIAN, H., RAJPUT, C., ELZOHEIRY, M. & SAJJAN, U. 2020. Rhinovirus and Innate Immune Function of Airway Epithelium. *Front Cell Infect Microbiol*, 10, 277.
- GARIBAY-CERDENARES, O., HERNANDEZ-RAMIREZ, V., OSORIO-TRUJILLO, J., GALLARDO-RINCON, D. & TALAMAS-ROHANA, P. 2015. Haptoglobin and CCR2 receptor expression in ovarian cancer cells that were exposed to ascitic fluid: exploring a new role of haptoglobin in the tumoral microenvironment. *Cell Adhesion & Migration*, 9, 394-405.
- GEROVAC, B. J., FREGIEN, N. L. J. A. J. O. R. C. & BIOLOGY, M. 2016. IL-13 inhibits multicilin expression and ciliogenesis via janus kinase/signal transducer and activator of transcription independently of Notch cleavage. 54, 554-561.
- GEROVAC, B. J., VALENCIA, M., BAUMLIN, N., SALATHE, M., CONNER, G. E. & FREGIEN, N. L. 2014. Submersion and hypoxia inhibit ciliated cell differentiation in a notch-dependent manner. *American journal of respiratory cell and molecular biology*, 51, 516-525.
- GERSEMANN, M., BECKER, S., NUDING, S., ANTONI, L., OTT, G., FRITZ, P., OUE, N., YASUI, W., WEHKAMP, J. & STANGE, E. F. 2012. Olfactomedin-4 is a glycoprotein secreted into mucus in active IBD. *Journal of Crohn's and Colitis*, 6, 425-434.
- GHAREBAGHI, R., HEIDARY, F., MORADI, M. & PARVIZI, M. 2020. Metronidazole; a Potential Novel Addition to the COVID-19 Treatment Regimen. *Arch Acad Emerg Med*, 8, e40.
- GHORANI-AZAM, A., RIAHI-ZANJANI, B. & BALALI-MOOD, M. 2016. Effects of air pollution on human health and practical measures for prevention in Iran. *Journal of research in medical sciences: the official journal of Isfahan University of Medical Sciences*, 21.
- GILLETTE, D. D., SHAH, P. A., CREMER, T., GAVRILIN, M. A., BESECKER, B. Y., SARKAR, A., KNOELL, D. L., CORMET-BOYAKA, E., WEWERS, M. D. & BUTCHAR, J. P. 2013. Analysis of human bronchial epithelial cell proinflammatory response to Burkholderia cenocepacia infection: inability to secrete IL-1 β . *Journal of Biological Chemistry*, 288, 3691-3695.
- GIUFFRIDA, P., CAPRIOLI, F., FACCIOTTI, F. & DI SABATINO, A. 2019. The role of interleukin-13 in chronic inflammatory intestinal disorders. *Autoimmunity reviews*, 18, 549-555.
- GNANAMANI, A., HARIHARAN, P. & PAUL-SATYASEELA, M. 2017. Staphylococcus aureus: Overview of bacteriology, clinical diseases, epidemiology, antibiotic resistance and therapeutic approach. *Frontiers in Staphylococcus aureus*, 4, 28.
- GOMI, K., ARBELAEZ, V., CRYSTAL, R. G. & WALTERS, M. S. J. P. O. 2015. Activation of NOTCH1 or NOTCH3 signaling skews human airway basal cell differentiation toward a secretory pathway. 10, e0116507.
- GORDON, S. & PLÜDDEMANN, A. 2018. Macrophage clearance of apoptotic cells: a critical assessment. *Frontiers in immunology*, 9, 127.
- GOUR, N. & WILLS-KARP, M. 2015. IL-4 and IL-13 signaling in allergic airway disease. *Cytokine*, 75, 68-78.
- GOVINDARAJAN, B. & GIPSON, I. K. 2010. Membrane-tethered mucins have multiple functions on the ocular surface. *Experimental eye research*, 90, 655-663.
- GRAHAM, C. L. B., NEWMAN, H., GILLETT, F. N., SMART, K., BRIGGS, N., BANZHAF, M. & ROPER, D. I. 2021. A Dynamic Network of Proteins Facilitate Cell Envelope Biogenesis in Gram-Negative Bacteria. *Int J Mol Sci*, 22.
- GREENBERG, J. A., HRUSCH, C. L., JAFFERY, M. R., DAVID, M. Z., DAUM, R. S., HALL, J. B., KRESS, J. P., SPERLING, A. I. & VERHOEF, P. A. 2018. Distinct T-helper cell responses to Staphylococcus aureus bacteremia reflect immunologic comorbidities and correlate with mortality. *Critical care*, 22, 1-13.

- GRIBBEN, K., WYSS, A., POOLE, J., FARAZI, P., WICHMAN, C., RICHARDS-BARBER, M., BEANE FREEMAN, L., HENNEBERGER, P., UMBACH, D. & LONDON, S. 2022. CC16 polymorphisms in asthma, asthma subtypes, and asthma control in adults from the Agricultural Lung Health Study. *Respiratory Research*, 23, 1-11.
- GUILLOT, L., NATHAN, N., TABARY, O., THOUVENIN, G., LE ROUZIC, P., CORVOL, H., AMSELEM, S. & CLEMENT, A. 2013. Alveolar epithelial cells: master regulators of lung homeostasis. *Int J Biochem Cell Biol*, 45, 2568-73.
- GÜNTHER, J. & SEYFERT, H.-M. The first line of defence: insights into mechanisms and relevance of phagocytosis in epithelial cells. *Seminars in immunopathology*, 2018. Springer, 555-565.
- HACKETT, N. R., SHAYKHIEV, R., WALTERS, M. S., WANG, R., ZWICK, R. K., FERRIS, B., WITOVER, B., SALIT, J. & CRYSTAL, R. G. 2011. The human airway epithelial basal cell transcriptome. *PLoS one*, 6, e18378.
- HÅHEIM, L. L. 2020. Epithelial cilia is the first line of defence against Coronavirus; addressing the observed age-gradient in the COVID-19 infection. *Medical Hypotheses*, 143, 110064.
- HAIR, P. S., ECHAGUE, C. G., SHOLL, A. M., WATKINS, J. A., GEOGHEGAN, J. A., FOSTER, T. J. & CUNNION, K. M. 2010. Clumping factor A interaction with complement factor I increases C3b cleavage on the bacterial surface of *Staphylococcus aureus* and decreases complement-mediated phagocytosis. *Infect Immun*, 78, 1717-27.
- HAITCHI, H. M., YOSHISUE, H., RIBBENE, A., WILSON, S. J., HOLLOWAY, J. W., BUCCHIERI, F., HANLEY, N. A., WILSON, D. I., ZUMMO, G. & HOLGATE, S. T. J. E. R. J. 2009. Chronological expression of ciliated bronchial epithelium 1 during pulmonary development.
- HANCOCK, R. E., HANEY, E. F. & GILL, E. E. 2016. The immunology of host defence peptides: beyond antimicrobial activity. *Nature Reviews Immunology*, 16, 321-334.
- HAQUE, M., SARTELLI, M., MCKIMM, J. & BAKAR, M. A. 2018. Health care-associated infections—an overview. *Infection and drug resistance*, 11, 2321.
- HARKINS, C. P., PETTIGREW, K. A., ORAVCOVÁ, K., GARDNER, J., HEARN, R. R., RICE, D., MATHER, A. E., PARKHILL, J., BROWN, S. J. & PROBY, C. M. 2018. The microevolution and epidemiology of *Staphylococcus aureus* colonization during atopic eczema disease flare. *Journal of Investigative Dermatology*, 138, 336-343.
- HASAN, S., SEBO, P. & OSICKA, R. 2018. A guide to polarized airway epithelial models for studies of host–pathogen interactions. *The FEBS journal*, 285, 4343-4358.
- HEUKELS, P., MOOR, C. C., VON DER THÜSEN, J. H., WIJSENBEK, M. S. & KOOL, M. 2019. Inflammation and immunity in IPF pathogenesis and treatment. *Respir Med*, 147, 79-91.
- HEWITT, R. J. & LLOYD, C. M. 2021. Regulation of immune responses by the airway epithelial cell landscape. *Nature Reviews Immunology*, 21, 347-362.
- HIEMSTRA, P. S., GROOTAERS, G., VAN DER DOES, A. M., KRUL, C. A. & KOOTER, I. M. 2018. Human lung epithelial cell cultures for analysis of inhaled toxicants: Lessons learned and future directions. *Toxicology in vitro*, 47, 137-146.
- HIEMSTRA, P. S., TETLEY, T. D. & JANES, S. M. 2019. Airway and alveolar epithelial cells in culture. *European Respiratory Journal*, 54.
- HILLIGAN, K. L. & RONCHESE, F. 2020. Antigen presentation by dendritic cells and their instruction of CD4+ T helper cell responses. *Cellular & molecular immunology*, 17, 587-599.
- HILLYER, P., SHEPARD, R., UEHLING, M., KRENZ, M., SHEIKH, F., THAYER, K. R., HUANG, L., YAN, L., PANDA, D. & LUONGO, C. 2018. Differential responses by human respiratory epithelial cell lines to respiratory syncytial virus reflect distinct patterns of infection control. *Journal of virology*, 92, e02202-17.
- HOGAN, B. L., BARKAUSKAS, C. E., CHAPMAN, H. A., EPSTEIN, J. A., JAIN, R., HSIA, C. C., NIKLASON, L., CALLE, E., LE, A. & RANDELL, S. H. 2014. Repair and regeneration of the respiratory system: complexity, plasticity, and mechanisms of lung stem cell function. *Cell stem cell*, 15, 123-138.
- HOLLENHORST, M. I., JURASTOW, I., NANDIGAMA, R., APPENZELLER, S., LI, L., VOGEL, J., WIEDERHOLD, S., ALTHAUS, M., EMPTING, M., ALTMÜLLER, J., HIRSCH, A. K. H., FLOCKERZI,

- V., CANNING, B. J., SALIBA, A. E. & KRASTEVA-CHRIST, G. 2020. Tracheal brush cells release acetylcholine in response to bitter tastants for paracrine and autocrine signaling. *Faseb j*, 34, 316-332.
- HORANI, A., NATH, A., WASSERMAN, M. G., HUANG, T. & BRODY, S. L. 2013. Rho-associated protein kinase inhibition enhances airway epithelial Basal-cell proliferation and lentivirus transduction. *American journal of respiratory cell and molecular biology*, 49, 341-347.
- HSIA, C. C., HYDE, D. M. & WEIBEL, E. R. 2016. Lung structure and the intrinsic challenges of gas exchange. *Comprehensive Physiology*, 6, 827.
- HSU, B.-M., CHEN, J.-S., LIN, I., HSU, G.-J., KONER, S., HUSSAIN, B., HUANG, S.-W. & TSAI, H.-C. 2021. Molecular and Anti-Microbial Resistance (AMR) Profiling of Methicillin-Resistant Staphylococcus aureus (MRSA) from Hospital and Long-Term Care Facilities (LTCF) Environment. *Antibiotics*, 10, 748.
- HUITEMA, L., PHILLIPS, T., ALEXEEV, V., TOMIC-CANIC, M., PASTAR, I. & IGOUCHEVA, O. 2021. Intracellular escape strategies of Staphylococcus aureus in persistent cutaneous infections. *Exp Dermatol*, 30, 1428-1439.
- HURLEY, M. N. 2018. Staphylococcus aureus in cystic fibrosis: problem bug or an innocent bystander? : Eur Respiratory Soc.
- HYNDS, R. E., BONFANTI, P. & JANES, S. M. 2018a. Regenerating human epithelia with cultured stem cells: feeder cells, organoids and beyond. *EMBO molecular medicine*, 10, 139-150.
- HYNDS, R. E., GOWERS, K. H., NIGRO, E., BUTLER, C. R., BONFANTI, P., GIANGRECO, A., PRÊLE, C. M. & JANES, S. M. 2018b. Cross-talk between human airway epithelial cells and 3T3-J2 feeder cells involves partial activation of human MET by murine HGF. *PLoS One*, 13, e0197129.
- ITALIANI, P. & BORASCHI, D. 2017. Induction of innate immune memory by engineered nanoparticles: a hypothesis that may become true. *Frontiers in Immunology*, 8, 734.
- IWASAKI, A. & MEDZHITOV, R. 2015. Control of adaptive immunity by the innate immune system. *Nature immunology*, 16, 343-353.
- JACKSON, N. D., EVERMAN, J. L., CHIOCCIOLI, M., FERIANI, L., GOLDFARB MUREN, K. C., SAJUTHI, S. P., RIOS, C. L., POWELL, R., ARMSTRONG, M. & GOMEZ, J. 2020. Single-cell and population transcriptomics reveal pan-epithelial remodeling in type 2-high asthma. *Cell reports*, 32, 107872.
- JAGUIN, M., HOULBERT, N., FARDEL, O. & LECUREUR, V. 2013. Polarization profiles of human M-CSF-generated macrophages and comparison of M1-markers in classically activated macrophages from GM-CSF and M-CSF origin. *Cellular immunology*, 281, 51-61.
- JAIN, R., BARKAUSKAS, C. E., TAKEDA, N., BOWIE, E. J., AGHAJANIAN, H., WANG, Q., PADMANABHAN, A., MANDERFIELD, L. J., GUPTA, M. & LI, D. 2015. Plasticity of Hopx⁺ type I alveolar cells to regenerate type II cells in the lung. *Nature communications*, 6, 1-11.
- JAMIESON, K. C., WIEHLER, S., MICHI, A. N. & PROUD, D. 2020. Rhinovirus induces Basolateral release of IL-17C in highly differentiated airway epithelial cells. *Frontiers in Cellular and Infection Microbiology*, 10, 103.
- JANEWAY JR, C. A. & MEDZHITOV, R. 2002. Innate immune recognition. *Annual review of immunology*, 20, 197-216.
- JENUL, C. & HORSWILL, A. R. 2019. Regulation of Staphylococcus aureus virulence. *Microbiology spectrum*, 7, 7.2. 29.
- JIANG, D., SCHAEFER, N. & CHU, H. W. 2018. Air-liquid interface culture of human and mouse airway epithelial cells. *Lung Innate Immunity and Inflammation*. Springer.
- JIANG, X. 2018. Silencing of heart and neural crest derivatives expressed transcript 2 attenuates transforming growth factor- β 1-enhanced apoptosis of human bronchial epithelial cells. *Oncology Letters*, 16, 4997-5005.
- JIN, L., HU, S., TU, T., HUANG, Z., TANG, Q., MA, J., WANG, X., LI, X., ZHOU, X. & SHUAI, S. 2018. Global long noncoding RNA and mRNA expression changes between prenatal and neonatal lung tissue in pigs. *Genes*, 9, 443.

- JIN, T., MOHAMMAD, M., PULLERITS, R. & ALI, A. 2021. Bacteria and host interplay in staphylococcus aureus septic arthritis and sepsis. *Pathogens*, 10, 158.
- JOHNSON, D. C. 2011. Airway mucus function and dysfunction. *N Engl J Med*, 364, 978; author reply 978.
- JONES, E., SHENG, J., CARLSON, J. & WANG, S. 2021. Aging-induced fragility of the immune system. *Journal of theoretical biology*, 510, 110473.
- JUNTILA, I. S. 2018. Tuning the cytokine responses: an update on interleukin (IL)-4 and IL-13 receptor complexes. *Frontiers in immunology*, 9, 888.
- KAISANI, A., DELGADO, O., FASCIANI, G., KIM, S. B., WRIGHT, W. E., MINNA, J. D. & SHAY, J. W. 2014. Branching morphogenesis of immortalized human bronchial epithelial cells in three-dimensional culture. *Differentiation*, 87, 119-126.
- KALAFATI, L., HATZIOANNOU, A., HAJISHENGALLIS, G. & CHAVAKIS, T. 2022. The role of neutrophils in trained immunity. *Immunological Reviews*.
- KANASHIRO, A., HIROKI, C. H., DA FONSECA, D. M., BIRBRAIR, A., FERREIRA, R. G., BASSI, G. S., FONSECA, M. D., KUSUDA, R., CEBINELLI, G. C. M., DA SILVA, K. P., WANDERLEY, C. W., MENEZES, G. B., ALVES-FIHO, J. C., OLIVEIRA, A. G., CUNHA, T. M., PUPO, A. S., ULLOA, L. & CUNHA, F. Q. 2020. The role of neutrophils in neuro-immune modulation. *Pharmacol Res*, 151, 104580.
- KAPPELMAYER, J. & NAGY, B., JR. 2017. The Interaction of Selectins and PSGL-1 as a Key Component in Thrombus Formation and Cancer Progression. *Biomed Res Int*, 2017, 6138145.
- KARAUZUM, H. & DATTA, S. K. 2017. Adaptive Immunity Against Staphylococcus aureus. *Curr Top Microbiol Immunol*, 409, 419-439.
- KAUR, B. P. & SECORD, E. 2019. Innate immunity. *Pediatric Clinics*, 66, 905-911.
- KE, Y., REDDEL, R. R., GERWIN, B. I., MIYASHITA, M., MCMENAMIN, M., LECHNER, J. F. & HARRIS, C. C. 1988. Human bronchial epithelial cells with integrated SV40 virus T antigen genes retain the ability to undergo squamous differentiation. *Differentiation*, 38, 60-6.
- KETTLE, R., SIMMONS, J., SCHINDLER, F., JONES, P., DICKER, T., DUBOIS, G., GIDDINGS, J., VAN HEEKE, G. & JONES, C. E. 2010. Regulation of neuregulin 1 β -induced MUC5AC and MUC5B expression in human airway epithelium. *American journal of respiratory cell and molecular biology*, 42, 472-481.
- KIEDROWSKI, M. R. & BOMBERGER, J. M. 2018. Viral-bacterial co-infections in the cystic fibrosis respiratory tract. *Frontiers in immunology*, 9, 3067.
- KIEDROWSKI, M. R., PAHARIK, A. E., ACKERMANN, L. W., SHELTON, A. U., SINGH, S. B., STARNER, T. D. & HORSWILL, A. R. 2016. Development of an in vitro colonization model to investigate Staphylococcus aureus interactions with airway epithelia. *Cellular microbiology*, 18, 720-732.
- KIM, J., KIM, B. E., AHN, K. & LEUNG, D. Y. 2019. Interactions between atopic dermatitis and Staphylococcus aureus infection: clinical implications. *Allergy, asthma & immunology research*, 11, 593-603.
- KIM, S. J., CHANG, J. & SINGH, M. 2015. Peptidoglycan architecture of Gram-positive bacteria by solid-state NMR. *Biochim Biophys Acta*, 1848, 350-62.
- KING, N. E., SUZUKI, S., BARILLA, C., HAWKINS, F. J., RANDELL, S. H., REYNOLDS, S. D., STRIPP, B. R. & DAVIS, B. R. 2020. Correction of airway stem cells: genome editing approaches for the treatment of cystic fibrosis. *Human Gene Therapy*, 31, 956-972.
- KLEVENS, R. M., MORRISON, M. A., NADLE, J., PETIT, S., GERSHMAN, K., RAY, S., HARRISON, L. H., LYNFIELD, R., DUMYATI, G., TOWNES, J. M., CRAIG, A. S., ZELL, E. R., FOSHEIM, G. E., MCDUGAL, L. K., CAREY, R. B. & FRIDKIN, S. K. 2007. Invasive methicillin-resistant Staphylococcus aureus infections in the United States. *Jama*, 298, 1763-71.
- KOAY, T. W., OSTERHOF, C., ORLANDO, I. M., KEPPNER, A., ANDRE, D., YOUSEFIAN, S., ALONSO, M. S., CORREIA, M., MARKWORTH, R. & SCHÖDEL, J. 2021. Androglobin gene expression patterns and FOXJ1-dependent regulation indicate its functional association with ciliogenesis. *Journal of Biological Chemistry*, 296.

- KOKELJ, S., ÖSTLING, J., GEORGI, B., FROMELL, K., EKDAHL, K. N., OLSSON, H. K. & OLIN, A.-C. 2021. Smoking induces sex-specific changes in the small airway proteome. *Respiratory research*, 22, 1-17.
- KOO, J. S., YOON, J.-H., GRAY, T., NORFORD, D., JETTEN, A. M. & NETTESHEIM, P. 1999. Restoration of the mucous phenotype by retinoic acid in retinoid-deficient human bronchial cell cultures: changes in mucin gene expression. *American Journal of Respiratory Cell and Molecular Biology*, 20, 43-52.
- KORSUN, N., ANGELOVA, S., TRIFONOVA, I., GEORGIEVA, I., VOLEVA, S., TZOTCHEVA, I., MILEVA, S., IVANOV, I., TCHERVENIAKOVA, T. & PERENOVSKA, P. 2019. Viral pathogens associated with acute lower respiratory tract infections in children younger than 5 years of age in Bulgaria. *Brazilian Journal of Microbiology*, 50, 117-125.
- KOTTON, D. N. & MORRISEY, E. E. 2014. Lung regeneration: mechanisms, applications and emerging stem cell populations. *Nature medicine*, 20, 822-832.
- KREDA, S. M., DAVIS, C. W. & ROSE, M. C. 2012. CFTR, mucins, and mucus obstruction in cystic fibrosis. *Cold Spring Harbor perspectives in medicine*, 2, a009589.
- KRISHNA, S. & MILLER, L. S. 2012. Host-pathogen interactions between the skin and *Staphylococcus aureus*. *Curr Opin Microbiol*, 15, 28-35.
- KRISMER, B., LIEBEKE, M., JANEK, D., NEGA, M., RAUTENBERG, M., HORNIG, G., UNGER, C., WEIDENMAIER, C., LALK, M. & PESCHEL, A. 2014. Nutrient Limitation Governs *Staphylococcus aureus* Metabolism and Niche Adaptation in the Human Nose. *PLOS Pathogens*, 10, e1003862.
- KUBELKOVA, K. & MACELA, A. 2019. Innate immune recognition: an issue more complex than expected. *Frontiers in cellular and infection microbiology*, 9, 241.
- KUEK, L. E. & LEE, R. J. 2020. First contact: the role of respiratory cilia in host-pathogen interactions in the airways. *American Journal of Physiology-Lung Cellular and Molecular Physiology*, 319, L603-L619.
- KUMAR, N., DAVID, M. Z., BOYLE-VAVRA, S., SIETH, J. & DAUM, R. S. 2015. High *Staphylococcus aureus* colonization prevalence among patients with skin and soft tissue infections and controls in an urban emergency department. *Journal of clinical microbiology*, 53, 810-815.
- KUMPITSCH, C., KOSKINEN, K., SCHÖPF, V. & MOISSEL-EICHINGER, C. 2019. The microbiome of the upper respiratory tract in health and disease. *BMC biology*, 17, 1-20.
- LAARMAN, A. J., MIJNHEER, G., MOOTZ, J. M., VAN ROOIJEN, W. J., RUYKEN, M., MALONE, C. L., HEEZIUS, E. C., WARD, R., MILLIGAN, G. & VAN STRIJP, J. A. 2012. *Staphylococcus aureus* Staphopain A inhibits CXCR2-dependent neutrophil activation and chemotaxis. *The EMBO journal*, 31, 3607-3619.
- LAFFORGUE, O., PONCET, S., SEYSSIECQ, I. & FAVIER, J. Rheological characterization of macromolecular colloidal gels as simulant of bronchial mucus. AIP Conference Proceedings, 2017. AIP Publishing LLC, 110003.
- LAM, J. H., SMITH, F. L. & BAUMGARTH, N. 2020. B cell activation and response regulation during viral infections. *Viral immunology*, 33, 294-306.
- LAM, M., LAMANNA, E. & BOURKE, J. E. 2019. Regulation of airway smooth muscle contraction in health and disease. *Smooth Muscle Spontaneous Activity*, 381-422.
- LAMBRECHT, B. N., HAMMAD, H. & FAHY, J. V. 2019. The cytokines of asthma. *Immunity*, 50, 975-991.
- LANGHANS, S. A. 2018. Three-Dimensional in Vitro Cell Culture Models in Drug Discovery and Drug Repositioning. *Front Pharmacol*, 9, 6.
- LECHNER, J. F., HAUGEN, A., MCCLENDON, I. A. & WARD PETTIS, E. 1982. Clonal growth of normal adult human bronchial epithelial cells in a serum-free medium. *In vitro*, 18, 633-642.
- LEE, A. S., DE LENCASTRE, H., GARAU, J., KLUYTMANS, J., MALHOTRA-KUMAR, S., PESCHEL, A. & HARBARTH, S. 2018a. Methicillin-resistant *Staphylococcus aureus*. *Nature reviews Disease primers*, 4, 1-23.

- LEE, B., MOON, K. M. & KIM, C. Y. 2018b. Tight junction in the intestinal epithelium: its association with diseases and regulation by phytochemicals. *Journal of immunology research*, 2018.
- LEEMAN, M., CHOI, J., HANSSON, S., STORM, M. U. & NILSSON, L. 2018. Proteins and antibodies in serum, plasma, and whole blood—size characterization using asymmetrical flow field-flow fractionation (AF4). *Analytical and bioanalytical chemistry*, 410, 4867-4873.
- LESIMPLE, P., VAN SEUNINGEN, I., BUISINE, M.-P., COPIN, M.-C., HINZ, M., HOFFMANN, W., HAJJ, R., BRODY, S. L., CORAUX, C. & PUCHELLE, E. 2007. Trefoil factor family 3 peptide promotes human airway epithelial ciliated cell differentiation. *American journal of respiratory cell and molecular biology*, 36, 296-303.
- LEVINSON, W. 2014. *Review of medical microbiology and immunology*, McGraw-Hill Education.
- LI, Z., LEVAST, B. & MADRENAS, J. 2017. Staphylococcus aureus Downregulates IP-10 Production and Prevents Th1 Cell Recruitment. *J Immunol*, 198, 1865-1874.
- LIMOLI, D. H. & HOFFMAN, L. R. 2019. Help, hinder, hide and harm: what can we learn from the interactions between Pseudomonas aeruginosa and Staphylococcus aureus during respiratory infections? *Thorax*, 74, 684-692.
- LIN, W.-H. W., TSAY, A. J., LALIME, E. N., PEKOSZ, A. & GRIFFIN, D. E. 2021. Primary differentiated respiratory epithelial cells respond to apical measles virus infection by shedding multinucleated giant cells. *Proceedings of the National Academy of Sciences*, 118.
- LIU, H., PERLMAN, H., PAGLIARI, L. J. & POPE, R. M. 2001. Constitutively activated Akt-1 is vital for the survival of human monocyte-differentiated macrophages: role of Mcl-1, independent of nuclear factor (NF)- κ B, Bad, or caspase activation. *Journal of Experimental Medicine*, 194, 113-126.
- LIU, M., GUO, S., HIBBERT, J. M., JAIN, V., SINGH, N., WILSON, N. O. & STILES, J. K. 2011. CXCL10/IP-10 in infectious diseases pathogenesis and potential therapeutic implications. *Cytokine & growth factor reviews*, 22, 121-130.
- LIU, X., ORY, V., CHAPMAN, S., YUAN, H., ALBANESE, C., KALLAKURY, B., TIMOFEEVA, O. A., NEALON, C., DAKIC, A., SIMIC, V., HADDAD, B. R., RHIM, J. S., DRITSCHILO, A., RIEGEL, A., MCBRIDE, A. & SCHLEGEL, R. 2012. ROCK inhibitor and feeder cells induce the conditional reprogramming of epithelial cells. *Am J Pathol*, 180, 599-607.
- LIU, Z., LIAO, F., SCOZZI, D., FURUYA, Y., PUGH, K. N., HACHEM, R., CHEN, D. L., CANO, M., GREEN, J. M. & KRUPNICK, A. S. 2019. An obligatory role for club cells in preventing obliterative bronchiolitis in lung transplants. *JCI insight*, 4.
- LIVAK, K. J. & SCHMITTGEN, T. D. 2001. Analysis of relative gene expression data using real-time quantitative PCR and the 2⁻ $\Delta\Delta$ CT method. *methods*, 25, 402-408.
- LONGO, D. M., LOUIE, B., WANG, E., POS, Z., MARINCOLA, F. M., HAWTIN, R. E. & CESANO, A. 2012. Inter-donor variation in cell subset specific immune signaling responses in healthy individuals. *American journal of clinical and experimental immunology*, 1, 1.
- LORENG, T. D. & SMITH, E. F. 2017. The central apparatus of cilia and eukaryotic flagella. *Cold Spring Harbor perspectives in biology*, 9, a028118.
- LOW, D. E. 2013. Toxic shock syndrome: major advances in pathogenesis, but not treatment. *Crit Care Clin*, 29, 651-75.
- LOWY, F. D. 1998. Staphylococcus aureus infections. *New England journal of medicine*, 339, 520-532.
- LUENGEN, A. E., KНИЕBS, C., BUHL, E. M., CORNELISSEN, C. G., SCHMITZ-RODE, T., JOCKENHOEVEL, S. & THIEBES, A. L. 2020. Choosing the right differentiation medium to develop Mucociliary phenotype of primary nasal epithelial cells in vitro. *Scientific reports*, 10, 1-11.
- LUMB, A. B. 2016. *Nunn's applied respiratory physiology eBook*, Elsevier Health Sciences.
- MA, J., RUBIN, B. K. & VOYNOW, J. A. 2018. Mucins, mucus, and goblet cells. *Chest*, 154, 169-176.
- MACINTYRE, C. R., CHUGHTAI, A. A., ZHANG, Y., SEALE, H., YANG, P., CHEN, J., PAN, Y., ZHANG, D. & WANG, Q. 2017. Viral and bacterial upper respiratory tract infection in hospital health care workers over time and association with symptoms. *BMC infectious diseases*, 17, 1-9.

- MACKELLAR, M. & VIGERUST, D. J. 2016. Role of haptoglobin in health and disease: a focus on diabetes. *Clinical Diabetes*, 34, 148-157.
- MAKITA, S., TAKATORI, H. & NAKAJIMA, H. 2021. Post-Transcriptional Regulation of Immune Responses and Inflammatory Diseases by RNA-Binding ZFP36 Family Proteins. *Front Immunol*, 12, 711633.
- MALVIN, N. P., KERN, J. T., LIU, T.-C., BRODY, S. L. & STAPPENBECK, T. S. 2019. Autophagy proteins are required for club cell structure and function in airways. *American Journal of Physiology-Lung Cellular and Molecular Physiology*, 317, L259-L270.
- MARIÑO CRESPO, Ó., CUEVAS ÁLVAREZ, E., HARDING, A. L., MURDOCH, C., FERNÁNDEZ BRIERA, A. & GIL MARTÍN, E. 2019. Haptoglobin expression in human colorectal cancer.
- MARSHALL, J. S., WARRINGTON, R., WATSON, W. & KIM, H. L. 2018. An introduction to immunology and immunopathology. *Allergy, Asthma & Clinical Immunology*, 14, 1-10.
- MARTINEZ-ANTON, A., SOKOLOWSKA, M., KERN, S., DAVIS, A. S., ALSAATY, S., TAUBENBERGER, J. K., SUN, J., CAI, R., DANNER, R. L. & EBERLEIN, M. 2013. Changes in microRNA and mRNA expression with differentiation of human bronchial epithelial cells. *American journal of respiratory cell and molecular biology*, 49, 384-395.
- MARTINOVICH, K. M., IOSIFIDIS, T., BUCKLEY, A. G., LOOI, K., LING, K.-M., SUTANTO, E. N., KICIC-STARCEVICH, E., GARRATT, L. W., SHAW, N. C. & MONTGOMERY, S. 2017. Conditionally reprogrammed primary airway epithelial cells maintain morphology, lineage and disease specific functional characteristics. *Scientific reports*, 7, 1-13.
- MAURIZI, E., ADAMO, D., MAGRELLI, F. M., GALAVERNI, G., ATTICO, E., MERRA, A., MAFFEZZONI, M. B. R., LOSI, L., GENNA, V. G. & SCEBERRAS, V. 2021. Regenerative Medicine of Epithelia: Lessons From the Past and Future Goals. *Frontiers in Bioengineering and Biotechnology*, 9, 193.
- MCGUINNESS, W. A., KOBAYASHI, S. D. & DELEO, F. R. 2016. Evasion of Neutrophil Killing by *Staphylococcus aureus*. *Pathogens*, 5.
- MCNEIL, J. C., FLORES, A. R., KAPLAN, S. L. & HULTEN, K. G. 2021. The indirect impact of the SARS-CoV-2 pandemic on invasive group A *Streptococcus*, *Streptococcus Pneumoniae* and *Staphylococcus Aureus* infections in Houston area children. *The Pediatric Infectious Disease Journal*, 40, e313-e316.
- MEDINA, L. M. P., BECKER, A.-K., MICHALIK, S., YEDAVALLY, H., RAINERI, E. J., HILDEBRANDT, P., SALAZAR, M. G., SURMANN, K., PFÖRTNER, H. & MEKONNEN, S. A. 2019. Metabolic cross-talk between human bronchial epithelial cells and internalized *Staphylococcus aureus* as a driver for infection. *Molecular & Cellular Proteomics*, 18, 892-908.
- METERSKY, M. L., AKSAMIT, T. R., BARKER, A., CHOATE, R., DALEY, C. L., DANIELS, L. A., DIMANGO, A., EDEN, E., GRIFFITH, D., JOHNSON, M., KNOWLES, M., O'DONNELL, A. E., OLIVIER, K., SALATHE, M., THOMASHOW, B., TINO, G., TURINO, G., WINTHROP, K. L. & MANNINO, D. 2018. The Prevalence and Significance of *Staphylococcus aureus* in Patients with Non-Cystic Fibrosis Bronchiectasis. *Ann Am Thorac Soc*, 15, 365-370.
- MILLER, A. J. & SPENCE, J. R. 2017. In vitro models to study human lung development, disease and homeostasis. *Physiology*, 32, 246-260.
- MINDAYE, S. T., ILYUSHINA, N. A., FANTONI, G., ALTERMAN, M. A., DONNELLY, R. P. & EICHELBERGER, M. C. 2017. Impact of influenza A virus infection on the proteomes of human bronchoepithelial cells from different donors. *Journal of proteome research*, 16, 3287-3297.
- MKRTCHYAN, H. V., XU, Z., YACOUB, M., TER-STEPANYAN, M. M., KARAPETYAN, H. D., KEARNS, A. M., CUTLER, R. R., PICHON, B. & HAMBARDZUMYAN, A. D. 2017. Detection of diverse genotypes of Methicillin-resistant *Staphylococcus aureus* from hospital personnel and the environment in Armenia. *Antimicrob Resist Infect Control*, 6, 19.
- MOHAMED, A. A. & ALAWNA, M. 2020. Role of increasing the aerobic capacity on improving the function of immune and respiratory systems in patients with coronavirus (COVID-19): A review. *Diabetes Metab Syndr*, 14, 489-496.

- MONTGOMERY, C. P., BOYLE-VAVRA, S. & DAUM, R. S. 2010. Importance of the global regulators Agr and SaeRS in the pathogenesis of CA-MRSA USA300 infection. *PLoS One*, 5, e15177.
- MONTGOMERY, C. P., DANIELS, M., ZHAO, F., ALEGRE, M.-L., CHONG, A. S. & DAUM, R. S. 2014. Protective immunity against recurrent *Staphylococcus aureus* skin infection requires antibody and interleukin-17A. *Infection and immunity*, 82, 2125-2134.
- MONTORO, D. T., HABER, A. L., BITON, M., VINARSKY, V., LIN, B., BIRKET, S. E., YUAN, F., CHEN, S., LEUNG, H. M. & VILLORIA, J. J. N. 2018. A revised airway epithelial hierarchy includes CFTR-expressing ionocytes. 560, 319.
- MOOKHERJEE, N., ANDERSON, M. A., HAAGSMAN, H. P. & DAVIDSON, D. J. 2020. Antimicrobial host defence peptides: functions and clinical potential. *Nature reviews Drug discovery*, 19, 311-332.
- MOREILHON, C., GRAS, D., HOLOGNE, C., BAJOLET, O., COTTREZ, F., MAGNONE, V., MERTEN, M., GROUX, H., PUCHELLE, E. & BARBRY, P. 2005. Live *Staphylococcus aureus* and bacterial soluble factors induce different transcriptional responses in human airway cells. *Physiological genomics*, 20, 244-255.
- MORENO-VILLANUEVA, M., FEIVESON, A. H., KRIEGER, S., KAY BRINDA, A., VON SCHEVEN, G., BÜRKLE, A., CRUCIAN, B. & WU, H. 2018. Synergistic effects of weightlessness, isoproterenol, and radiation on DNA damage response and cytokine production in immune cells. *International journal of molecular sciences*, 19, 3689.
- MORETTA, A., SCIEUZO, C., PETRONE, A. M., SALVIA, R., MANNIELLO, M. D., FRANCO, A., LUCCHETTI, D., VASSALLO, A., VOGEL, H., SGAMBATO, A. & FALABELLA, P. 2021. Antimicrobial Peptides: A New Hope in Biomedical and Pharmaceutical Fields. *Front Cell Infect Microbiol*, 11, 668632.
- MORGENE, M. F., BOTELHO-NEVERS, E., GRATTARD, F., PILLET, S., BERTHELOT, P., POZZETTO, B. & VERHOEVEN, P. O. 2018. *Staphylococcus aureus* colonization and non-influenza respiratory viruses: Interactions and synergism mechanisms. *Virulence*, 9, 1354-1363.
- MORRISON, C. B., EDWARDS, C. E., SHAFFER, K. M., ARABA, K. C., WYKOFF, J. A., WILLIAMS, D. R., ASAKURA, T., DANG, H., MORTON, L. C. & GILMORE, R. C. 2022. SARS-CoV-2 infection of airway cells causes intense viral and cell shedding, two spreading mechanisms affected by IL-13. *Proceedings of the National Academy of Sciences*, 119, e2119680119.
- MOU, H., VINARSKY, V., TATA, P. R., BRAZAUSKAS, K., CHOI, S. H., CROOKE, A. K., ZHANG, B., SOLOMON, G. M., TURNER, B. & BIHLER, H. 2016. Dual SMAD signaling inhibition enables long-term expansion of diverse epithelial basal cells. *Cell stem cell*, 19, 217-231.
- MOU, H., YANG, Y., RIEHS, M. A., BARRIOS, J., SHIVARAJU, M., HABER, A. L., MONTORO, D. T., GILMORE, K., HAAS, E. A. & PAUNOVIC, B. 2021. Airway basal stem cells generate distinct subpopulations of PNECs. *Cell reports*, 35, 109011.
- MROCHEN, D. M., FERNANDES DE OLIVEIRA, L. M., RAAFAT, D. & HOLTFRETER, S. 2020. *Staphylococcus aureus* host tropism and its implications for murine infection models. *International journal of molecular sciences*, 21, 7061.
- MUDHUNE, S., WAMAE, M. & REGION, N. S. F. P. D. I. T. E. A. 2009. Report on invasive disease and meningitis due to *Haemophilus influenzae* and *Streptococcus pneumoniae* from the Network for Surveillance of Pneumococcal Disease in the East African Region. *Clinical Infectious Diseases*, 48, S147-S152.
- MUNYE, M. M., SHOEMARK, A., HIRST, R. A., DELHOVE, J. M., SHARP, T. V., MCKAY, T. R., O'CALLAGHAN, C., BAINES, D. L., HOWE, S. J. & HART, S. L. 2017. BMI-1 extends proliferative potential of human bronchial epithelial cells while retaining their mucociliary differentiation capacity. *Am J Physiol Lung Cell Mol Physiol*, 312, L258-L267.
- MURPHY, K. & WEAVER, C. 2016. *Janeway's immunobiology*, Garland Science.
- NAKAUCHI, M., NAGATA, N., TAKAYAMA, I., SAITO, S., KUBO, H., KAIDA, A., OBA, K., ODAGIRI, T. & KAGEYAMA, T. 2019. Propagation of rhinovirus C in differentiated immortalized human airway HBEC3-KT epithelial cells. *Viruses*, 11, 216.

- NARYZHNY, S. & LEGINA, O. 2021. Haptoglobin as a biomarker. *Biomeditsinskaya khimiya*, 67, 105-118.
- NAWROTH, J. C., VAN DER DOES, A. M., RYAN, A. & KANSO, E. 2020. Multiscale mechanics of mucociliary clearance in the lung. *Philosophical Transactions of the Royal Society B*, 375, 20190160.
- NEUPANE, A. S., WILLSON, M., CHOJNACKI, A. K., CASTANHEIRA, F. V. E. S., MOREHOUSE, C., CARESTIA, A., KELLER, A. E., PEISELER, M., DIGIANDOMENICO, A. & KELLY, M. M. 2020. Patrolling alveolar macrophages conceal bacteria from the immune system to maintain homeostasis. *Cell*, 183, 110-125. e11.
- NGUYEN, H.-H., TRAN, B.-T., MULLER, W. & JACK, R. S. 2012. IL-10 acts as a developmental switch guiding monocyte differentiation to macrophages during a murine peritoneal infection. *The Journal of Immunology*, 189, 3112-3120.
- NIE, X., KITAOKA, S., TANAKA, K., SEGI-NISHIDA, E., IMOTO, Y., OGAWA, A., NAKANO, F., TOMOHIRO, A., NAKAYAMA, K. & TANIGUCHI, M. 2018. The innate immune receptors TLR2/4 mediate repeated social defeat stress-induced social avoidance through prefrontal microglial activation. *Neuron*, 99, 464-479. e7.
- NIKOLIĆ, M. Z., CARITG, O., JENG, Q., JOHNSON, J.-A., SUN, D., HOWELL, K. J., BRADY, J. L., LARESGOITI, U., ALLEN, G. & BUTLER, R. 2017. Human embryonic lung epithelial tips are multipotent progenitors that can be expanded in vitro as long-term self-renewing organoids. *Elife*, 6, e26575.
- NOGUCHI, M., FURUKAWA, K. T. & MORIMOTO, M. 2020. Pulmonary neuroendocrine cells: physiology, tissue homeostasis and disease. *Disease models & mechanisms*, 13, dmm046920.
- O'BOYLE, N., SUTHERLAND, E., BERRY, C. C. & DAVIES, R. L. 2018. Optimisation of growth conditions for ovine airway epithelial cell differentiation at an air-liquid interface. *PLoS One*, 13, e0193998.
- O'CALLAGHAN, R. J. 2018. The Pathogenesis of Staphylococcus aureus Eye Infections. *Pathogens*, 7.
- O'HALLORAN, D. P., WYNNE, K. & GEOGHEGAN, J. A. 2015. Protein A is released into the Staphylococcus aureus culture supernatant with an unprocessed sorting signal. *Infect Immun*, 83, 1598-609.
- OHLSEN, K., DANDEKAR, G., SCHWARZ, R. & DANDEKAR, T. 2008. New trends in pharmacogenomic strategies against resistance development in microbial infections. *Pharmacogenomics*, 9, 1711-23.
- OKUDA, K., DANG, H., KOBAYASHI, Y., CARRARO, G., NAKANO, S., CHEN, G., KATO, T., ASAKURA, T., GILMORE, R. C., MORTON, L. C., LEE, R. E., MASCENIK, T., YIN, W. N., BARBOSA CARDENAS, S. M., O'NEAL, Y. K., MINNICK, C. E., CHUA, M., QUINNEY, N. L., GENTZSCH, M., ANDERSON, C. W., GHIO, A., MATSUI, H., NAGASE, T., OSTROWSKI, L. E., GRUBB, B. R., OLSEN, J. C., RANDELL, S. H., STRIPP, B. R., TATA, P. R., O'NEAL, W. K. & BOUCHER, R. C. 2021. Secretory Cells Dominate Airway CFTR Expression and Function in Human Airway Superficial Epithelia. *Am J Respir Crit Care Med*, 203, 1275-1289.
- ONYIAH, J. C. & COLGAN, S. P. 2016. Cytokine responses and epithelial function in the intestinal mucosa. *Cellular and Molecular Life Sciences*, 73, 4203-4212.
- OSTEDGAARD, L. S., MONINGER, T. O., MCMENIMEN, J. D., SAWIN, N. M., PARKER, C. P., THORNELL, I. M., POWERS, L. S., GANSEMER, N. D., BOUZEK, D. C., COOK, D. P., MEYERHOLZ, D. K., ABOU ALAIWA, M. H., STOLTZ, D. A. & WELSH, M. J. 2017. Gel-forming mucins form distinct morphologic structures in airways. *Proceedings of the National Academy of Sciences*, 114, 6842-6847.
- OUADAH, Y., ROJAS, E. R., RIORDAN, D. P., CAPOSTAGNO, S., KUO, C. S. & KRASNOW, M. A. 2019. Rare Pulmonary Neuroendocrine Cells Are Stem Cells Regulated by Rb, p53, and Notch. *Cell*, 179, 403-416.e23.
- PAGET, C. & TROTTEIN, F. 2013. Role of type 1 natural killer T cells in pulmonary immunity. *Mucosal Immunol*, 6, 1054-67.

- PALMA MEDINA, L. M., BECKER, A.-K., MICHALIK, S., SURMANN, K., HILDEBRANDT, P., GESELL SALAZAR, M., MEKONNEN, S. A., KADERALI, L., VÖLKER, U. & VAN DIJL, J. M. 2020. Interaction of *Staphylococcus aureus* and host cells upon infection of bronchial epithelium during different stages of regeneration. *ACS infectious diseases*, 6, 2279-2290.
- PARK, I.-K., MORRISON, S. J. & CLARKE, M. F. J. T. J. O. C. I. 2004. Bmi1, stem cells, and senescence regulation. 113, 175-179.
- PARK, Y.-H., KIM, D., DAI, J. & ZHANG, Z. 2015. Human bronchial epithelial BEAS-2B cells, an appropriate in vitro model to study heavy metals induced carcinogenesis. *Toxicology and applied pharmacology*, 287, 240-245.
- PARKER, D. & PRINCE, A. Immunopathogenesis of *Staphylococcus aureus* pulmonary infection. *Seminars in immunopathology*, 2012. Springer, 281-297.
- PARKUNAN, S. M., RANDALL, C. B., ASTLEY, R. A., FURTADO, G. C., LIRA, S. A. & CALLEGAN, M. C. 2016. CXCL1, but not IL-6, significantly impacts intraocular inflammation during infection. *Journal of leukocyte biology*, 100, 1125-1134.
- PAULI, N. T., KIM, H. K., FALUGI, F., HUANG, M., DULAC, J., HENRY DUNAND, C., ZHENG, N. Y., KAUR, K., ANDREWS, S. F., HUANG, Y., DEDENT, A., FRANK, K. M., CHARNOT-KATSIKAS, A., SCHNEEWIND, O. & WILSON, P. C. 2014. *Staphylococcus aureus* infection induces protein A-mediated immune evasion in humans. *J Exp Med*, 211, 2331-9.
- PELZEK, A. J., SHOPSIN, B., RADKE, E. E., TAM, K., UEBERHEIDE, B. M., FENYÖ, D., BROWN, S. M., LI, Q., RUBIN, A. & FULMER, Y. 2018. Human memory B cells targeting *Staphylococcus aureus* exotoxins are prevalent with skin and soft tissue infection. *MBio*, 9, e02125-17.
- PENA, R. T., BLASCO, L., AMBROA, A., GONZÁLEZ-PEDRAJO, B., FERNÁNDEZ-GARCÍA, L., LÓPEZ, M., BLERIOT, I., BOU, G., GARCÍA-CONTRERAS, R. & WOOD, T. K. 2019. Relationship between quorum sensing and secretion systems. *Frontiers in microbiology*, 10, 1100.
- PETERS-HALL, J. R., COQUELIN, M. L., TORRES, M. J., LARANGER, R., ALABI, B. R., SHO, S., CALVA-MORENO, J. F., THOMAS, P. J., SHAY, J. W. J. A. J. O. P.-L. C. & PHYSIOLOGY, M. 2018. Long-term Culture and Cloning of Primary Human Bronchial Basal Cells that Maintain Multipotent Differentiation Capacity and CFTR Channel Function.
- PICKENS, C. I. & WUNDERINK, R. G. 2022. Methicillin-Resistant *Staphylococcus aureus* Hospital-Acquired Pneumonia/Ventilator-Associated Pneumonia. *Semin Respir Crit Care Med*.
- PIDWILL, G. R., GIBSON, J. F., COLE, J., RENSHAW, S. A. & FOSTER, S. J. 2021. The role of macrophages in *Staphylococcus aureus* infection. *Frontiers in Immunology*, 3506.
- PIETROCOLA, G., NOBILE, G., RINDI, S. & SPEZIALE, P. 2017. *Staphylococcus aureus* Manipulates Innate Immunity through Own and Host-Expressed Proteases. *Front Cell Infect Microbiol*, 7, 166.
- PILIPONSKY, A. M. & ROMANI, L. 2018. The contribution of mast cells to bacterial and fungal infection immunity. *Immunological reviews*, 282, 188-197.
- PIPER, S. N. C., FERGUSON, J., KAY, L., PARKER, L. C., SABROE, I., SLEEMAN, M. A., BRIEND, E. & FINCH, D. K. 2013. The role of interleukin-1 and interleukin-18 in pro-inflammatory and anti-viral responses to rhinovirus in primary bronchial epithelial cells. *PLoS One*, 8, e63365.
- PLASSCHAERT, L. W., ŽILIONIS, R., CHOO-WING, R., SAVOVA, V., KNEHR, J., ROMA, G., KLEIN, A. M. & JAFFE, A. B. 2018. A single-cell atlas of the airway epithelium reveals the CFTR-rich pulmonary ionocyte. *Nature*, 560, 377-381.
- PLEUGER, C., LEHTI, M. S., COOPER, M., O'CONNOR, A. E., MERRINER, D. J., SMYTH, I. M., COTTLE, D. L., FIETZ, D., BERGMANN, M. & O'BRYAN, M. K. 2019. CBE1 is a manchette-and mitochondria-associated protein with a potential role in somatic cell proliferation. *Endocrinology*, 160, 2573-2586.
- PRASAD, S. V., FIEDORUK, K., DANILUK, T., PIKTEL, E. & BUCKI, R. 2019. Expression and function of host defense peptides at inflammation sites. *International journal of molecular sciences*, 21, 104.

- PROVIDENCE, K. M., HIGGINS, S. P., MULLEN, A., BATTISTA, A., SAMARAKOON, R., HIGGINS, C. E., WILKINS-PORT, C. E. & HIGGINS, P. J. 2008. SERPINE1 (PAI-1) is deposited into keratinocyte migration "trails" and required for optimal monolayer wound repair. *Archives of Dermatological Research*, 300, 303-310.
- PUNDIR, P., LIU, R., VASAVDA, C., SERHAN, N., LIMJUNYAWONG, N., YEE, R., ZHAN, Y., DONG, X., WU, X. & ZHANG, Y. 2019. A connective tissue mast-cell-specific receptor detects bacterial quorum-sensing molecules and mediates antibacterial immunity. *Cell host & microbe*, 26, 114-122. e8.
- RAJAN, D., MCCRACKEN, C. E., KOPLEMANN, H. B., KYU, S. Y., LEE, F. E.-H., LU, X. & ANDERSON, L. J. 2014. Human rhinovirus induced cytokine/chemokine responses in human airway epithelial and immune cells. *PLoS One*, 9, e114322.
- RAJPUT, C., HAN, M., ISHIKAWA, T., LEI, J., GOLDSMITH, A. M., JAZAERI, S., STROUPE, C. C., BENTLEY, J. K. & HERSHENSON, M. B. 2021. Rhinovirus C infection induces type 2 innate lymphoid cell expansion and eosinophilic airway inflammation. *Frontiers in immunology*, 12, 649520.
- RAMIREZ, R. D., SHERIDAN, S., GIRARD, L., SATO, M., KIM, Y., POLLACK, J., PEYTON, M., ZOU, Y., KURIE, J. M., DIMAIO, J. M., MILCHGRUB, S., SMITH, A. L., SOUZA, R. F., GILBEY, L., ZHANG, X., GANDIA, K., VAUGHAN, M. B., WRIGHT, W. E., GAZDAR, A. F., SHAY, J. W. & MINNA, J. D. 2004. Immortalization of human bronchial epithelial cells in the absence of viral oncoproteins. *Cancer Res*, 64, 9027-34.
- RANDELL, S. H., WALSTAD, D. L., SCHWAB, U. E., GRUBB, B. R. & YANKASKAS, J. R. 2001. Isolation and culture of airway epithelial cells from chronically infected human lungs. *In Vitro Cellular & Developmental Biology-Animal*, 37, 480-489.
- RANDOLPH, G. J. 2011. No need to coax monocytes. *Science*, 332, 1268-1269.
- RAO, D. A. 2018. T Cells That Help B Cells in Chronically Inflamed Tissues. *Front Immunol*, 9, 1924.
- RAO, V., THAKUR, S., RAO, J., ARAKERI, G., BRENNAN, P. A., JADHAV, S., SAYEED, M. S. & RAO, G. 2020. Mesenchymal stem cells-bridge catalyst between innate and adaptive immunity in COVID 19. *Med Hypotheses*, 143, 109845.
- RAWLINS, E. L., OKUBO, T., XUE, Y., BRASS, D. M., AUTEN, R. L., HASEGAWA, H., WANG, F. & HOGAN, B. L. 2009. The role of Scgb1a1+ Clara cells in the long-term maintenance and repair of lung airway, but not alveolar, epithelium. *Cell Stem Cell*, 4, 525-34.
- RAYNER, R. E., MAKENA, P., PRASAD, G. L. & CORMET-BOYAKA, E. 2019. Optimization of normal human bronchial epithelial (NHBE) cell 3D cultures for in vitro lung model studies. *Scientific reports*, 9, 1-10.
- REAME, N. K. 2020. Toxic Shock Syndrome and Tampons: The Birth of a Movement and a Research 'Vagenda'. *The Palgrave Handbook of Critical Menstruation Studies*, 687-703.
- REDEGELD, F. A., YU, Y., KUMARI, S., CHARLES, N. & BLANK, U. 2018. Non-IgE mediated mast cell activation. *Immunological reviews*, 282, 87-113.
- REINER, R. C., WELGAN, C. A., CASEY, D. C., TROEGER, C. E., BAUMANN, M. M., NGUYEN, Q. P., SWARTZ, S. J., BLACKER, B. F., DESHPANDE, A., MOSSER, J. F., OSGOOD-ZIMMERMAN, A. E., EARL, L., MARCZAK, L. B., MUNRO, S. B., MILLER-PETRIE, M. K., RODGERS KEMP, G., FROSTAD, J., WIENS, K. E., LINDSTEDT, P. A., PIGOTT, D. M., DWYER-LINDGREN, L., ROSS, J. M., BURSTEIN, R., GRAETZ, N., RAO, P. C., KHALIL, I. A., DAVIS WEAVER, N., RAY, S. E., DAVIS, I., FARAG, T., BRADY, O. J., KRAEMER, M. U. G., SMITH, D. L., BHATT, S., WEISS, D. J., GETHING, P. W., KASSEBAUM, N. J., MOKDAD, A. H., MURRAY, C. J. L. & HAY, S. I. 2019. Identifying residual hotspots and mapping lower respiratory infection morbidity and mortality in African children from 2000 to 2017. *Nat Microbiol*, 4, 2310-2318.
- REYNOLDS, S. D., REYNOLDS, P. R., PRYHUBER, G. S., FINDER, J. D., STRIPP, B. R. J. A. J. O. R. & MEDICINE, C. C. 2002. Secretoglobins SCGB3A1 and SCGB3A2 define secretory cell subsets in mouse and human airways. 166, 1498-1509.
- REYNOLDS, S. D., RIOS, C., WESOLOWSKA-ANDERSEN, A., ZHUANG, Y., PINTER, M., HAPPOLDT, C., HILL, C. L., LALLIER, S. W., COSGROVE, G. P., SOLOMON, G. M., NICHOLS, D. P. & SEIBOLD, M.

- A. 2016. Airway Progenitor Clone Formation Is Enhanced by Y-27632-Dependent Changes in the Transcriptome. *Am J Respir Cell Mol Biol*, 55, 323-36.
- RIEDER, S. A., NAGARKATTI, P. & NAGARKATTI, M. 2011. CD1d-independent activation of invariant natural killer T cells by staphylococcal enterotoxin B through major histocompatibility complex class II/T cell receptor interaction results in acute lung injury. *Infect Immun*, 79, 3141-8.
- RIERA ROMO, M., PÉREZ-MARTÍNEZ, D. & CASTILLO FERRER, C. 2016. Innate immunity in vertebrates: an overview. *Immunology*, 148, 125-139.
- RIO, D. C., ARES, M., HANNON, G. J. & NILSEN, T. W. J. C. S. H. P. 2010. Purification of RNA using TRIzol (TRI reagent). 2010, pdb. prot5439.
- ROCHE, F. M., DOWNER, R., KEANE, F., SPEZIALE, P., PARK, P. W. & FOSTER, T. J. 2004. The N-terminal A domain of fibronectin-binding proteins A and B promotes adhesion of *Staphylococcus aureus* to elastin. *J Biol Chem*, 279, 38433-40.
- ROCK, J. R., ONAITIS, M. W., RAWLINS, E. L., LU, Y., CLARK, C. P., XUE, Y., RANDELL, S. H. & HOGAN, B. L. M. 2009. Basal cells as stem cells of the mouse trachea and human airway epithelium. *Proceedings of the National Academy of Sciences*, 106, 12771-12775.
- ROCK, J. R., RANDELL, S. H. & HOGAN, B. L. 2010. Airway basal stem cells: a perspective on their roles in epithelial homeostasis and remodeling. *Disease models & mechanisms*, 3, 545-556.
- ROSALES, C. 2018. Neutrophil: a cell with many roles in inflammation or several cell types? *Frontiers in physiology*, 113.
- ROSENBERG, H. F., DYER, K. D. & FOSTER, P. S. 2013. Eosinophils: changing perspectives in health and disease. *Nature Reviews Immunology*, 13, 9-22.
- ROSS, A. J., DAILEY, L. A., BRIGHTON, L. E., DEVLIN, R. B. J. A. J. O. R. C. & BIOLOGY, M. 2007. Transcriptional profiling of mucociliary differentiation in human airway epithelial cells. 37, 169-185.
- RUIZ GARCÍA, S., DEPREZ, M., LEBRIGAND, K., CAVARD, A., PAQUET, A., ARGUEL, M.-J., MAGNONE, V., TRUCHI, M., CABALLERO, I. & LEROY, S. 2019. Novel dynamics of human mucociliary differentiation revealed by single-cell RNA sequencing of nasal epithelial cultures. *Development*, 146, dev177428.
- RYAN, R., FAILLER, M., REILLY, M. L., GARFA-TRAORE, M., DELOUS, M., FILHOL, E., REBOUL, T., BOLEFEYSOT, C., NITSCHKÉ, P. & BAUDOUIN, V. J. H. M. G. 2017. Functional characterization of tektin-1 in motile cilia and evidence for TEK1 as a new candidate gene for motile ciliopathies. 27, 266-282.
- SAAEELDIN, I. M., TUKUR, H. A., ALJUMAAH, R. S. & SINDI, R. A. 2020. Rocking the Boat: The Decisive Roles of Rho Kinases During Oocyte, Blastocyst, and Stem Cell Development. *Front Cell Dev Biol*, 8, 616762.
- SANTACROCE, L., CHARITOS, I. A., BALLINI, A., INCHINGOLO, F., LUPERTO, P., DE NITTO, E. & TOPI, S. 2020. The human respiratory system and its microbiome at a glimpse. *Biology*, 9, 318.
- SATIR, P. 2005. Tour of organelles through the electron microscope: A reprinting of Keith R. Porter's classic Harvey Lecture with a new introduction. *The Anatomical Record*, 287, 1184-1204.
- SCHILDERS, K. A., EENJES, E., VAN RIET, S., POOT, A. A., STAMATIALIS, D., TRUCKENMÜLLER, R., HIEMSTRA, P. S. & ROTTIER, R. J. 2016. Regeneration of the lung: Lung stem cells and the development of lung mimicking devices. *Respir Res*, 17, 44.
- SCHILLING, E.-M., SCHERER, M. & STAMMINGER, T. 2021. Intrinsic Immune Mechanisms Restricting Human Cytomegalovirus Replication. *Viruses*, 13, 179.
- SCHNEIDER, C., O'LEARY, C. E. & LOCKSLEY, R. M. 2019. Regulation of immune responses by tuft cells. *Nat Rev Immunol*, 19, 584-593.
- SCHOENBRUNNER, N. J., GUPTA, A. P., YOUNG, K. K., WILL, S. G. J. B. M. & PROTOCOLS 2017. Covalent modification of primers improves PCR amplification specificity and yield. 2, bpx011.
- SCHULTE, W., BERNHAGEN, J. & BUCALA, R. 2013. Cytokines in sepsis: potent immunoregulators and potential therapeutic targets--an updated view. *Mediators Inflamm*, 2013, 165974.

- SCHWARTBECK, B., BIRTEL, J., TREFFON, J., LANGHANKI, L., MELLMANN, A., KALE, D., KAHL, J., HIRSCHHAUSEN, N., NEUMANN, C. & LEE, J. C. 2016. Dynamic in vivo mutations within the *ica* operon during persistence of *Staphylococcus aureus* in the airways of cystic fibrosis patients. *PLoS pathogens*, 12, e1006024.
- SCHWARZE, J., HAMELMANN, E., BRADLEY, K. L., TAKEDA, K. & GELFAND, E. W. 1997. Respiratory syncytial virus infection results in airway hyperresponsiveness and enhanced airway sensitization to allergen. *The Journal of clinical investigation*, 100, 226-233.
- SCUDIERI, P., MUSANTE, I., VENTURINI, A., GUIDONE, D., GENOVESE, M., CRESTA, F., CACI, E., PALLESCHI, A., POETA, M., SANTAMARIA, F., CICIRIELLO, F., LUCIDI, V. & GALIETTA, L. J. V. 2020. Ionocytes and CFTR Chloride Channel Expression in Normal and Cystic Fibrosis Nasal and Bronchial Epithelial Cells. *Cells*, 9.
- SEIBOLD, M. A. 2018. Interleukin-13 Stimulation Reveals the Cellular and Functional Plasticity of the Airway Epithelium. *Annals of the American Thoracic Society*, 15, S98-S102.
- SEIBOLD, P., AUVINEN, A., AVERBECK, D., BOURGUIGNON, M., HARTIKAINEN, J. M., HOESCHEN, C., LAURENT, O., NOËL, G., SABATIER, L., SALOMAA, S. & BLETTNER, M. 2020. Clinical and epidemiological observations on individual radiation sensitivity and susceptibility. *Int J Radiat Biol*, 96, 324-339.
- SELL, E. A., ORTIZ-CARPENA, J. F., DE'BROSKI, R. H. & COHEN, N. A. 2021. Tuft cells in the pathogenesis of chronic rhinosinusitis with nasal polyps and asthma. *Annals of Allergy, Asthma & Immunology*, 126, 143-151.
- SHAMBAT, S. M., CHEN, P., HOANG, A. T. N., BERGSTEN, H., VANDENESCH, F., SIEMENS, N., LINA, G., MONK, I. R., FOSTER, T. J. & ARAKERE, G. 2015. Modelling staphylococcal pneumonia in a human 3D lung tissue model system delineates toxin-mediated pathology. *Disease models & mechanisms*, 8, 1413-1425.
- SHARMA-KUINKEL, B. K., MONGODIN, E. F., MYERS, J. R., VORE, K. L., CANFIELD, G. S., FRASER, C. M., RUDE, T. H., FOWLER, V. G., JR. & GILL, S. R. 2015. Potential Influence of *Staphylococcus aureus* Clonal Complex 30 Genotype and Transcriptome on Hematogenous Infections. *Open Forum Infect Dis*, 2, ofv093.
- SHARMA, L., FENG, J., BRITTO, C. J. & DELA CRUZ, C. S. 2020. Mechanisms of Epithelial Immunity Evasion by Respiratory Bacterial Pathogens. *Front Immunol*, 11, 91.
- SHAYKHIEV, R. 2019. Emerging biology of persistent mucous cell hyperplasia in COPD. BMJ Publishing Group Ltd.
- SHINJI, H., YOSIZAWA, Y., TAJIMA, A., IWASE, T., SUGIMOTO, S., SEKI, K. & MIZUNOE, Y. 2011. Role of fibronectin-binding proteins A and B in in vitro cellular infections and in vivo septic infections by *Staphylococcus aureus*. *Infect Immun*, 79, 2215-23.
- SHUKLA, S. D., VANKA, K. S., CHAVELIER, A., SHASTRI, M. D., TAMB UWALA, M. M., BAKSHI, H. A., PABREJA, K., MAHMOOD, M. Q. & O'TOOLE, R. F. 2020. Chronic respiratory diseases: An introduction and need for novel drug delivery approaches. *Targeting Chronic Inflammatory Lung Diseases Using Advanced Drug Delivery Systems*. Elsevier.
- SIDDIQUI, S., JOHANSSON, K., JOO, A., BONSER, L. R., KOH, K. D., LE TONQUEZE, O., BOLOURCHI, S., BAUTISTA, R. A., ZLOCK, L., ROTH, T. L., MARSON, A., BHAKTA, N. R., ANSEL, K. M., FINKBEINER, W. E., ERLE, D. J. & WOODRUFF, P. G. 2021. Epithelial miR-141 regulates IL-13-induced airway mucus production. *JCI Insight*, 6.
- SIMON, A. K., HOLLANDER, G. A. & MCMICHAEL, A. 2015. Evolution of the immune system in humans from infancy to old age. *Proceedings of the Royal Society B: Biological Sciences*, 282, 20143085.
- SINGH, B. K., LI, N., MARK, A. C., MATEO, M., CATTANEO, R. & SINN, P. L. J. J. O. V. 2016. Cell-to-cell contact and nectin-4 govern spread of measles virus from primary human myeloid cells to primary human airway epithelial cells. *JVI*. 00266-16.
- SLEIGH, M. A. 2016. *The Biology of Cilia and Flagella: International Series of Monographs on Pure and Applied Biology: Zoology*, Elsevier.

- SMITH, C., ODD, D., HARWOOD, R., WARD, J., LINNEY, M., CLARK, M., HARGREAVES, D., LADHANI, S. N., DRAPER, E., DAVIS, P. J., KENNY, S. E., WHITTAKER, E., LUYT, K., VINER, R. & FRASER, L. K. 2022. Deaths in children and young people in England after SARS-CoV-2 infection during the first pandemic year. *Nat Med*, 28, 185-192.
- SMITH, E. J., VISAI, L., KERRIGAN, S. W., SPEZIALE, P. & FOSTER, T. J. 2011. The Sbi protein is a multifunctional immune evasion factor of *Staphylococcus aureus*. *Infect Immun*, 79, 3801-9.
- SÖKELAND, G. & SCHUMACHER, U. 2019. The functional role of integrins during intra- and extravasation within the metastatic cascade. *Mol Cancer*, 18, 12.
- SOLANKI, S. S., SINGH, P., KASHYAP, P., SANSI, M. S. & ALI, S. A. 2021. Promising role of defensins peptides as therapeutics to combat against viral infection. *Microbial Pathogenesis*, 155, 104930.
- SOLLBERGER, G., TILLEY, D. O. & ZYCHLINSKY, A. 2018. Neutrophil Extracellular Traps: The Biology of Chromatin Externalization. *Dev Cell*, 44, 542-553.
- SONG, D., CAHN, D. & DUNCAN, G. A. 2020. Mucin biopolymers and their barrier function at airway surfaces. *Langmuir*, 36, 12773-12783.
- SONG, H., YAO, E., LIN, C., GACAYAN, R., CHEN, M. H. & CHUANG, P. T. 2012. Functional characterization of pulmonary neuroendocrine cells in lung development, injury, and tumorigenesis. *Proc Natl Acad Sci U S A*, 109, 17531-6.
- SOONG, G., MARTIN, F. J., CHUN, J., COHEN, T. S., AHN, D. S. & PRINCE, A. 2011. *Staphylococcus aureus* protein A mediates invasion across airway epithelial cells through activation of RhoA GTPase signaling and proteolytic activity. *J Biol Chem*, 286, 35891-35898.
- SORIANO, J. B., KENDRICK, P. J., PAULSON, K. R., GUPTA, V., ABRAMS, E. M., ADEDOYIN, R. A., ADHIKARI, T. B., ADVANI, S. M., AGRAWAL, A. & AHMADIAN, E. 2020. Prevalence and attributable health burden of chronic respiratory diseases, 1990–2017: a systematic analysis for the Global Burden of Disease Study 2017. *The Lancet Respiratory Medicine*, 8, 585-596.
- SPAAN, A. N., REYES-ROBLES, T., BADIOU, C., COCHET, S., BOGUSLAWSKI, K. M., YOONG, P., DAY, C. J., DE HAAS, C. J., VAN KESSEL, K. P., VANDENESCH, F. J. C. H. & MICROBE 2015. *Staphylococcus aureus* targets the Duffy antigen receptor for chemokines (DARC) to lyse erythrocytes. 18, 363-370.
- SPAAN, A. N., SUREWAARD, B. G., NIJLAND, R. & VAN STRIJP, J. A. 2013. Neutrophils versus *Staphylococcus aureus*: a biological tug of war. *Annual review of microbiology*, 67, 629-650.
- STEAD, M. B. & KUSHNER, S. R. 2016. Method for isolating total RNA from cells. Google Patents.
- STEINSTRÄESSER, L., KRANEBURG, U., JACOBSEN, F. & AL-BENNA, S. 2011. Host defense peptides and their antimicrobial-immunomodulatory duality. *Immunobiology*, 216, 322-33.
- STEWART, C. E., TORR, E. E., MOHD JAMILI, N. H., BOSQUILLON, C. & SAYERS, I. 2012. Evaluation of differentiated human bronchial epithelial cell culture systems for asthma research. *Journal of allergy*, 2012.
- STIER, M. T., BLOODWORTH, M. H., TOKI, S., NEWCOMB, D. C., GOLENIIEWSKA, K., BOYD, K. L., QUITALIG, M., HOTARD, A. L., MOORE, M. L. & HARTERT, T. V. 2016. Respiratory syncytial virus infection activates IL-13–producing group 2 innate lymphoid cells through thymic stromal lymphopoietin. *Journal of Allergy and Clinical Immunology*, 138, 814-824. e11.
- STONE, A., QUITTELL, L., ZHOU, J., ALBA, L., BHAT, M., DECELIE-GERMANA, J., RAJAN, S., BONITZ, L., WELTER, J. J., DOZOR, A. J., GHERSON, I., LOWY, F. D. & SAIMAN, L. 2009. *Staphylococcus aureus* nasal colonization among pediatric cystic fibrosis patients and their household contacts. *Pediatr Infect Dis J*, 28, 895-9.
- STRAY-PEDERSEN, A., SORTE, H. S., SAMARAKOON, P., GAMBIN, T., CHINN, I. K., AKDEMIR, Z. H. C., ERICHSEN, H. C., FORBES, L. R., GU, S., YUAN, B. J. J. O. A. & IMMUNOLOGY, C. 2017. Primary immunodeficiency diseases: genomic approaches delineate heterogeneous Mendelian disorders. 139, 232-245.
- STUBBS, J., VLADAR, E., AXELROD, J. & KINTNER, C. J. N. C. B. 2012. Multicilin promotes centriole assembly and ciliogenesis during multiciliate cell differentiation. 14, 140.

- TAM, K. & TORRES, V. J. 2019. Staphylococcus aureus secreted toxins and extracellular enzymes. *Microbiology spectrum*, 7, 7.2. 16.
- TARIQUE, A. A., LOGAN, J., THOMAS, E., HOLT, P. G., SLY, P. D. & FANTINO, E. 2015. Phenotypic, functional, and plasticity features of classical and alternatively activated human macrophages. *American journal of respiratory cell and molecular biology*, 53, 676-688.
- TATA, P. R., MOU, H., PARDO-SAGANTA, A., ZHAO, R., PRABHU, M., LAW, B. M., VINARSKY, V., CHO, J. L., BRETON, S. & SAHAY, A. J. N. 2013. Dedifferentiation of committed epithelial cells into stem cells in vivo. 503, 218.
- TAVARES, T. D., ANTUNES, J. C., PADRÃO, J., RIBEIRO, A. I., ZILLE, A., AMORIM, M. T. P., FERREIRA, F. & FELGUEIRAS, H. P. 2020. Activity of Specialized Biomolecules against Gram-Positive and Gram-Negative Bacteria. *Antibiotics (Basel)*, 9.
- TAYLOR, G., CHOPRA, D. & MATHIEU, P. 1993. Differences in secretory profiles of epithelial cell cultures derived from human tracheal and bronchial mucosa and submucosal glands. *Epithelial cell biology*, 2, 163-169.
- TAYLOR, T. A. & UNAKAL, C. G. 2021. Staphylococcus aureus. *StatPearls [Internet]*.
- TCHATCHOUANG, S., BIGNA, J. J., NZOUANKEU, A., FONKOUA, M.-C., NANSSEU, J. R., NDANGANG, M. S., KENMOE, S., PENLAP, V. B. & NJOUOM, R. 2018. Prevalence of respiratory bacterial infections in people with lower respiratory tract infections in Africa: the BARIAFRICA systematic review and meta-analysis protocol. *BMJ open*, 8, e023592.
- TENG, T.-S., JI, A.-L., JI, X.-Y. & LI, Y.-Z. 2017. Neutrophils and immunity: from bactericidal action to being conquered. *Journal of immunology research*, 2017.
- TILLEY, A. E., WALTERS, M. S., SHAYKHIEV, R. & CRYSTAL, R. G. 2015. Cilia dysfunction in lung disease. *Annual review of physiology*, 77, 379-406.
- TING, H.-A. & VON MOLTKE, J. 2019. The immune function of tuft cells at gut mucosal surfaces and beyond. *The Journal of Immunology*, 202, 1321-1329.
- TORR, E., HEATH, M., MEE, M., SHAW, D., SHARP, T. V. & SAYERS, I. 2016. Expression of polycomb protein BMI-1 maintains the plasticity of basal bronchial epithelial cells. *Physiological Reports*, 4, e12847.
- TOUZELET, O., BROADBENT, L., ARMSTRONG, S. D., ALJABR, W., CLOUTMAN-GREEN, E., POWER, U. F. & HISCOX, J. A. 2020. The secretome profiling of a pediatric airway epithelium infected with hRSV identified aberrant apical/basolateral trafficking and novel immune modulating (CXCL6, CXCL16, CSF3) and antiviral (CEACAM1) proteins. *Molecular & Cellular Proteomics*, 19, 793-807.
- TOWNLEY, R. G., SAPKOTA, M. & SAPKOTA, K. 2011. IL-13 and its genetic variants: effect on current asthma treatments. *Discovery medicine*, 12, 513-523.
- TRABER, K. E., LEE, E., BENSON, S., CORRIGAN, R., CANTERA, M., SHOPSIN, B. & NOVICK, R. P. 2008. agr function in clinical Staphylococcus aureus isolates. *Microbiology (Reading)*, 154, 2265-2274.
- TRAVAGLINI, K. J., NABHAN, A. N., PENLAND, L., SINHA, R., GILLICH, A., SIT, R. V., CHANG, S., CONLEY, S. D., MORI, Y., SEITA, J., BERRY, G. J., SHRAGER, J. B., METZGER, R. J., KUO, C. S., NEFF, N., WEISSMAN, I. L., QUAKE, S. R. & KRASNOW, M. A. 2020. A molecular cell atlas of the human lung from single-cell RNA sequencing. *Nature*, 587, 619-625.
- TROTTEIN, F. & PAGET, C. 2018. Natural Killer T Cells and Mucosal-Associated Invariant T Cells in Lung Infections. *Front Immunol*, 9, 1750.
- TSAO, P.-N., VASCONCELOS, M., IZVOLSKY, K. I., QIAN, J., LU, J. & CARDOSO, W. V. 2009. Notch signaling controls the balance of ciliated and secretory cell fates in developing airways.
- TURNER, J., ROGER, J., FITAU, J., COMBE, D., GIDDINGS, J., HEEKE, G. V. & JONES, C. E. 2011a. Goblet cells are derived from a FOXJ1-expressing progenitor in a human airway epithelium. *American Journal of Respiratory Cell and Molecular Biology*, 44, 276-284.

- TURNER, J., ROGER, J., FITAU, J., COMBE, D., GIDDINGS, J., HEEKE, G. V., JONES, C. E. J. A. J. O. R. C. & BIOLOGY, M. 2011b. Goblet cells are derived from a FOXJ1-expressing progenitor in a human airway epithelium. *44*, 276-284.
- TYNER, J. W., KIM, E. Y., IDE, K., PELLETIER, M. R., ROSWIT, W. T., MORTON, J. D., BATTAILE, J. T., PATEL, A. C., PATTERSON, G. A. & CASTRO, M. 2006. Blocking airway mucous cell metaplasia by inhibiting EGFR antiapoptosis and IL-13 transdifferentiation signals. *The Journal of clinical investigation*, *116*, 309-321.
- UALIYEVA, S., HALLEN, N., KANAOKA, Y., LEDDEROSE, C., MATSUMOTO, I., JUNGER, W. G., BARRETT, N. A. & BANKOVA, L. G. 2020. Airway brush cells generate cysteinyl leukotrienes through the ATP sensor P2Y2. *Sci Immunol*, *5*.
- UEBELE, J., HABENICHT, K., TICHA, O. & BEKEREDJIAN-DING, I. 2020. Staphylococcus aureus Protein A Induces Human Regulatory T Cells Through Interaction With Antigen-Presenting Cells. *Frontiers in immunology*, *11*, 2553.
- ULFIG, A. & LEICHERT, L. I. 2021. The effects of neutrophil-generated hypochlorous acid and other hypohalous acids on host and pathogens. *Cell Mol Life Sci*, *78*, 385-414.
- VAN BELKUM, A. 2016. Hidden Staphylococcus aureus carriage: overrated or underappreciated? *MBio*, *7*, e00079-16.
- VAN CLEEMPUT, J., POELAERT, K. C. K., LAVAL, K., VANDERHEIJDEN, N., DHAENENS, M., DALED, S., BOYEN, F., PASMANS, F. & NAUWYNCK, H. J. 2020. An Alphaherpesvirus Exploits Antimicrobial β -Defensins To Initiate Respiratory Tract Infection. *J Virol*, *94*.
- VAN DEN ELSEN, P. J. 2011. Expression regulation of major histocompatibility complex class I and class II encoding genes. *Front Immunol*, *2*, 48.
- VAN DER DOES, A. M., AMATNGALIM, G. D., KEIJSER, B., HIEMSTRA, P. S. & VILLENAVE, R. 2018. Contribution of host defence proteins and peptides to Host-Microbiota interactions in chronic inflammatory lung diseases. *Vaccines*, *6*, 49.
- VAN LOMMEL, A. 2001. Pulmonary neuroendocrine cells (PNEC) and neuroepithelial bodies (NEB): chemoreceptors and regulators of lung development. *Paediatr Respir Rev*, *2*, 171-6.
- VAUGHAN, M. B., RAMIREZ, R. D., WRIGHT, W. E., MINNA, J. D. & SHAY, J. W. 2006. A three-dimensional model of differentiation of immortalized human bronchial epithelial cells. *Differentiation*, *74*, 141-148.
- VAZ, M., HWANG, S. Y., KAGIAMPAKIS, I., PHALLEN, J., PATIL, A., O'HAGAN, H. M., MURPHY, L., ZAHNOW, C. A., GABRIELSON, E., VELCULESCU, V. E., EASWARAN, H. P. & BAYLIN, S. B. 2017. Chronic Cigarette Smoke-Induced Epigenomic Changes Precede Sensitization of Bronchial Epithelial Cells to Single-Step Transformation by KRAS Mutations. *Cancer Cell*, *32*, 360-376.e6.
- VESTERGAARD, M., FREES, D. & INGMER, H. 2019. Antibiotic resistance and the MRSA problem. *Microbiology spectrum*, *7*, 7.2. 18.
- VILLENAVE, R., SHIELDS, M. D. & POWER, U. F. 2013. Respiratory syncytial virus interaction with human airway epithelium. *Trends in microbiology*, *21*, 238-244.
- VLADAR, E. K. & BRODY, S. L. 2013. Analysis of ciliogenesis in primary culture mouse tracheal epithelial cells. *Methods in enzymology*. Elsevier.
- VOGEL, D. Y., GLIM, J. E., STAVENUITER, A. W., BREUR, M., HEIJNEN, P., AMOR, S., DIJKSTRA, C. D. & BEELEN, R. H. 2014. Human macrophage polarization in vitro: maturation and activation methods compared. *Immunobiology*, *219*, 695-703.
- VU, V. Q. 2011. ggbiplot: A ggplot2 based biplot. R package version 0.55.
- WALDMAN, A. D., FRITZ, J. M. & LENARDO, M. J. 2020. A guide to cancer immunotherapy: from T cell basic science to clinical practice. *Nature Reviews Immunology*, *20*, 651-668.
- WALTERS, M. S., GOMI, K., ASHBRIDGE, B., MOORE, M. A., ARBELAEZ, V., HELDRICH, J., DING, B.-S., RAFII, S., STAUDT, M. R. & CRYSTAL, R. G. 2013. Generation of a human airway epithelium derived basal cell line with multipotent differentiation capacity. *Respiratory research*, *14*, 1-18.

- WANG, G., LOU, H. H., SALIT, J., LEOPOLD, P. L., DRISCOLL, S., SCHYMEINSKY, J., QUAST, K., VISVANATHAN, S., FINE, J. S. & THOMAS, M. J. 2019. Characterization of an immortalized human small airway basal stem/progenitor cell line with airway region-specific differentiation capacity. *Respiratory research*, 20, 1-14.
- WANG, H., HE, L., LIU, B., FENG, Y., ZHOU, H., ZHANG, Z., WU, Y., WANG, J., GAN, Y. & YUAN, T. 2018a. Establishment and comparison of air-liquid interface culture systems for primary and immortalized swine tracheal epithelial cells. *BMC cell biology*, 19, 1-10.
- WANG, X.-Y., CHEN, S.-H., ZHANG, Y.-N. & XU, C.-F. 2018b. Olfactomedin-4 in digestive diseases: a mini-review. *World journal of gastroenterology*, 24, 1881.
- WANG, X., ZHAO, H., WANG, B., ZHOU, Y., XU, Y., RAO, L., AI, W., GUO, Y., WU, X., YU, J., HU, L., HAN, L., CHEN, S., CHEN, L. & YU, F. 2022. Identification of methicillin-resistant *Staphylococcus aureus* ST8 isolates in China with potential high virulence. *Emerg Microbes Infect*, 11, 507-518.
- WANG, Y., TANG, Z., HUANG, H., LI, J., WANG, Z., YU, Y., ZHANG, C., LI, J., DAI, H. & WANG, F. 2018c. Pulmonary alveolar type I cell population consists of two distinct subtypes that differ in cell fate. *Proceedings of the National Academy of Sciences*, 115, 2407-2412.
- WHITSETT, J. A. 2018. Airway epithelial differentiation and mucociliary clearance. *Annals of the American Thoracic Society*, 15, S143-S148.
- WHITSETT, J. A. & ALENGHAT, T. 2015. Respiratory epithelial cells orchestrate pulmonary innate immunity. *Nature immunology*, 16, 27.
- WILDEN, J. J., HRINCIUS, E. R., NIEMANN, S., BOERGELING, Y., LÖFFLER, B., LUDWIG, S. & EHRHARDT, C. 2020. Impact of *Staphylococcus aureus* Small Colony Variants on Human Lung Epithelial Cells with Subsequent Influenza Virus Infection. *Microorganisms*, 8, 1998.
- WILSON, K. 2015. *Modelling the airway epithelium in vitro as a tool for understanding pulmonary innate defence mechanisms*. University of Sheffield.
- WOLF, S., PEREZ, G. F., MUKHARESH, L., ISAZA, N., PRECIADO, D., FREISHTAT, R. J., PILLAI, D., ROSE, M. C. & NINO, G. 2017. Conditional reprogramming of pediatric airway epithelial cells: A new human model to investigate early-life respiratory disorders. *Pediatr Allergy Immunol*, 28, 810-817.
- WOLFE, M. S. J. B. 2006. The γ -secretase complex: membrane-embedded proteolytic ensemble. 45, 7931-7939.
- WOOD, C., SAHL, J., MALTINSKY, S., COYNE, B., RUSSAKOFF, B., YAGÜE, D. P., BOWERS, J. & PEARSON, T. 2021. SaQuant: a real-time PCR assay for quantitative assessment of *Staphylococcus aureus*. *BMC Microbiol*, 21, 174.
- WU, H. & TANG, N. 2021. Stem cells in pulmonary alveolar regeneration. *Development*, 148.
- WU, R., MARTIN, W. R., ROBINSON, C. B., ST GEORGE, J. A., PLOPPER, C. G., KURLAND, G., LAST, J. A., CROSS, C. E., MCDONALD, R. J. & BOUCHER, R. J. A. J. R. C. M. B. 1990. Expression of mucin synthesis and secretion in human tracheobronchial epithelial cells grown in culture. 3, 467-478.
- WU, R., YANKASKAS, J., CHENG, E., KNOWLES, M. & BOUCHER, R. 1985. Growth and differentiation of human nasal epithelial cells in culture: serum-free, hormone-supplemented medium and proteoglycan synthesis. *American Review of Respiratory Disease*, 132, 311-320.
- WU, X. & XU, F. 2014. Dendritic cells during *Staphylococcus aureus* infection: subsets and roles. *J Transl Med*, 12, 358.
- WYNN, T. A. 2015. Type 2 cytokines: mechanisms and therapeutic strategies. *Nature Reviews Immunology*, 15, 271-282.
- XIAO, S., JONES, R. M., ZHAO, P. & LI, Y. 2019. The dynamic fomite transmission of Methicillin-resistant *Staphylococcus aureus* in hospitals and the possible improved intervention methods. *Building and Environment*, 161, 106246.
- XU, D. & LU, W. 2020. Defensins: A Double-Edged Sword in Host Immunity. *Front Immunol*, 11, 764.
- YAGHI, A. & DOLOVICH, M. B. 2016. Airway Epithelial Cell Cilia and Obstructive Lung Disease. *Cells*, 5.

- YAN, N. & CHEN, Z. J. 2012. Intrinsic antiviral immunity. *Nature immunology*, 13, 214-222.
- YANG, C., YANG, X., DU, J., WANG, H., LI, H., ZENG, L., GU, W. & JIANG, J. 2015. Retinoic acid promotes the endogenous repair of lung stem/progenitor cells in combined with simvastatin after acute lung injury: a stereological analysis. *Respir Res*, 16, 140.
- YANG, J., HERNANDEZ, B. J., MARTINEZ ALANIS, D., NARVAEZ DEL PILAR, O., VILA-ELLIS, L., AKIYAMA, H., EVANS, S. E., OSTRIN, E. J. & CHEN, J. 2016. The development and plasticity of alveolar type 1 cells. *Development*, 143, 54-65.
- YANG, S. & YU, M. 2021. Role of goblet cells in intestinal barrier and mucosal immunity. *Journal of Inflammation Research*, 14, 3171.
- YATES, L. L., MITCHISON, H. M. & DEAN, C. H. 2018. Cilia in Lung Development and Disease. *Cilia*. CRC Press.
- YEASMIN, R., BREWER, A., FINE, L. R. & ZHANG, L. 2021. Molecular Dynamics Simulations of Human Beta-Defensin Type 3 Crossing Different Lipid Bilayers. *ACS Omega*, 6, 13926-13939.
- YOKOYAMA, R., ITOH, S., KAMOSHIDA, G., TAKII, T., FUJII, S., TSUJI, T. & ONOZAKI, K. 2012. Staphylococcal superantigen-like protein 3 binds to the Toll-like receptor 2 extracellular domain and inhibits cytokine production induced by Staphylococcus aureus, cell wall component, or lipopeptides in murine macrophages. *Infection and immunity*, 80, 2816-2825.
- YOSHISUE, H., PUDDICOMBE, S. M., WILSON, S. J., HAITCHI, H. M., POWELL, R. M., WILSON, D. I., PANDIT, A., BERGER, A. E., DAVIES, D. E. & HOLGATE, S. T. 2004. Characterization of CBE1, a Ciliated Cell-associated Gene Induced During Mucociliary Differentiation. *American Journal of Respiratory Cell and Molecular Biology*.
- YU, X., NG, C. P., HABACHER, H. & ROY, S. 2008. Foxj1 transcription factors are master regulators of the motile ciliogenic program. *Nature genetics*, 40, 1445-1453.
- ZANIN, M., BAVISKAR, P., WEBSTER, R. & WEBBY, R. 2016. The interaction between respiratory pathogens and mucus. *Cell host & microbe*, 19, 159-168.
- ZARAGOSI, L., DEPREZ, M. & BARBRY, P. 2020. Using single-cell RNA sequencing to unravel cell lineage relationships in the respiratory tract. *Biochemical Society Transactions*, 48, 327-336.
- ZECCONI, A. & SCALI, F. 2013. Staphylococcus aureus virulence factors in evasion from innate immune defenses in human and animal diseases. *Immunology letters*, 150, 12-22.
- ZHAI, W., WU, F., ZHANG, Y., FU, Y. & LIU, Z. 2019. The Immune Escape Mechanisms of Mycobacterium Tuberculosis. *Int J Mol Sci*, 20.
- ZHANG, L., HOU, X., SUN, L., HE, T., WEI, R., PANG, M. & WANG, R. 2018. Staphylococcus aureus Bacteriophage Suppresses LPS-Induced Inflammation in MAC-T Bovine Mammary Epithelial Cells. *Front Microbiol*, 9, 1614.
- ZHANG, Y., VELEZ-DELGADO, A., MATHEW, E., LI, D., MENDEZ, F. M., FLANNAGAN, K., RHIM, A. D., SIMEONE, D. M., BEATTY, G. L. & DI MAGLIANO, M. P. 2016. Abstract A096: Myeloid cells are required for pancreatic carcinogenesis and PD-1/PD-L1 checkpoint activation. AACR.
- ZHOU, J., ZHOU, X.-D., XU, R., DU, X.-Z., LI, Q., LI, B., ZHANG, G.-Y., CHEN, L.-X., PERELMAN, J. M. & KOLOSOV, V. P. 2021. The Degradation of Airway Epithelial Tight Junctions in Asthma Under High Airway Pressure Is Probably Mediated by Piezo-1. *Frontiers in physiology*, 12, 637790.
- ZHOU, W., HASHIMOTO, K., MOORE, M. L., ELIAS, J. A., ZHU, Z., DURBIN, J., COLASURDO, G., RUTIGLIANO, J. A., CHIAPPETTA, C. L. & GOLENIEWSKA, K. 2006. IL-13 is associated with reduced illness and replication in primary respiratory syncytial virus infection in the mouse. *Microbes and infection*, 8, 2880-2889.
- ZHU, Q., WEN, W., WANG, W. & SUN, B. 2019. Transcriptional regulation of virulence factors Spa and ClfB by the SpoVG-Rot cascade in Staphylococcus aureus. *Int J Med Microbiol*, 309, 39-53.
- ZHU, Y., CHIDEKEL, A. & SHAFFER, T. H. 2010. Cultured human airway epithelial cells (calu-3): a model of human respiratory function, structure, and inflammatory responses. *Critical care research and practice*, 2010.
- ZIHNI, C., MILLS, C., MATTER, K. & BALDA, M. S. 2016. Tight junctions: from simple barriers to multifunctional molecular gates. *Nature reviews Molecular cell biology*, 17, 564-580.

ZUYDERDUYN, S., NINABER, D. K., SCHRUMPF, J. A., VAN STERKENBURG, M. A., VERHOESEL, R. M., PRINS, F. A., VAN WETERING, S., RABE, K. F. & HIEMSTRA, P. S. 2011. IL-4 and IL-13 exposure during mucociliary differentiation of bronchial epithelial cells increases antimicrobial activity and expression of antimicrobial peptides. *Respiratory research*, 12, 1-12.